Université du Québec

Institut National de la Recherche Scientifique

Centre Eau Terre Environnement

LA GÉODÉSIE SPATIALE EN SOUTIEN À LA GESTION DE L'EAU SOUTERRAINE AU MEXIQUE CENTRAL

SPACE GEODESY TO SUPPORT GROUNDWATER MANAGEMENT IN CENTRAL MEXICO

Par

Pascal CASTELLAZZI

Thèse présentée pour l'obtention du grade de

Philosophiae Doctor (Ph. D.) en Sciences de la Terre

Jury d'évaluation :

Examinateur externe :	Dr. Tom Farr, JPL/NASA
Examinateur externe :	Dr. Sergey Samsonov, NRCAN
Président du jury de thèse et examinateur interne :	Dr. Monique Bernier, INRS-ETE
Co-directeur de recherche :	Dr. Alfonso Rivera, NRCAN
Co-directeur de recherche :	Dr. Jaime Garfias, UAEM
Directeur de recherche :	Dr. Richard Martel, INRS-ETE

Table des matières

Résumé – Français

Les populations établies sur les zones arides du monde dépendent largement des eaux souterraines pour assurer leurs besoins vitaux en eau, leur production alimentaire, et leur développement économique et humain. Ainsi, les ressources en eaux souterraines sont d'une importance cruciale et ont bien souvent une place importante dans les politiques internes de ces régions. De plus, ces ressources sont souvent partagées entre différents pays ou nations, ayant des manières différentes de les considérer, et plus spécifiquement, de les gérer. Dès lors, il est important de développer des outils permettant d'évaluer la pérennité des stocks en eau souterraine de manière fiable, apolitique, et au-delà de toute frontière. A travers l'étude d'une région particulièrement préoccupée par cette question, le Mexique Central, cette thèse propose d'évaluer l'utilisation de la géodésie spatiale comme outil de gestion des stocks d'eau souterraine.

Durant la décennie 2000-2010, deux techniques permettant de suivre les variations des stocks d'eau souterraine depuis l'espace ont été développées: l'interférométrie radar, et la gravimétrie par satellite. L'interférométrie radar, ou InSAR, permet de suivre les mouvements du sol avec une précision suffisante pour détecter les effets induits par les changements de pression hydrostatique dans les aquifères. La gravimétrie par satellite, utilisant les données de la mission GRACE, permet pour sa part de suivre les changements du champ gravitationnel dans le temps induits par les variations des masses d'eau. Ces deux techniques ont des limitations majeures ne permettant pas de les utiliser individuellement et directement comme outils de gestion des stocks d'eau souterraine. Par contre, la thèse développe des applications de ces deux techniques, les comparent, et présente une méthodologie qui les combinent en perspective d'une utilisation opérationnelle pour la gestion de l'eau.

La zone d'étude est localisée au Mexique Central et s'étend sur environ 200 000 km^2, de la ville de Mexico dans le Sud, aux environs de Zacatecas dans le Nord. Dans cette région, la surexploitation des aquifères engendre une subsidence de l'ordre de 5 à 15 cm/an affectant de manière importante l'intégrité des infrastructures urbaines. Certaines zones agricoles dépendantes de l'irrigation et situées à la périphérie des villes principales contribuent également à la surexploitation. Malgré les déficits locaux en eau, la perte de masse liée est la surexploitation des aquifères est faible, suggérant que l'eau

pompée reste en partie présente dans les systèmes hydrologiques régionaux. Les résultats suggèrent également qu'une meilleure compréhension de la détection des changements de masses est nécessaire afin de pouvoir en faire un outil de gestion.

Abstract – English

Human settlements located in arid areas of the World are largely dependent on groundwater resources to sustain their vital needs, their food production, and their economic and human development. In such places, groundwater resources are of great importance, and have often a central place within the internal politics. In addition, these resources are often shared between different cities, countries, or nations using different management practices. In such context, it is of major importance to develop tools allowing groundwater storage monitoring which are effective, apolitical, and applicable beyond boundaries. Through the study of a region particularly affected by these preoccupations, Central Mexico, this thesis explores the contribution of space geodesy toward this objective.

From 2000 to 2010, two techniques allowing groundwater storage change monitoring from space were developed: radar interferometry, and satellite gravimetry. Radar interferometry, or InSAR, allows monitoring ground level changes related to hydrostatic pressure changes within aquifers. Satellite gravimetry relying on data from the GRACE mission allows monitoring temporal changes of the gravity field linked to groundwater mass changes. These two techniques have major limitations preventing them from being used directly as water management tools. This thesis illustrates the applicability of the techniques, presents a comparison of the observations from the two techniques, and presents a methodology for combining them in the perspective of an operational use for groundwater management.

The study area is localised in Central Mexico and extends over around 200 000 km^2, from Mexico City to the South, to the Zacatecas area to the North. In this region, groundwater overexploitation causes subsidence rates generally ranging from 5 to 15 cm/yr and affecting significantly urban infrastructure integrity. Several agricultural areas depending on irrigation are surrounding some of the main cities, which also contribute to groundwater overexploitation. Despite these important regional deficits, the large-scale groundwater mass loss is low, suggesting that the extracted groundwater remains within the hydrologic systems. Results also suggest that a better understanding of groundwater mass changes is necessary in the perspective of developing the needed groundwater management tools.

Resumen – Español

Las poblaciones que se asienta en zonas áridas son dependientes en gran medida del agua subterránea para satisfacer sus necesidades vitales, la producción alimentaria, así como para el desarrollo económico y humano. De este modo, los recursos hídricos son de importancia crucial y juegan un rol crucial en las políticas internas de estas regiones. Además, estos recursos son a menudo compartidos entre diferentes países, que, asimismo, tienen diferentes maneras de considerarla y de administrarla. En tal sentido, es de importancia crucial desarrollar herramientas que permitan evaluar la sustentabilidad de las aguas subterráneas de manera fiable, apolítica, así como más allá de las fronteras. A través del estudio de un área particularmente afectada por esta compleja problemática ambiental, la región central de México, esta tesis extiende las aportaciones de la geodesia espacial con el fin de aportar elementos que sustenten respuestas a esta problemática.

Durante la década 2000-2010, dos técnicas han sido desarrolladas con base a la información satelital, que permiten seguir las variaciones del almacenamiento de agua subterránea: la interferometría radar y la gravimetría. La interferometría radar, o InSAR, permite seguir la consolidación diferencial del terreno con una precisión suficiente para detectar los efectos inducidos por los cambios de la presión hidrostática en un acuífero. La gravimetría satelital, con base a los datos de los satélites GRACE, permite seguir los cambios temporales del campo gravitacional inducido por las variaciones de las masas de agua. Estas técnicas tienen limitaciones mayores que no permiten ser utilizadas directamente como herramientas de gestión del almacenamiento del agua subterránea. Esta tesis ilustra las aplicaciones de ambas técnicas, su comparación, sus límites, así como presenta una metodología para un uso combinado con el fin de una utilización operacional para la gestión sustentable del agua.

La zona estudiada está localizada en la región central de México y se extiende sobre aproximadamente 200 000 km^2, desde la ciudad de México al sur hasta el extremo del Estado del Zacatecas al norte. En esta región, la sobreexplotación de los acuíferos engendra una consolidación diferencial del terreno que fluctúa entra 5 y 15 cm/año, que afecta la integridad de la infraestructura urbana. Algunas zonas agrícolas dependientes de la irrigación, situadas en la periferia de las principales ciudades, también contribuyen

a la sobreexplotación. A pesar del déficit localizado, la pérdida de masa relacionada a la sobreexplotación de los acuíferos es reducida, sugiriendo que el agua extraída por bombeo resta en parte en los sistemas hidrológicos regionales. Los resultados también sugieren que una mejor comprensión de la detección de los cambios de masa por gravimetría es necesaria para poder convertirse en una herramienta de gestión.

Remerciements

Je remercie mes directeurs de thèse : Richard Martel (INRS), Alfonso Rivera (CGC), et Jaime Garfias (UAEM). Ils ont su former une équipe d'encadrement efficace, complémentaire, et organisée. Leur ouverture d'esprit m'a permis de combiner leur expertise en hydrogéologie avec de la géodésie, alors que ce n'est pas leur expertise principale. C'est justement avec cette ouverture d'esprit que les frontières entre les domaines peuvent s'ouvrir et créer des opportunités d'applications nouvelles. J'espère être inspiré de la même ouverture d'esprit pour le reste de ma carrière de chercheur.

Je remercie les chercheurs m'ayant permis de développer mon expertise en géodésie, alors que ce n'était pas initialement mon champ d'expertise : Laurent Longuevergne (CNRS), Angus Calderhead (INRS), Devin Galloway (USGS), Jonathan Normand (USC), Jianliang Huang (CCCOT) et Tom Farr (JPL/NASA).

Je remercie ma famille, Christian, Claudine, Julien et Nicolas Castellazzi. Leurs encouragements et leur support ont été essentiels à la réussite de ce projet de thèse. Je remercie mes amis, notamment Jeremy Longuet, Guillaume Nielsen, Vincent Taillard, Charles Brouard, Laetitia Pertuis, Najim Chaoui. Je remercie aussi Joanie Coté pour son soutien.

Je remercie toutes les agences ayant fourni, ou ayant aidé à récolter les données utilisées dans cette thèse : L'Agence Spatiale Canadienne (ASC), l'Agence Spatiale Européenne, l'Alaska Satellite Facility (ASF), la Comission Nacional del Agua (CNA). Je remercie également les agences ayant contribuées directement au financement de la thèse : le Consejo Nacional de Ciencia y Tecnología (CONACyT), le Ministère des Relations Internationales et de la Francophonie du gouvernement du Québec (MRIFQ), le Fonds de Recherche du Québec - Nature et Technologies (FRQNT), ainsi que le Conseil de Recherches en Sciences Naturelles et en Génie du Canada (CRSNG - fond de subvention à la découverte du professeur Richard Martel).

Avant-propos

Cette thèse de doctorat présente les résultats et la synthèse de travaux effectués entre Janvier 2012 et Mai 2017. La totalité des travaux présentés proviennent de la collaboration de chercheurs issus de cinq organismes : l'Institut National de la Recherche Scientifique (INRS, Québec, Canada), La Commission Géologique du Canada (CGC, Québec, Canada), L'Université Autonome de l'État de Mexico (UAEM, Toluca, Mexique), le Centre Canadien de Cartographie et d'Observation de la Terre (CCCOT, Ottawa, Canada) et le Centre National de la Recherche Scientifique (CNRS, France).

Pascal Castellazzi, étudiant au doctorat à l'INRS (Québec, Canada) a effectué les travaux décrits dans cette thèse sous la supervision de trois chercheurs issus d'institutions différentes : Richard Martel (INRS), Alfonso Rivera (CGC), et Jaime Garfias (UAEM). Le directeur principal à l'origine de ce travail de la thèse est le Professeur Richard Martel, INRS-ETE, Québec, QC, Canada.

Format de la thèse

Cette thèse est dite ‘par article’, c’est-à-dire qu’elle comprend une partie de synthèse en français, et une succession de chapitres structurés à la manière d’articles scientifiques écrits en anglais. Ce format de thèse permet à l’étudiant à la fois de valider sa thèse académiquement, mais aussi de publier son travail dans des revues accessibles par ses paires. Le premier chapitre est en français, les cinq suivants sont en anglais.

La partie synthèse constitue le premier chapitre, et présente de manière concise et synthétique l’ensemble des résultats présentés dans les parties suivantes. Cette partie se termine par une conclusion générale tirant essence de tous les travaux effectués durant la thèse. Les articles sont organisés de manière logique. Chaque partie de la thèse fait environ une trentaine de pages.

Le style de référencement des citations utilisé correspond à celui d’un des articles de la thèse, présenté au Chapitre 4 et publié dans la revue *Water Ressources Research*. Une seule bibliographie est présentée, regroupant toutes les références citées dans l’ensemble du document. Les références d’un même premier auteur et de la même année sont différenciées par une lettre (a, b, et c) après l’indication de l’année de publication, et ce de manière consistante dans la totalité de la thèse.

La numérotation des figures, des tableaux et des équations commence à 1 pour chaque chapitre. Le format de présentation des équations varie selon les journaux ciblés pour la publication des articles présentés dans les Chapitres 2 à 6. Les figures présentes dans la synthèse (Chapitre 1) sont en français, sauf lorsqu’elles sont reprises d’articles en anglais soumis ou publiés.

Structure de la thèse

La thèse est présentée par une succession de six chapitres structurés dans l'ordre suivant:

1. **Synthèse :**

Cette partie présente d'abord la problématique, les principes, l'utilisation, et les applications liées aux techniques utilisées. Il s'en suit un résumé des contributions scientifiques et une réflexion sur les travaux effectués ainsi que sur les limitations et le potentiel des méthodes employées en perspective de résoudre la problématique.

2. **Article 1 (Castellazzi et al. 2016a):**

LAND SUBSIDENCE IN MAJOR CITIES OF CENTRAL MEXICO: INTERPRETING INSAR-DERIVED LAND SUBSIDENCE MAPPING WITH HYDROGEOLOGICAL DATA

Castellazzi, P., N. Arroyo-Domínguez, R. Martel, A. I. Calderhead, J. C. L. Normand, J. Gárfias, and A. Rivera (2016). *International Journal of Applied Earth Observation and Geoinformation*, 47, 102-111. doi:10.1016/j.jag.2015.12.002.

Article Accepté le 1er décembre 2015.

3. **Article 2 (Castellazzi et al. 2017a) :**

INSAR TO SUPPORT SUSTAINABLE URBANIZATION OVER COMPACTING AQUIFERS: THE CASE OF TOLUCA VALLEY, MEXICO

Castellazzi, P., J. Garfias, R. Martel, C. Brouard, and A. Rivera (2017). *International Journal of Applied Earth Observation and Geoinformation*, 63, 33-44. doi:10.1016/j.jag.2017.06.011.

Article Accepté le 26 Juin 2017.

4. **Article 3 (Castellazzi et al. 2016b) :**

GROUNDWATER DEPLETION IN CENTRAL MEXICO: USE OF GRACE AND INSAR TO SUPPORT WATER RESOURCES MANAGEMENT

Castellazzi, P., R. Martel, A. Rivera, J. Huang, P. Goran, A. I. Calderhead, E. Chaussard, J. Garfias, and J. Salas (2016)., *Water Resources Research*. doi:10.1002/2015WR018211.

Article Accepté le 5 Juillet 2016.

5. **Article 4 (Castellazzi et al. 2016c) :**

ASSESSING GROUNDWATER DEPLETION AND DYNAMICS USING GRACE AND INSAR: POTENTIAL AND LIMITATIONS

Castellazzi, P., R. Martel, D. L. Galloway, L. Longuevergne, and A. Rivera (2016), *Groundwater*. doi: 10.1111/gwat.12453.

Article Accepté le 25 Juillet 2016.

6. **Article 5 (Castellazzi et al. 2017b – en révision) :**

COMBINING GRACE AND INSAR FOR QUANTITATIVE MAPPING OF GROUNDWATER DEPLETION AT THE WATER MANAGEMENT SCALE

Castellazzi, P., Longevergne, L., Martel, R., Rivera, A., Brouard, C., and E. Chaussard. (2017 – en révision).

Soumis à la revue *Remote Sensing of Environment* le 14 mars 2017.

7. **Autres contributions**

Cette section liste les autres contributions scientifiques effectuées durant le programme de doctorat (2012-2017).

Contributions de l'étudiant et des collaborateurs

L'étudiant est à l'origine des idées, des travaux de terrains et des analyses présentés dans les cinq articles de la thèse. Il est aussi à l'origine de l'écriture des articles et de leurs corrections après révision par des pairs. Durant ses séjours au Mexique, l'étudiant a également pu apprendre l'espagnol.

Dr Richard Martel a dirigé l'étudiant durant sa thèse, a apporté un soutien financier, ainsi que son support pendant les travaux de terrain et durant l'écriture des articles. Dr Alfonso Rivera a codirigé l'étudiant, il a engament apporté son expertise sur la gestion de l'eau au Mexique et pour l'écriture et la correction des articles. Dr Jaime Garfias a codirigé l'étudiant et a apporté son support quant à l'organisation des travaux de terrain. Dr Devin L. Galloway a fourni son expertise sur l'interprétation des données issues de l'InSAR en hydrogéologie. Dr Laurent Longuevergne a fourni une aide quant au traitement et à l'interprétation des données issues du capteur GRACE. Dr Angus Calderhead à apporter son expertise au début des travaux de thèse pour permettre à l'étudiant de mieux incorporer ses travaux dans la continuité des travaux précédents. Dr Estelle Chaussard a apporté son support quant au traitement des données radar et à l'interprétation des résultats. Dr Jianliang Huang a fourni une version des données GRACE utilisée dans la thèse et a apporté son expertise sur l'utilisation de ses données. Charles Brouard a aidé à la création des algorithmes utilisés pour le traitement des données GRACE et InSAR (notament pour l'inversion utilisée dans le dernier article). Dr Norma Arroyo-Domínguez a aidé au traitement des données SAR pour la région de Toluca.

Liste des abréviations

LSP: Lerma-Santiago-Pacifico water basin

GRACE: Gravity Recovery and Climate Experiment

InSAR: Interferometric Synthetic Aperture Radar

GLDAS: Global Land Data Assimilation System

SAR: Synthetic Aperture Radar

SBAS: Small Baseline Subset Interferometry

PSI: Permanent Scatterer Interferometry

LOS: Line Of Sight

GWS: Groundwater Storage

TWS: Total Water Storage

SWS: Surface Water Storage

SMS: Soil Moisture Storage

SIS: Snow and Ice Water Storage

LSM: Land Surface Model

SMP: Soil Moisture Probe

WTE: Water Thickness Equivalent

MCM: Million Cubic Meters

NDVI: Normalized Difference Vegetation Index

CONAGUA: Comisión Nacional del Agua

CFE: Comisión Federal de Electricidad

NAMO: *Nivel de Aguas Máximas Ordinarias* – Maximum Ordinary Water Level

Définitions utiles

Géodésie : Science qui étudie les dimensions et la forme de la Terre ainsi que les variations temporelles de sa surface et de son champ de gravité.

Interférométrie radar : Technique utilisant simultanément deux radars à synthèse d'ouverture ou le même radar à des instants différents pour étudier les différences de phase des images générées afin de générer des modèles numériques d'élévation ou de mesurer des déplacements de la surface de la terre.

Gravimétrie par satellite : La gravimétrie est une méthode qui étudie les variations spatiales ou temporelles du champ de gravité. La gravimétrie par satellite réfère à l'étude des variations temporelles du champ de gravité tel que mesuré par les satellites de la mission Gravity Recovery And Climate Experiment (GRACE).

Aquifère : Formation géologique contenant de façon temporaire ou permanente de l'eau mobilisable, constituée de roches perméables et capable de la restituer naturellement ou par exploitation.

Subsidence : La subsidence est un lent affaissement du sol vers le bas. Elle peut notamment se produire par compaction d'un aquifère poreux surexploité.

Objectif de la thèse

Les travaux décrits dans cette thèse visent à tester l'utilisation de données issues de capteurs orbitaux dans la perspective d'un suivi global des ressources en eau souterraine, de leur gestion durable, et de prévenir la subsidence. Le Mexique Central est la region d'étude permettant de tester la méthodologie et les differentes techniques.

Ainsi la question posée est la suivante :

Comment pouvons-nous effectuer un suivi global des ressources en eau souterraine dans le but d'en assurer la bonne gestion et de prévenir la subsidence?

Qui se traduit en anglais de la manière suivante:

How can we monitor groundwater resources globally to support their sustainable management and prevent land subsidence?

1. SYNTHÈSE

1.1. L'EAU SOUTERRAINE

1.1.1. GÉNÉRALITÉS

L'eau souterraine est l'eau saturant un milieu poreux ou fracturé sous la surface du sol. Elle fait partie intégrante du cycle de l'eau, qu'il est essentiel de comprendre préalablement à la lecture de la thèse présentée. Le cycle de l'eau est un modèle conceptuel permettant de représenter le parcours de l'eau entre les grands réservoirs d'eau liquide (Figure 1). Les flux d'eau s'évaporant des océans et des terres circulent dans l'atmosphère et retombent sous forme de précipitation. La précipitation liquide retombant sur les continents s'écoule à leur surface, s'évapore, ou s'infiltre. La partie infiltrée recharge les nappes d'eau souterraine. Les variations spatiales de l'infiltration, aussi appelé recharge, forme des gradients de niveau d'eau souterraine qui sont à l'origine de l'écoulement souterrain.

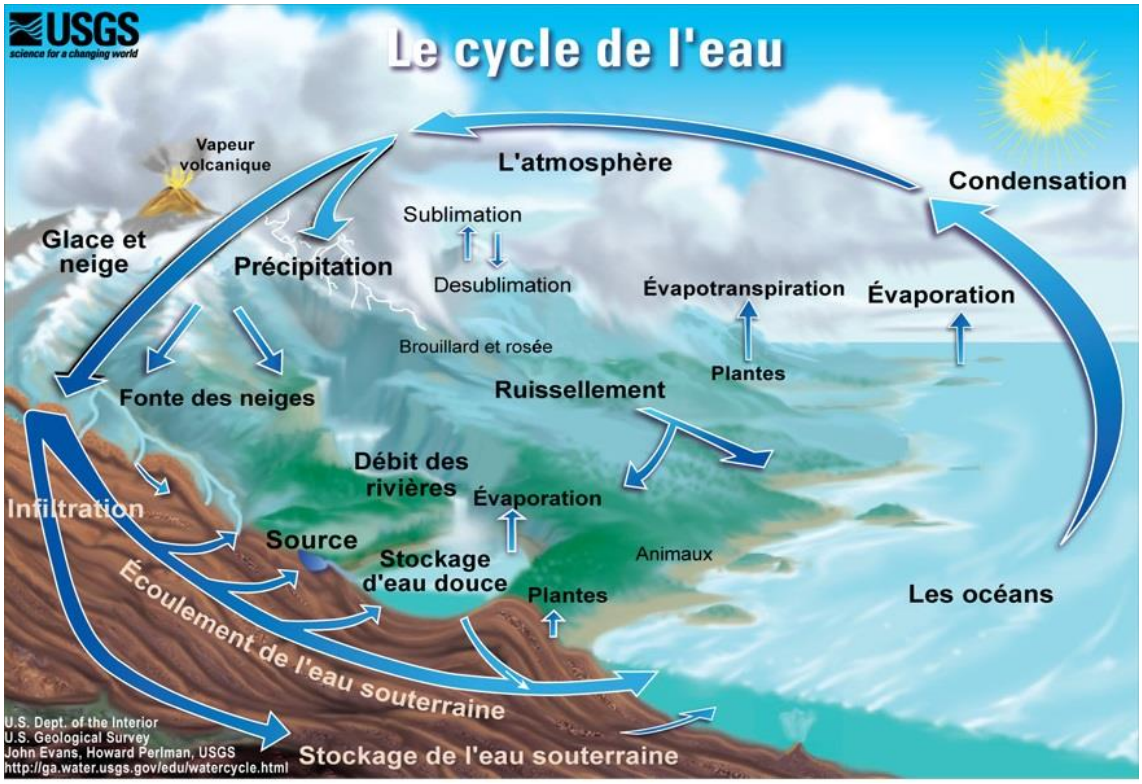

Figure 1 : Le cycle de l'eau (source : USGS).

Les différents compartiments du stockage de l'eau sont d'importants sujets d'études en sciences de la Terre. Chaque compartiment a son importance propre pour le climat et pour les communautés humaines. L'hydrogéologie se concentre sur l'étude de l'eau souterraine, notamment de son écoulement, de ses caractéristiques chimiques, et sur tous facteurs influant son extraction pour les communautés humaines. Cette thèse se concentre principalement sur ce dernier thème.

Les hydrogéologues définissent un aquifère comme une unité de stockage de l'eau souterraine. En fait, il existe deux courants de pensée majeurs lorsqu'il s'agit de délimiter un aquifère. Il y a premièrement une vision géologique, ou un aquifère est défini par une unité ou un ensemble d'unités géologiques. Il y a deuxièmement une vision hydraulique, ou un aquifère est défini comme une unité d'écoulement. A l'heure actuelle, il semble qu'aucun consensus n'existe sur l'utilisation d'une ou l'autre approche. Cependant, il semble logique de privilégier l'approche hydraulique pour les études sur la dynamique d'écoulement, ou sur la diffusion de contaminants. Alors qu'il semble davantage approprié de recourir à l'approche géologique pour les études hydrogéochimiques ou isotopiques, ou lorsque une séquence géologique très marquée, continue, et d'importance majeure, est présente.

Différentes échelles d'études des eaux souterraines existent. Ces échelles d'étude sont reliées à différents systèmes d'écoulements ayant des processus de recharge, des temps de transport, et des échelles de profondeur différents. La Figure 2 présente une vue générale des échelles d'étude inspirée de Toth (1963). Plus d'information sur ces différentes échelles d'étude est présentée en détail au Chapitre 5.

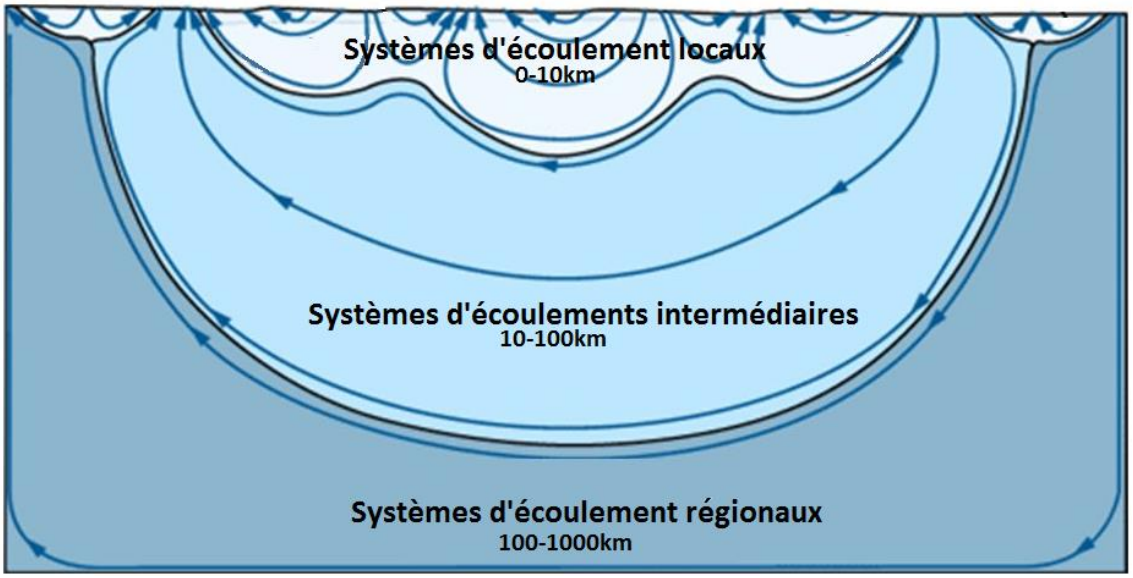

Figure 2 : Les différentes échelles de circulation des eaux souterraines (figure inspiré de Toth, 1963).

1.1.2. LA SUREXPLOITATION DES RESSOURCES EN EAU SOUTERRAINE

L'eau souterraine est surexploitée lorsque les flux d'eau entrant dans l'aquifère sont inférieurs aux flux d'eau sortant. L'équilibre entre les flux entrant et sortant d'un aquifère influe sur le stockage de l'eau dans l'aquifère, selon l'équation suivante :

Equation 1: $\Delta GWS = R - (D + P)$

ΔGWS étant la variation de stockage de l'eau dans l'aquifère, R étant le flux de recharge entrant dans l'aquifère, D étant la décharge naturelle d'eau souterraine vers, par exemple, une rivière ou un autre aquifère, et P est le pompage anthropogénique. Les flux R, D et P doivent être considérés dans les mêmes unités, par exemple, en m^3/an.

Le calcul de chaque flux s'effectue de manière séparée. La décharge anthropique se calcul généralement à travers l'installation d'instruments de mesure du débit sur chaque puits en pompage. Le calcul de la décharge naturelle s'effectue au cas par cas, selon le milieu récepteur. Dans le cas d'une rivière, l'analyse du débit de la rivière et de ses tributaires permet de conclure sur le débit d'eau souterraine rechargeant la rivière ou quittant la rivière pour recharger l'aquifère.

La recharge est certainement le flux le plus difficile à estimer. De nombreuses méthodes existent. Une vue d'ensemble sur ces méthodes est fournies par Scanlon et al. (2012).

Une approche largement simplifiée permet de les classer en deux catégories. Premièrement, les méthodes empiriques sont basées sur l'analyse de courbes de fluctuation des niveaux d'eau dans des puits ou sur l'analyse des gradients spatiaux des niveaux d'eau. Ces méthodes sont particulièrement efficaces lorsque les puits d'observations sont nombreux et qu'une bonne connaissance physique de l'aquifère est déjà disponible. L'analyse des gradients permet, à travers l'application de la loi de Darcy, d'estimer les flux d'eau en transfert entre les zones de recharge et les zones de résurgence ou de pompage. Deuxièmement, les méthodes basées sur des bilans de surface utilisent l'équation suivante :

Equation 2: $R = P - E - Ru$

R étant le flux de recharge arrivant à l'aquifère, *P* étant la précipitation, *E* étant l'évapotranspiration, et Ru étant le ruissellement de surface. Ces méthodes, dites de 'bilan hydrique de surface' considèrent la recharge comme le résiduel d'une équation de partitionnement de la précipitation.

En utilisant une approche basée sur les flux entrant et sortant des aquifères, Wada et al. (2010) présente une carte du déficit dans les aquifères de surface sur la Terre (Figure 3c). Il présente aussi les données d'estimation des flux entrant (Figure 3a) et des flux sortant (Fig.3b) ayant permis le calcul du déficit (Figure 3c).

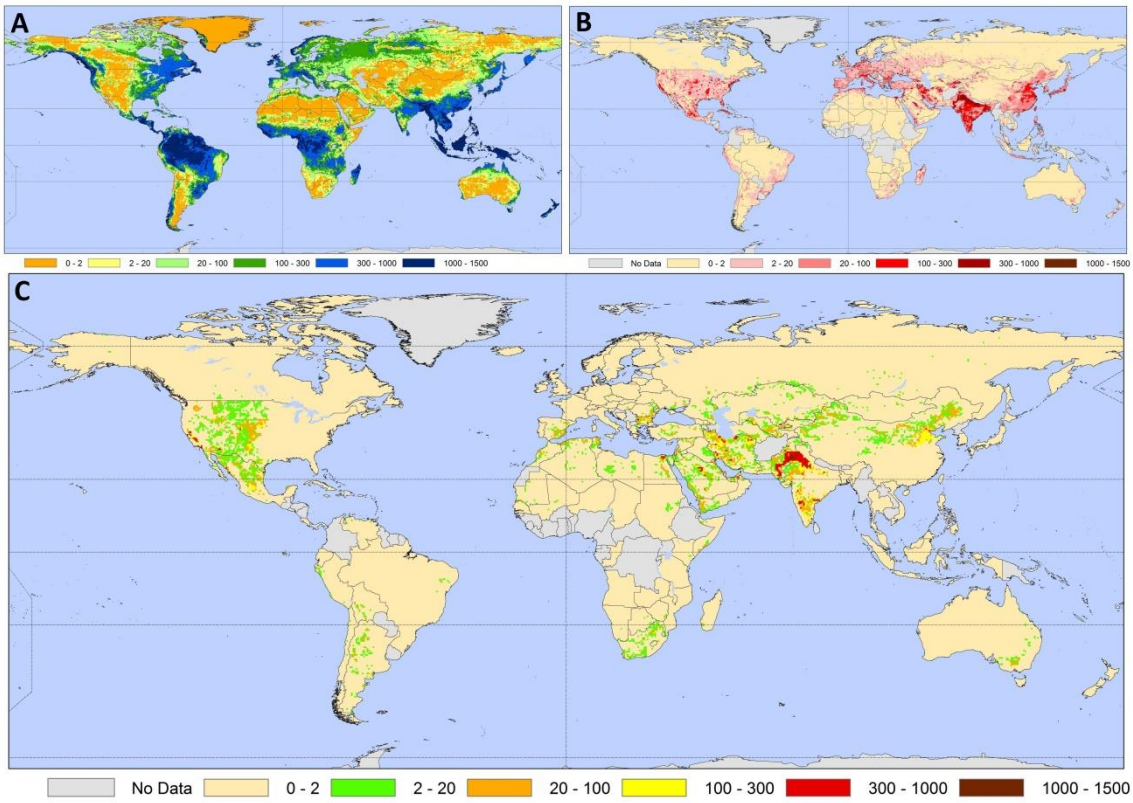

Figure 3 : Les aquifères surexploités dans le monde (source : Wada et al. 2010). (A) représente le flux entrant en mm/an (recharge), (B) le flux sortant (exploitation) et (C) déficit des eaux souterraine (mm/an).

Plus récemment, des données géodésiques issues de GRACE ont permis la détection des pertes de masse dans les aquifères et de produire une carte globale (Figure 4). Il est intéressant de noter les différences majeures entre la carte basée sur un bilan d'eau de surface et celle basée sur les variations de masse. Une différence particulièrement évidente est visible dans la zone étudiée dans cette thèse : le Mexique Central. En effet, la Figure 3 suggère un déficit dans cette région, ce qui n'est pas le cas de la Figure 4. Ces différences s'expliquent possiblement par le fait que ces mesures sont issues de résiduels entre des paramètres différents. Finalement, à la vue de différences si évidentes, il est facile de constater le manque de connaissances exactes quant aux zones où les aquifères sont surexploités, les causes de la surexploitation, et le manque de consensus sur leurs détection et évaluation. Selon les deux estimations (Figure 3 et Figure 4), la surexploitation des eaux souterraines est préoccupante, particulièrement dans les zones arides ou c'est souvent la seule source d'eau pouvant approvisionner/déservir la population à un coût de production raisonnable.

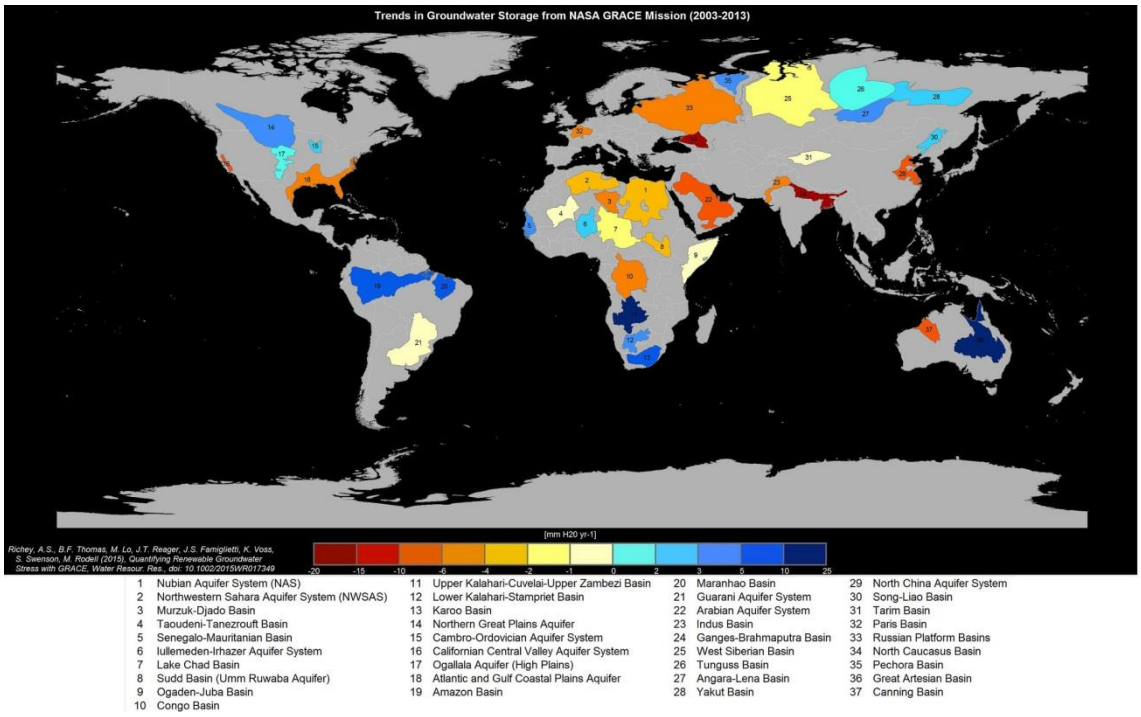

Figure 4 : Carte des aquifères surexploités dans le monde. La figure provient de Richey et al. 2015.

1.2. L'EAU SOUTERRAINE AU MEXIQUE

1.2.1. IMPORTANCE

Les ressources en eau souterraine sont d'importances majeures au Mexique Central, car elle constitue souvent la seule ressource en eau disponible en qualité et quantité suffisante. Des villes de taille importante se sont initialement développées grâce à l'abondance des ressources en eau malgré le climat aride du Mexique Central. Cependant, le développement incontrôlé de ces villes a engendré une situation ou l'exploitation des eaux souterraines n'est pas durable. La Figure 5 présente les principaux facteurs du déficit en eau souterraine au Mexique: la densité de la population (Figure 5a), les taux de précipitation annuels (Figure 5b), et la présence de lacs ou de réservoirs pouvant constituer des sources d'eau alternative à l'eau souterraine (Figure 5c). Finalement, la Figure 5 présente également la carte nationale des aquifères administratifs en déficit du Mexique (CONAGUA, 2009a).

La région de Mexico est la plus peuplée du pays, et c'est aussi une région ou les aquifères sont largement en déficit, malgré un taux de précipitation annuel d'environ 1000 mm/an. Au nord de Mexico, la région du Bajio présente des déficits importants car

les précipitations sont faibles (autour de 500 mm/an), malgré une concentration de population moindre, la région de Guadalajara présente peu de déficit dans les aquifères, notamment car, étant située en bas de basin (voir chapitre 4) et recevant les principaux effluents de la région, l'eau de surface est la source principale des eaux utilisées. Ainsi, la présence de lacs et réservoir a permis de largement réduire la dépendance aux eaux souterraines. Enfin, la partie nord du Mexique Central fait face à des déficits importants malgré une population de faible densité. Les taux de précipitation très bas (250 à 350 mm/an) ne permettent pas aux aquifère de se recharger suffisamment.

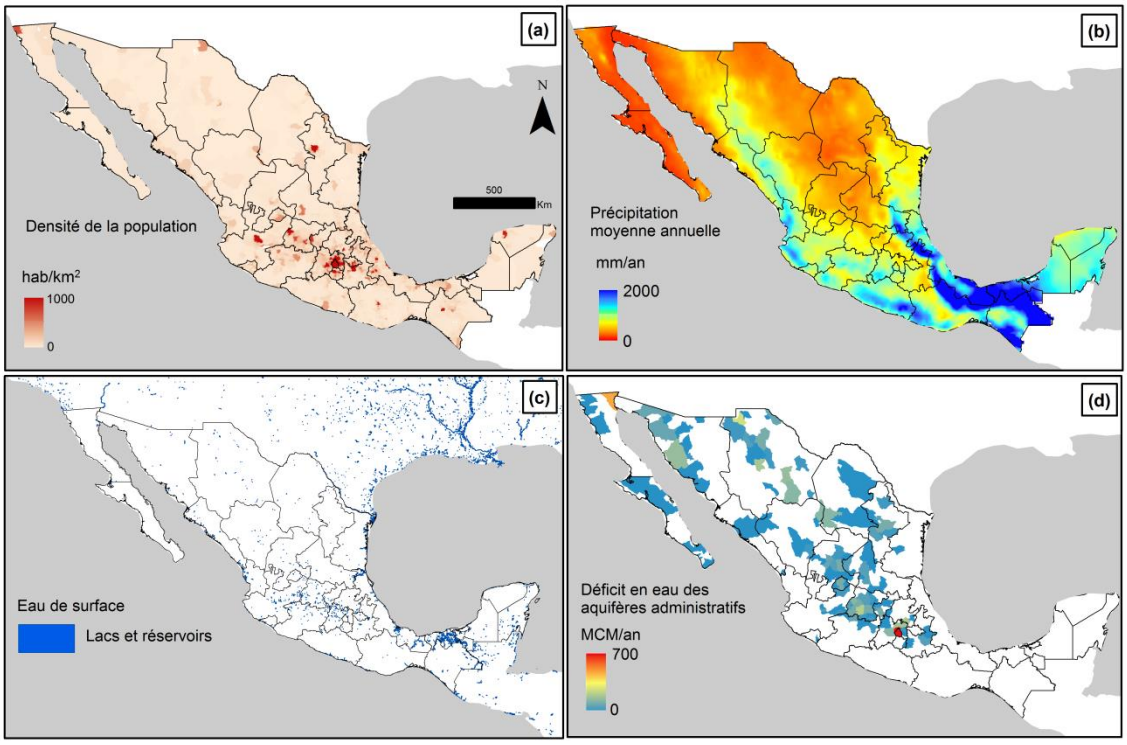

Figure 5: Densité de la population (a), taux de précipitation moyen annuel (b), carte des lacs et réservoirs (c), et carte des aquifères en déficit utilisée pour leur gestion (d). (Sources: a - Center for International Earth Science Information Network; b - WorldClim/Hijmans et al. 2005; c - The Global Lakes and Wetlands Database; d - CONAGUA, 2009a).

1.2.2. PROBLÉMATIQUES

a) Évaluer la durabilité de l'approvisionnement en eau souterraine

Les agences chargées de la gestion des ressources en eau souterraine ont généralement pour but d'assurer la pérennité de la ressource lorsque c'est possible, c'est-à-dire lorsque l'aquifère est naturellement rechargé à des taux pouvant compenser les taux de pompage et assurer à l'aquifère un état d'équilibre (voir Bredehoeft et al. 2002 pour une définition détaillée de l'état d'équilibre d'un aquifère). Lorsque le pompage n'est pas durable, comme c'est forcément le cas pour les aquifères fossiles ne recevant aucun flux entrant, la ressource doit alors être gérée et des solutions alternatives doivent être identifiées à l'avance. En d'autres termes, la surexploitation d'un aquifère n'engendre pas forcément des conséquences graves tant qu'elle est bien connue et quantifiée, et que la gestion de l'aquifère est adaptée à sa dynamique de confinement et de recharge (Bredehoeft et al. 2002).

Au Mexique, l'agence gouvernementale responsable de la gestion des ressources en eau souterraine est la *Comisión Nacional del Agua* (CNA ou CONAGUA). La CNA reconnait 693 aquifères administratifs, pour lesquels elle évalue la durabilité des stocks d'eau. Pour cela, l'agence se base sur deux méthodes différentes dépendamment de la disponibilité des données pour chaque aquifère. Plus de détails sur ces calculs sont fournis à la section 4.2 de ce document.

La première méthode de calcul du budget en eau des aquifères est la méthode privilégiée par la CNA si les données nécessaires sont disponibles. C'est une approche basée sur les observations d'écoulement. Les zones de recharge et de résurgence sont délimitées, puis les flux entrants ou sortants sont mesurés par la loi de Darcy (Darcy, 1856). Cette méthode nécessite des données de terrain telles que des observations de niveau statique dans les puits. L'avantage majeur de cette méthode est qu'elle ne requiert pas l'estimation de paramètres dont l'évaluation est difficile ou imprécise, tels que l'évapotranspiration ou le ruissellement. La deuxième méthode consiste à évaluer les flux d'eau entrants dans l'aquifère par un budget de surface ou la précipitation, l'évapotranspiration, le ruissellement et le changement de stockage dans la zone insaturée sont estimés. La recharge est alors un résiduel de la précipitation à laquelle on soustrait les estimations des autres flux. Le principal problème de cet approche est qu'elle ne considère pas l'état dynamique de l'aquifère (Bredehoeft et al. 2002), et que

les erreurs liées au calcul des paramètres nécessaires s'accumulent dans l'estimation finale de la recharge.

Les estimations fournies par l'analyse des budgets en eau montrent que 173 des 653 aquifères administratifs sont en déficit (Figure 5d). Ces aquifères se trouvent majoritairement au centre, au nord, et au nord-ouest du Mexique. Les imprécisions liées aux estimations effectuées par les budgets en eau sont importantes, telles que suggérées par Calderhead et al. (2011), qui estime le déficit annuel de l'aquifère de la Vallée de Toluca à environ le double qu'officiellement publié par la CONAGUA. Les cartes de subsidence fournies par Chaussard et al. (2014b) suggèrent également que le déficit est parfois observable dans des régions où il n'est pas officiellement publié. De plus, les effets de la 'fermeture' (la perte des connections hydrologiques) des bassins versant ont été montrés par Wester et al. (2011). Toutes ces observations sont autant de preuves qu'une méthode alternative d'observation et de mesure du déficit doit être développée, que ce soit pour appuyer le système de gestion présentement en place, ou soit, dans un futur plus lointain, pour le remplacer. Les chapitres 4, 5 et 6 de cette thèse présentent des solutions issues des dernières avancées de la géodésie spatiale.

b) La compaction des aquifères et ses conséquences

La surexploitation des aquifères peut induire des conséquences directes et à court terme sur la stabilité des infrastructures urbaines. En effet, elle engendre une baisse des pressions hydrostatiques dans l'aquifère, et selon la compressibilité et l'épaisseur de celui-ci, elle peut engendrer sa compaction et l'affaissement du sol. La perte de pression hydrostatique a une ampleur supérieure dans les aquifères confinés, et la compaction de ce type d'aquifère peut facilement atteindre des taux importants (plusieurs dizaines de centimètres par an). Ces processus sont décrits en détail au Chapitre 5 de la thèse.

Les changements de pression hydrostatique se traduisent à l'échelle des pores par une augmentation de la contrainte effective, telle que décrite par la théorie de la poro-élasticité (Terzaghi, 1925 ; Biot, 1940) :

Equation 3: $\sigma_t = \sigma_e + p$

Ou p est la pression interstitielle, σ_t est la contrainte verticale totale, et σ_e est la contrainte effective. Dans le cas d'une contrainte totale constante, en régime permanent

et à l'équilibre, l'équation peut être simplifiée et exprimée en terme de changement (Δ) de contrainte :

Equation 4: $\Delta\sigma_e = -\Delta p = -\rho\, g\, \Delta h$

Ou ρ est la densité de l'eau, g est la constante gravitationnelle, et Δh est le changement de charge hydraulique. Le changement de charge hydraulique est important dans un aquifère confiné, puisque le coefficient d'emmagasinement est faible (voir chapitre 5 pour une description détaillée).

La portion du coefficient d'emmagasinement liée à la compressibilité de l'aquifère est appelée l'emmagasinement spécifique (*Ss*).

Equation 5: $Ss = Ssk + Ssw = \rho\, g\, (\alpha + n\, \beta w)$

Equation 6: $\Delta u = b\, Ss\, \Delta h$

Où *b* est l'épaisseur de l'aquifère, *Ssk* est l'emmagasinement squelettique spécifique relié à la compressibilité de la matrice de solide de l'aquifère (α), Ssw est l'emmagasinement spécifique de l'eau relié à la compressibilité de l'eau (βw), et *n* est la porosité de l'aquifère. Finalement, le déplacement vertical (Δu) induit par un changement de pression hydraulique s'exprime ainsi :

À travers les équations 4 à 6, il est possible de se rendre compte que la compaction d'un aquifère est largement dépendante de trois facteurs : la perte de pression hydraulique (Δh), l'épaisseur de l'aquifère (*b*), et sa compressibilité (α). Dès lors qu'un aquifère présente des hétérogénéités majeures dans l'un de ces trois paramètres, de grandes variations sur les taux de subsidence sont observées en surface. L'apparition de fractures est un signe parfaitement visible de ces hétérogénéités. La fracturation ou la fissuration du sol pose des problèmes majeurs pour l'intégrité des infrastructures. Ce point est largement développé au le Chapitre 3.

Une autre conséquence importante de la compaction des aquifères est la diminution irréversible de sa porosité et de son emmagasinement spécifique. Ainsi, la fraction inélastique de la compaction détermine la perte de volume qui n'est pas récupérable si le niveau de pression (les niveaux d'eau) remonte. Ce phénomène est particulièrement préoccupant, puisqu'il engendre une diminution de la qualité de l'aquifère, dans le sens ou l'aquifère ne pourra plus stocker autant d'eau pour les générations futures.

1.3. UTILISATION DE LA GÉODÉSIE EN HYDROGÉOLOGIE QUANTITATIVE

1.3.1. INTERFÉROMÉTRIE RADAR

a) Principes

Les satellites SAR (Synthethic Aperture Radar), orbitent la terre et émettent une onde électromagnétique à haute résolution depuis une distance d'environ 700 km. Cette onde est renvoyée par la surface de la Terre et le signal de retour est récupéré par une antenne positionnée sur le satellite. Ainsi, une image est acquise, où chaque pixel contient de l'information sur l'amplitude (la puissance) et la phase de l'onde électromagnétique renvoyée par l'aire au sol couverte par le pixel. Les éléments au sol revoient des signaux d'amplitude et de phase différents dépendamment de leur taille, rugosité, composition, teneur en humidité, et distance au satellite. Des informations sur l'état du sol et son évolution peuvent ainsi être récupérées. Parmi les données récupérées, celles concernant les variations du niveau du sol dans le temps est particulièrement utiles en génie civil, en sismologie, en volcanologie, et en hydrogéologie.

Toutes les techniques InSAR (Interferometric Synthetic Aperture Radar) fonctionnent sur des principes de base similaires. Le mouvement est détecté en comparant la phase du retour d'un signal électromagnétique envoyé sur Terre (Figure 6).

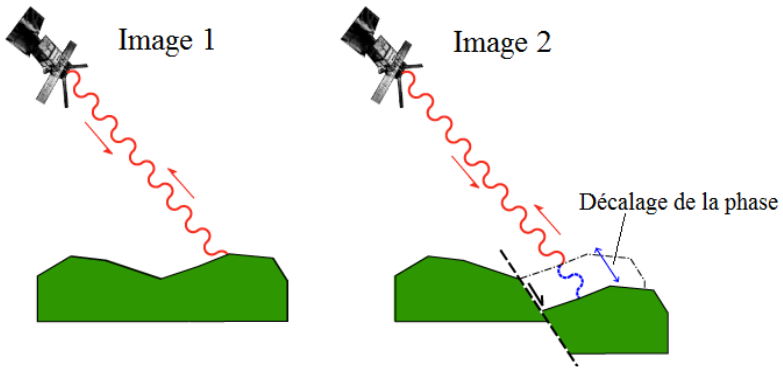

Figure 6 : Le mouvement du sol provoque un décalage du signal de phase. Ainsi, si la valeur de la phase varie le long d'une série temporelle d'images, elle traduit un déplacement du niveau du sol.

Des paires d'images radar acquises depuis des positions orbitales planifiées pour être identiques sont utilisées. Les deux images sont co-registrées, c'est-à-dire que la première est ré-échantillonnée pour être parfaitement compatible pixel à pixel avec la seconde. Toutes les informations contenues dans la seconde image sont alors comparables à celle de la deuxième, notamment les valeurs d'amplitude et de phase du signal de retour. Les techniques diffèrent dans la manière dont sont choisies les paires d'images dans un ensemble d'images ainsi que dans les principes utilisées pour discriminer l'information de phase importante des informations inutiles (bruit). Dans tous les cas, le mouvement est mesuré dans le sens de la visée du satellite, c'est-à-dire selon un angle généralement compris entre 20 et 45 degrés par rapport à la verticale.

b) Produire des données de déformation à partir d'images radar

L'interférométrie d'images radar (InSAR) permet de produire des données de déformation du sol à partir d'images radar. La technique fut développée dans les années 1990 (Massonet et Feigl, 1998), après la mise en orbite des satellites radar de premières générations tels qu'ERS-1 et RADARSAT-1. Au début des années 2000, elle connut un véritable tournant grâce à l'arrivée de techniques permettant l'intégration de plus de deux images et les algorithmes de réduction des perturbations atmosphériques (Ferretti et al, 2001 ; Berardino et al. 2002). Aujourd'hui, à part certaines applications spécifiques, ces algorithmes dits 'avancés' ont largement supplanté les techniques de première génération. Une vue d'ensemble des principes et particularité des nouvelles techniques InSAR est fournie par Crosetto et al. (2016).

Le SBAS-InSAR (Berardino et al. 2002) récupère les principes des premières générations de traitement InSAR. Une analyse préliminaire d'une série temporelle d'images radar permet de déceler les paires d'images pouvant former les meilleures paires interférométriques. Il s'agit généralement de sélectionner les séries d'images ayant des géométries d'acquisition idéales et des erreurs de positionnement orbital faibles. La particularité du SBAS, tout comme les techniques plus anciennes (comme le D-InSAR), est d'être basée sur l'utilisation d'images dont la résolution a été diminuée, réduisant ainsi la variance locale et lissant ainsi le bruit. Le bruit est efficacement réduit au prix d'une résolution diminuée par un facteur allant généralement de 3 à 10. La résolution finale en plan est alors souvent entre 8 et 30 m, selon la résolution des images initiales et le facteur de diminution de la résolution choisie. A partir des images co-registrées de basse résolution, une carte de différence de phases entre les deux images

est produite, appelée interférogramme. Après une éventuelle filtration de cette carte (souvent par l'application d'un filtre passe-bas) et l'application de corrections liées à des erreurs de parallaxe, la phase est 'déroulée'. Cette étape permet de transformer un interférogramme dont les valeurs de différence de phases vont de $-\pi$ à $+\pi$, en une carte de déplacement en millimètre du mouvement entre les deux acquisitions formant les deux images d'un interférogramme.

Le PSI (Ferretti et al. 2001; Hooper et al. 2004) permet de suivre les variations des niveaux de sol renvoyant un signal de phase cohérent et stable. Il a l'avantage d'être utilisable a la résolution des 'cibles', c'est-à-dire des éléments au sol renvoyant le signal, tels les éléments durs (béton, métal) et anguleux (coins de bâtiments par exemple) présents au sol. Dans un premier temps, il est nécessaire d'identifier les points pour lesquels la phase est systématiquement renvoyée de manière puissante et cohérente. Deux critères sont identifiés pour la détection de ces cibles : la stabilité de l'amplitude du signal de retour et la cohérence interférométrique du signal de phase. Une fois les points au sol détectés (appelé 'Persistent Scatterers'), les valeurs de phase sont récupérées pour chaque acquisition et pour chaque point, créant une série temporelle de variations de la phase en chaque point. Une technique d'inversion est ensuite appliquée, permettant de transformer les variations de la phase dans le temps ($-\pi$ à$+\pi$) en déplacements du niveau du sol (en mm). A la différence du SBAS-InSAR, aucun lissage n'est appliqué. La résolution finale et la précision verticale est supérieure au SBAS-InSAR si les cibles au sol sont denses, comme c'est le cas en milieu urbain.

c) Choix de la stratégie de traitement

La Figure 7 illustre différents avantages et inconvénients des deux méthodes. Elle présente les résultats des traitements SBAS-InSAR et PSI appliqués sur la même série temporelle de données Sentinel-1A, prisent entre 2014 et 2016 sur une partie de la ville de Toluca au Mexique. Le SBAS-InSAR (Figure 7a) présente des résultats robustes libres de toute erreur évidente. Le PSI (Figure 7b) produit des résultats à la résolution des cibles réfléchissantes au sol, telles que les coins anguleux des toits, les rebords des bâtiments ou des routes. Bien que les résultats soient globalement similaires, ils divergent à certains endroits à cause de deux facteurs. Premièrement, le PSI permet la mise en évidence de zones d'affaissement plus petites lorsque la densité des cibles est suffisante. (Figure 7b – cercle noir). Deuxièmement, lorsque le déplacement est supérieur à un quart de la longueur d'onde (en bande C, la longueur d'onde est

d'environ 5,6 cm), des erreurs d'inversion peuvent se produire lorsque la phase est inversée dans le temps (Figure 7b, cercles blancs). Les algorithmes spatiaux de déroulement de la phase ne présentent pas ces erreurs tant que le déplacement est progressif dans l'espace. En d'autres mots, le SBAS est approprié aux déplacements spatialement progressifs, et le PSI permet une meilleure résolution en milieu urbain si le déplacement est faible et progressif dans le temps.

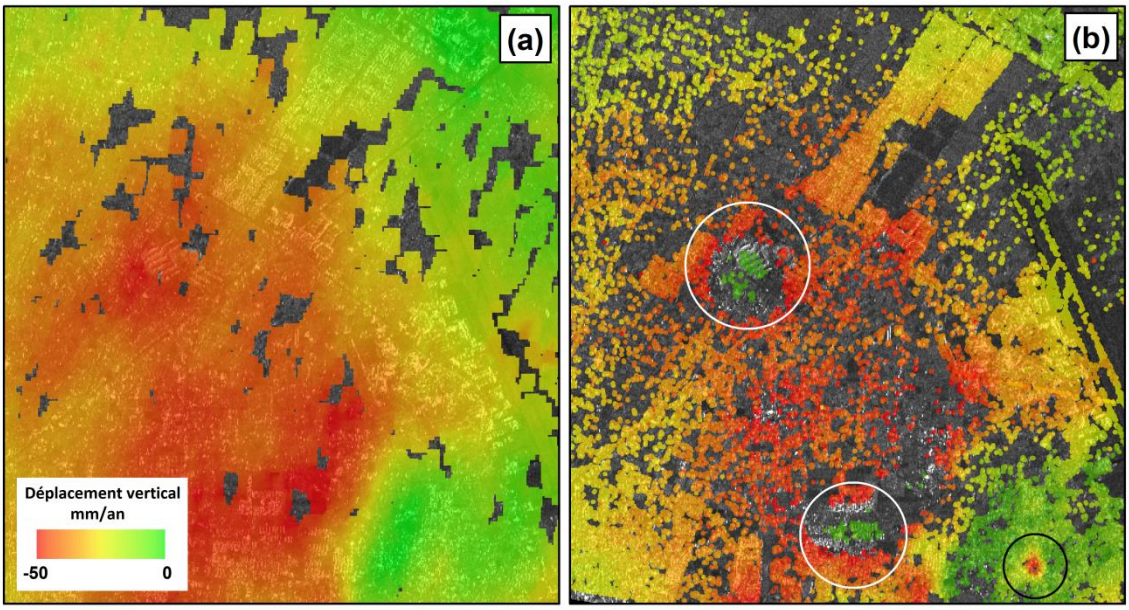

Figure 7 : Comparaison entre les résultats de traitement SBAS-InSAR (a) et PSI (b) de 25 images Sentinel-1A sur la Vallée de Toluca. Les zones vertes sont stables. Le PSI permet d'obtenir une meilleure précision spatiale en milieu urbain permettant de voir certains détails importants (cercle noir). Cependant, des erreurs d'inversion peuvent apparaître si le déplacement dépasse 1,4 cm entre deux acquisitions de la série temporelle utilisée (cercles blancs).

Les déplacements liés à la compaction d'un aquifère surexploité présentent des variations spatiales en accord avec les variations des épaisseurs des couches les plus compressibles. Ces couches étant généralement d'épaisseur progressive spatialement, les déplacements observés le sont généralement aussi. Il est alors souvent possible d'utiliser le PSI. Cependant, la précision spatiale et verticale n'étant souvent pas une priorité pour les applications visant la détection et la quantification de la subsidence, de nombreux auteurs privilégient le SBAS-InSAR pour sa capacité à produire des cartes de

déplacements dans les zones légèrement végétalisées et moins cohérentes (e.g. Chaussard et al. 2014b). Lorsque l'InSAR est utilisé pour observer les dommages aux infrastructures urbaines liés à la subsidence, le PSI est à privilégier (voir exemple d'application dans le Chapitre 3).

d) Principales applications en hydrogéologie

L'interférométrie radar, et notamment les techniques InSAR avancées (SBAS, PSI, et autres variantes), a vu son champ d'application s'élargir considérablement lors des dix dernières années. De nombreuses images satellites sont maintenant disponibles, et les capteurs récents ont un meilleur positionnement orbital rendant la technique plus facile à appliquer (moins de compensation de parallaxe à appliquer). Les apports de l'InSAR en sismologie, en volcanologie et pour l'étude des glissements de terrain sont évidents. Les applications en hydrogéologie se sont développées surtout entre 2005 et 2010. Galloway et Hoffmann (2007) présentent une vision complète des applications de l'InSAR en hydrogéologie.

1.3.2. MESURES GRAVIMÉTRIQUES SPATIALES (GRACE)

a) Principes

Selon la loi de Newton, des corps ayant une masse s'attirent. Un satellite en orbite est donc attiré par la Terre et il doit, pour garder son altitude constante, obtenir une vitesse précise de parcours orbital. La Terre n'étant pas constituée de masses uniformes, la valeur de gravité varie spatialement et temporellement, et de légères variations de vitesse et d'altitude sont observées lors du suivi des capteurs orbitaux. À travers une technologique innovante, le système orbital Gravity Recovery And Climate Experiment (GRACE) permet de mesurer ces variations dans le temps, et en tout point de la Terre.

Le système GRACE comprend deux satellites distants d'environ 200 km et positionnés sur une orbite polaire basse, à environ 400 km d'altitude. Un télémètre en bande K permet le suivi continuel de la distance entre les deux satellites. La variation de distance entre les deux satellites est comparée sur plusieurs passages et à des temps différents et permet de produire des cartes de variations temporelles de la gravité, renseignant alors sur les phénomènes ayant une influence rapide sur la gravité.

Les facteurs influençant la gravité à l'échelle du mois et de l'année sont mal connus. Cependant, il est souvent considéré dans la littérature que les contributeurs principaux à

ces variations sont les stocks d'eau. Ainsi, les données GRACE peuvent être interprétées selon l'équation suivante :

Equation 7: ΔTWS = ΔSWS + ΔGWS + ΔSMS + ΔSIS

TWS est le stockage d'eau terrestre (ou total) tel que mesuré directement par le système GRACE, *SWS* représente l'eau stockée dans les rivières et lacs, *SMS* représente l'eau stockée sous forme d'humidité dans le sol, et *SIS* l'eau stockée sous forme solide (neige, glace). S'il est possible d'obtenir des estimations pour trois des quatre paramètres de l'équation, les données GRACE permettent alors d'obtenir le quatrième. Par exemple, en hydrogéologie, l'équation peut être utilisée de la manière suivante :

Equation 8: ΔGWS = ΔTWS – (ΔSWS + + ΔSMS + ΔSIS)

b) Traitement des données issues de GRACE

De la réception des données de distance entre les satellites à la production de cartes mensuelles de variation gravimétrique, plusieurs étapes de traitement sont nécessaires. Dans tous les cas, une stratégie de séparation des artefacts et du bruit dominant le signal doit être adoptée. Chaque stratégie est appelée 'solution'. Il en existe de nombreuses disponibles gratuitement sur internet (Voir section 5.2.2c). Ces étapes complexes sont généralement réalisées par des spécialistes en géodésie.

Les solutions sont généralement classées en deux types. Le premier type est les solutions non-contraintes, qui n'utilisent aucun *a priori* pour la séparation du bruit et du signal, mais un algorithme de reconnaissance des artéfacts typiques de GRACE et des filtres passe-bas pour la réduction des hautes fréquences bruitées. Ainsi, des filtres optimisés pour les données GRACE ont vu le jour, comme le filtre DDK (Kusche et al. 2007) (Figure 8e). Le deuxième type comprend les solutions contraintes qui utilisent un *a priori* sur la définition des artefacts et du bruit afin de les séparer en des données utiles. La solution du Groupe de Recherches de Géodésie Spatiale (GRGS, appartenant au Centre National d'Etudes Spatiales) par exemple (Figure 9a), prend comme *a priori* que les données finales doivent ressembler (dans leur domaine spectral) aux estimations d'humidité de sol fournies par les modèles de surfaces (LSM). À travers une décomposition en harmonique sphérique, les coefficients définissant les variations ne

ressemblant pas à ces modèles sont diminués, et les coefficients ressemblant aux modèles de surface sont augmentés. Il en résulte une carte dont les artefacts sont peu apparents. Les Figures 8b, 8c, 8d, 8e et 8f présentent des données finales de tendance de *ΔTWS* en WTE (Water Thickness Equivalent). Les zones rouges présentent une dimution naturelle ou anthropique des stocks en eau.

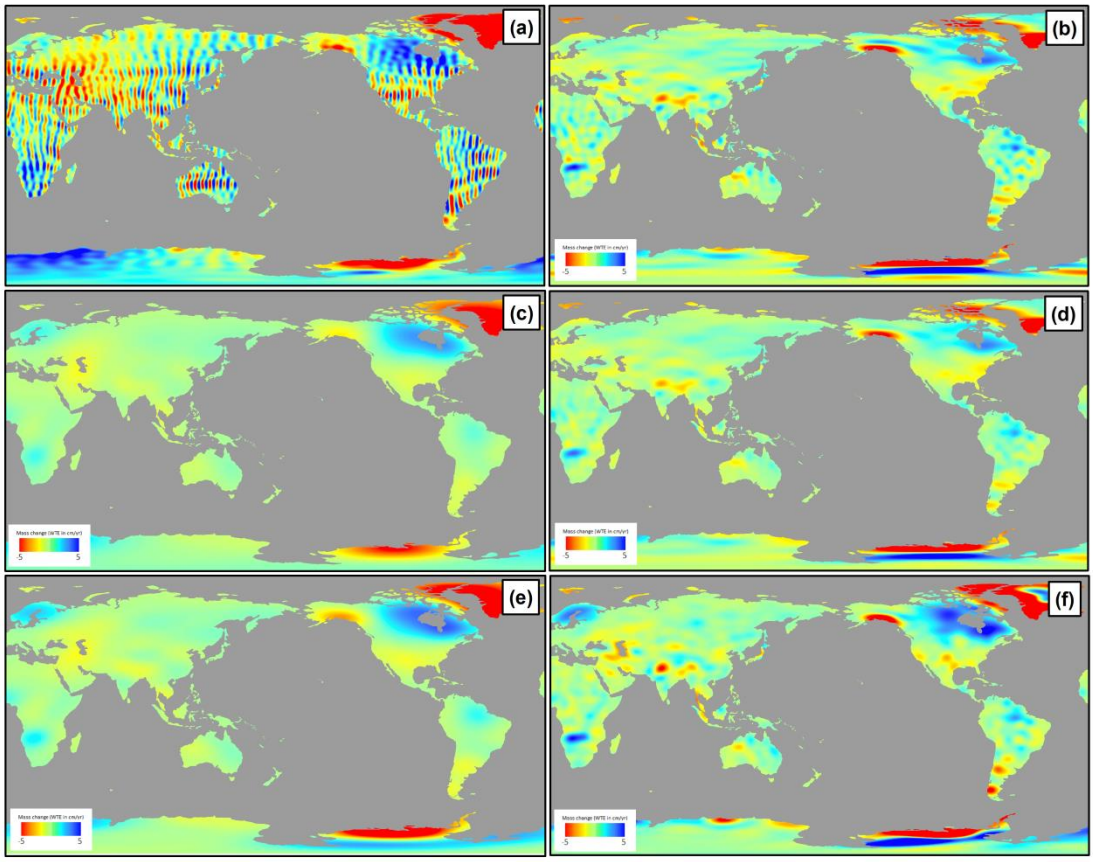

Figure 8 : Tendance TWS (08/2002-08/2014) de différentes solutions GRACE non – contraintes : (a) originales, (b) 'destrippées' en utilisant l'algorithme proposé par Swenson et Wahr (2006), (c) lissées par un filtre Gaussian de 700 km de rayon, (d) 'destrippées' lissées par un filtre Gaussian de 200 km, (e) 'destrippées' et lissées en une seule étape par un filtre DDK fort de degré 1 (Kusche et al. 2007), (f) 'destrippées' et lissées en une seule étape par un filtre DDK faible de degré 5 (Kusche et al. 2007, 2009)

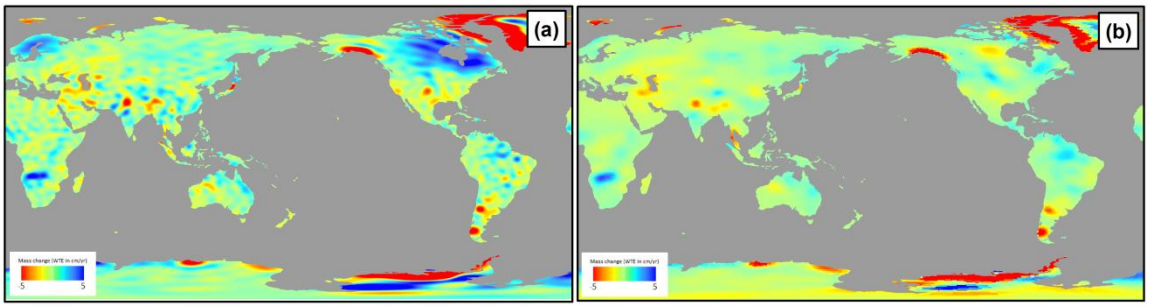

Figure 9 : Tendance TWS (08/2002-08/2014) de deux solutions GRACE contraintes : (a) la solution stabilisée du GRGS RL03, (b) la solution MASCON régularisée de CSR (Save et al. 2016).

c) Principales applications en hydrogéologie

Le principal avantage apporté par le capteur GRACE pour les applications en hydrogéologie est lié à sa caractéristique de mesure par variations de masse. Dans le cas de l'eau, la masse est directement reliée au volume, puisque sa densité est égale à 1 et est quasiment constante. Ce type de mesure gravimétrique n'est pas disponible autrement à ces échelles spatiales. Le suivi des variations des masses d'eau par GRACE à plusieurs autres avantages. Premièrement, il permet de suivre l'état complet des variations des stocks, prenant en compte directement les effets dynamiques des flux dans les aquifères (Bredehoeft, 2002). Deuxièmement, les mesures prennent en compte les variations de masse en profondeur, c'est-à-dire tous les aquifères, peu importe leur profondeur. Finalement, les données sont disponibles gratuitement et globalement pour les hydrogéologues. Il est alors facile de comprendre pourquoi le capteur GRACE a créé un engouement évident dans la communauté des sciences hydrologiques. Tel que présenté au Chapitre 6 de cette thèse, une certaine incompréhension existe toujours sur les meilleures stratégies de traitement à adopter.

1.4. Principales limitations des techniques géodésiques

Cette section présente une discussion sur les limitations de la gravimétrie par satellite et de l'interférométrie en perspective de leur incorporation dans des systèmes opérationnels du suivi des stocks d'eau souterraine.

a) Résolution

Le capteur GRACE possède des caractéristiques de résolution très atypiques pour les spécialistes de la télédétection et de l'hydrogéologie. En fait, il s'agit d'une résolution par 'champ de masse', c'est-à-dire qu'une forte variation de masse affectera une zone plus large qu'une faible variation de masse. Les masses telles que détectées par GRACE ont ainsi des effets de fuites les unes vers les autres. Seule une simulation permet de bien se rendre compte de la résolution et du comportement du capteur GRACE (Figure 10 et 11).

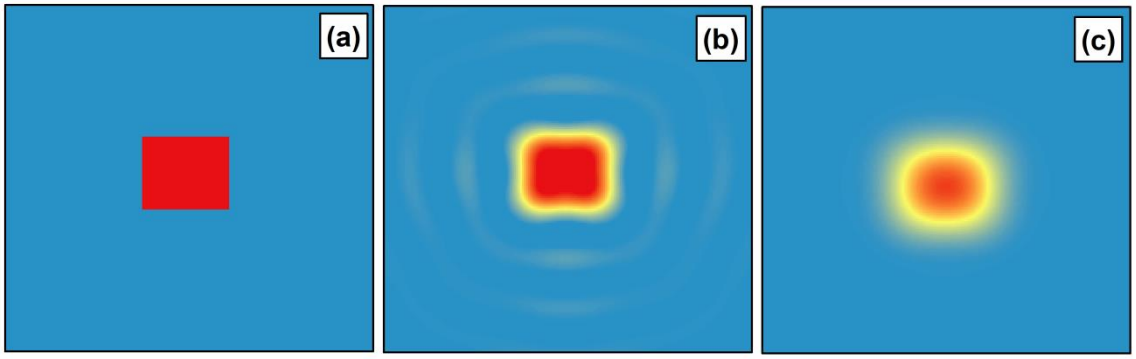

Figure 10: Simulation de la détection par GRACE d'un changement d'une masse synthétique entourée de masses stables. La partie (a) montre une masse synthétique d'environ 1000 km de côté. Elle est ensuite définie sur 60 ordre et degrés d'harmoniques sphériques (b) où l'on peut noter la présence de 'vagues' atour de la masse synthétique, puis lissée par un filtre Gaussien de 300 km de côté (c). Ce processus simule le post-traitement d'une des versions GRACE utilisée fréquemment.

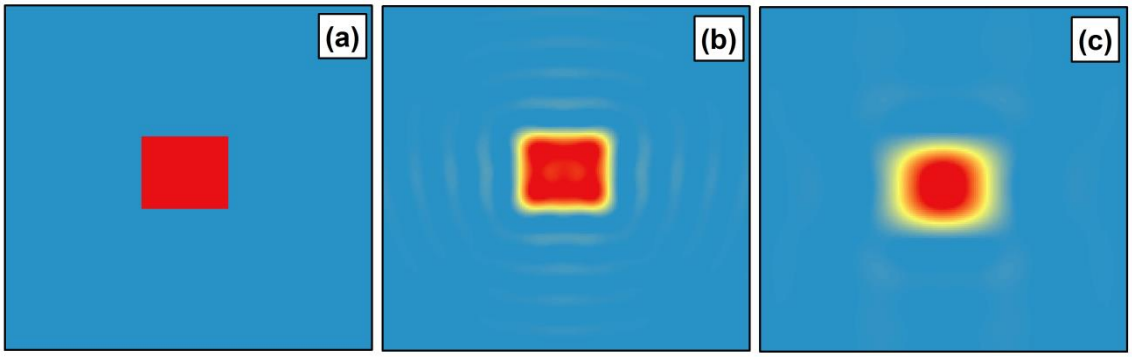

Figure 11 : Résultats d'une simulation similaire à celle montrée dans la figure précédente avec une définition du signal sur 96 ordres et degrés d'harmoniques sphériques (b) et l'utilisation d'un filtre DDK5 (c - Kusche et al. 2009). Un important gain en résolution est observable par rapport à la solution GRACE précédente. La

comparaison avec la figure précédente illustre les différences de résolution entre différentes solutions GRACE.

Initialement, lorsque les solutions majoritairement utilisée incluaient l'application d'un filtre Gaussien de 300 km de rayon (Figure 10c), certains auteurs parlaient d'une intégration spatiale sur une zone d'au moins 200 000 km^2 pour obtenir des données finales (TWS ou GWS) peu affectées par les fuites spatiales. Avec une meilleure expérience de l'utilisation des données GRACE, et la possibilité de mieux simuler les effets des fuites spatiales à l'aide de simulations sur des données synthétiques (tels que les exemples des Figures 10 et 11), il fut ensuite possible d'utiliser les données GRACE sur des zones d'études plus petites, de l'ordre de 100 000 km^2 (Castellazzi et al. 2016b).

Les données de type 'MASCONS' (e.g. Save et al. 2016), issues de l'inversion directe des données de distance inter-satellites sur des aires prédéfinies (souvent arbitraires : pixels ou polygones) permettent théoriquement d'obtenir des données de plus haute résolution. Les produits GRACE 'MASCONS' présentement distribuées sont calculés à partir d'aires définies par des pixels de 1 à 3 degrés. En pratique, les zones 'MASCONS' adjacentes ne sont pas complétement indépendantes, et l'apport de ces solutions en termes de gain de résolution est présentement encore mal compris.

L'utilisation des données GRACE sur des zones d'une taille inférieure à 100 000 km^2 semble tout de même possible, à partir du moment où il existe une connaissance détaillée des zones influant le TWS à l'intérieur et aux environs de la zone d'étude. Une application de ce type est présentée au chapitre 6 de la thèse (Castellazzi et al. 2017b – en révision).

b) Couverture spatiale et temporelle des deux techniques

Les données GRACE sont disponibles depuis avril 2002, et sont discontinues depuis 2014. La majorité des solutions (contraintes ou non) sont disponibles à une résolution temporelle mensuelle. Bien que certains centres de traitement (e.g. GRGS) proposent des solutions à une résolution temporelle de 10 jours, rares sont les applications pouvant en tirer parti.

Les capteurs SAR présentent des caractéristiques de couverture et de résolutions variées définies lors de la conception initiale de la mission. La plupart des capteurs peuvent fournir des images compatibles à un intervalle de 12 à 45 jours. Certains capteurs, tels

que Terrasar-X et Sentinel-1 ayant un cycle orbital court, sont construits de manière optimale pour l'InSAR. Ces deux capteurs ont également été conçus en tandem, c'est-à-dire qu'ils sont suivis par un satellite identique, donc produisant des données compatibles, repassant sur leur trace après la moitié de la durée d'un cycle orbital normal. C'est ainsi que le tandem SENTINEL-1A/B possède une résolution temporelle de 6 jours depuis 2015.

Les images produites par les capteurs SAR couvrent des zones carrées ou rectangulaires sur une superficie allant de 10 km sur 10 km à 350 km sur 350 km, soit une couverture de l'ordre de 100 km^2 à 120 000 km^2. Les images de haute résolution sont généralement acquises en contrepartie d'une couverture plus faible. Les images à large couverture sont acquises selon des modes d'acquisitions complexes, appelés TOPSAR (Figure 12) ou SCANSAR. Ces images sont créées par une suite d'acquisitions d'images plus petites. Ces petites acquisitions sont ensuite rassemblées en une seule image par calibration et co-registration.

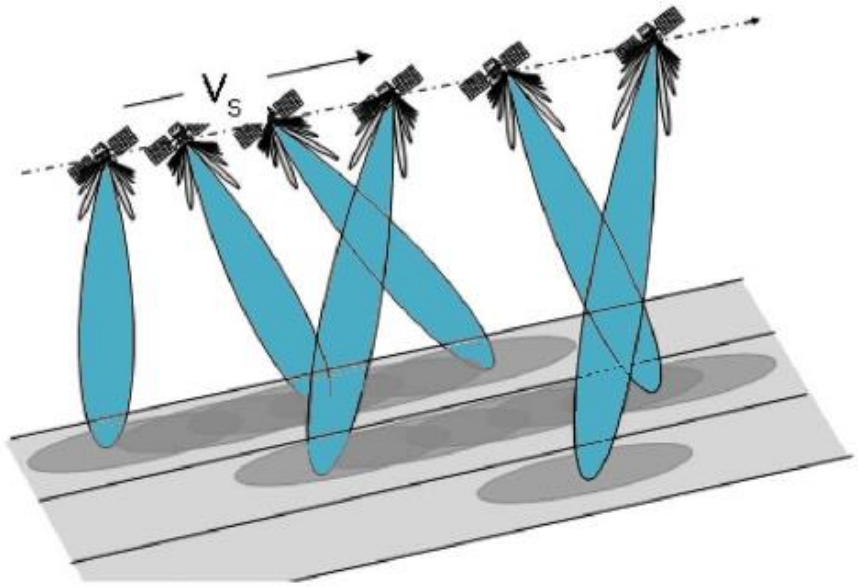

Figure 12 : Mode d'acquisition 'Interferometric Wide Swath' des capteurs Sentinel-1A et B. Ce mode d'acquisition forme une image de taille importante par la modification de l'angle de visée entre chacune des trois parties de l'image finale. Ce mode est appelé TOPSAR (Terrain Observation with Progressive Scans SAR). Le vecteur Vs represente la direction et la vitesse de dépalcement du satellite.

c) Précision

La précision verticale de l'InSAR dépend fortement de la capacité à soustraire l'influence atmosphérique des interférogrammes. En effet, les décalages de phase induits par les différences spatiales dans la composition de l'atmosphère sont une source d'erreur importante. L'utilisation d'un grand nombre d'images SAR et d'un procédé de traitement par série temporelle permet en grande partie d'enlever ses effets, car le signal atmosphérique n'est pas récurant sur une série d'interférogrammes. Le signal lié à la subsidence est quant à lui souvent persistent et/ou récurant sur tous les interférogrammes. La précision finale de l'InSAR dépend également d'autres facteurs, tels que la précision du Modèle Numérique d'Élévation (MNE) utilisé pour enlever la composante topographique de la différence de phase. La précision finale obtenue est de l'ordre de 1cm/an avec les données en Bande L, et peut aller jusqu'à 1mm/an (Rucci et al. 2012) avec les données en bande C ou X ayant une densité temporelle élevée (Sentinel-1, TerraSAR-X). Une manière empirique de quantifier l'erreur de la technique est d'effectuer un traitement interférométrique sur une zone stable et d'observer la variabilité des valeurs de déplacement mesurées (Figure 13). La précision spatiale horizontale dépend du type de traitement et de la résolution des données initiales utilisées. Elle s'étend d'environ 60 m pour des données de type RADARSAT-2 fine interprétées selon la technique SBAS-InSAR à quelques mètres pour des données de type RADARSAT-2 ultrafine interprétées selon la technique PSI en milieu urbain.

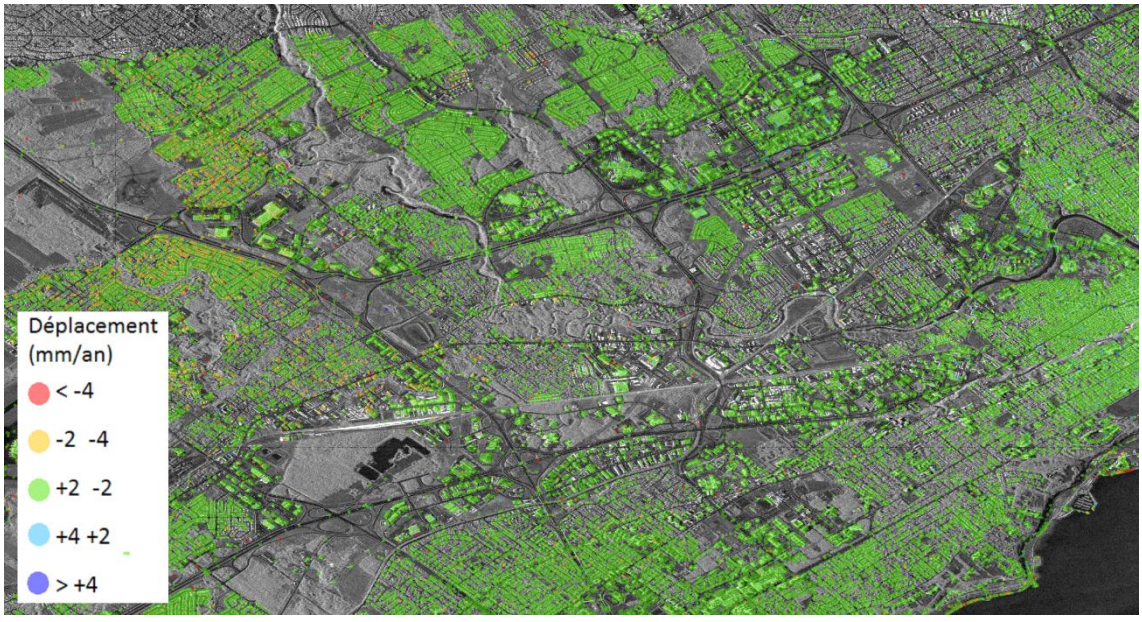

Figure 13 : Traitement par PSI effectué sur 35 images RADARSAT-2 de résolution 'ultrafine' (de l'ordre de 2m) sur une ville canadienne globalement stable. Cet exemple

illustre bien la précision d'une telle série de données, ou la grande majorité des points de réflexion du signal sont stables et montrent des taux de déplacements entre -2 et +2mm/an.

Le seuil de détection système GRACE est de l'ordre de 1 km^3 (Longuevergne et al. 2010, 2013; Scanlon et al. 2012) mais varie largement en fonction des zones adjacentes à l'aire étudiée. La résolution spatiale minimale du système est mal connue, mais Longuevergne et al. (2010, 2013) propose une estimation de la résolution de 'plusieurs centaines de kilomètres'. La résolution spatiale dépend de la stratégie de traitement, telle que mis en évidence au Chapitre 6. L'analyse des données GRACE sur des lacs ayant subi des changements de masse important a pu mettre en évidence la résolution en 'champs de masse' du capteur GRACE (Longuevergne et al. 2013). C'est-à-dire qu'un changement de masse suffisant (de l'ordre de 1 km^3 d'eau par an) sur une zone restreinte peut être détecté si les zones adjacentes ne présentent pas des variations de masses très différentes. Les changements de masse aux environs de la zone auront plus d'influence si la zone est retreinte que si elle est de taille importante.

d) Disponibilité actuelle et future des données

Alors que le premier capteur GRACE est présentement en fin de vie, un deuxième système GRACE permettant d'assurer la continuité des séries temporelles est en préparation. Le système GRACE-2 est également supposé fournir une meilleure résolution spatiale que son prédécesseur. Son lancement est prévu pour 2017. Il semble donc que la continuité des données GRACE est pour l'instant assurée jusqu'aux environs de 2025. La série temporelle totale sera alors de plus de 20 ans. La couverture spatiale des données GRACE est totale, le système offre une vision des changements de masse sur la Terre entière.

Les satellites radar à synthèse d'ouverture (SAR) présentement en opération sont de troisième génération (ALOS-2, Sentinel-1, et bientôt Radarsat-3) et ont été mis en orbite en 2014. Étant donné que ces capteurs orbitaux ont une durée de vie pouvant aller jusqu'à 17 ans (Radarsat-1 a duré 17 ans alors qu'il n'était prévu que pour 5 ans), il est raisonnable de penser que l'acquisition des données des capteurs SAR sont pour le moment garanties jusqu'au environ de 2030. Certains systèmes SAR de quatrième génération sont déjà en préparation, tel le système NiSAR issu de la collaboration entre les agences spatiales américaine (NASA) et indienne (ISRO).

Les limitations des techniques InSAR proviennent de trois facteurs :

1) la disponibilité des données issues de capteurs SAR pour la zone d'étude. La production de séries interférométriques de déplacement nécessite généralement au moins une quinzaine d'images acquises de la même manière à un certain nombre de cycles orbitaux d'écart. L'étude d'un mouvement passé est conditionnée par la présence d'images d'archives de qualité appropriée et en quantité suffisante. Le Tableau 1 présente les caractéristiques des principaux capteurs SAR utilisés pour des applications interférométriques.

2) l'inversion de phases/déplacements pour des déplacements ayant une forte composante non-linéaire. Les techniques utilisant un déroulement de phase spatial, telles que le SBAS-InSAR, sont plus appropriées pour ce genre de mouvement. Seulement, lorsque le mouvement affecte une zone de petite étendue spatiale (de l'ordre de 0 à 20 m de large ; comme c'est souvent le cas pour les effondrements liés à la présence de karsts), le lissage spatial nécessaire à l'interprétation de la différence de phase peut rendre le signal de déplacement indécelable.

3) la présence de végétation sur la zone d'étude. Les variations de valeurs de phase sont alors affectées par la dispersion du signal engendrée par le feuillage. L'utilisation de longueurs d'ondes plus grandes (Bande L) permet, dans une certaine mesure, de diminuer cet impact.

Tableau 1 : Caractéristiques et accessibilités des données des principales données SAR existantes (ASE : Agence Spatiale Européenne; ASC : Agence Spatiale Canadienne ; ASF : Alaskan Sattellite Facility ; DLR : German Aerospace Center).

Capteur	Longueur d'onde	Période d'opération	Duré des cycles orbitaux	Accessibilité des données
ERS-1	C	1991-2000	35 jours	Disponible sur demande à l'ASE
ERS-2	C	1995-2011	35 jours	Disponible sur demande à l'ASE
RADARSAT-1	C	1998-2012	24 jours	Sur proposition à l'ASC
ENVISAT	C	2003-2010	35 jours	Disponible sur demande à l'ASE
ALOS-1	L	2007-2011	46 jours	Disponibles facilement sur le portail Vertex de l'ASF
TERRASAR-X	X	2007 - présent	11 jours	Sur proposition à DLR

RADARSAT-2	C	2008 - présent	24 jours	Sur proposition à l'ASC
ALOS 2	L	2014 -présent	14 jours	Restreinte pour le moment
SENTINEL-1	C	2014 - présent	12 ou 6 jours	Accès libre (ASE)

1.5. SYNTHÈSE DES CONTRIBUTIONS

Les chapitres suivants de cette thèse présentent les principales avancées scientifiques présentées sous forme d'articles scientifiques publiés ou soumis à des revues scientifiques. Cette section en présente une synthèse des principales avancées, qui peuvent être regroupées en quatre catégories:

a) Utilisation de l'InSAR pour détecter et cartographier la surexploitation de l'eau souterraine

Les chapitres 2, 4, 5 et 6 de cette thèse présentent une analyse des données et des méthodes à utiliser pour l'utilisation de l'InSAR pour la détection et la cartographie des aquifères compressibles surexploitées. Des données issues de RADARSAT-2 sont analysées dans le Chapitre 2, où l'étude InSAR ne concerne que les zones urbaines. Cette partie de l'étude a permis, par exemple, de mettre en évidence une diminution significative de la subsidence sur la ville de Querétaro liée à une modification majeure dans la stratégie d'approvisionnement en eau de la ville (Figures 14 et 15). Dans les Chapitres 4 et 6, des données ALOS-1 acquises avec une longueur d'onde radar plus grande permettent une détection de la surexploitation des eaux souterraines de manière globale, dans tous types de couverture au sol. Une méthode d'interpolation est présentée dans les chapitres 4 et 6 pour rendre la couverture de la détection complète à partir de données radar en bande L. Avec de telles données, le seuil de détection est de 1cm/an. Il est possible d'obtenir un seuil de détection plus petit avec les données radar en bande C, permettant la détection du déficit dans les aquifères les moins compressibles, mais il est alors impossible d'obtenir une détection continue dans l'espace, i.e. égale dans tous types de couverture au sol (végétation, constructions etc.). Des perspectives intéressantes apportées par l'arrivée des données des satellites de 3^{ième} génération tels que Sentinel-1 et ALOS-2 sont présentées au Chapitre 5.

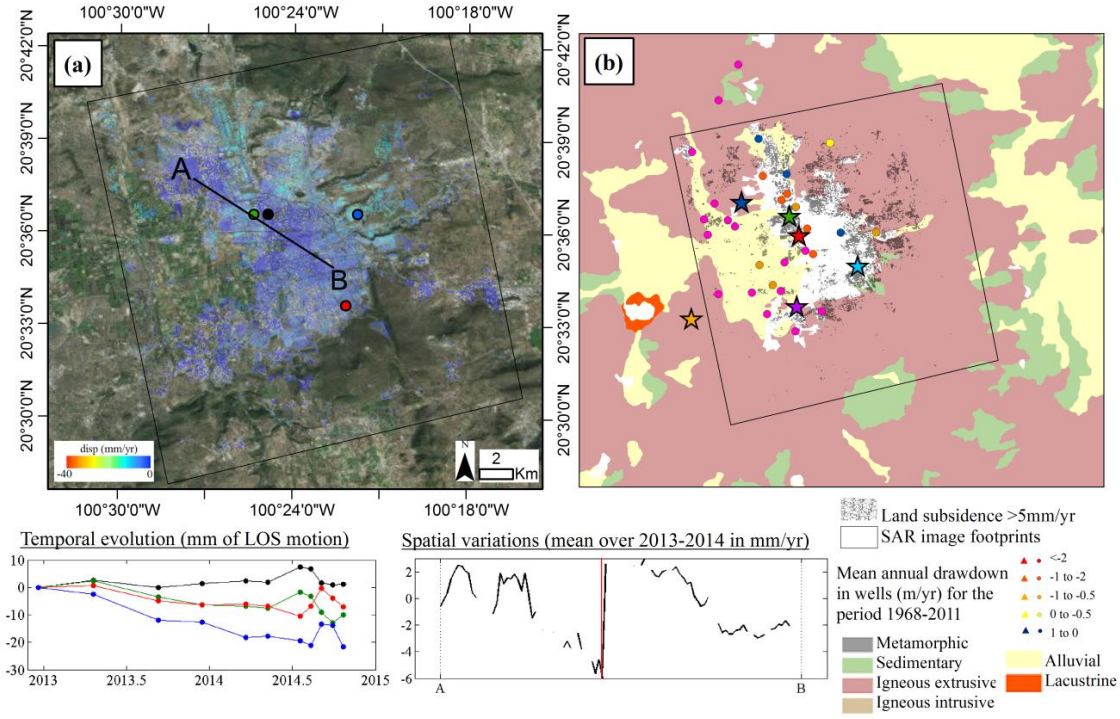

Figure 14 : Subsidence dans la Ville de Querétaro pour la période 2012-2014. Les valeurs mesurées sont environs 5 fois plus petites que celles mesurées à des dates antérieures (Farina et al. 2008; Chaussard et al. 2014). La figure provient de Castellazzi et al. 2016a.

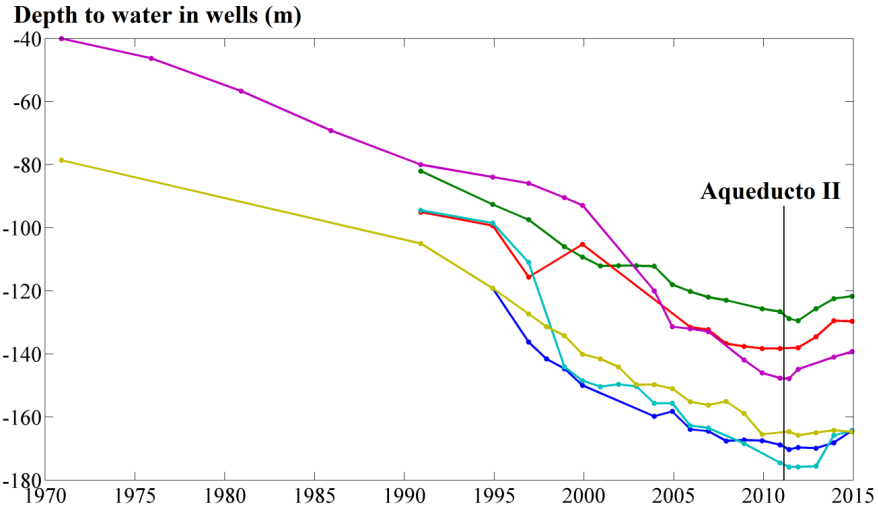

Figure 15 : La diminution de la subsidence pour la ville de Querétaro s'explique par un changement important de la stratégie d'approvisionnement en eau de la ville. Environ la moitié des puits de pompage ont été arrêtés lors du projet 'Aqueducto II', ce qui a permis la stabilisation des niveaux d'eau de l'aquifère et la diminution quasi-totale de la subsidence (Figure 14). La figure provient de Castellazzi et al. 2016a.

b) Utilisation de l'InSAR pour limiter les conséquences de la compaction des aquifères

Le Chapitre 3 présente une application différente de l'InSAR, indépendante des autres applications présentées dans les autres chapitres. Il illustre une application opérationnelle de l'InSAR pour aider la gestion du développement urbain sur les aquifères en compaction. Il présente et compare les résultats de deux types de traitement InSAR sur trois types de données radar, issues d'Envisat, de Radarsat-2, et de Sentinel-1. Des différences dans la qualité des résultats sont mises en évidence et permettent de bien visualiser les progrès des données SAR lors des deux dernières décennies.

L'application principale présentée dans ce Chapitre est un tracé de fractures engendrées par la compaction de l'aquifère de la Vallée de Toluca uniquement par InSAR. Il s'agit de démontrer l'utilisation de l'InSAR comme méthode indépendante permettant de cartographier les fractures engendrées par la compaction d'un aquifère surexploitée (Figure 16 - Castellazzi et al. 2017a). Les résultats permettent d'aider et d'informer les prises de décision en matière d'urbanisme. La méthode consiste à appliquer des traitements additionnels sur les résultats finaux d'une carte de déplacement produite par un calcul InSAR de type PSI. Ce traitement consiste premièrement en une interpolation spatiale, puis un lissage (filtre Gaussien) de la carte de déplacement moyen annuel. Deuxièmement, les gradients horizontaux sont calculés et les fractures sont tracées manuellement. Une validation de terrain effectuée en janvier 2017 a permis de prouver que la technique est efficace sur au moins 2/3 des fractures tracées.

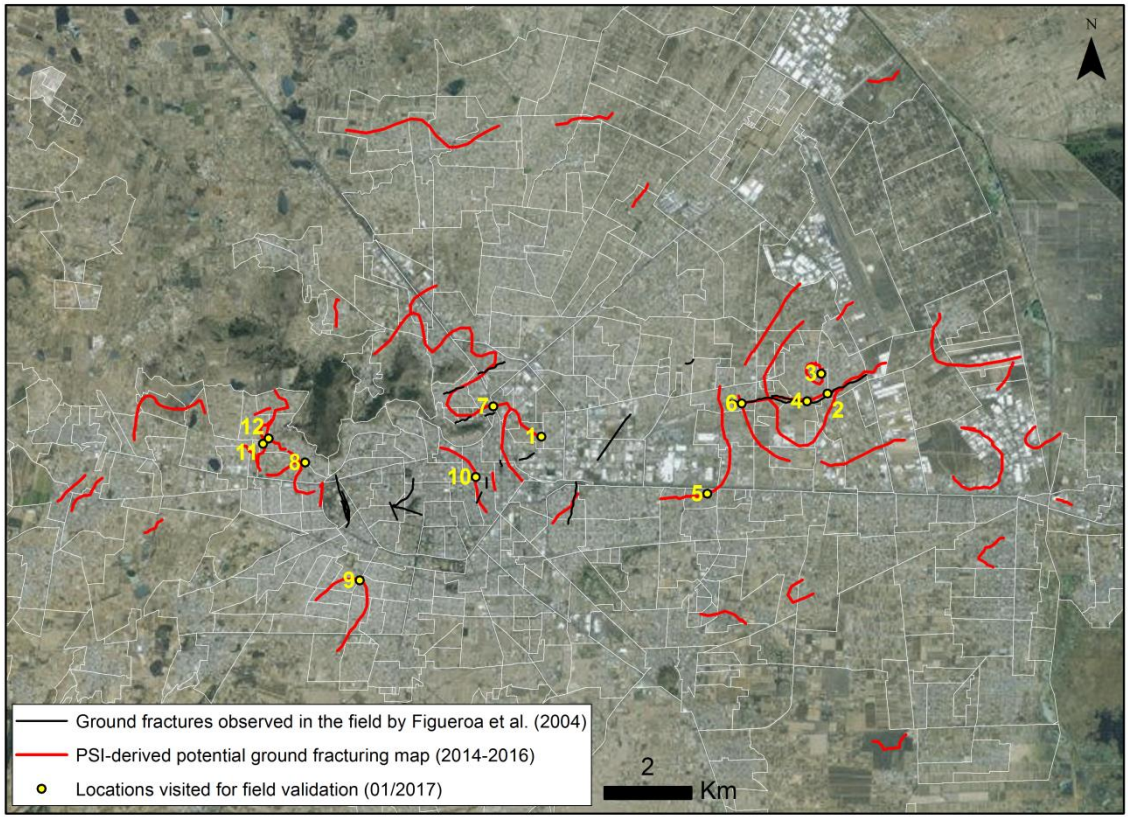

Figure 16 : Carte des fractures sur la Vallée de Toluca dérivé du traitement InSAR d'images Sentinel-1A. Cette figure provient de Castellazzi et al. 2017a (en révision). Les points jaunes montrent les endroits visités sur le terrain pour validation. Des fractures importantes et évidentes ont été repérées sur 2/3 des points environs.

c) Combinaison InSAR/GRACE pour la cartographie quantitative des variations de stockage de l'eau dans les aquifères

Le Chapitre 4 présente les avancées récentes de l'InSAR et des capteurs GRACE dans un article conceptuel rassemblant environ une centaine de références importantes. L'article présente notamment les différents types de traitement InSAR, ainsi qu'une vue d'ensemble sur les données disponibles. Une observation importante concerne l'augmentation notoire de la couverture des données InSAR acquises par les principaux capteurs récents. Alors que les capteurs de 2^{ième} génération tels que Alos-1, Radarsat-2 et Envisat pouvaient obtenir des images de haute résolution sur des étendues limitées de l'ordre de 10-50 km, certains modes d'acquisition des capteurs récents permettent d'acquérir des images sur des étendues allant jusqu'à 120 000 km^2 (Figure 17).

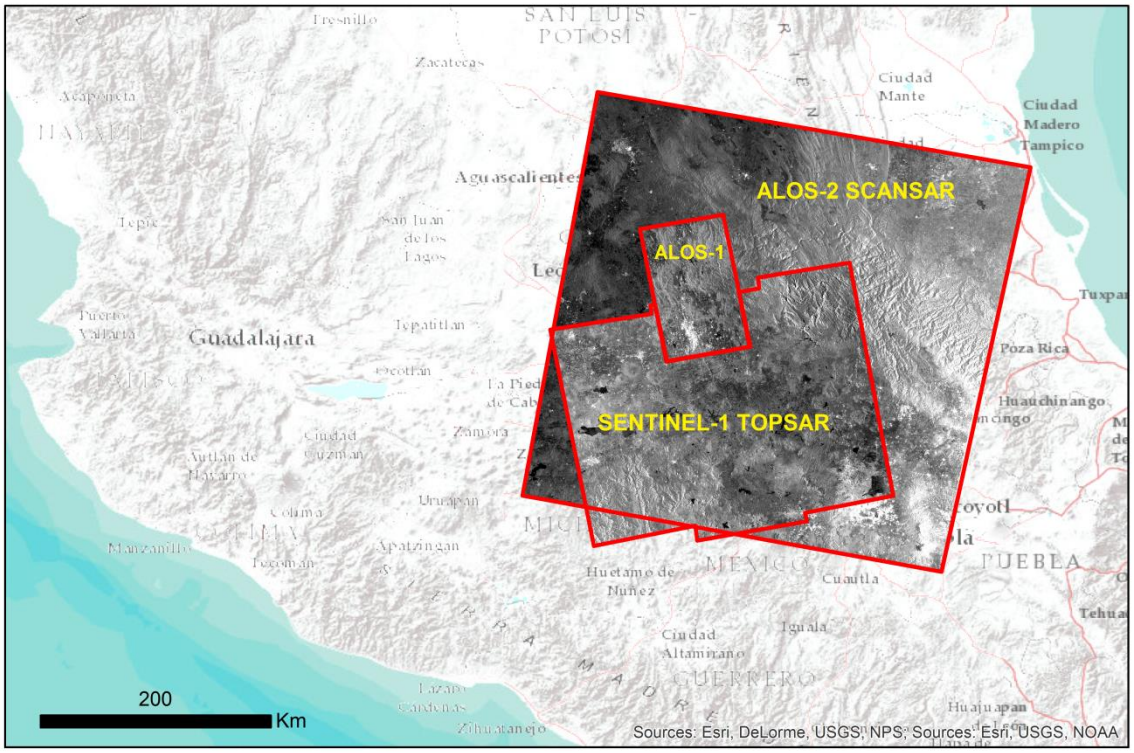

Figure 17 : Différence de couverture entre les images ALOS-1 FBS (représentant une échelle typique de couverture des images SAR issues des 1ères et 2^{ieme} générations des capteurs SAR), les images ALOS-2 ScanSAR, et les images Sentinel-1 TOPSAR. En vue d'une utilisation conjointe avec GRACE, les modes d'acquisition TOPSAR et ScanSAR sont particulièrement intéressants, ils couvrent environ 40 000 et 120 000 km^2, respectivement. L'aire couverte par l'image ALOS-2 ScanSAR est similaire à l'aire minimale d'interprétation des données GRACE.

Les échelles d'étude des capteurs GRACE et InSAR se rapprochant, il est alors possible d'entrevoir des applications conjointes. Le Chapitre 5 propose des pistes de réflexions sur ces applications possibles, ainsi qu'une présentation complète des prochaines avancées prévues pour chaque méthode.

d) Test d'une stratégie de combinaison InSAR/GRACE : inversion par modélisation directe des concentrations de masse

Alors que les idées de combinaisons GRACE/InSAR, leurs potentiels scientifiques, et les défis qui y sont reliés sont développés principalement au Chapitre 5, le Chapitre 6

illustre avec un exemple pratique l'une de ces applications. Dans cette application, il s'agit d'utiliser la cartographie non-quantitative de la surexploitation de l'eau souterraine fournie par l'InSAR pour reconcentrer le signal quantitatif GRACE et en augmenter la résolution (Figure 18). Un protocole d'inversion jointe est utilisé pour concentrer les pertes de masses observées par GRACE sur les zones de déficits en eau souterraine observées par InSAR. Les résultats obtenus sont tout à fait comparables aux budgets en eau des aquifères utilisés pour la gestion de l'eau souterraine au Mexique Central (Figure 18).

La combinaison GRACE/InSAR proposé consiste à tester des valeurs différentes pour chaque MASCON en simulant la manière dont GRACE verrait ces changements de masses. Un algorithme génétique fut utilisé pour trouver la sélection de valeurs de déficit en eau (une pour chaque MASCON), qui après troncature en harmonique sphérique et filtration, permet de mieux reproduire le signal GRACE détecté. L' 'option 1' (Figure 18) conserve la donnée quantitative fournit par l'InSAR, alors que l' 'option 2' n'utilise l'InSAR que pour délimiter les zones de variations de stockage de l'eau souterraine. La première option permet d'obtenir des résultats convaincants (Figure 19).

Alors que les capteurs SAR de dernières générations fournissent des images à la couverture étendue (Figure 17), la disponibilité de ces données n'était pas suffisante au moment de l'étude. Ainsi, un nombre important de données ALOS-1 ont dû être traitées (plus de 700 au total) et ont permis d'offrir une couverture spatiale suffisante pour être utilisées conjointement avec les données GRACE.

Figure 18 (page suivante): Schéma de la combinaison GRACE/InSAR permettant la cartographie à haute résolution des pertes de masses dans les aquifères à une résolution d'environ 25km.

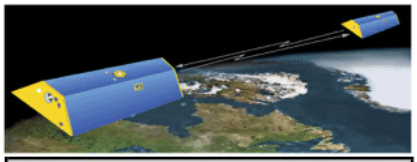

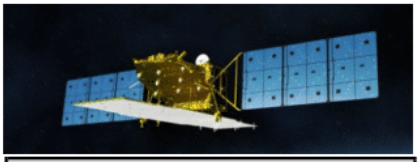

GRACE

L-Band SAR

Traitements jusqu'au 'Niveau 2'

Conversion en WTE

SBAS-InSAR

Carte de subsidence - haute résolution 1

Isolation des mouvements de sol reliés à la compaction des aquifères

Carte de tendance TWS

Carte de subsidence - haute résolution 2

Décomposition du signal (soustraction de SMS, SWS, SIS)

Rééchantillonnage

Carte de tendance GWS

Carte des zones de déficit en eau souterraine à 0.25 deg.

Délimitation des MASCONs (+/- 35 000km^2)

option 1

option 2

une masse par MASCON répartie également sur les zones de subsidence

Optimization itérative par algorythme génétique

une masse par MASCON multipliée par le taux de subsidence de chaque pixel

Modélisation de l'observation des masses synthétiques par GRACE

Modélisation de l'observation des masses synthétiques par GRACE

Calcul du résiduel entre le modèle et la carte de tendance GWS provenant de GRACE

Calcul du résiduel entre le modèle et la carte de tendance GWS provenant de GRACE

Le plus petit résiduel détermine la meilleure combinaison de valeurs

Le plus petit résiduel détermine la meilleure combinaison de valeurs

Carte de déficit des eaux souterraines à la résolution des MASCONs

Carte de déficit des eaux souterraines à une résolution de 0.25 deg.

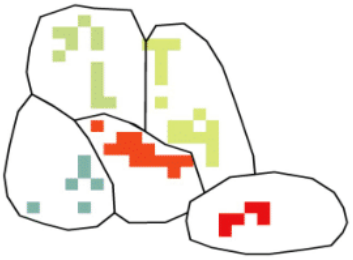

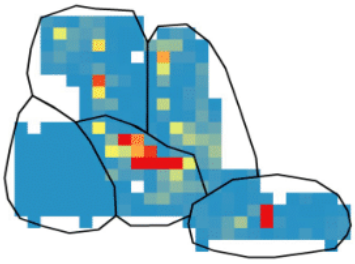

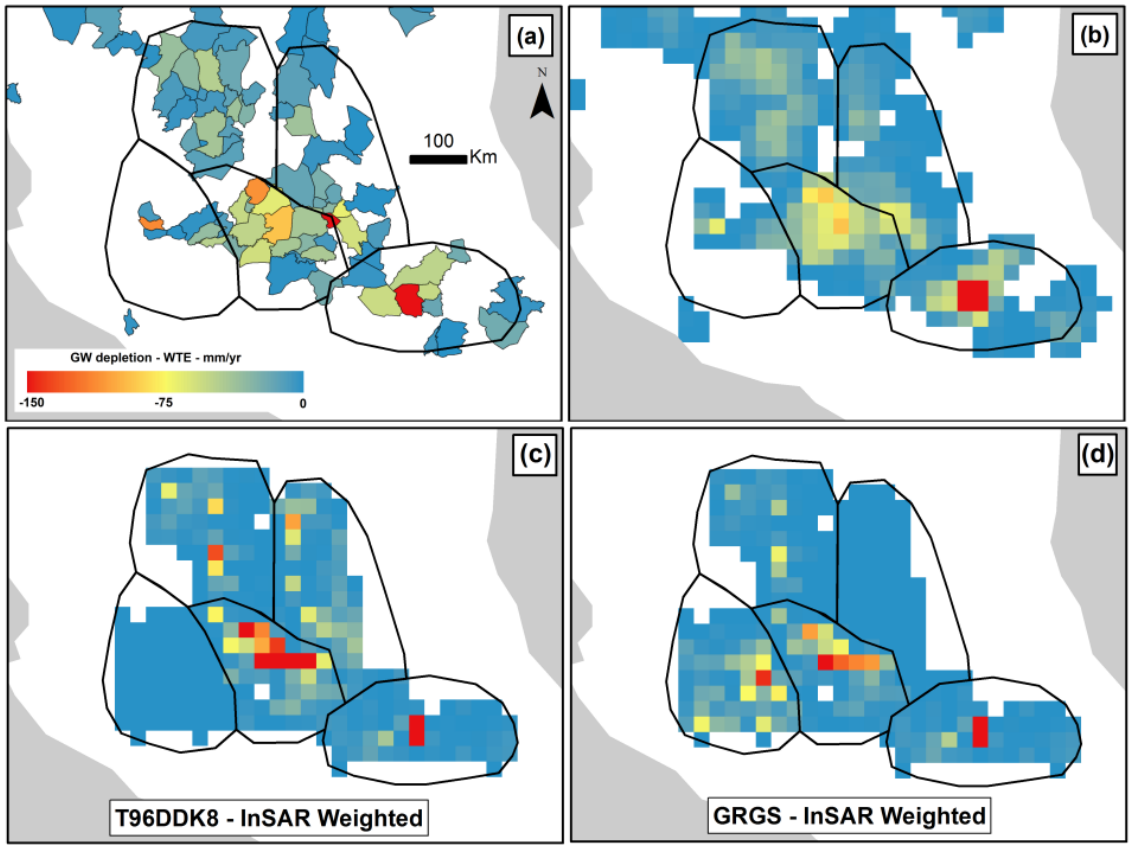

Figure 19 : Principaux résultats de la concentration des masses mesurées par GRACE. Les résultats de l'InSAR ont été utilisés comme a priori spatial de la répartition de ces masses. La carte (a) présente les aquifères en déficit selon le système de gestion de l'eau souterraine au Mexique Central (CONAGUA, 2009a), la carte (b) présente la même carte après conversion à une résolution de 0.25 degré. Les cartes (c) et (d) présentent les résultats du calcul présenté dans la Figure 18 (option 2) en utilisant deux solutions GRACE différentes. Ces cartes de déficit en eau souterraine entièrement produites par géodésie spatiale et sans données de terrain ouvrent des perspectives importantes pour la gestion des aquifères surexploités à travers le monde. Cette figure provient de Castellazzi et al. (2017b – en révision) et est expliquée davantage au Chapitre 6.

1.6. DISCUSSION ET PERSPECTIVE DE DÉVELOPPEMENT

L'InSAR a connu ses débuts à la fin des années 1990 (Massonet et Feigl, 1998), et a dès lors connu un développement très rapide, notamment à partir de l'arrivée des algorithmes de traitement par séries temporelles (Ferretti et al. 2001 ; Berardino et al. 2002). Environ quinze ans plus tard, l'Agence Spatiale Européenne (ASE) dirige la

construction et le lancement des satellites Sentinel-1A et 1B destinés à fournir des données optimisées et gratuites pour des applications scientifiques et commerciales de l'InSAR. La technique a donc subi un essor important et rapide. Elle a permis de fournir des données sans précédent aux domaines des géosciences, ce qui permet de justifier les coûts des plateformes spatiales SAR récentes. En parallèle, les stratégies de traitement se sont diversifiées et les avantages et limitations de chacune des techniques sont maintenant bien compris (Crossetto et al. 2016). Certaines applications en hydrogéologie sont illustrées dans cette thèse. Tels que détaillé dans les trois premiers chapitres, deux types d'applications de l'InSAR sont particulièrement intéressantes en hydrogéologie : la cartographie et la quantification des risques liées aux conséquences de la surexploitation d'aquifères compressibles (subsidence et fracturation des sols - Chapitre 2 et 3), et la détection et la cartographie globale des aquifères compressibles surexploités (Chapitre 4). D'autres applications récentes portent notamment sur l'utilisation de données de compaction pour déduire les paramètres d'emmagasinement des aquifères confinés (Zhang et al. 2016).

Les outils d'exploitation des données SAR et des algorithmes InSAR se développent rapidement. Malheureusement, les logiciels de traitement ayant une interface conviviale telle que SARSCAPE (http://www.sarmap.ch/) ou GAMMA (http://www.gamma-rs.ch/) restent relativement dispendieux pour les équipes de recherche n'étant pas spécialisées dans ces applications. Le traitement de données des dernières générations telles que celles récupérées par Sentinel-1 et ALOS-2 est plus facile que celui des données des générations antérieures. Les trajectoires orbitales sont plus précises (la ligne de base tridimensionnelle est généralement 2 à 5 fois plus petite), ce qui mène à une simplification des corrections de parallaxe à apporter aux interférogrammes (voir Chapitre 3). D'un autre côté, la densité temporelle plus importante (jusque 6 jours pour le système orbital Sentinel-1) permet une soustraction des perturbations atmosphérique précise et efficace. Il est alors facile de prévoir l'arrivée de l'automatisation du traitement InSAR, ou aucune intervention de l'utilisateur ne sera nécessaire pour produire des résultats fiables. Ces améliorations dans le traitement et l'accessibilité des données SAR et de leurs produits de traitement continuent à promouvoir l'expansion de la technique. Elles sont particulièrement profitables aux groupes de recherche axés sur la phénoménologie, ayant une expertise davantage reliée aux phénomènes observés qu'aux méthodes/outils d'observation. On assiste donc présentement aux débuts

opérationnels et commerciaux (voir par exemple : http://tre-altamira.com/) d'une technique ayant bénéficié de 15 ans de développement très intense.

La gravimétrie spatiale est plus récente. Le capteur GRACE qui est la source des données utilisées dans cette thèse, est de première génération. Les premières applications de GRACE se sont concentrées sur les régions montrant une adéquation importante entre la connaissance préalable de la région et la tendance des données GRACE de base (solutions non contraintes de type detripping+T60G300, voir Chapitre 6). Le capteur GRACE a alors bénéficié d'un support important de la communauté scientifique et a été rapidement considéré comme étant utile et globalement efficace.

Néanmoins, faire de GRACE un outil de détection des aquifères en déficit est difficile. GRACE est efficace dans certaines régions étudiées (e.g. Feng et al 2013), mais il ne permet pas pour autant la détection systématique et globale de la surexploitation des aquifères. Ainsi, comme c'est le cas dans cette thèse (Chapitre 4), les observations GRACE ne sont pas forcément en accord avec la connaissance locale sur l'exploitation durable des aquifères (Castellazzi et al. 2016b). Pourtant, dans d'autres aquifères à travers le monde, certaines versions de GRACE peuvent être en accord avec les connaissances préalables d'une région ou d'un aquifère. Il est raisonnable de penser que là où la variance entre les solutions GRACE issues de traitements différents est importante, et en l'absence de lignes directrices sur le choix de la solution à utiliser, GRACE ne peut pas être utilisé comme un outil de gestion. La technique ne peut alors en aucun cas être considérée comme un outil global de détection de la surexploitation. Dès lors, il est permis de se questionner sur la fiabilité générale du système, y compris dans la quantification des variations de masses d'eau lorsque GRACE est en accord avec la littérature ou les données existantes. En l'absence totale de possibilité de calibrer et valider GRACE pour comprendre complètement les données existantes (par exemple, des données de microgravité terrestre), le système reste à ce jour un outil intéressant à des fins de recherche mais il est incapable de supporter seul la gestion de l'eau souterraine (voir Alley et Konikow, 2016).

De manière générale, les discordances entre les observations GRACE et la connaissance préalable des aquifères peuvent s'expliquer par quatre facteurs. Premièrement, le choix de la solution GRACE est bien souvent à la discrétion des auteurs. Il n'y a actuellement aucun article de référence sur la comparaison des solutions (contraintes ou non)

permettant de trancher quelle solution est la plus efficace à adopter selon le contexte ou la zone étudiée. Une certaine confusion existe donc quant à la stratégie de traitement des données et au choix des solutions. Deuxièmement, la décomposition du signal GRACE pour obtenir une estimation de la tendance de stockage d'eau dans les aquifères se base sur deux hypothèses : les compartiments SMS, SWS et SIS sont les seuls contribuant aux changements de masse convertis en TWS et mesurés par GRACE, et les estimations des compartiments tels que SMS et SIS par des modèles sont fiables. Bien qu'aucune preuve n'existe sur l'influence importante d'autres paramètres, aucun auteur n'a pu prouver que les paramètres considérés rassemblent l'entièreté du signal GRACE. Alors que les effets induits par l'ajustement isostatique sont bien connus (Huang et al. 2012), les effets des séismes ou du transport sédimentaire sur les variations temporelles de la force gravitationnelle sont encore peu connus. Troisièmement, les particularités phénoménologiques liées à la détection des masses d'eau et leur comparaison avec d'autres méthodes de mesure de la durabilité des stocks d'eau souterraine (par exemple, le bilan en eau, voir Chapitre 4) ne prennent pas en compte l'aspect dynamique des eaux souterraines (Brodehoeft, 2002). Quatrièmement, les différences d'échelles entre les observations GRACE (de l'ordre de 100 000 km^2) et les autres échelles d'étude plus communément considérées (aquifères, régions - de l'ordre de 100 à 10 000 km^2) posent de nombreux défis pour l'interprétation des données GRACE.

L'inversion des données GRACE telle que montrée au Chapitre 6 est prometteuse car elle permet de transférer l'observation gravimétrique des stocks d'eau souterraine à l'échelle de sa gestion opérationnelle. Il est possible d'utiliser l'InSAR comme *a priori* spatial de localisation des changements de masses liés aux eaux souterraines (Chapitre 6). Cependant, en l'absence de connaissances sur la répartition spatiale des autres contributions aux changements de masses (variations des autres compartiments de stockage de l'eau, volcanisme, séisme), il semble difficile d'obtenir une inversion du signal suffisamment fiable pour en faire un outil de gestion des aquifères. L'obtention d'*a priori* spatiaux pour les autres contributions aux changements de masses inclus dans le signal GRACE reste un thème encore peu exploré par la communauté scientifique. Sans la cartographie complète et l'inclusion de toutes les contributions dans les algorithmes d'inversion, les résultats seront systématiquement biaisés par ces contributions non prises en compte. L'exercice d'inversion permet cependant d'aller

plus loin dans l'analyse spatiale des données GRACE qu'en utilisant les méthodes consistant à utiliser une moyenne uniforme sur un bassin versant ou une région.

Les deux techniques GRACE et InSAR sont promises à un avenir intéressant. D'un côté, les applications InSAR de grande échelle ne nécessiteront plus le traitement de très nombreuses (trente ou plus) séries temporelles d'images SAR (voir Chapitre 4 et 5), car les images disponibles actuellement couvrent des superficies plus importantes tout en maintenant la même résolution (jusqu'à 120 000 km^2). D'un autre côté, le principal axe d'amélioration développé pour les prochaines missions GRACE est la résolution spatiale. Par contre, peu d'information sont disponibles quant à l'échelle de cette amélioration. Il est important de noter que la différence dans les échelles d'études considérées par GRACE et InSAR est en train de se résorber ce qui facilitera l'usage combiné des deux techniques.

L'évolution des techniques géodésiques est à suivre avec attention, alors que les avancées rapides des technologies électroniques et informatiques fournissent un axe important d'innovation dans ce secteur. La quantité de données SAR utilisables dans les traitements InSAR a cru de manière très importante avec l'arrivée de la troisième génération de satellite proposant des modes d'imagerie automatisés acquérant des données à l'échelle globale sans qu'elles aient été commandées préalablement (e.g. les données Sentinel-1 Interferometric Wide). Ces données sont utiles dans la mesure ou la communauté scientifique ne peut pas systématiquement localiser et prévoir les futures besoins en images (e.g. il est souvent impossible de prévoir les séismes ou de localiser les catastrophes naturelles à venir). De plus, certains systèmes satellites de troisième génération proposent des séries temporelles avec une fréquence de six jours et produisent donc environ 60 images par série temporelle par année. Considérant que ces images sont de 7 à 12 fois plus pesantes (en capacité de stockage informatique), une série temporelle annuelle complète arrive à des dimensions de données qui sont difficilement traitables avec un ordinateur personnel. Il est donc d'importance cruciale de considérer dorénavant le *cloud computing* plutôt que le travail sur poste pour effectuer des traitements de données SAR à l'échelle d'un bassin versant, d'un pays, et aux échelles où GRACE est typiquement utilisée.

Une avancé intéressante dans l'évolution des capteurs SAR est l'arrivée d'une bande S intermédiaire entre les bandes C et L, telle que promise par le capteur NISAR (NASA-

ISRO Synthetic Aperture Radar). En effet, la bande C est très sensible aux pertes de cohérence en zone végétalisée, limitant ses applications aux milieux urbains. La bande L, telle qu'utilisée aux Chapitre 4 et 6, permet une cartographie globale des mouvements de sols dans presque tous les contextes (sauf dans les zones de haute végétation et les forêts – voir Chapitre 4 et 5), mais son application n'est limitée qu'à la détection de mouvements importants (supérieurs à 1cm/an). La bande S proposée par la future mission NISAR proposera donc un compromis intéressant entre les deux options présentement disponibles.

Peu d'informations précises sont publiées sur les avancées attendues des futures générations des satellites GRACE. Alors qu'une augmentation de la fréquence temporelle ne serait pas utile aux échelles spatiales d'études considérées, l'augmentation des stocks de données et le *cloud computing* ne sont pas à prévoir pour les futures applications. Une augmentation de la résolution est possible, mais il semble impossible, étant donné les limites inhérentes aux principes de mesures GRACE, qu'elle atteigne un ordre de grandeur de plus. L'utilisation des futures capteurs GRACE en tant qu'outil de gestion des eaux souterraines nécessitera toujours des inversions basées sur des *a priori* spatiaux de localisation de masses telles que présentée au Chapitre 6.

L'utilisation des données GRACE est présentement sujette à controverse dans la communauté scientifique. Alors que de nombreuses publications ont vu le jour, les plus populaires où celles ayant le plus d'impact (Rodell et al. 2009 en Inde ; Famiglietti et al. en Californie, et Richey et al. 2015 globalement) ont systématiquement fait l'objet de commentaires et de discussions (Long et al. 2016 en Inde ; Sahoo et al. 2016) concernant la carte globale proposée (Richey et al. 2015). Alley et Konikow (2015) ont proposé un article intéressant tentant d'établir des lignes directrices sur l'utilisation de GRACE pour des applications quantitatives et phénoménologiques reliées à l'eau souterraine. Il semble qu'une majorité de publications sujettes à la controverse est mise en doute par la communauté scientifique en raison de la tendance à développer des applications de GRACE sans mettre en évidence ses limitations.

La philosophie de recherche adoptée pour la thèse est dans la lignée de celle proposée par Alley et Konikow (2015) ou par Scanlon et al. (2012), en se basant sur la phénoménologie des aquifères et les apports de GRACE pour l'étude de celles-ci. La recherche proposée au Chapitre 5 en est le parfait exemple.

La confusion de la communauté scientifique sur la valeur et l'interprétation des données GRACE ralentit à juste titre son intégration comme outil de gestion des eaux souterraines. Néanmoins, les travaux effectués dans cette thèse montrent bien le potentiel d'utilisation de GRACE à ces fins lorsque la localisation des pertes de masses contribuant au signal de GRACE est possible. Il faudra attendre qu'un consensus existe dans les traitements à apporter aux données GRACE (type de solutions, contraintes des solutions, interprétation systématique des pertes de masses, connaissance de tous les paramètres des changements de masses) pour que le système de mesure bénéficie de la confiance générale de la communauté scientifique, ouvrant ainsi la porte aux applications opérationnelles en gestion de l'eau. Cependant, il est nécessaire de noter l'importance du système GRACE pour les sciences hydrologiques. Il s'agit de données sur les masses d'eau, et donc directement transposables en volume. En ce sens, elles sont sans précédents et vont mener à des découvertes majeures en hydrologie. Elles sont d'autant plus intéressantes qu'elles permettront un suivi apolitique des stocks en eau et indépendant des systèmes de gouvernance, en faisant de GRACE un outil particulièrement intéressant pour étudier les ressources transfrontalières actuellement sujettes à de nombreuses préoccupations dans certaines régions du monde.

1.7. CONCLUSION DES TRAVAUX

Cette thèse de doctorat présente les avancées récentes des deux principales techniques géodésiques utilisées pour étudier les variations des stocks d'eau souterraine. Des applications nouvelles y sont proposées, telles que la détection des aquifères compressibles surexploités à l'échelle des basins versant (plus de 100 000 km^2) ou la comparaison des différentes mesures géodésiques avec les systèmes de gestion de l'eau présentement en place. La thèse présente également une application particulièrement intéressante : la combinaison de InSAR et GRACE pour la cartographie quantitative des déficits en eau dans les aquifères (Castellazzi et al. 2016c, 2017b). Cet axe de recherche très prometteur est basé sur une inversion jointe, où l'InSAR sert d'*a priori* spatial pour reconcentrer les variations de masses détectées par GRACE.

Les résultats de la thèse quant aux avancées liées à l'utilisation de l'InSAR (détection des aquifères surexploitées et des fractures) sont très convaincants. Ces résultats sont suffisamment fiables et sont facilement vérifiables sur le terrain. Il est alors clair que l'InSAR a atteint un certain niveau de maturité, tant dans l'obtention et la disponibilité des données initiales que dans les stratégies de traitements disponibles. L'InSAR est un outil particulièrement efficace permettant des applications opérationnelles intéressantes pour, par exemple, la conciliation de l'extraction de l'eau avec un développement urbain durable (Castellazzi et al. 2017). D'un autre côté, l'autre technique géodésique largement exploré dans cette thèse est moins convaincante. En effet, les données GRACE nécessite de nombreuses étapes de traitement pour pouvoir être utilisées en hydrologie ou en hydrogéologie. Plusieurs stratégies de traitement existent et mènent à des résultats et des interprétations parfois différentes. Ainsi, le système de mesure GRACE ne semble pas être d'une maturité suffisante pour être utilisé plus amplement dans la gestion de l'eau. Par contre, des espoirs importants existent, et les applications possibles sont sans précédents en science hydrologique. Il est important de noter que les satellites SAR présentement en opération sont de troisième génération, alors que le capteur GRACE n'est qu'à sa première version. Il est raisonnable de penser, que malgré les limitations inhérentes d'un système de mesure comme GRACE (l'altitude du capteur ne permettant pas, *a priori*, une augmentation significative de la résolution), les avancées liées aux développements des prochains capteurs GRACE favoriseront fortement les applications jointes GRACE/InSAR présentées dans cette thèse.

2. LAND SUBSIDENCE IN MAJOR CITIES OF CENTRAL MEXICO: INTERPRETING INSAR-DERIVED LAND SUBSIDENCE MAPPING WITH HYDROGEOLOGICAL DATA

Pascal Castellazzi

Institut national de la recherche scientifique, Centre Eau, Terre et Environnement, Université du Québec, 490 rue de la Couronne, Québec, QC, Canada, G1K 9A9, Phone : 418 570 3630, Fax : 418 654 2600. Email: pascal.castellazzi@ete.inrs.ca

Norma Arroyo-Domínguez

Universidad Autónoma del Estado de México. Centro Interamericano de Recursos del Agua Carretera Toluca-Atlacomulco, km 14.5. Ciudad Universitaria, C.P.50110, Toluca, Estado de México. Mexico. Phone: 0052 722 296 5550 ext. 106. Email: norarroydo@gmail.com

Richard Martel

Institut national de la recherche scientifique, Centre Eau, Terre et Environnement , Université du Québec, 490 rue de la Couronne, Québec, QC, Canada, G1K 9A9, Phone : 418 654 2683, Fax : 418 654 2600. Email : richard.martel@ete.inrs.ca

Angus Calderhead

Institut national de la recherche scientifique, Centre Eau, Terre et Environnement, Université du Québec, 490 rue de la Couronne, Québec, QC, Canada, G1K 9A9, Email : angus.calderhead@ete.inrs.ca

Jonathan Normand

California Institute of Technology. 1200 E California Blvd, Pasadena, CA 91125, United States. Email: jonathan.normand@gmail.com

Jaime Gárfias

Universidad Autónoma del Estado de México. Centro Interamericano de Recursos del Agua Carretera Toluca-Atlacomulco, km 14.5. Ciudad Universitaria, C.P.50110, Toluca, Estado de México. Mexico. Phone: 0052 722 296 5550 ext. 106. Email: jgarfiass@uaemex.mx

This chapter is published as: Castellazzi et al. (2016), Land subsidence in major cities of Central Mexico: Interpreting InSAR-derived land subsidence mapping with hydrogeological data, Int. J. Appl. Earth Obs. Geoinf. 47, 102-111. http://dx.doi.org/10.1016/j.jag.2015.12.002

Alfonso Rivera

Geological Survey of Canada. Natural Resources Canada. 490, rue de la Couronne. Québec (Quebec) G1K 9A9, Canada. Phone 418 654 2688, Fax: 001 418 654 2615. Email: arivera@canada.ca

Abstract

Significant structural damages to urban infrastructures caused by compaction of over-exploited aquifers are an important problem in Central Mexico. While the case of Mexico City has been well-documented, insight into land subsidence problems in other cities of Central Mexico is still limited. Among the cities concerned, we present and discuss the cases of five of them, located within the Trans-Mexican Volcanic Belt (TMVB): Toluca, Celaya, Aguascalientes, Morelia, and Queretaro. Applying the SBAS-InSAR method to C-Band RADARSAT-2 data, five high resolution ground motion time-series were produced to monitor the spatio-temporal variations of displacements and fracturing from 2012 to 2014. The study presents recent changes of land subsidence rates along with concordant geological and water data. It aims to provide suggestions to mitigate future damages to infrastructure and to assist in groundwater resources management.

Aguascalientes, Celaya, Morelia and Queretaro (respectively in order of decreasing subsidence rates) are typical cases of fault-limited land subsidence of Central Mexico. It occurs as a result of groundwater over-exploitation in lacustrine and alluvial deposits covering highly variable bedrock topography, typical of horst-graben geological settings. Aguascalientes and Toluca show high rates of land subsidence (up to 10 cm/yr), while Celaya and Morelia show lower rates (from 2 to 5 cm/yr). Comparing these results with previous studies, it is inferred that the spatial patterns of land subsidence have changed in the city of Toluca. This change appears to be mainly controlled by the spatial heterogeneity of compressible sediments since no noticeable change occurred in groundwater extraction and related drawdown rates. While land subsidence of up to 8 cm/yr has been reported in the Queretaro Valley before 2011, rates inferior to 1cm/yr are measured in 2013-2014. The subsidence has been almost entirely mitigated by major changes in the water management practices of the city, i.e. a

This chapter is published as: Castellazzi et al. (2016), Land subsidence in major cities of Central Mexico: Interpreting InSAR-derived land subsidence mapping with hydrogeological data, Int. J. Appl. Earth Obs. Geoinf. 47, 102-111. http://dx.doi.org/10.1016/j.jag.2015.12.002

122 km long pipeline bringing surface water from an adjacent state allowed to cease pumping in half of the wells.

Keywords: Land subsidence, InSAR, Central Mexico, groundwater depletion.

2.1. INTRODUCTION

Unsustainable groundwater pumping is seen in several regions of the World (e.g. Wada et al. 2010). Groundwater sustainability is often defined through a water budget approach, as the balance between inputs and outputs of an aquifer system (see e.g. Alley et al. 1999). A negative water balance may imply progressive and negative impacts on the environmental equilibrium and on the communities who rely on these water resources. While the impacts should be limited to what is considered environmentally, economically, and socially acceptable, there are no obvious solutions to this problem. As it occurs globally (e.g. Famiglietti, 2014), there is an urgent need for cost-effective and globally applicable methods to study groundwater depletion and its related impacts.

Typical water budget approaches overlook the dynamic effects of over-pumping, i.e. storage influences the governing parameters regulating inflows and outflows (Bredehoeft, 2002). Integrated flow models can be used to simulate the dynamic effects of overpumping and associated ground deformation, but have historically only been used reliably when calibrated with costly field campaigns. The lack of reliable data hinders the calibration and validation of the much-needed groundwater management models. The need for reliable data is a major challenge in hydrogeology.

Several space-borne remote-sensing techniques can be used to study groundwater overexploitation and its consequences on human settlements without having to rely on extensive field data campaigns, i.e. multispectral, radar and gravimetry, Among these, Synthetic Aperture Radar Interferometry (InSAR, Massonet and Feigl, 1998) has been effective in studying the aquifer reaction to over-pumping (Galloway and Hoffmann, 2007) and its consequence on urban infrastructures (e.g. Bru et al. 2013). InSAR uses the phase history of at least two SAR images acquired with a minimal spatial baseline to retrieve ground displacement along the satellite Line Of Sight (LOS). In the last decade, this technique was subject to major methodological developments (e.g. SBAS-InSAR:

This chapter is published as: Castellazzi et al. (2016), Land subsidence in major cities of Central Mexico: Interpreting InSAR-derived land subsidence mapping with hydrogeological data, Int. J. Appl. Earth Obs. Geoinf. 47, 102-111. http://dx.doi.org/10.1016/j.jag.2015.12.002

Berardino et al. 2002; PS-InSAR: Hooper et al. 2004; and Squee-SAR: Ferretti et al. 2011) and the increasing availability of SAR imagery products. InSAR is particularly efficient to monitor progressive ground movements, making it an appropriate method to study depleting aquifers undergoing overexploitation and land subsidence. However, the inversion of InSAR-derived land subsidence maps into a volume of groundwater storage change is not possible without extensive lithological data and is restricted by the spatial variability of the lithological compressibility.

Aquifer overexploitation implies changes in water levels and pore pressure. The decrease in pore pressure implies an increase in effective stress (Terzaghi, 1925; Biot, 1941). When the aquifer system contains compressible sediments such as clays and silts, an effective stress increase leads to a matrix re-configuration and land subsidence. This phenomenon varies spatially according to sediment compressibility and water pressure change patterns, leading to damages on urban infrastructures. Damages are accentuated in areas where faults and subsidence with high spatial variability occurs. It is essential to identify subsidence patterns and faulting in order to mitigate future damages and adapt groundwater management accordingly. Land subsidence also implies a largely non-recoverable physical change within the aquifer by impacting its capacity to store water for future generations.

The five central Mexican cities in this study match all criteria enumerated by Burbey (2002), who lists conditions favouring the occurrence of pumping-induced ground deformation and faulting: (1) arid to semiarid climate, (2) long-term pumping of groundwater that results in large water-level declines, (3) considerable thickness of accumulated compressible layers, (4) variable distribution of compressible layers, (5) variability in the values of the compression index of the granular material, and (6) existence of discontinuity structures such as pre-pumping faults that allows for stress accumulation.

2.2. OBJECTIVES

In this paper, we apply the SBAS-InSAR technique on high resolution SAR images to provide an up-to-date assessment of land subsidence in five cities of the Trans-Mexican Volcanic Belt. We reveal temporal variations over a two years period with fine spatial details. Using both geological maps and groundwater level variation data, we discuss

This chapter is published as: Castellazzi et al. (2016), Land subsidence in major cities of Central Mexico: Interpreting InSAR-derived land subsidence mapping with hydrogeological data, Int. J. Appl. Earth Obs. Geoinf. 47, 102-111. http://dx.doi.org/10.1016/j.jag.2015.12.002

the governing parameters explaining spatial and temporal variations of subsidence for each city. We provide an analysis of the evolution of land subsidence at a decadal time scale by comparing the results with previous studies. For changes detected, concordant water and geological data assist in identifying the causes. The study aims to contribute to future urban developments and water distribution plans.

2.3. STUDY AREA

The population density of the area and the locations of the five cities are shown on Figure 1. The cities of Toluca, Morelia, Queretaro, Celaya and Aguascalientes (respectively, from South to Nord) rely mainly on groundwater to sustain both industrial and domestic water needs. Additionally, irrigation is used to sustain intensive agricultural activities in the regions of Toluca, Celaya and Aguascalientes (INEGI, 2005). While the highlands of Central Mexico are densely populated and are of major importance in the Mexican economy, precipitation is low, i.e. the cities studied rely on over-exploited groundwater resources (CONAGUA, 2013a; Table 1).

Among the cities within the region facing both aquifer depletion and subsidence, Mexico city has been well documented by InSAR, (e.g. Yan et al. 2012, Osmanoglu et al. 2011; Chaussard et al. 2014b) but the groundwater depletion and induced land subsidence in the other cities is poorly documented. At a larger scale, land subsidence is detected by InSAR in 21 locations of Central Mexico (Chaussard et al. 2014b), but there is still a need for fine-scale mapping to better understand the land subsidence arising from groundwater over-exploitation in Central Mexico and provide guidance for future urban development. Geologically, the cities presented in this study are within the Trans-Mexican Volcanic Belt (TMVB), a 1000 km long Neogene continental volcanic arc (see Ferrari et al. 1994, 2012). In the five cities, the aquifer-systems from which groundwater is pumped are formed by typical layer sequences of extrusive rocks and volcanic deposits (aquifers) separated by alluvial and lacustrine deposits (aquitards). The thickness of confining alluvial and lacustrine deposits and their occurrence between volcaniclastic and basaltic sequences controls the type of aquifer confinement and, consequently, the spatial patterns of aquifer-system compaction in each city.

This chapter is published as: Castellazzi et al. (2016), Land subsidence in major cities of Central Mexico: Interpreting InSAR-derived land subsidence mapping with hydrogeological data, Int. J. Appl. Earth Obs. Geoinf. 47, 102-111. http://dx.doi.org/10.1016/j.jag.2015.12.002

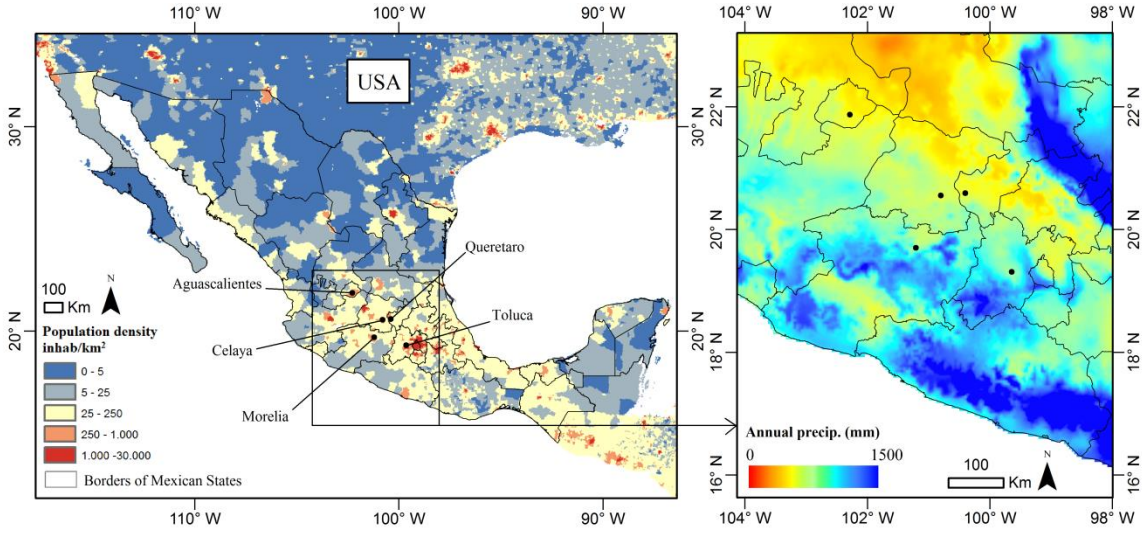

Figure 1: Location, population density (left) and annual precipitation (right) of the five cities in the study.

Table 1: Population, annual precipitation and water balance in the aquifers from which groundwater is extracted for the cities in the study.

City	Population of the metropolitan area[1]	1950-2000 Average Annual precip.(in mm)[2]	Official Aquifer unit[3]	Water balance of the aquifer in MCM/yr [3]	Main Groundwater uses
Toluca	1 936 126	810	Valle de Toluca	-134	City of Toluca City of Mexico Irrigation
Querétaro	1 097 025	565	Valle de Queretaro	-68	City of Queretaro
Aguascalientes	932 369	515	Valle de Aguascalientes	-110	City of Aguascalientes Irrigation
Celaya	602 045	625	Valle de Celaya	-132	Irrigation (~80%) City of Celaya
Morelia	829 625	781	Morelia - Queréndaro	-31	City of Morelia

1. INEGI (2005). Delimitación de las Zonas Metropolitanas de México.
2. WorldClim (2005) - Global Climate Data - http://www.worldclim.org/download
3. CONAGUA (2013a) - Units are in MCM: Million Cubic Meters

This chapter is published as: Castellazzi et al. (2016), Land subsidence in major cities of Central Mexico: Interpreting InSAR-derived land subsidence mapping with hydrogeological data, Int. J. Appl. Earth Obs. Geoinf. 47, 102-111. http://dx.doi.org/10.1016/j.jag.2015.12.002

2.4. MATERIAL AND METHODS

2.4.1. SAR DATASETS AND INSAR PROCESSING

The InSAR time-series relies on 69 RADARSAT-2 images and 14 ENVISAT ASAR images over the five cities, as shown in table 2. RADARSAT-2 images were acquired from December 2012 to December 2014. Their nominal pixel footprint is approximately 1.6 m by 2.8 m (respectively Range x Azimuth) for Ultrafine acquisitions and 5.2 m by 7.7 m for Fine acquisitions (MDA, 2014). ENVISAT ASAR acquisitions were acquired in IMS_1P mode, with a resolution of 8 m by 4 m.

The Small Baseline Subset algorithm (SBAS-InSAR; Berardino et al. 2002) integrated in ENVI through the SARScape module was used to process the images. The SBAS processing method consists in creating all possible interferograms within a temporal and a spatial baseline threshold. These interferograms are integrated in an interconnected network and inverted for the phase change through time relative to the first SAR acquisition. In this study, a total of 332 interferograms were created to build the six land subsidence time-series (Table 2). The mean connection number per image was kept above 5 to assure sufficient redundancy and connection graph density. The topographic phase was removed by using the SRTM Digital Elevation Model with a 30 m by 30 m pixel footprint (Farr et al. 2007) oversampled to 10m x 10m using a bilinear interpolation. The process implies the positioning of reference points with known rates of land subsidence. They were set in agreement with water management agencies recommendations for Celaya and Aguascalientes, and were based on previous studies for Toluca (Calderhead et al. 2010), Morelia (Farina et al. 2008) and Queretaro (Farina et al. 2008). The numbers of looks were selected though trial-and-error, to improve processing speed while preserving spatially variable subsidence patterns. For the city of Celaya, the process is optimized for retrieval of spatial land subsidence patterns by selecting a lower number of looks (i.e keeping a higher resolution at the cost of a lower noise/signal ratio) and by reducing the spatial filtering. Phase unwrapping is performed with a Minimum Cost Flow (MCF) algorithm. The unwrapping coherence threshold was adjusted by trial and error to values ranging from 0.2 to 0.3. The threshold was adjusted to limit unwrapping errors by selecting a useful phase history while still keeping the unity of the area to unwrap. From all the unwrapped interferograms of each time-series, the LOS displacements time-series were retrieved using a linear fitting.

This chapter is published as: Castellazzi et al. (2016), Land subsidence in major cities of Central Mexico: Interpreting InSAR-derived land subsidence mapping with hydrogeological data, Int. J. Appl. Earth Obs. Geoinf. 47, 102-111. http://dx.doi.org/10.1016/j.jag.2015.12.002

Finally, a coherence mask of 0.4 was applied to the final results. Spatial transections are used to identify the spatial variability of land subsidence. Faults with significant (>5 mm/yr) differential movements were identified, and shown as red lines in the transections graphs.

Table 2: SBAS processing parameters of the RADARSAT-2 and ENVISAT time-series (ASC for Ascending, DES for Descending).

City	SAR Mode Path	Number of acquisitions	Time-series Start/End	Median incidence angle	Number of interferograms	Mean connetion per image	Number of looks (Rg/Az)
Toluca	RADARSAT-2 Fine ASC	21	2012-03-08 2014-11-17	19.4	85	8.1	1/3
	ENVISAT ASAR IMS DES	14	2003-03-26 2008-05-28	20.0	39	6	1/3
Querétaro	RADARSAT-2 Ultrafine ASC	11	2013-01-03 2014-11-06	47.8	49	8.9	6/6
Aguascalientes	RADARSAT-2 Ultrafine DES	12	2012-12-18 2014-11-14	29.5	48	8.0	5/5
Celaya	RADARSAT-2 Ultrafine DES	13	2012-12-25 2014-11-21	24.7	53	8.2	2/2
Morelia	RADARSAT-2 Ultrafine DES	12	2012-12-15 2014-11-11	39.3	58	9.6	5/5

2.4.2. GROUNDWATER AND GEOLOGY

Comisión Nacional del Agua (CONAGUA) and *Comisión Estatal de Aguas - Querétaro* provided the data on water resources. The monitoring of water levels performed by CONAGUA consists in annual or semi-annual surveys; which started in 1968 in most states. There are no available datasets to interpret the depth, the confinement, and the extent of the aquifer from which water is pumped, i.e. the hydrogeological characterization and interpretation is limited. Linear regressions are created for each well level history and according to the time period encompassed by the available data. The resulting dataset shows the annual velocity of drawdown for each well for the time period for which data were available. *Instituto Nacional de Estadística y Geografía (INEGI)* provided the geological data used in this study to interpret the causes and origins of the deformation.

This chapter is published as: Castellazzi et al. (2016), Land subsidence in major cities of Central Mexico: Interpreting InSAR-derived land subsidence mapping with hydrogeological data, Int. J. Appl. Earth Obs. Geoinf. 47, 102-111. http://dx.doi.org/10.1016/j.jag.2015.12.002

2.5. RESULTS AND DISCUSSION

2.5.1. WATER EXTRACTION, GEOLOGICAL SETTINGS, LAND SUBSIDENCE MAPPING, AND DETECTION OF RECENTLY ACTIVE FAULTS

a) Toluca

The geological setting of the Toluca Valley is described by Honorio and Hernandez (1982) and Calderhead et al. (2011). The hydrogeological setting of the area is complex (Figure 2b); water is extracted from three main confined basaltic aquifer units, isolated by fine grained alluvial and lacustrine sediments. In the Toluca Valley, water is extracted for municipal and agricultural needs within the Valley, but also to supply 38% of Mexico City's water needs via a network of wells called the *Sistema Lerma*. Groundwater over-exploitation led to progressive changes in hydrodynamic behaviour and hydrochemistry of the aquifer (Rudolph at al., 2006; Del Campo et al. 2014). Drawdown rates in observation wells are highly variable and reflect the hydrogeological complexity of the Valley. Nevertheless, the vast majority of the observation wells show water level drawdowns of ~50 cm/yr (Figure 2b).

This chapter is published as: Castellazzi et al. (2016), Land subsidence in major cities of Central Mexico: Interpreting InSAR-derived land subsidence mapping with hydrogeological data, Int. J. Appl. Earth Obs. Geoinf. 47, 102-111. http://dx.doi.org/10.1016/j.jag.2015.12.002

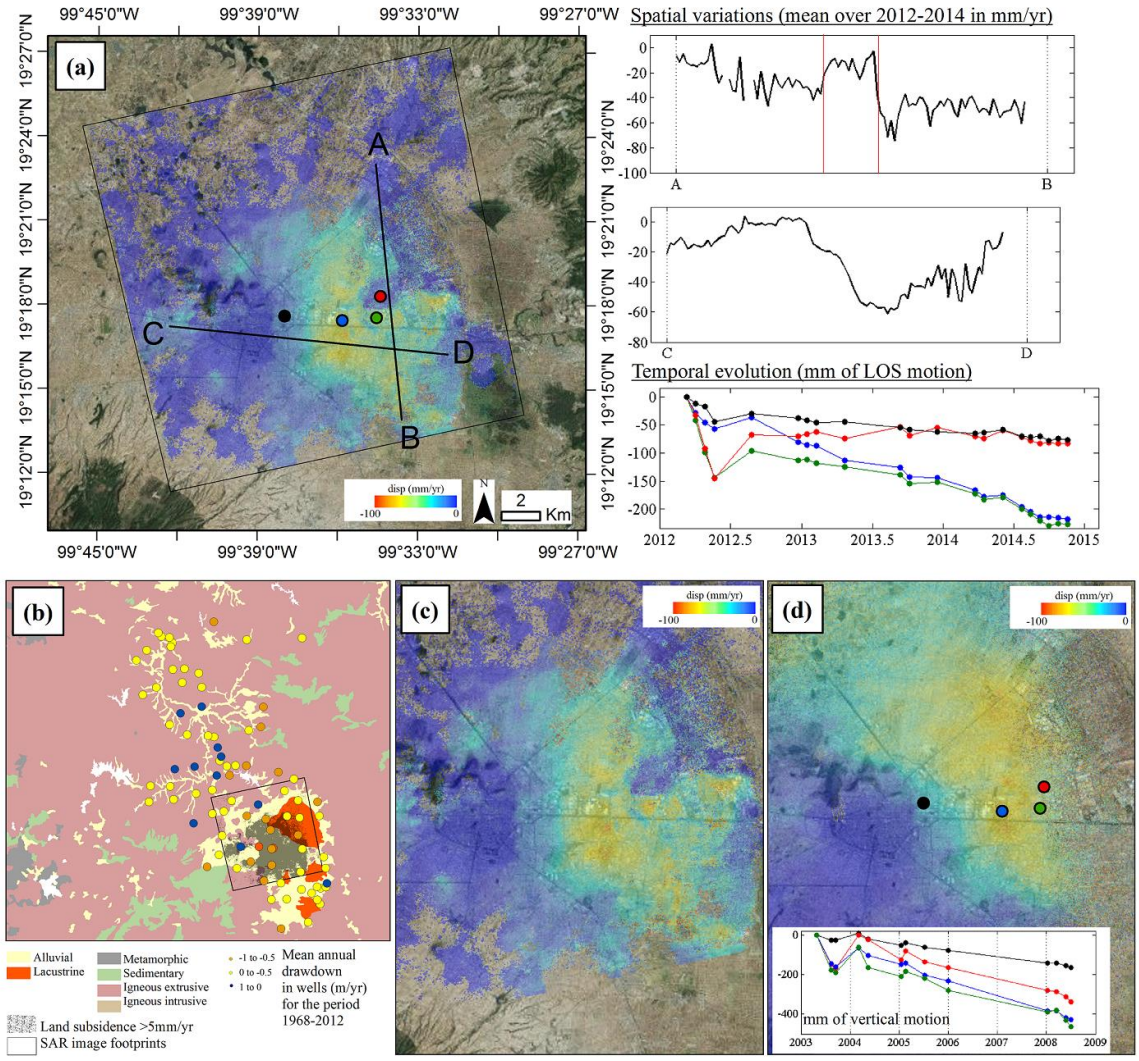

Figure 2: (a) Average annual LOS displacement in Toluca Valley from 2012-03-08 to 2014-11-17 with spatial and temporal variations (graphs, red bar indicates fractures with important differential movement during 2012-2014). (b) Geological map of Toluca Valley and mean annual drawdown rates in wells. (c) and (d) Comparison between annual vertical displacement rates measured in 2012-2014 with RADARSAT-2 n 2003-2008 with ENVISAT. To compare results from RADARSAT-2 (c) and ENVISAT (d), the horizontal motion was assumed to be negligible in the vertical displacements calculation.

The city of Toluca faces important land subsidence with high spatial variability in some areas (sections AB and CD in Figure 2a). Generally, subsidence rates agree well with previous InSAR observations using different SAR time-series (Calderhead et al. 2010;

Chaussard et al. 2014b). When comparing InSAR results from RADARSAT-2 in 2012-2014 and from ENVISAT ASAR in 2003-2008, we observe that the highest subsidence rates occurred further South in recent years (Figure 2c,d), below the Toluca-Mexico highway (beside the blue point of Figure 2d). Although the spatial patterns of land subsidence changed, the maximum subsidence rates observed are similar for both time-periods. No significant changes have occurred in the groundwater extraction policy of the Toluca Valley. Consequently, we suggest that the changes in spatial patterns of land subsidence arise from the spatial heterogeneity of compressible sediment layers, rather than from a change in groundwater drawdown rates. A geological feature controlling compressible sediment thickness is apparent in section AB, and is concordant with fractures observed on the field (red bars on the graph). Stable areas (in blue) are located at either higher elevations or in the city center where there are no compressible sediments (Figure 2a). The city center is mostly built on stable basaltic bedrock. The alluvial and lacustrine sediments occur mostly in the eastern part of the city (section AB). This area experiences subsidence rates of up to 9 cm/yr (Figure 2a). Subsidence rates are generally constant in time; although we are able to identify a coseismic LOS displacement of up to 6cm resulting from the Guerrero–Oaxaca earthquake that occurred on March 20th 2012 (magnitude of 7.4; curves for the red and green dots on Figure 2a).

b) Celaya

The number of extraction wells in the city of Celaya largely increased in the past decades. There were less than 100 wells in 1956, increasing up to 2162 in 1998. While the number of wells is now stable, groundwater extraction keeps increasing with a rising demand for water. The water is extracted from a regional unconfined aquifer (Carranco-Lozada et al. 2013), but the hydrogeology is more complex locally due to discontinuous clayey aquitards (Farina et al. 2008). An important variability is observed in the average drawdown rates in wells, but as the aquifer is to a certain extent homogeneous and regional, this is mainly explained by the fact that only seven groundwater level measurements were considered (Figure 3b). Fault activity vastly controls the sediment thickness and the creation of sedimentary basins. Consequently, the subsidence-induced surficial fractures (Fig.3a) tend to be oriented similarly to the underlying faults. This phenomenon is described as Subsidence-Creep-Fault Process (SCFP, Avila-Olivera et

al. 2008). The city lies on an alluvial and fluvio-lacustrine deposits that settled over the cretaceous basement. The basement topography forms a depressed block bordered by two parallel normal faults, in a Horst-Graben configuration (Graben means 'ditch' or 'trench'). In Celaya, compressible sediment thickness is controlled by a 200 m deep and approximately 300 m wide graben oriented NNW-SSE. (Carranco-Lozada et al. 2013, Farina et al. 2008) controls the orientation of the subsidence-induced fracturing (section AB in Fig 3a).

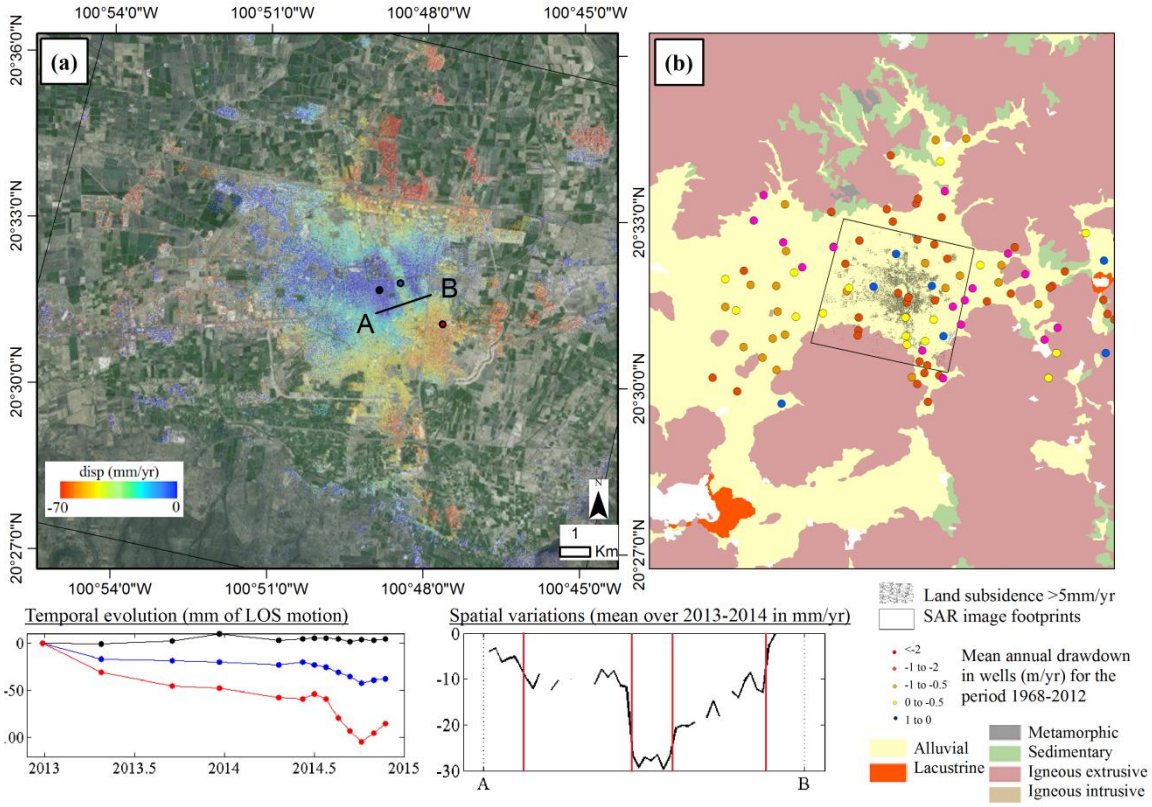

Figure 3: (a) Average annual LOS displacement in the city of Celaya from 2012-12-25 to 2014-11-21, with spatial and temporal variations (graphs below the red bar indicates fractures with important differential movement during 2013-2014). (b) Geological map and mean annual drawdown rates in wells.

The city of Celaya faces land subsidence rates of up to 10 cm/yr with highly variable and distinctive spatial patterns. As described by Carranco-Lozada (2013), six main fractures occur in the city, among which three show important activity during the 2013-2014 periods (section AB – Figure 3). While the depth to water level is over 100 m deep

in most areas, the sediment thickness over the basaltic bedrock is only about 60m on the western side of the graben (black dot) and approximately 250 m inside the graben (blue dot, see detailed explanation in Trujillo-Candelaria, 1985, 1991; Huizar-Alvarez et al. 2011). The results presented herein show good agreement with previous studies (Farina et al. 2008), suggesting that no major change in the spatial and temporal patterns of land subsidence have occurred after 2013. Land subsidence rates are generally constant in time and no elastic motion is measured. However, seasonal variations in land subsidence rates are observed from June to December 2014. Rainy seasons occurring from June to October might temporarily reduce groundwater drawdowns and related aquifer-system compaction (see red dot, Figure 3a).

c) Queretaro

The city of Queretaro is built on a small graben bounded by two nearly-N-S oriented faults. The bedrock is composed of Miocene-Pliocene andesitic lavas and basalts sequences covered by fluvial or lacustrine sediments (Aguirre-Diaz et al. 2005; Farina et al. 2008). Groundwater is extracted from the multi-layered semi-confined aquifer system composed of clay overlying sequences of silts and sands. Up until 2011, the vast majority of observation wells show alarming rates of drawdowns of more than 2 m/yr (Figure 2b).

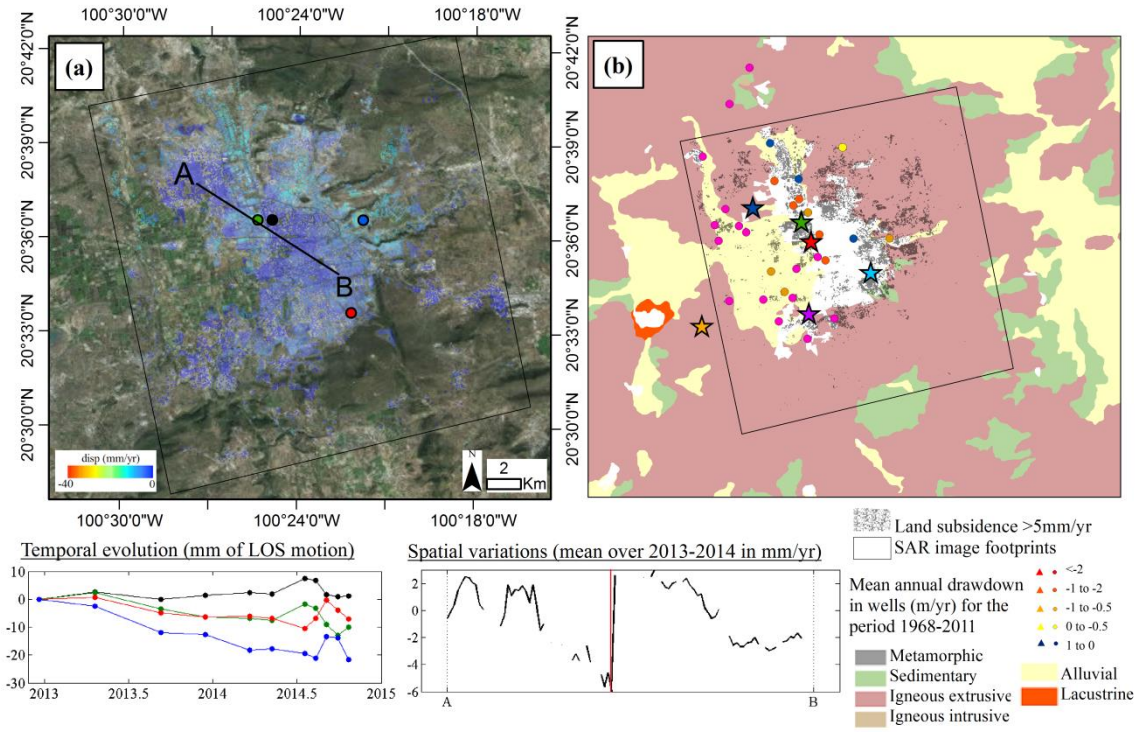

This chapter is published as: Castellazzi et al. (2016), Land subsidence in major cities of Central Mexico: Interpreting InSAR-derived land subsidence mapping with hydrogeological data, Int. J. Appl. Earth Obs. Geoinf. 47, 102-111. http://dx.doi.org/10.1016/j.jag.2015.12.002

Figure 4 (previous page): (a) Average annual LOS displacement in Queretaro Valley from 2013-01-03 to 2014-11-06, with spatial and temporal variations (graphs below). (b) The geological map and mean annual drawdown rates in wells. Stars indicate the location of the wells for which water level time-series are shown on Fig.7. Red bar indicates fractures with important differential movement during 2013-2014.

While previous studies mention subsidence rates from 3 to 8 cm/yr during the time period 2003-2011 in the city of Queretaro (Pacheco et al. 2006; Farina et al. 2008; Chaussard et al. 2014b), only a maximum of 0.6 cm/yr was observed in 2013 and 2014 (Figure 4a). Water extraction in the unconfined aquifer (Pacheco et al. 2006) induced important subsidence rates of up to 8 cm/yr and six fractures in the 2006-2011 time-periods. Almost none of these fractures showed significant differential motion in 2013-2014. Differential movement of up to 6 mm/yr is still observable along the *5 de Febrero* fault (crossed by section AB, green and black dots). Since the aquifer level stabilized as of 2011 by adjusting extraction rates to natural recharge rates (see part 5.2, Fig.7), seasonal patterns of ground level variations related to seasonal groundwater level fluctuations can now be observed. 10 mm of uplift is detected during the rainy season in some areas (Figure 4a - green and black dot), while it is observed two to three months later in others (Figure 4a - red and blue dot). This uplift is generally in phase with the annual peak in groundwater recharge rates and groundwater levels, occurring during and shortly after the rainy season. The response of ground level observed could be delayed (red and blue dot, compared to black and green dot) depending on the distance from groundwater recharge areas and aquifer transmissivity. The time-lag could also be related to changes in the groundwater extraction scheme, but no information is currently available to support this explanation. Note that the SAR images used have a large incidence angle of 47.8^0, implying that the LOS displacement is particularly sensitive to horizontal motion. Nevertheless, it is observed that land subsidence in the Queretaro Valley has significantly decreased in 2013 and 2014.

d) Morelia

Although no water data could be obtained for the city of Morelia, Cigna (2012) provides some information on the extraction of water for the city and explains the poor spatial

correlation between water extraction rates and subsidence by the lithological heterogeneity. Land subsidence in Morelia is largely fault-limited (Figure 5a, sections AB and CD, Cigna et al. 2012). While some of these faults may still be active, the average displacement rates due to paleoseismic activity are at least one order of magnitude smaller than the vertical displacement due to groundwater extraction as reported by Garduño-Monroy et al. (2001) and Cigna et al. (2012). As for the city of Celaya, Morelia's land subsidence is largely driven by SCFP (Avila-Olivera et al, 2008, 2010).

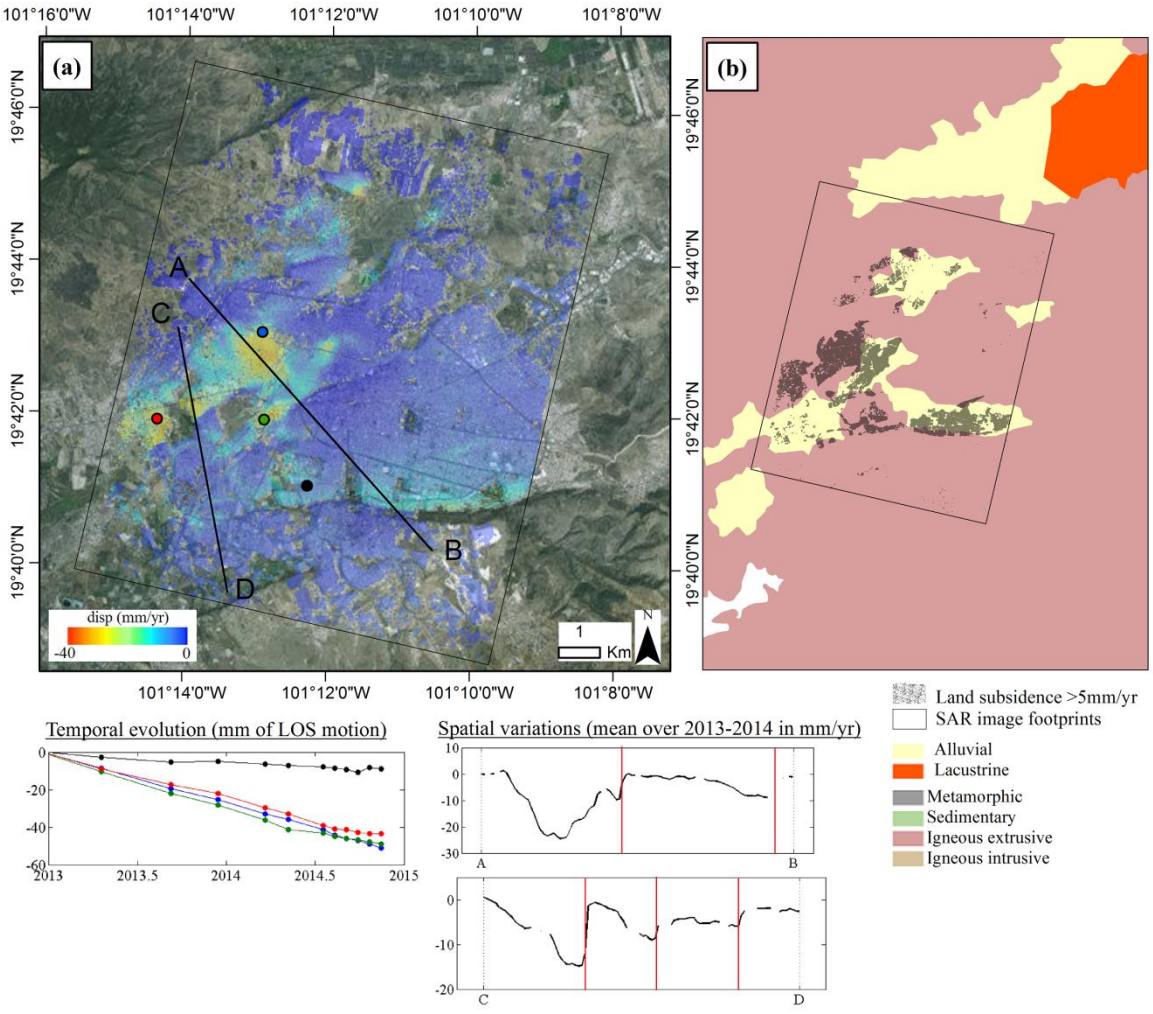

Figure 5: (a) Average annual LOS displacement in the city of Morelia from 2012-12-15 to 2014-11-11, with spatial and temporal variations (graphs below). (b) Geological map and mean annual drawdown rates in wells. Red bar indicates fractures with important differential movement during 2013-2014.

This chapter is published as: Castellazzi et al. (2016), Land subsidence in major cities of Central Mexico: Interpreting InSAR-derived land subsidence mapping with hydrogeological data, Int. J. Appl. Earth Obs. Geoinf. 47, 102-111. http://dx.doi.org/10.1016/j.jag.2015.12.002

The city of Morelia faces land subsidence along a series of East-West oriented fractures. Land subsidence was up to 4 cm/yr and constant throughout the year (Figure 5a). InSAR results show that land subsidence rates are within the temporal variations previously observed by Cigna (2012) during the time-period of 2003 to 2010. During 2013 and 2014, the SBAS-InSAR technique does not detect any important temporal variations of subsidence rates.

e) Aguascalientes

The city of Aguascalientes is located over the Ojocaliente–Aguascalientes–Encarnación aquifer system, a vast unconfined aquifer system encompassing three Mexican states. The city is settled over a tectonic graben delimited at the surface by a topographic depression and bordered by two normal faults oriented N-S. A mix of tertiary and quaternary alluvial and fluvial sediments makes the aquifer system highly heterogeneous (Fig 2a in Pacheco-Martinez et al. 2013; Figure 6b). Pacheco-Martinez et al. (2013) show that water levels are declining faster in the urban area than anywhere else in the Valley. Figure 6a does not show such observation but confirms the drawdown rates given by the same author: almost the totality of the observation wells are declining between 1 and 2 m/yr. Pacheco-Martinez et al. (2013) note that in 2013, 3285 wells were extracting a volume of groundwater equivalent to twice the recharge of the Valley. Ground fracturing has been reported prior to groundwater extraction in the Aguascalientes Valley (Aranda-Gómez, 1989; Pacheco-Martinez et al. 2013), which leads to believe that they have tectonic origins. These fractures are tectonically inactive, but their motion was reactivated by stress related to groundwater pumping (SCFP, section CD on Figure 6a).

This chapter is published as: Castellazzi et al. (2016), Land subsidence in major cities of Central Mexico: Interpreting InSAR-derived land subsidence mapping with hydrogeological data, Int. J. Appl. Earth Obs. Geoinf. 47, 102-111. http://dx.doi.org/10.1016/j.jag.2015.12.002

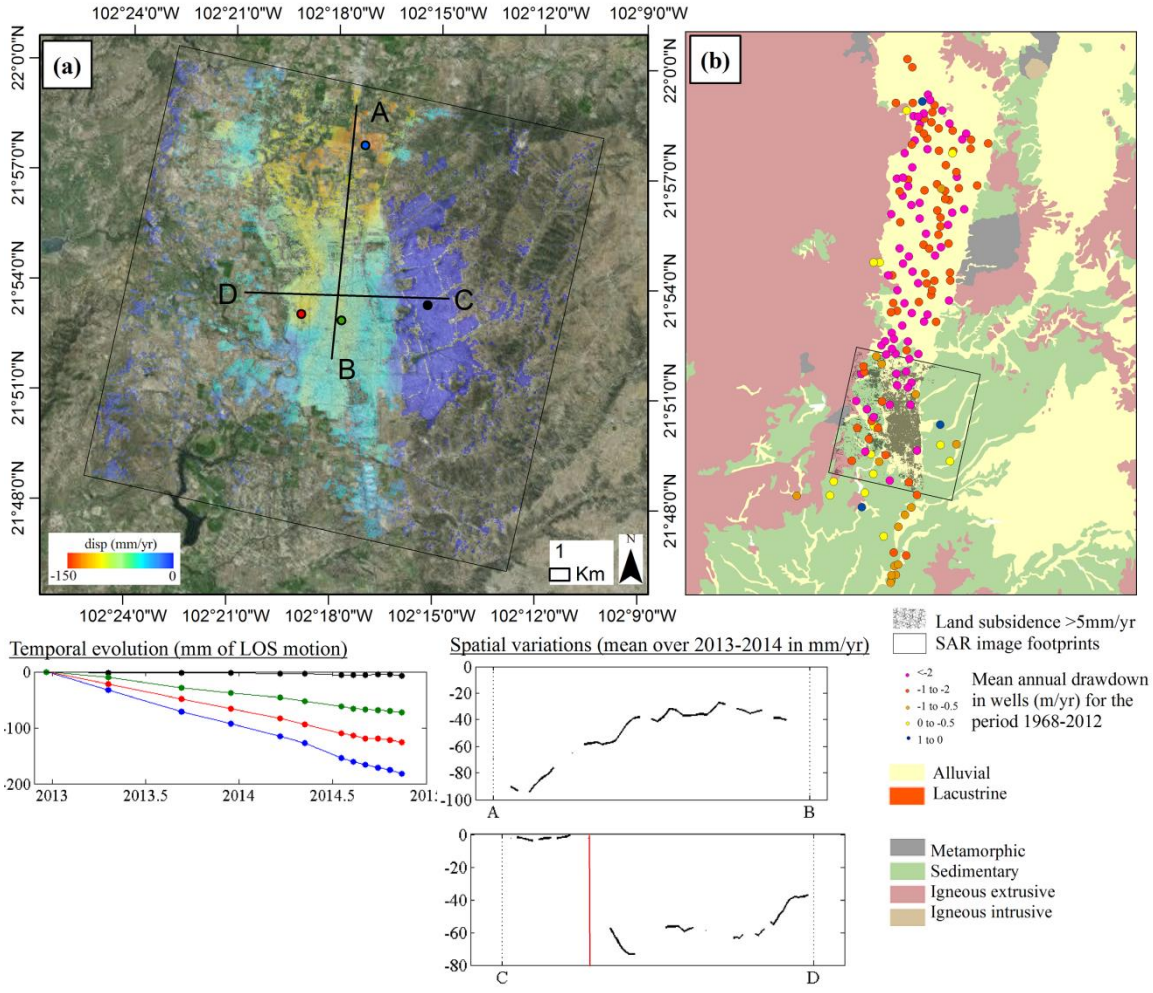

Figure 6: (a) Average annual LOS displacement in the city of Aguascalientes from 2012-12-18 to 2014-11-14, with spatial and temporal variations (graphs below). (b) Geological map and mean annual drawdown rates in wells. The red bar indicates fractures with important differential movement during 2013-2014.

Aguascalientes shows the highest land subsidence rates and spatial variability of the 5 cities studied. Section CD (Figure 6a) is perpendicular to the graben and shows a differential movement up to 8 cm/yr on the eastern border of the graben. Section AB is parallel to the graben orientation and shows that land subsidence rates are gradually increasing from B to A, where it reaches 10 cm/yr (blue dot on Figure 6a). The Aguascalientes Valley manifests alarming rates of drawdowns in pumping wells; most of the wells show drawdowns greater than 1 m/yr (Figure 6b). Thickness of compressible sediment is highly variable and ranges from no compressible sediments in the highest part of the Valley to 400 m thickness of potentially compressible alluvial sediments in the center (Figure 6b, see Pacheco-Martinez et al. 2013 for a more detailed

This chapter is published as: Castellazzi et al. (2016), Land subsidence in major cities of Central Mexico: Interpreting InSAR-derived land subsidence mapping with hydrogeological data, Int. J. Appl. Earth Obs. Geoinf. 47, 102-111. http://dx.doi.org/10.1016/j.jag.2015.12.002

geological description). During 2013 and 2014, the SBAS-InSAR technique does not detect any important temporal variations of subsidence rates.

Table 3: Inter-comparison between InSAR-derived land subsidence mapping in 2012, 2013 and 2014 and previous studies.

City	LOS velocity (cm/yr) in 2013-2014 with RADARSAT-2	Spatial variability of subsidence	Comparison with previous InSAR studies				
			Reference	SAR Sensor	Study time-span	Subsidence rates (cm/yr)	Subsidence Evolution
Toluca	7-9	Patchy and fault-limited	Chaussard et al. 2014b	ALOS PALSAR	2007-2011	5-7	Increase
			Calderhead et al. 2010	RADARSAT-1, ENVISAT ASAR	1995-2008	7-11	Stable
			Davila-Hernandez et al. 2014	ENVISAT ASAR	2003-2010	8	Stable
Querétaro	< 1	Patchy	Farina et al. 2008	ENVISAT ASAR	2003-2005	6-8	Strong decrease
			Chaussard et al. 2014b	ALOS PALSAR	2007-2011	3-5	Strong decrease
Aguascalientes	8-12	Fault-limited	Chaussard et al. 2014b	ALOS PALSAR	2007-2011	5-8	Increase
Celaya	4-6	Fault-limited	Farina et al. 2008	ENVISAT ASAR	2003-2006	2-3	Stable
			Chaussard et al. 2014b	ALOS PALSAR	2007-2011	6-8	Decrease
Morelia	3-4	Fault-limited	Farina et al. 2008	ENVISAT ASAR	2003-2005	1-4	High temporal fluctuations
			Chaussard et al. 2014b	ALOS PALSAR	2007-2011	5-7	
			Cigna et al. 2012	ENVISAT ASAR	2003-2010	7-8	

This chapter is published as: Castellazzi et al. (2016), Land subsidence in major cities of Central Mexico: Interpreting InSAR-derived land subsidence mapping with hydrogeological data, Int. J. Appl. Earth Obs. Geoinf. 47, 102-111. http://dx.doi.org/10.1016/j.jag.2015.12.002

2.5.2. DECADAL SCALE EVOLUTION OF LAND SUBSIDENCE

Results from the InSAR analysis during 2012 to 2014 were compared to previous InSAR studies in order to identify if any major changes occurred on a decadal time scale (Table 3). InSAR observations measured for the same location may vary between authors, who used different SAR satellites or different acquisition modes, because the sensibility to vertical displacement changes according to the SAR acquisitions geometry (i.e. incidence angle). Nevertheless, even if incidence angle are not always provided by authors, the most obvious trends in land subsidence patterns can be inferred.

To provide water for the city of Queretaro, a pipeline was built in 2011 under the name *Proyecto Aqueducto II* (CONAGUA, 2011a) bringing water to the city from Rio Moctezuma, located 122 km away. The project was designed to bring 50 MCM /yr (million cubic meters per year) to the city of Queretaro since 2011, and to cease operation of approximately half of the production wells. The project was effective in reducing drawdowns rates, and increases in water level have been observed in some wells (Fig.7). In 2013 and 2014, we detect low ground motion rates within the range of seasonal ground level variations possibly related to the natural and seasonal water pressures change within the aquifer (Figure 4 red and blue dots). These seasonal fluctuations are around one order of magnitude smaller than the subsidence reported before 2011 (Farina et al. 2008; Chaussard et al. 2014b). This observation suggests that the aquifer has reached a new balance, where ground level follows (with possible delay) the seasonal groundwater level pattern (as measured in 2014, Fig.4a), inducing intermittent subsidence and uplift effects (Fig.4a, black dot). Further studies will help with monitoring the aquifer reaction to such an important change to the water supply scheme.

This chapter is published as: Castellazzi et al. (2016), Land subsidence in major cities of Central Mexico: Interpreting InSAR-derived land subsidence mapping with hydrogeological data, Int. J. Appl. Earth Obs. Geoinf. 47, 102-111. http://dx.doi.org/10.1016/j.jag.2015.12.002

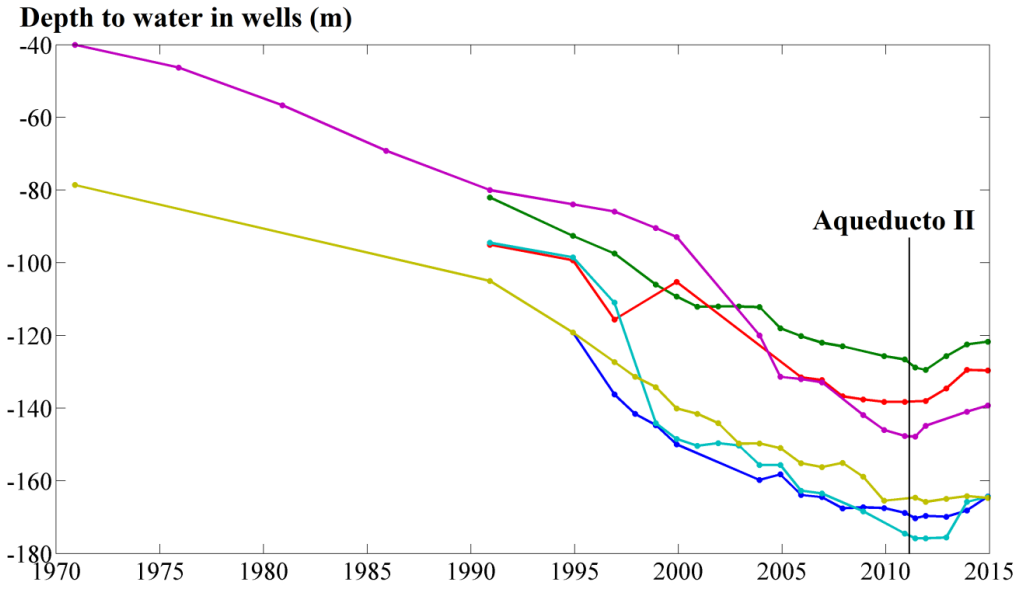

Figure 7: Temporal evolution of depth to water in six wells within the semi-confined aquifer of Queretaro Valley. From 2011, around half of the water supply was assured by importing surface water (Project Aqueducto II). Consequently, groundwater drawdowns and related aquifer compaction were significantly reduced (Figure 4a). Seasonal groundwater level variations cannot be seen on the graph since measurements were taken once per year. Locations of the six wells are drawn on Fig.4b.

2.6. CONCLUSION

Until almost a decade ago, the only well documented case of land subsidence in Mexico was Mexico City. Over the past ten years, increasing accessibility to SAR images has allowed the detection of land subsidence in several other major cities of Central Mexico. In this study, the use of high resolution InSAR time series enables land subsidence mapping with finer spatial resolution and identify active faults. Since the effects of land subsidence on urban infrastructures are accentuated in areas where faults are present, it is essential to identify these faults in order to mitigate future damages and assist in the management of the groundwater resources. In addition, our RADARSAT-2 InSAR results (2012-2014) were compared with results obtained with older SAR acquisitions from ENVISAT ASAR (2003-2009) and with InSAR observations from other authors, allowing us to observe potential changes in land subsidence over a decadal time scale.

This chapter is published as: Castellazzi et al. (2016), Land subsidence in major cities of Central Mexico: Interpreting InSAR-derived land subsidence mapping with hydrogeological data, Int. J. Appl. Earth Obs. Geoinf. 47, 102-111. http://dx.doi.org/10.1016/j.jag.2015.12.002

Based on our results, the cities of Toluca and Aguascalientes are facing important and constant rates of land subsidence of up to 10 cm/yr. Celaya and Morelia are facing lower rates in the order of 4 to 6 cm/yr. The spatial variability of subsidence in the Toluca Valley is mainly controlled by clayey lacustrine deposits imbedded between pyroclastic and basaltic deposits. In Aguascalientes, Queretaro, Celaya and Morelia, the horst-graben configurations explain the high spatial variability of compressible sediment thickness and the groundwater extraction-induced subsidence. As a result, fractures occur with a similar orientation as the normal paleoseismic fault forming the grabens.

While four among the five cities studied showed overall temporally constant land subsidence rates, the subsidence in the Queretaro Valley was almost entirely mitigated by the creation of important surface water imports and transportation infrastructures. Even if the aquifer may have undergone a largely unrecoverable compaction during the past decades, a light uplift should be expected in the next years as the groundwater level slowly recovers. As the aquifer was over-exploited and clays compacted, the aquifer storage decreased. The aquifer porosity and storage loss will largely be unrecoverable. The fault-driven land subsidence seen in Celaya, Morelia, Aguascalientes and parts of Toluca is typical for central Mexican cities with over-pumped aquifers. Ongoing monitoring by radar satellites will assist aquifer managers in making informed decisions on their valued water resources.

2.7. ACKNOWLEDGEMENTS

The authors would like to thank the Ministère des Relations internationales Francophonie et Commerce extérieur du Québec (MRIFCE - Québec) and the Consejo Nacional de Ciencia y Tecnología (CONACyT - Mexico) for their financial supports. We acknowledge Natural Resources Canada and the Canadian Space Agency for their help in obtaining Radarsat-2 acquisitions over Mexico under the MURF #CG0063. The authors also thank José Trujillo-Candelaria and Sergio Murillo for their technical supports.

3. InSAR to support sustainable urbanization over compacting aquifers: the case of Toluca Valley, Mexico

Pascal Castellazzi

PhD. candidate. Institut national de la recherche scientifique, Centre Eau, Terre et Environnement, Université du Québec, 490 rue de la Couronne, Québec, QC, Canada, G1K 9A9, Phone : 418 570 3630, Fax : 418 654 2600. Email: pascal.castellazzi@ete.inrs.ca

Jaime Garfias

Professor. Universidad Autónoma del Estado de México. Centro Interamericano de Recursos del Agua Carretera Toluca-Atlacomulco, km 14.5. Ciudad Universitaria, C.P.50110, Toluca, Estado de México. Mexico. Phone: 0052 722 296 5550 ext. 106. Email: jgarfiass@uaemex.mx

Richard Martel

Professor. Institut national de la recherche scientifique, Centre Eau, Terre et Environnement , Université du Québec, 490 rue de la Couronne, Québec, QC, Canada, G1K 9A9, Phone : 418 654 2683, Fax : 418 654 2600. Email : richard.martel@ete.inrs.ca

Charles Brouard

Computer analyst. Institut national de la recherche scientifique, Centre Eau, Terre et Environnement , Université du Québec, 490 rue de la Couronne, Québec, QC, Canada, G1K 9A9, Phone : 418 654 2683, Fax : 418 654 2600. Email : charles.brouard@gmail.com

Alfonso Rivera

Research scientist. Geological Survey of Canada. Natural Resources Canada. 490, rue de la Couronne. Quebec (Quebec) G1K 9A9, Canada. Phone 418 654 2688, Fax: 001 418 654 2615. Email: alfonso.rivera@canada.ca

This chapter is published as: Castellazzi et al. (2017), InSAR to support sustainable urbanization over compacting aquifers: The case of Toluca Valley, Mexico, Int. J. Appl. Earth Obs. Geoinf. 63, 33-44. https://doi.org/10.1016/j.jag.2017.06.011

Keywords

InSAR; Subsidence; Groundwater depletion; Mexico; Urban development; Ground Fracturing

Abstract

This paper illustrates how InSAR alone can be used to delineate potential ground fractures related to aquifer system compaction. An InSAR-derived ground fracturing map of the Toluca Valley, Mexico, is produced and validated through a field campaign. The results are of great interest to support sustainable urbanization and show that InSAR processing of open-access Synthetic Aperture Radar (SAR) data from the Sentinel-1 satellites can lead to reliable and cost-effective products directly usable by cities to help decision-making.

The Toluca Valley Aquifer (TVA) sustains the water needs of two million inhabitants living within the valley, a growing industry, an intensively irrigated agricultural area, and 38% of the water needs of the megalopolis of Mexico City, located 40 km east of the valley. Ensuring water sustainability, infrastructure integrity, along with supporting the important economic and demographic growth of the region, is a major challenge for water managers and urban developers. This paper presents a long-term analysis of ground fracturing by interpreting 13 years of InSAR-derived ground displacement measurements. Small Baseline Subset (SBAS) and Persistent Scatterer Interferometry (PSI) techniques are applied over three SAR datasets totalling 93 acquisitions from Envisat, Radarsat-2, and Sentinel-1A satellites covering the period from 2003 to 2016.

From 2003 to 2016, groundwater level declines of up to 1.6 m/yr, land subsidence up to 77 mm/yr, and major infrastructure damages are observed. Groundwater level data show highly variable seasonal responses according to their connectivity to recharge areas. However, the trend of groundwater levels consistently range from -0.5 to -1.5 m/yr regardless of the well location and depth. By analysing the horizontal gradients of vertical land subsidence, we provide a potential ground fracture map to assist in future urban development planning in the Toluca Valley.

This chapter is published as: Castellazzi et al. (2017), InSAR to support sustainable urbanization over compacting aquifers: The case of Toluca Valley, Mexico, Int. J. Appl. Earth Obs. Geoinf. 63, 33-44. https://doi.org/10.1016/j.jag.2017.06.011

3.1. INTRODUCTION

Several factors can cause land subsidence: tectonic motion, sediment consolidation, increase in surface loading and geostatic pressure, fluid withdrawal and decrease in hydrostatic pressure, Glacial Isostatic Adjustment (GIA), mining, hydro-chemical erosion of karst, and decomposition of the organic components of soils (see e.g., Yuill et al., 2009). While some of these factors are rarely impacting human settlements due to their low amplitude and/or large spatial extent, others can cause local and regional-scale subsidence with high spatial variability, which impacts infrastructures stability and integrity. The hydrostatic pressure changes occurring when an aquifer is over-pumped can lead to important land subsidence if the aquifer comprises compressible sediment layers. It has been reported in several cities worldwide, the most known cases being Mexico (Osmanoğlu et al., 2011), Venice (Teatini et al., 2005), Las Vegas (Amelung et al., 1999), and Shanghai (Dong et al., 2014). Such phenomena are often described by the poro-elasticity theory, which explains the response of an aquifer matrix to a given hydrostatic pressure change (Terzhagi, 1925, Biot, 1941). The main controlling factors of aquifer compactions are: the amplitude of the hydrostatic pressure change linked to the groundwater overexploitation (which greatly depends on aquifer confinement, see e.g. Castellazzi et al 2016c), the depth of the aquifer, and its compressibility. An overview of such processes and their mathematical representations are provided in Galloway and Burbey (2011).

InSAR is increasingly popular to monitor ground movements. It consists of comparing radar phase backscattering at different times in order to retrieve the phase variations over time and invert them into displacements. Instruments consist of an emitter antenna and a receptor antenna. It can be ground-based (Bozzano et al. 2011), but it is more often deployed on a polar-orbiting satellite. In this configuration, InSAR users are constrained by the design and the orbital characteristics of the satellite. However, a wide variety of resolution, coverage, and acquisition angles (Line Of Sight - LOS) options are now available. The temporal density of any InSAR-based monitoring is limited by the satellite repeat path, which ranges from 45 to 6 days depending on its altitude and orbital configuration. Space-borne InSAR is now routinely used for groundwater studies (Galloway and Hoffman, 2007) and for infrastructure stability monitoring (e.g. Ng et al. 2012). The increasing popularity of time-series InSAR techniques among non-InSAR

This chapter is published as: Castellazzi et al. (2017), InSAR to support sustainable urbanization over compacting aquifers: The case of Toluca Valley, Mexico, Int. J. Appl. Earth Obs. Geoinf. 63, 33-44. https://doi.org/10.1016/j.jag.2017.06.011

specialists demonstrates a certain maturity in InSAR processing research (Crossetto et al. 2016). Up to few years ago, InSAR users had to produce time-consuming and sometimes complicated proposals with space agencies in order to obtain SAR images and perform InSAR processing. SAR archive data from past missions are now often available for free and through user-friendly portals (for example, the Alaskan Satellite Facility portal: https://vertex.daac.asf.alaska.edu). Furthermore, the European Space Agency (ESA) Copernicus program has provided free and high-quality SAR data from Sentinel-1A and 1B satellites since 2014.

Central Mexico faces numerous and important cases of aquifer-system compaction and accompanying ground subsidence related to groundwater depletion. A decade ago, only the case of Mexico City was well documented, but several recent studies documented subsidence in other cities in the region as well. It is now well-known that almost every city in Central Mexico is facing land subsidence issues (Chaussard et al. 2014b; Castellazzi et al. 2016a), among which the most affected are (from South to North): Mexico, Toluca, Queretaro, Celaya, Irapuato, and Aguascalientes. Municipal and industrial groundwater extraction is the main cause of subsidence and ground fracturing in cities. Some municipalities, such as Celaya, Toluca, and Aguascalientes are surrounded by agricultural areas relying on irrigation, which also contributes to groundwater depletion and subsidence. Chaussard et al. (2014b) provide a large-scale overview of the subsidence issues in cities of Central Mexico and describes the controlling factors of its spatial patterns. Castellazzi et al. (2016a) provide a description of the main hydrogeological settings and present the recent (2012-2014) subsidence rates and fracturing patterns for five of these cities. Brunori et al. (2015) present a previously undocumented case study in Ciudad Guzman, Jalisco.

In the Toluca Valley, groundwater stakeholders are trying to reconcile the water needs of its important and ever-growing population with infrastructure integrity and security. This paper compares the growth of both the population and the urban area within the valley, the evolution of the vertical land subsidence patterns and horizontal gradients, and the evolution of groundwater levels from the largest available period of time. Some cities in the region are currently addressing the ground subsidence issue (e.g., Queretaro, see Castellazzi et al., 2016a), hence we present a comprehensive analysis of the current situation for the purpose of comparative monitoring to be used when

This chapter is published as: Castellazzi et al. (2017), InSAR to support sustainable urbanization over compacting aquifers: The case of Toluca Valley, Mexico, Int. J. Appl. Earth Obs. Geoinf. 63, 33-44. https://doi.org/10.1016/j.jag.2017.06.011

appropriate mitigation measures take place. This paper also aims to assess the advantages of the recent open-access Sentinel-1 data for operational use of InSAR to delineate potential ground fractures. Such application is valuable to conciliate groundwater extraction and sustainable urbanization in municipalities extracting water from aquifer-systems prone to differential compaction.

3.2. STUDY AREA

The Toluca Valley is part of the Lerma-Santiago-Pacifico (LSP) water basin. It is located in State of Mexico (Fig. 1) and extends over 2,000 km2. Its shape is rectangular; the east and south boundaries are delimited by topographic heights, while the northwest side is delimited for water management purposes, where the valley opens to a flatter landscape. The Nevado de Toluca volcano (4860 masl) delimits the Valley on the Southwest side and is its most iconic feature. Toluca, the main city, is located approximately at its center and at 2600 masl. The valley is separated from Mexico City by the Sierra Las Cruces mountain range to the east. Because of its proximity to the megalopolis of Mexico City around 40km east, and its privileged position toward with respect to transportation corridors, Toluca has undergone important industrial and demographic growth during the last four decades (Fig. 2). In 2010, it was the fifth largest city in the country with a population of around 0.8 million inhabitants. According to the National Population Council (CONAPO), the population is expected to increase by 30% from 2010 to 2030. The total population living within the Toluca valley is currently close to 2 million.

This chapter is published as: Castellazzi et al. (2017), InSAR to support sustainable urbanization over compacting aquifers: The case of Toluca Valley, Mexico, Int. J. Appl. Earth Obs. Geoinf. 63, 33-44. https://doi.org/10.1016/j.jag.2017.06.011

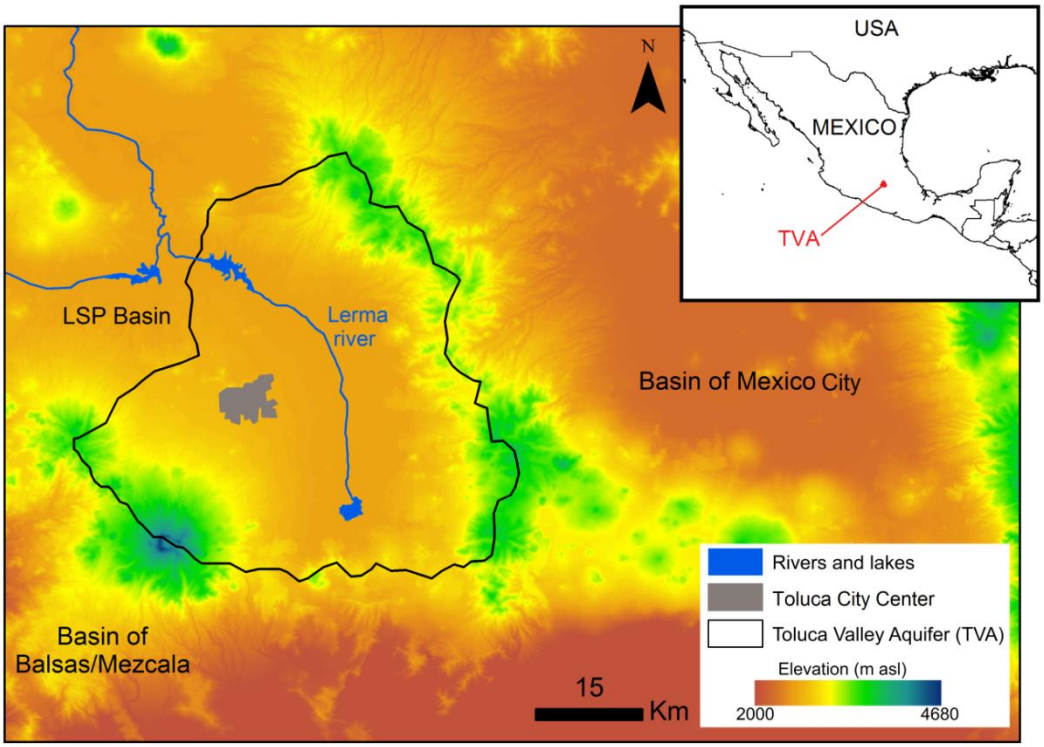

Figure 1: Location and Digital Elevation Model (DEM) of the Toluca Valley (DEM from SRTM Plus v3.0 dataset).

This chapter is published as: Castellazzi et al. (2017), InSAR to support sustainable urbanization over compacting aquifers: The case of Toluca Valley, Mexico, Int. J. Appl. Earth Obs. Geoinf. 63, 33-44. https://doi.org/10.1016/j.jag.2017.06.011

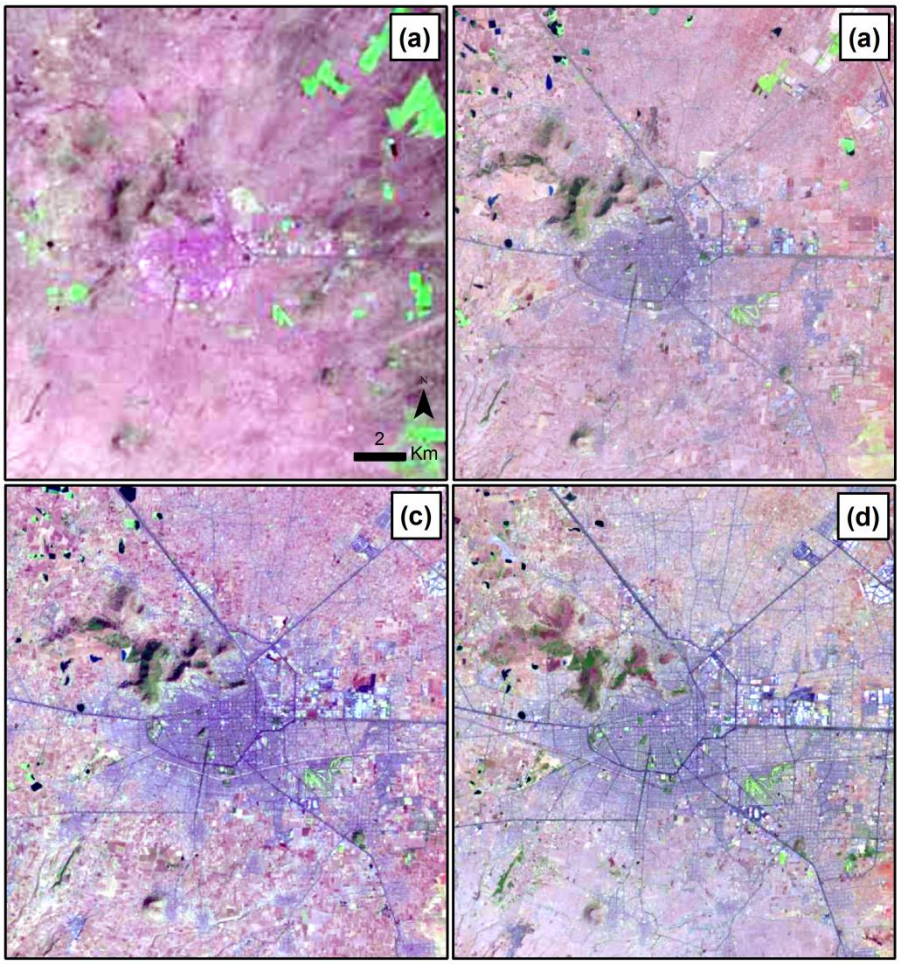

Figure 2: Landsat color-composite images of Toluca from (a) 1973, (b) 1989, (c) 2002, and (d) 2013. The rapid expansion of the city and the development of important transportation corridors are clear. The images are available in the USGS LandsatLook Viewer (https://landsatlook.usgs.gov/). Further information on the growth of Toluca during 1720-2006 is presented in del Campo et al. (2014).

The Toluca Valley Aquifer (TVA) is a complex aquifer-system located within the Trans-Mexican Volcanic Belt (TMVB), a 1000 km long Neogene continental volcanic arc (Ferrari et al., 2012). The TVA basement consists of andesitic rocks, over which lays a complex stratigraphy comprising volcaniclastic and basaltic deposits separated by alluvial and lacustrine sequences. Aquifer-systems are mainly composed of volcanogenic and alluvial deposits, while aquitards are composed of lacustrine clays (Fig. 3). An andesitic volcanic cone is located below the city center, which controls the sediment thickness and limits the land subsidence at this location (Calderhead et al., 2011).

This chapter is published as: Castellazzi et al. (2017), InSAR to support sustainable urbanization over compacting aquifers: The case of Toluca Valley, Mexico, Int. J. Appl. Earth Obs. Geoinf. 63, 33-44. https://doi.org/10.1016/j.jag.2017.06.011

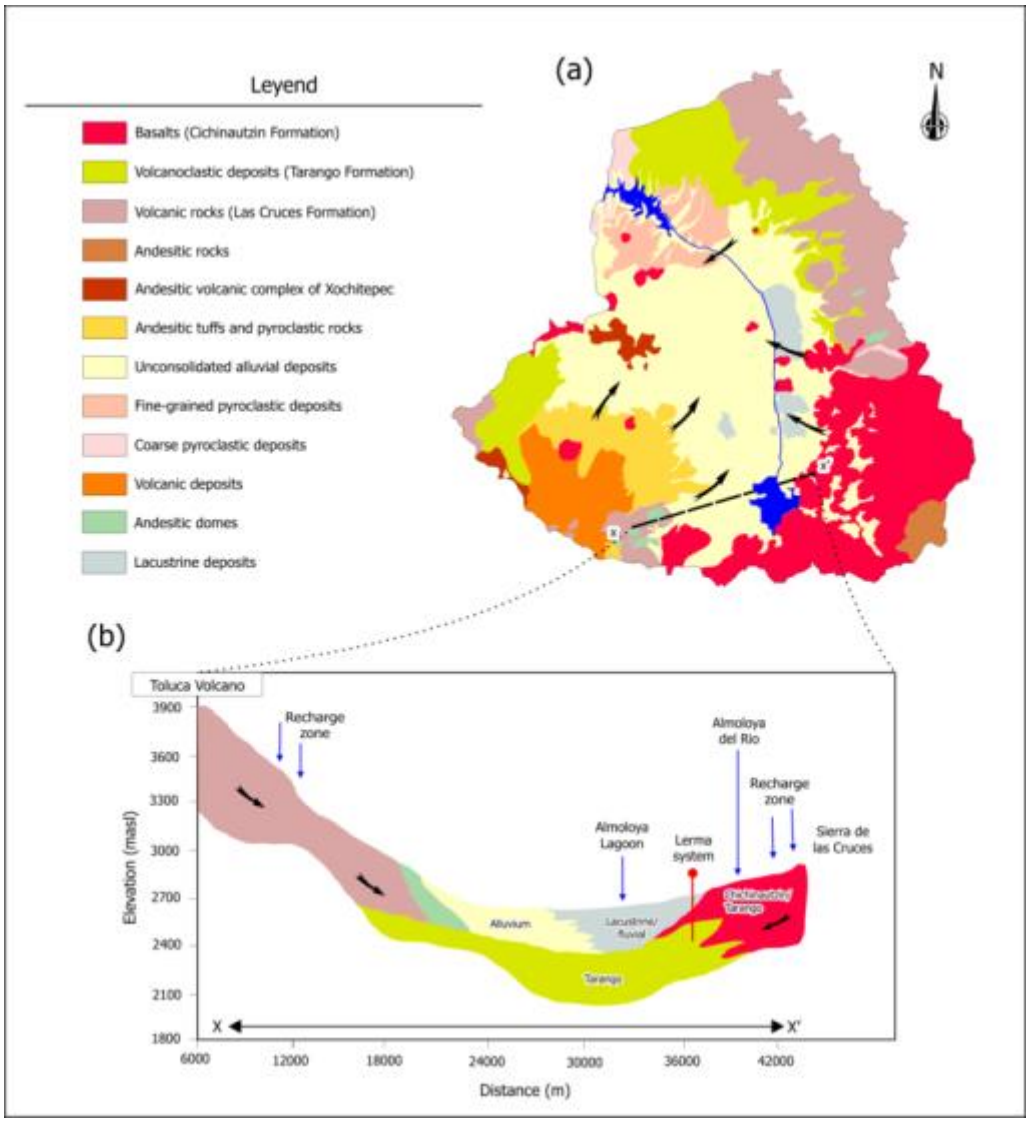

Figure 3: (a) Geological scheme of the Toluca valley aquifer and (b) west-east cross section through the southern Toluca basin from Nevado de Toluca volcano to the foothills of the Sierra de las Cruces mountain range. The arrows represent the direction of groundwater flow (Modified from Hancox et al. 2010 and Calderhead et al. 2012b).

Several studies have focused on the hydrodynamics, hydrochemistry, groundwater depletion, and the related subsidence within the TVA. Esteller and Andreu (2005) and Esteller et al. (2012) provided information on the changes in groundwater chemistry due to groundwater depletion. Rudolph et al. (2006) described the progressive hydrodynamic changes in the valley, which include the gradual extinction of lagoons, springs, and wetlands. Calderhead et al. (2011) provided an insight into groundwater dynamics and related aquifer-system compaction rates by integrating InSAR results and groundwater flow modeling to simulate future compaction rates (Calderhead, 2011,

This chapter is published as: Castellazzi et al. (2017), InSAR to support sustainable urbanization over compacting aquifers: The case of Toluca Valley, Mexico, Int. J. Appl. Earth Obs. Geoinf. 63, 33-44. https://doi.org/10.1016/j.jag.2017.06.011

2012a, 2012b). More recently, Davila-Hernandez (2014) used InSAR to compare hydraulic head losses in observation wells and land subsidence rates. Chaussard et al. (2014) and Castellazzi et al. (2016a) provided an overview of land subsidence problems in several cities of Central Mexico, including Toluca, by using time-series InSAR.

Although the compaction rates within the City of Toluca are well known and mapped, most studies have relied on short time-period monitoring of usually 4 years or less (Chaussard et al., 2014, Castellazzi et al., 2016a). Given the increasing availability of archives from SAR satellites from all three generations of SAR satellites, it is now possible to follow subsidence rates over larger time-series and to provide insight into the decadal-scale evolution of subsidence patterns. Such monitoring is particularly useful as the urban area and the transportation infrastructures are developing at alarming rates (Fig. 2, Mexico Daily News, 2015) and as the groundwater crisis remains unsolved.

3.3. Material and Methods

3.3.1. Groundwater level monitoring

More than 10 water level data loggers (Solinst levellogger model 3001 or equivalent) were placed in monitoring wells in 2007, 2009 and 2012. The disaffected extraction wells in which pressure loggers were installed were chosen according to the recommendations of local water managers. In 2015, the loggers were retrieved and the recorded data were analysed and entered into Matlab 2015a. No information on the stratigraphy of these observations wells are available. As the study focuses on the long term level variations, no barometric corrections are applied.

3.3.2. InSAR data

93 selected subsets of SAR images are used. They are all centered on the city of Toluca and cover from 7 to 15 km of distance in any direction from the city center. The SBAS-InSAR algorithm was applied over 33 Envisat ASAR IMS images, 19 Radarsat-2 Fine images, and 41 Sentinel-1A Interferometric Wide (IW) images covering different time periods (Table 1 - Fig. 4). For all InSAR processing, the topographic component of the

This chapter is published as: Castellazzi et al. (2017), InSAR to support sustainable urbanization over compacting aquifers: The case of Toluca Valley, Mexico, Int. J. Appl. Earth Obs. Geoinf. 63, 33-44. https://doi.org/10.1016/j.jag.2017.06.011

phase variation signal was corrected using a Digital Elevation Model (DEM) with a 30 m resolution (ASTER GDEM Validation Team, 2009).

Table 1: Details of the SAR imagery used in the study. The temporal gap between Envisat ASAR and Radarsat-2 time-series is filled by interpolating linearly the Envisat ASAR results.

Dataset	*Mode*	*Start and end of the time series*		*Number of acquisitions*	*Nominal Resolution (Rg x Az in m)*	*Path*	*Approx. LOS angle (deg)*
Sentinel-1A	*IW1*	*2014-10-08*	*2016-04-12*	*41*	*5 x 20*	*DES*	*27-32*
Radarsat-2	*Fine Quad-Pol*	*2012-05-19*	*2014-10-24*	*19*	*5.2 x 7.6*	*ASC*	*~19*
Envisat ASAR	*IMS*	*2003-03-26*	*2010-10-20*	*33*	*8 x 4*	*DES*	*19-26*

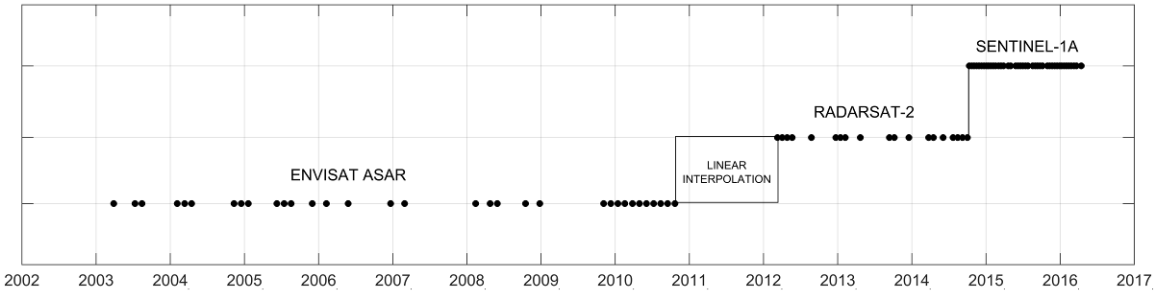

Figure 4: A total of 93 SAR acquisitions from three orbital sensors are used to retrieve ground deformation data over 13 years from 2003-03-26 to 2016-04-12. Sentinel-1A images are available every 12 days and allow subsidence monitoring at a finer temporal resolution.

3.3.3. INSAR PROCESSING

A comprehensive overview of the InSAR processing strategies used in this study and others is given by Crosetto et al. (2016). SAR data are processed using the Small BAseline Subset (SBAS-InSAR) algorithm (Berardino et al., 2002) and a Persistent Scatterers Interferometry (PSI) algorithm (Ferretti et al., 2001), both incorporated into the ENVI platform through the SARSCAPE 5.2 module (http://www.sarmap.ch/). SBAS is used for all three SAR time-series to produce combinable ground subsidence maps with the highest spatial coverage possible, thus highlighting the temporal

evolution of subsidence patterns for the period 2003-2016. The PSI technique is only applied to the Sentinel-1A dataset to produce a gradient map at the highest resolution possible and for the most recent time-period. Its ability to precisely delineate ground fractures related to differential subsidence is tested.

For PSI processing, images are oversampled by a factor of 4 in range and co-registered. Amplitude and coherence criterions are used to select the phase signal linked to high-quality ground targets, called 'Persistent Scatterers' (PS). The phase ambiguity is solved by using a linear temporal inversion algorithm. Thus, displacement/time estimates for phase/time observations at every point are obtained. Only PS points with a coherence value of at least 0.85/1 are taken into account.

For SBAS processing, the SAR images are down-sampled by a factor of 3 to 5 in order to improve the signal/noise ratio, increase the interferometric coherence, speed up the process, and improve the spatial phase unwrapping. All interferograms using SAR images pairs below a certain threshold of temporal and tridimensional (3D distance difference in acquisition geometries) baselines are produced and represented in a 'connection graph'. To assure the robustness of the atmospheric corrections and the final results, connection graphs are visually checked and optimized taking into account that (1) each SAR image is used to produce at least three interferograms and (2) the mean number of interferograms per image is at least 5. The image pairs are co-registered and interferograms are produced, filtered, and unwrapped. Then, a visual check is performed in order to remove the pairs affected by irregular residual fringes, unusual atmospheric effects, or significant unwrapping errors. A coherence mask of 0.2 is applied over the final results. The reference point (assuming no displacement) is taken at the same location for all processing at the center of the city, where urban development induces high interferometric coherence and where no land subsidence occurs (Castellazzi et al., 2016a).

InSAR techniques allow ground displacement measurements along the SAR acquisition geometry, also referred to as LOS angle (Table 1). It is possible to infer the horizontal and vertical ground motion by relating two InSAR results taken with different LOS angle (usually, ascending and descending satellite paths are used). This is particularly interesting for application to fault movements and earthquakes, as determining the motion direction and angle is crucial for characterizing the underlying strains. In the

This chapter is published as: Castellazzi et al. (2017), InSAR to support sustainable urbanization over compacting aquifers: The case of Toluca Valley, Mexico, Int. J. Appl. Earth Obs. Geoinf. 63, 33-44. https://doi.org/10.1016/j.jag.2017.06.011

case of the Toluca Valley, it is assumed throughout the study that, as observed in Mexico City (Chaussard et al. 2014), LOS angle motion detected by InSAR is entirely controlled by the vertical component of ground motion. Consequently, all three SBAS-InSAR LOS-angle time-series are converted into vertical displacement time series considering the horizontal component of displacement as negligible. They are co-registered and linked together in order to produce a continuous time series of vertical displacement. In this perspective, the 2010-10 to 2012-05 temporal gap between the Envisat and Radarsat-2 time-series (Table 1 - Fig. 4) is filled using the mean vertical displacement rate from Envisat time-series (2003/03 to 2010/10). The second link between Radarsat-2 and Sentinel-1A data is done by shortening the Radarsat-2 time-series at the exact date at which the Sentinel-1A time-series starts. Comparisons with well data are performed by averaging the resulting 13-years' time-series over a radius of 100 m around each well.

3.3.4. INFERRING HORIZONTAL GRADIENTS OF VERTICAL GROUND DISPLACEMENTS

Ground ruptures and fracturing can occur as a result of differential subsidence. They potentially causes important damage to urban infrastructures such as buildings, roads, pavement, communication and electricity lines, and water pipes, hence the need to monitor them. This phenomenon occurs mainly where subsidence patterns are spatially variable, as localised differential subsidence induces strain, bending of the surface layer, and ultimately result in tension cracks and fractures (Holzer and Johnson, 1985). In this study, horizontal gradients of vertical subsidence are analysed in order to map areas prone to ground fracturing and thus provide operational support to urban planning.

All gradient calculations are based on the *imgradient* function implemented into Matlab 2015a. For the gradient derived from SBAS-InSAR, areas showing displacement rates of less than 0.5 cm/yr are masked in order to remove gradient values in areas where displacement rates are lower than a realistic SBAS-InSAR detection threshold. The calculation of gradients from the PSI-derived displacement-rate map is done to optimize and keep the gain in resolution linked to such target-based processing strategy. Before the gradient calculation, mean displacement-rate values of the PS points are fit on a 10-m resolution raster, interpolated with a Natural Neighbour algorithm, and a light Gaussian filtering (sigma = 60 m) was applied to reduce the local variance and smooth

This chapter is published as: Castellazzi et al. (2017), InSAR to support sustainable urbanization over compacting aquifers: The case of Toluca Valley, Mexico, Int. J. Appl. Earth Obs. Geoinf. 63, 33-44. https://doi.org/10.1016/j.jag.2017.06.011

out the noise patterns related to isolated unstable targets installed on stable ground. The gradient calculation is then computed similarly to the one derived from the SBAS-InSAR results, and sampled back as points in respect to the initial ground target map to remove the interpolation artifact and to ease interpretation. All gradient results are shown in a 1:100 000 ratio of annual vertical displacement to horizontal distance ratio, in $cm.km^{-1}.yr^{-1}$. The Matlab code used to convert the InSAR-derived displacement data in point-shapefile format into a gradient map in point-shapefile format (see Fig 9) is available upon request to the corresponding author.

3.3.5. FRACTURE DELINEATION AND FIELD VALIDATION

A potential ground fracturing map is created by delineating manually the main features of the horizontal gradient map derived from the PSI vertical displacement map. In order to verify the occurrence of these potential fractures, a field validation survey was conducted in January 2017 to visit several easily accessible locations chosen throughout the study area. Signs of fractures and damages to infrastructures were checked at the vicinity of the delineated features. At several locations, local inhabitants greatly helped in identifying the effects of land subsidence. This field validation step is essential to assess the validity of the final PSI-derived potential ground fracturing map. The final map will be provided to the City of Toluca and to groundwater managers as guidance for urban development planning. It may also be provided to other cities of the region as an example.

3.4. RESULTS AND DISCUSSION

3.4.1. GROUNDWATER DEPLETION AND LAND SUBSIDENCE

The accumulated compaction is as much as 1007 mm for the period of 2003-03-26 to 2016-04-12 (Fig. 5), corresponding to a mean rate of approximately -77 mm/yr. The highest subsidence rates are found on the western side of the urban area, along the industrial corridor located along the Toluca-Mexico highway. Groundwater level vs subsidence time-series are shown in Fig. 6 and Fig. 7, and a compilation of the groundwater drawdowns and subsidence rates, along with the main observation for each well, is provided in Table 2.

This chapter is published as: Castellazzi et al. (2017), InSAR to support sustainable urbanization over compacting aquifers: The case of Toluca Valley, Mexico, Int. J. Appl. Earth Obs. Geoinf. 63, 33-44. https://doi.org/10.1016/j.jag.2017.06.011

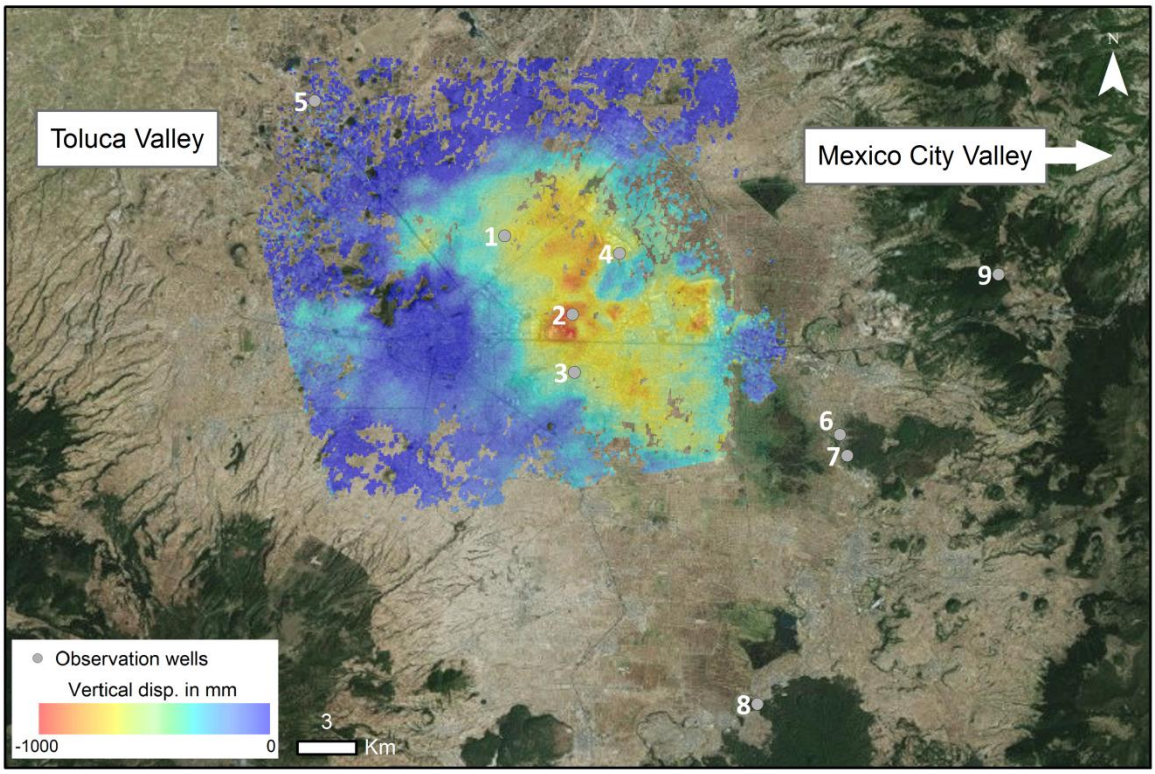

Figure 5: Total vertical subsidence for the period 2003-2016 produced by cumulating InSAR measurements from three SAR sensors. Some areas of the city have undergone 1m of subsidence in 13 years. Temporal variation of the groundwater levels are shown in Fig. 7 and 8 for the monitoring wells 1 to 9.

Wells 1, 2, 3, and 4 are located in highly subsiding areas. Seasonal variations of the water levels vary highly depending on the connections between the screened layer and the recharge zones. However, all of the four wells show negative level trends ranging from -1.12 to -0.28 m/yr. Well 2 and 3 are located in the industrial area, where important groundwater consumers are located. Water level from Well 2 is notably influenced by a pumping well located nearby, and a highly varying groundwater-level recovery and drawdown pattern is observed in relation to the pumping cycles of the extraction well. Important negative level trends can be observed in Well 1, 2, and 4, while level variations in Well 3 show an unexpected recovery from 2012, which could be potentially due to the decommissioning of a nearby pumping well. Well 4 is screened at the same depth as Well 1, and both show similar level trends. However, a noticeable difference in the seasonal cycles suggests

This chapter is published as: Castellazzi et al. (2017), InSAR to support sustainable urbanization over compacting aquifers: The case of Toluca Valley, Mexico, Int. J. Appl. Earth Obs. Geoinf. 63, 33-44. https://doi.org/10.1016/j.jag.2017.06.011

different hydraulic connections to their contributing recharge areas. Well 5 is located downgradient in the groundwater flow system, along the Toluca-Ixtlahuaca transportation axis, and away from the pumping centers. Even if only 2 years of data are available at this well, its shows both a seasonal signal and a strong negative level trend of -0.79 m/yr. This well, located on the lowest altitude of the valley, and along the groundwater discharge area of the TVA and away from all pumping centers provides information about the varying groundwater discharge rates, which are likely impacted by the groundwater extraction upstream.

Wells 6, 7, 8 and 9 are located outside of the InSAR subsidence survey. Well 6, 7 and 9 are located closer to the recharge area of the Sierra Las Cruces mountain range. Well 6 is strongly influenced by a pumping well drilled 20 meters away, and it shows frequent sudden level variations as much as 8m. The influencing pumping well is related to the *Systema Lerma* well system, providing water for exportation to Mexico City. Well 7 and 8 do not show the typical ample temporal patterns expected near a recharge area and are probably poorly connected to it. However, they both show slightly negative trends reflecting the regional scale groundwater depletion occurring within the valley. Well 9, located higher in the mountain range, shows very important amplitude and seasonal recharge patterns as much as 10m typical for a well located in the Sierra Las Cruces, where the recharge rates are the highest of the valley.

Table 2: Mean annual groundwater drawdowns and local land subsidence rates for the 9 monitoring wells showed in Fig. 5. Monitoring wells 6 to 9 are located outside of the InSAR subsidence survey.

Well number (Fig. 6)	GW level trend (m/yr)	Vertical displacement at the well	Observation
1	-0.69	-41	Strong seasonality and trend
2	-1.12	-70	Strong trend, affected by pumping well 20m away
3	-0.28	-43	Surprising reaction after 2012. (decommissioning of a nearby pumping well)

This chapter is published as: Castellazzi et al. (2017), InSAR to support sustainable urbanization over compacting aquifers: The case of Toluca Valley, Mexico, Int. J. Appl. Earth Obs. Geoinf. 63, 33-44. https://doi.org/10.1016/j.jag.2017.06.011

4	-0.66	-45	No seasonality, strong trend
5	-0.79	+2	Located downstream the aquifer Strong seasonality and trend. Displacement is below the detection threshold
6	-1.66	NA	Strong trend, affected by pumping well
7	-0.61	NA	-
8	-0.16	NA	-
9	-0.60	NA	At the recharge area – Large seasonal variations

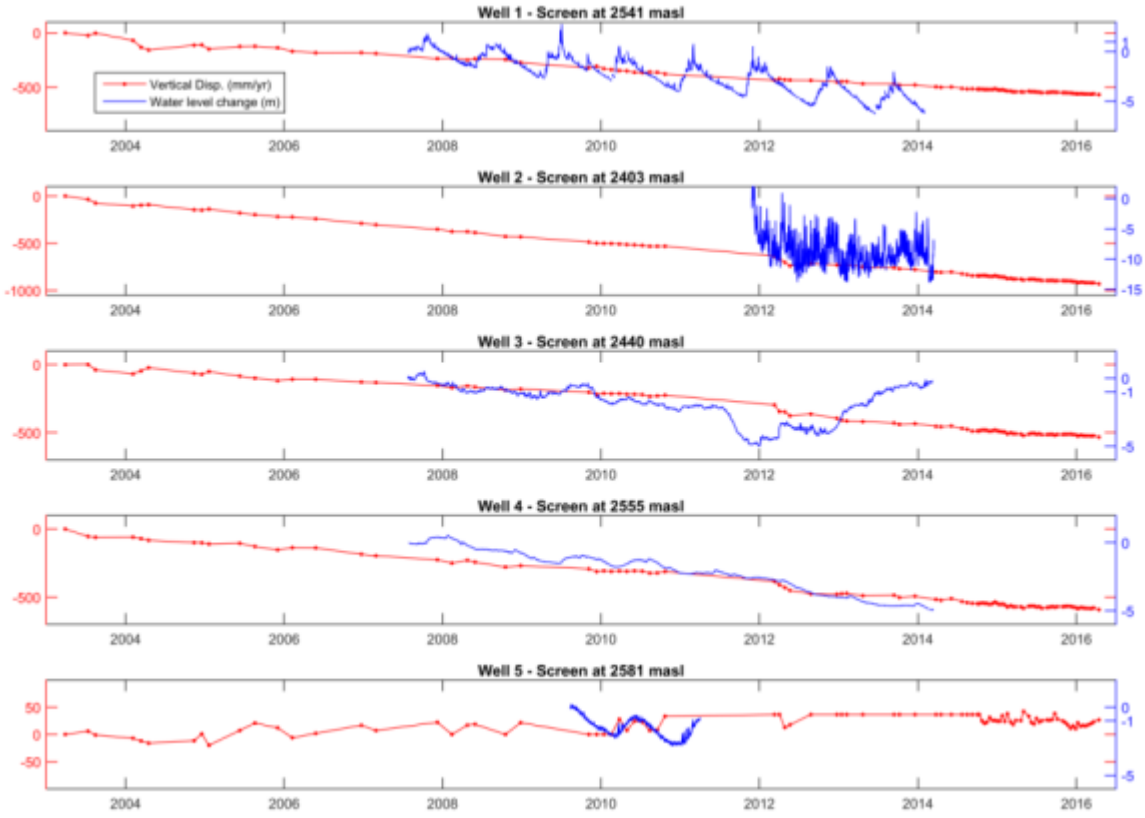

Figure 6: Groundwater level change in monitoring Wells 1 to 5 (Fig. 5) and InSAR-derived vertical subsidence at their vicinity.

This chapter is published as: Castellazzi et al. (2017), InSAR to support sustainable urbanization over compacting aquifers: The case of Toluca Valley, Mexico, Int. J. Appl. Earth Obs. Geoinf. 63, 33-44. https://doi.org/10.1016/j.jag.2017.06.011

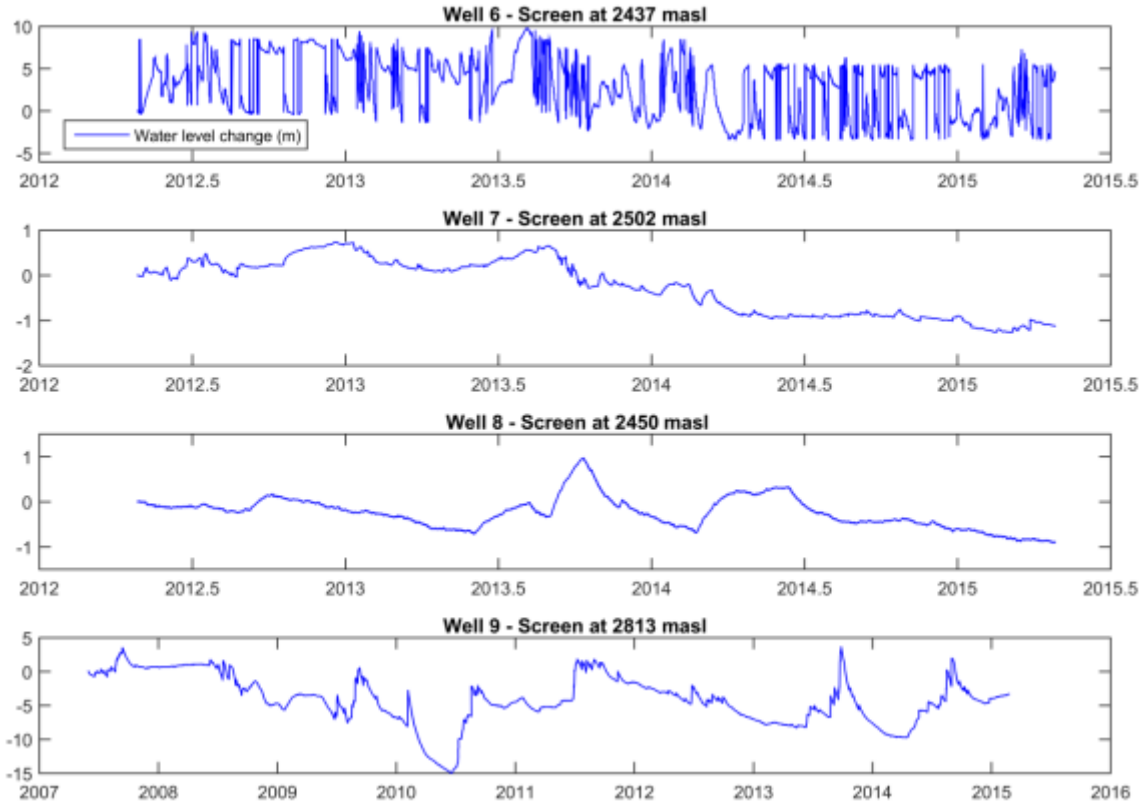

Figure 7: Groundwater level change in monitoring wells 6 to 9 (Fig. 5).

3.4.2. EVOLUTION OF LAND SUBSIDENCE FROM 2003 TO 2016

The three InSAR-derived mean annual vertical displacement maps and the derived gradient maps are shown on Fig. 8: Envisat ASAR for 2003-2010 (Fig.8a/d), Radarsat-2 for 2012-2014 (Fig. 8b/e), and Sentinel-1A for 2014-2016 (Fig. 8c/f). While no significant change in the maximum subsidence rates have occurred, the evolution of its spatial patterns is noticeable. The south-east and south-western sides of the urban area are facing generally increasing land subsidence rates. The latest measurements (Fig. 8, c and f) show that important land subsidence (superior to 50 mm/yr) is spreading to the east, along the Toluca-Mexico axis, and where important transportation infrastructure developments are planned to take place. The subsidence is also spreading to the west, which now shows rates of subsidence up to 55 mm/yr.

This chapter is published as: Castellazzi et al. (2017), InSAR to support sustainable urbanization over compacting aquifers: The case of Toluca Valley, Mexico, Int. J. Appl. Earth Obs. Geoinf. 63, 33-44. https://doi.org/10.1016/j.jag.2017.06.011

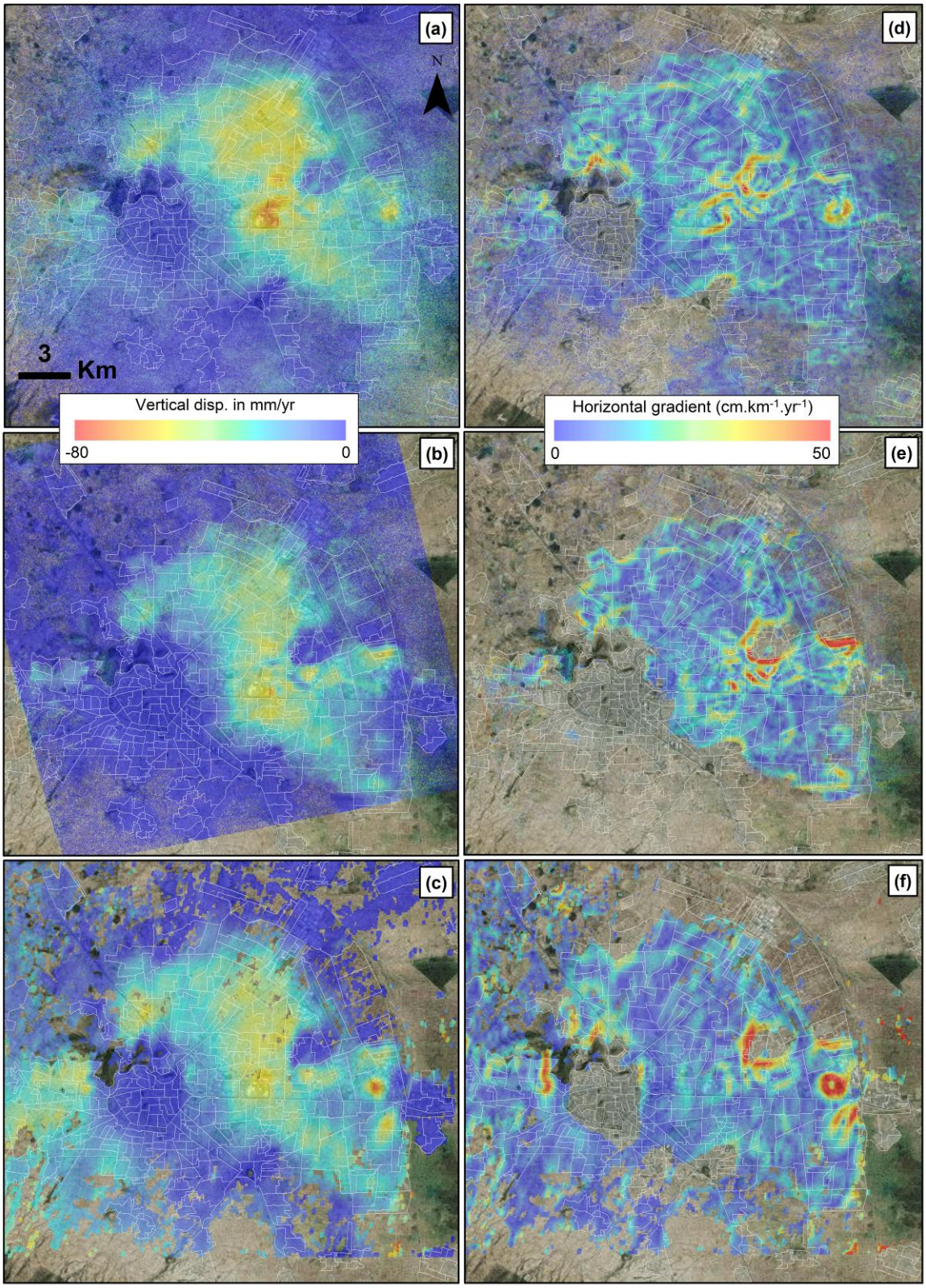

Figure 8: Vertical ground displacement for the periods 2003-2010 (a), 2011-2014 (b), and 2014-2016 (c) detected by Envisat, Radarsat-2, and Sentinel-1A, respectively. Horizontal gradients of vertical displacement rates are calculated for

This chapter is published as: Castellazzi et al. (2017), InSAR to support sustainable urbanization over compacting aquifers: The case of Toluca Valley, Mexico, Int. J. Appl. Earth Obs. Geoinf. 63, 33-44. https://doi.org/10.1016/j.jag.2017.06.011

each vertical ground displacement map and shown in (d) for (a), (e) for (b), and (f) for (c).

3.4.3. RECENT SUBSIDENCE RATES AND HORIZONTAL GRADIENTS

PSI processing was performed with 41 Sentinel-1A IW images to select and invert the phase variations into displacement for 567 728 detected coherent ground targets spread over 750 km^2 (about 1/3 of the total TVA area) and centered over the City of Toluca (Fig. 9). Subsidence rates range from 0 to -80 mm/yr of LOS displacement. The industrial complex, several housing districts, and the airport are affected by important and spatially varying land subsidence patterns (Fig. 9a). The largest rates of subsidence are found in the lacustrine sediments (Fig. 3 and 9a), and the smallest rates occur where slightly coarser-grained alluvial sediments occur, or where alluvial sediment layers are thinner.

The methodology used to compute gradient allows delineating fractures without showing the typical artifacts related to interpolation in areas of low PS point density (Fig. 9b). Important gradient patterns occur within the valley, and their patterns differ significantly from the latest surficial mapping from Figueroa (2004 – Fig. 9b). As the Figueroa (2004) report is based on local knowledge and field observation, it might overlook the less noticeable fractures where population density is lower or where no complaints from local inhabitants were received. In addition, several fractures noticed in the field before 2004 do not show differential movements from 2014-2016, confirming the variable dynamics of compaction of the TVA, with respect to variable temporal and spatial distributions of groundwater extraction and accompanying groundwater level drawdown and recovery. The most noticeable fractures (Fig. 9a and 9b) showed a differential displacement rate of around 30 mm/yr. Several subsidence horizontal gradient features show shapes aligned with mapped basaltic flows (Fig. 9b), which reflects the volcanic/alluvial history of TVA controlling the sediment thickness and the subsidence patterns.

This chapter is published as: Castellazzi et al. (2017), InSAR to support sustainable urbanization over compacting aquifers: The case of Toluca Valley, Mexico, Int. J. Appl. Earth Obs. Geoinf. 63, 33-44. https://doi.org/10.1016/j.jag.2017.06.011

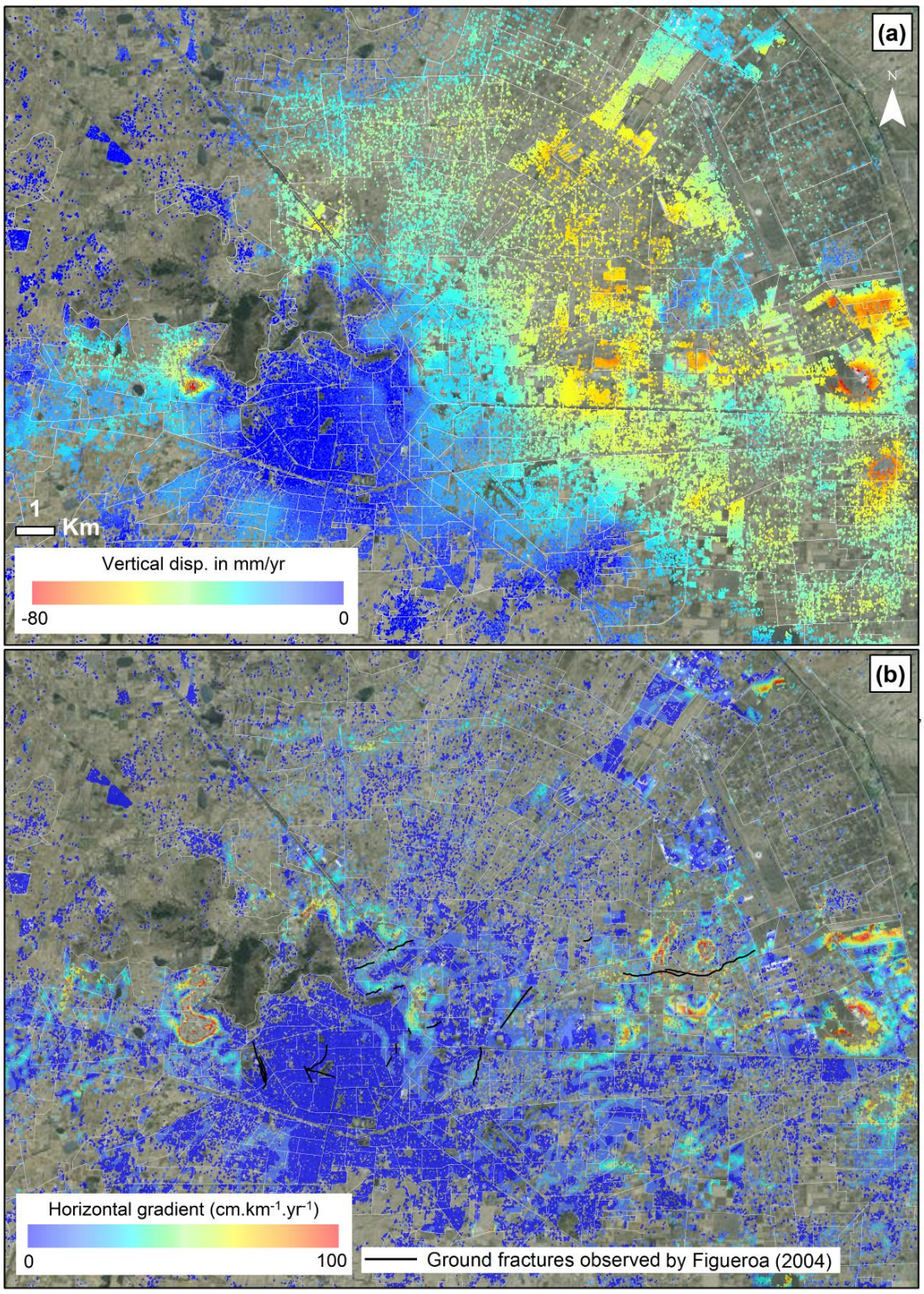

Figure 9: Vertical displacement rates for the period 2014-2016 measured by processing 42 Sentinel-1A images using the PSI algorithm (a). By solving the phase ambiguity individually for each ground target, PSI allows ground displacement measurements at the ground target resolution. The latest ground fracturing map by Figueroa (2004) is presented in (b – black lines). The PSI-derived horizontal

This chapter is published as: Castellazzi et al. (2017), InSAR to support sustainable urbanization over compacting aquifers: The case of Toluca Valley, Mexico, Int. J. Appl. Earth Obs. Geoinf. 63, 33-44. https://doi.org/10.1016/j.jag.2017.06.011

gradient map is used to manually delineate the potential ground fractures and provide an updated fracturing map (following section - Fig. 10).

3.4.4. PRODUCTION AND FIELD VALIDATION OF THE INSAR-DERIVED GROUND FRACTURING MAP

We suggest that the ground fracture mapping is more complete and reliable when derived from InSAR than when solely based on field observations (Figueroa et al. 2004). This hypothesis was tested through a field survey, which consisted in visiting several easily accessible potential fractures observed by InSAR (Fig. 10).

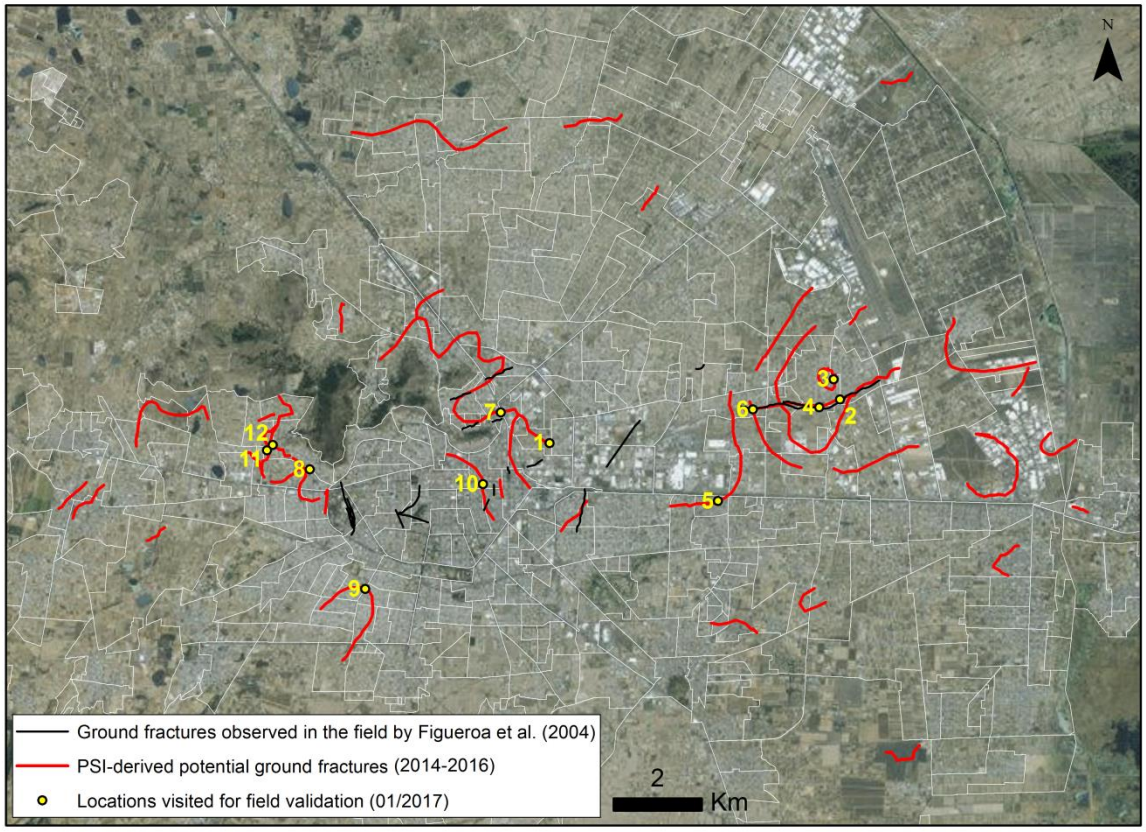

Figure 10: Comparison between potential surficial fractures manually drawn from the PSI-derived horizontal gradient map of vertical subsidence (Fig. 9) and the latest surficial fracture map from Figueroa et al. (2004) based on field observation.

Linear fractures were easily identified in the field at most locations (Points

1,2,3,4,6,8,11, and 12 - Fig. 10 and 11). No obvious fractures were identified at the locations 5, 9, 10 and 7 (Fig. 10). The detection of important subsidence gradients does not directly imply that a fractures is observable. Three factors are likely to compromise the identification of fractures in the field. First, we suggest that infrastructures close to the city center (Points 9 and 10) are better maintained and quickly repaired after been affected by differential subsidence. Second, the presence of high horizontal gradients of vertical subsidence does not necessarily imply observable ground fracturing. We suggest that where the strain is relieved progressively, in 'steps', it is divided over several smaller fractures, which compromises their identification. At these locations, damages to infrastructures might not be obvious enough to be observed while surveying, and might require a more in-depth and time-consuming field inspection. Third, the Gaussian filtering required to smooth out the noise (isolated unstable targets) and produce a usable gradient map leads to a decrease in resolution proportional to the Gaussian filter radius. It implies that fractures cannot be identified with a spatial precision sufficient for direct and effortless identification in the field. In most locations, the help of local inhabitants was essential to identify the fracture, which was not observable exactly in the field where it was drawn on the InSAR-derived map.

As ground fractures were found in 2/3 of the locations visited (e.g., Fig. 11), and given the difficulty of identifying such patterns in the field (i.e. some might have been missed), we conclude that the PSI-derived ground fractures map is generally reliable enough to provide guidance for urban development planning. Such a map can be used as is, i.e. as a potential ground fracturing map, but we recommend its use as an *a priori* map supporting a field-based ground fracture monitoring.

This chapter is published as: Castellazzi et al. (2017), InSAR to support sustainable urbanization over compacting aquifers: The case of Toluca Valley, Mexico, Int. J. Appl. Earth Obs. Geoinf. 63, 33-44. https://doi.org/10.1016/j.jag.2017.06.011

Figure 11: Examples of ground fractures observed in the field while surveying the areas identified by PSI. The locations visited are all marked on Fig. 10. In some locations, obvious linear ground fractures are found (e.g., points 8, 4, and 6), while in others, only discontinuous subsidence effects can be observed (e.g., points 11 and 3). The latter can be interpreted as secondary effects of structural damage suggesting the possible occurrence of differential subsidence and ground ruptures.

3.5. CONCLUSION

The TVA is highly heterogeneous, and hydraulic connections between aquifers and recharge areas are not fully understood. Consequently, it is notably difficult to accurately estimate the regional-scale groundwater depletion using only a few observation wells. However, given the drawdown rates observed in 9 wells monitored as part of this study, it is reasonable to estimate the regional groundwater level decline between 50 cm/yr to 80 cm/yr. This groundwater depletion leads to a land subsidence rate as much as 77mm/yr in average during 2003-2016 and recurrent damages to

infrastructures in both the eastern and western parts of the city. The city center, located on a thinner sediment layer deposited on an andesitic volcanic cone, does not face land subsidence issues. It is also one of the main geological structures controlling distribution and thickness of the compressible sediment and associated fracturing.

The latest surficial fracture map was published in 2004 (Figueroa Vega, 2004), and shows different patterns than the ones revealed by the InSAR analysis in this study. Fractures are neither regularly monitored by the scientific community nor by local governments, suggesting that related prevention or mitigation programs in place are insufficient. In the meantime, major infrastructure developments are planned to better link Toluca and Mexico, suggesting the acceleration of the expansion and densification of the city of Toluca. Nevertheless, the groundwater depletion issues remain unresolved.

Sentinel-1 IW data are particularly suitable for the application presented in this article. PSI processing can provide high-resolution ground displacement maps over urban areas, but is also more sensitive than SBAS to inversion errors when displacement rates are important or non-linear. The 12 day orbital repeat path frequency (or 6 days when using both Sentienl-1 satellites) greatly helps in solving the phase ambiguity during the PSI phase/time to displacement/time inversion. In addition, the temporal density of the Sentinel-1 system allows performing PSI-derived fault detection analysis such as presented in this article over much shorter periods of time (i.e., the last 4-6 months). Such analysis is of great interest for cities, as fractures would be detected at their most early stage and as field validation would potentially be easier, without a time gap allowing residents to repair or hide the fractures.

Theoretically, 30 C-Band images per year (corresponding to a 12 days repeat path frequency) can reveal up to 42 cm/yr of subsidence without unwrapping error and using a typical PSI-type processing (Crossetto et al., 2016). As compacting aquifer-systems produce subsidence rates usually ranging from a few mm/yr to around 30 cm/yr, Sentinel-1 SAR data are perfectly suitable for such application. The use of both Sentinel-1 satellites, simulating a 6 day repeat path frequency, is useful to double the threshold of maximum measurable displacement, and most of all to better remove the atmospheric phase shifts and obtain a better vertical precision and detection threshold. The latter opens perspectives for studying fractured rock aquifers (Schuite at al., 2015) or the least compressible sedimentary aquifers.

This chapter is published as: Castellazzi et al. (2017), InSAR to support sustainable urbanization over compacting aquifers: The case of Toluca Valley, Mexico, Int. J. Appl. Earth Obs. Geoinf. 63, 33-44. https://doi.org/10.1016/j.jag.2017.06.011

The low 3D perpendicular baseline (usually within the 20-100m range for any given image pair) and the high orbital precision also greatly help in providing clean interferograms without important residual fringe patterns. Given the availability of the Sentinel-1 IW data and the maturity of both InSAR algorithms and processing platforms, InSAR-derived ground fracturing maps can be routinely provided to cities built over compacting aquifers in the near future.

3.6. ACKNOWLEDGEMENTS

The authors would like to thank the *Ministère des Relations internationales Francophonie et Commerce extérieur du Québec* (MRIFCE - Québec) and the Consejo Nacional de Ciencia y Tecnología (CONACyT - Mexico), and the Natural Sciences and Engineering Research Council of Canada (NSERC – discovery grant of Richard Martel RGPIN-2016-06503) for their financial supports. We acknowledge Natural Resources Canada (NRCAN) and the Canadian Space Agency (CSA) for their help in obtaining Radarsat-2 acquisitions over Mexico under the MURF #CG0063. We acknowledge the European Space Agency (ESA) for providing Envisat ASAR images under project C1F.31647 and Sentinel-1 IW data. We also thank the French Center for Space Research (CNES) for proving a user-friendly access to Sentinel-1 data through the *Plateforme d'Exploitation des Produits Sentinel* (PEPS - https://peps.cnes.fr). We thank the SARMAP team for their help and their efforts in continuously improving the SARScape InSAR processing toolbox.

4. GROUNDWATER DEPLETION IN CENTRAL MEXICO: USE OF GRACE AND INSAR TO SUPPORT WATER RESOURCES MANAGEMENT

Pascal Castellazzi

Institut national de la recherche scientifique, Centre Eau, Terre et Environnement, Université du Québec, 490 rue de la Couronne, Québec, QC, Canada, G1K 9A9, Phone: 418 570 3630, Fax: 418 654 2600. Email: pascal.castellazzi@ete.inrs.ca

Richard Martel

Institut national de la recherche scientifique, Centre Eau, Terre et Environnement , Université du Québec, 490 rue de la Couronne, Québec, QC, Canada, G1K 9A9, Phone: 418 654 2683, Fax: 418 654 2600. Email: richard.martel@ete.inrs.ca

Alfonso Rivera

Geological Survey of Canada. Natural Resources Canada. 490, rue de la Couronne. Quebec (Quebec) G1K 9A9, Canada. Phone 418 654 2688, Fx: 001 418 654 2615. Email: alfonso.rivera@canada.ca

Jianliang Huang

Canadian Geodetic Survey, SGB. Natural Resources Canada / Government of Canada. 615 Booth Street, Ottawa, ON, K1A 0Y7, Canada. Phone: 343 292 6754. Email: jianliang.huang@canada.ca

Goran Pavlic

Surveyor General Branch. Natural Resources Canada / Government of Canada. 588 Booth Street # 341B, Ottawa, ON, K1A 0Y7, Canada. Phone: 343 292 6624. Email: goran.pavlic@canada.ca

Angus I. Calderhead

Institut national de la recherche scientifique, Centre Eau, Terre et Environnement, Université du Québec, 490 rue de la Couronne, Québec, QC, Canada, G1K 9A9, Phone: 418 570 3630, Fax: 418 654 2600. Email: angus.calderhead@ete.inrs.ca

This chapter is published as: Castellazzi et al. (2016), Groundwater depletion in Central Mexico: Use of GRACE and InSAR to support water resources management, Water Resour. Res. 52, 5985–6003, http://dx.doi.org/10.1002/2015WR018211

Estelle Chaussard

State University of New York at Buffalo. 714 Hochstetter Hall, Buffalo, NY 14260-1350, USA. Phone: 716 645 4291. E-mail: estellec@buffalo.edu

Jaime Garfias

Universidad Autónoma del Estado de México. Centro Interamericano de Recursos del Agua. Carretera Toluca-Atlacomulco, km 14.5. Ciudad Universitaria, C.P.50110, Toluca, Estado de México. Mexico. Phone: 0052 722 296 5550 ext. 106. Email: jgarfiass@uaemex.mx

Javier Salas

Universidad Autónoma del Estado de México. Centro Interamericano de Recursos del Agua. Carretera Toluca-Atlacomulco, km 14.5. Ciudad Universitaria, C.P.50110, Toluca, Estado de México. Mexico. Phone: 0052 722 296 5550 ext. 106. Email: proyectos@javiersalasg.com

Key Points

- InSAR and GRACE observations are compared with the groundwater management scheme
- Discordance between GRACE, InSAR, and water budgets suggests important wastewater recharge
- Co-interpreting GRACE and InSAR brings an unprecedented insight into groundwater sustainability

Abstract

Groundwater deficits occur in several areas of Central Mexico, where water resource assessment is limited by the availability and reliability of field data. In this context, GRACE and InSAR are used to remotely assess groundwater storage loss in one of Mexico's most important watersheds in terms of size and economic activity: the Lerma-Santiago-Pacifico (LSP). *In situ* data and Land Surface Models are used to subtract soil moisture and surface water storage changes from the total water storage change measured by GRACE satellites. As a result,

This chapter is published as: Castellazzi et al. (2016), Groundwater depletion in Central Mexico: Use of GRACE and InSAR to support water resources management, Water Resour. Res. 52, 5985–6003, http://dx.doi.org/10.1002/2015WR018211

groundwater mass change time-series are obtained for a 12 years period. ALOS-PALSAR images acquired from 2007 to 2011 were processed using the SBAS-InSAR algorithm to reveal areas subject to ground motion related to groundwater over-exploitation. In the perspective of providing guidance for groundwater management, GRACE and InSAR observations are compared with official water budgets and field observations.

InSAR-derived subsidence mapping generally agrees well with official water budgets, and shows that deficits occur mainly in cities and irrigated agricultural areas. GRACE does not entirely detect the significant groundwater losses largely reported by official water budgets, literature and InSAR observations. The difference is interpreted as returns of wastewater to the groundwater flow systems, which limits the watershed scale groundwater depletion but suggests major impacts on groundwater quality. This phenomenon is enhanced by ground fracturing as noticed in the field. Studying the fate of the extracted groundwater is essential when comparing GRACE data with higher resolution observations, and particularly in the perspective of further InSAR/GRACE combination in hydrogeology.

Keywords

Groundwater deficit, land subsidence, InSAR, GRACE, wastewater infiltration, Mexico.

4.1. INTRODUCTION

Groundwater sustainability assessment is crucial to assure water availability for future generations. In this perspective, groundwater managers usually rely on the water budget approach. By evaluating the balance between input and output of groundwater over an aquifer or region, managers compare supply and demand of water (Eq. 1):

$$\Delta GWS = R - (D + Q) \quad (1)$$

where ΔGWS is groundwater storage change over time, R is recharge rate, D is natural discharge, and Q is net extraction rate. A negative budget of the fluxes means a decrease in storage, i.e.a deficit. This approach is limited by the availability of *in situ*

This chapter is published as: Castellazzi et al. (2016), Groundwater depletion in Central Mexico: Use of GRACE and InSAR to support water resources management, Water Resour. Res. 52, 5985–6003, http://dx.doi.org/10.1002/2015WR018211

measurements, and the inaccuracies of pumping and recharge estimates. Additionally, it overlooks the impacts of storage changes on aquifer dynamics, e.g. changes in recharge and discharge (Bredehoeft, 2002) or in surface water/groundwater interactions. Temporal variations of GWS imply changes in Earth's gravity field, and when the aquifers comprise compressible sediments, ground level changes. By monitoring such effects, groundwater managers can directly observe GWS evolution over time.

In Mexico, groundwater fulfills more than 70% of the water needs for the 120 million inhabitants (INEGI, 2015). Annual rainfall rates show a smooth transition from high (>2500 mm/yr) in the South to low (<300 mm/yr) in the North (WorldClim – Hijmans et al. 2005). Population is mostly concentrated in the central part of the country, where rainfall ranges from 400 to 1000 mm/yr. The major economic and demographic centers are located in the highlands of Central Mexico, where access to water almost completely relies on over-exploited groundwater resources. The region is recognized as one of the most important cases of groundwater depletion in the World (e.g. Pacheco-Martínez et al. 2013; Chaussard et al, 2014b; Castellazzi et al. 2016a). Bottling, automobile, and agro-alimentary are the main water consuming industries in the cities. Farming relies intensively on irrigation which also greatly contributes to the depletion. Conciliating the demographic and economic growth with water sustainability is a major challenge for water managers of the region.

Groundwater storage change can be directly quantified using space-borne gravimetry. The Gravity Recovery And Climate Experiment (GRACE) consists of two identical satellites on a low near-polar orbit. A K-Band ranging system is used to track changes of the distance between both spacecraft. Distance measurements are converted into gravitational acceleration variations in space, and used to produce mean monthly Earth's gravity field models (Tapley et al. 2004). After post-processing and corrections for non-water mass changes, the monthly GRACE models can be further used to estimate the Total Water Storage (TWS) variations (Wahr et al. 1998). Typically, the surface water (ΔSWS) and the solid water (snow and ice – ΔSIS) contributions are extracted from field data and the soil moisture (ΔSMS) contribution can be extracted using Land Surface Model (LSM). Over the last decade, GRACE has greatly contributed to groundwater storage change estimations over large regions (Yeh et al. 2006; Rodell et al. 2007, 2009; Strassberg et al. 2009; Swenson et al. 2008b; Tiwari et

This chapter is published as: Castellazzi et al. (2016), Groundwater depletion in Central Mexico: Use of GRACE and InSAR to support water resources management, Water Resour. Res. 52, 5985–6003, http://dx.doi.org/10.1002/2015WR018211

al. 2009; Wada et al. 2010; Famiglietti et al. 2011; Henry et al. 2011; Scanlon et al. 2012; Huang et al. 2012; Feng et al. 2013). GRACE also shows great potential for large scale groundwater flow model calibration (Guntner et al. 2006; Hu and Jiao, 2015). The primary limitation of the GRACE system arises from the difficulty of isolating the mass variations signal over small watersheds. It is unable to provide TWS estimates at local (100 – 1,000 km^2) or regional (1,000 – 10,000 km^2) scales, where most groundwater management schemes occur. Initially, GRACE was considered applicable beyond scales ranging from 160,000 to 200,000 km^2 (Rodell et al. 1999; Longuevergne et al. 2010). More recently, novel processing strategies have improved its spatial resolution (Bruinsma et al. 2010, Ramillien et al. 2011, Save et al. 2012, Huang et al. 2012) and several authors have successfully used GRACE for water basins of 100,000 to 150,000km^2 (e.g. Long et al. 2014; Li et al. 2014; Billah et al. 2015) given that the effect of the low resolution and leakages in/out of the study area are secondary or can be accounted. In recent years, several global GRACE-derived groundwater stress and depletion maps were created (Gleeson et al. 2012; Famiglietti, 2014; Richey et al. 2015). Others have described the main limitations of using the GRACE system for groundwater management applications (Alley and Konikow, 2015).

Groundwater deficits may lead to compaction of the aquifer matrix and land subsidence. This phenomenon occurs in several parts of the World, including major cities such as Las Vegas, Shanghai, and Bangkok, and agricultural basins such as the Central Valley (CA, USA). It induces major and recurrent damages to urban infrastructures, increases in flood and water contamination risks, as well as non-recoverable losses in the aquifer's ability to store water. An overview of the mathematical representations of land subsidence processes and the available observation tools is provided by Galloway and Burbey (2011). Among the methods available to monitor ground deformations, Interferometric Synthetic Aperture Radar (InSAR - Rocca et al. 1997; Massonnet and Feigl, 1998) is non-invasive, has a large spatial coverage, a sufficient temporal frequency of observations (from 45 to 6 days depending on the space-borne SAR system), and a precision of up to a few mm/yr. Ground displacement in the radar Line Of Sight (LOS) direction is obtained by inverting the phase variations over a time-series of SAR images. Small Baseline Subset (SBAS) and Permanent Scatterer Interferometry (PSI) are among the main InSAR processing algorithms. The SBAS technique considers tens to hundreds of phase difference maps (interferograms) with small spatial and

This chapter is published as: Castellazzi et al. (2016), Groundwater depletion in Central Mexico: Use of GRACE and InSAR to support water resources management, Water Resour. Res. 52, 5985–6003, http://dx.doi.org/10.1002/2015WR018211

temporal baselines to maintain high interferometric coherence, and inverts this interferogram network to retrieve surface displacement through time (Bernardino et al. 2002; Lanari et al. 2004). PSI only uses the phase history of highly coherent and stable scattering targets (Ferretti et al. 2000a, 2000b, 2001). Due to an independent phase unwrapping for each scattering target, PSI provides greater accuracy and higher spatial resolution. However, it is limited to areas where stable targets occur (often man-made structures), which limits its use outside of urban areas. InSAR has contributed in providing valuable ground deformation data to hydrogeologists (Galloway et al. 1998, 2007, Amelung et al. 1999), and it is now routinely used to: (1) identify litho-stratigraphic boundaries (e.g. Chaussard et al. 2014b), (2) define aquifer material and heterogeneity (Bell et al. 2008; Xu et al. 2012), (3) estimate system properties (Hoffmann et al. 2001; Chaussard et al. 2014a; Reeves et al. 2011; Calderhead et al. 2011), and (4) constrain numerical models (Yan et al. 2008; Calderhead et al. 2011). However, further implementation of InSAR into groundwater studies is limited as the inversion of ground displacement maps into volume of depleted GWS is often confounded by the lack of sediment compressibility data.

Although groundwater depletion has been studied in several regions of Central Mexico (e.g. Esteller et al, 2002; Rudolph et al. 2006, Avila-Olivera et al. 2010, Calderhead et al. 2012b; Castellazzi et al. 2016a), no study were carried at the basin scale. This study is the first to assess water sustainability at the hydrologic scale and independently from officially published government data. Additionally, Central Mexico has never been mentioned in any of the global GRACE-derived groundwater depletion and stress maps (Famiglietti, 2014; Richey et al. 2015). Thus, there is methodological interest in understanding the reasons for the discordance between geodetic observations and the current hydrogeological knowledge of the region. Hence we present and interpret a unique and comprehensive dataset, including GRACE-derived groundwater storage change estimates, InSAR-derived land subsidence maps, water management tools and maps, and *in situ* observations. While conducting a case study, we compare GRACE and InSAR observations for the first time. In a context where scientists attempt to transpose these geodetic observations into water management schemes, there is a crucial need to compare these novel methods with the current state of groundwater management practices.

This chapter is published as: Castellazzi et al. (2016), Groundwater depletion in Central Mexico: Use of GRACE and InSAR to support water resources management, Water Resour. Res. 52, 5985–6003, http://dx.doi.org/10.1002/2015WR018211

4.2. STUDY AREA

In this study, we investigate the GWS of Central Mexico's main watershed during the period 2002-2014. The Lerma-Santiago-Pacifico (LSP) water basin extends over 133,484 km^2 and provides water for eight of Mexico's 35 most populated cities (Figure 1; Mexico, Guadalajara, Léon, Zapopan, Aguascalientes, Queretaro, Morelia, and Toluca). Around 20 million inhabitants live within the watershed, which encompasses eight states (Figure 1; Estado de Mexico, Michoacán, Queretaro, Guanajuato, Jalisco, Aguascalientes, Nayarit and Zacatecas). It also exports 38% of the water supply for the 26 million inhabitants of the metropolitan area of Mexico City, located 50 km outside of the southern tip of the watershed. Precipitation in LSP basin is typical for Central Mexico, and varies from 1,000 mm/yr in Toluca Valley, to around 400 mm/yr in the states of Aguascalientes and Zacatecas (Figure 1). Two new hydroelectric dams were constructed during the study period, namely La Yesca and El Cajon. They are possibly impacting the TWS measured over the basin.

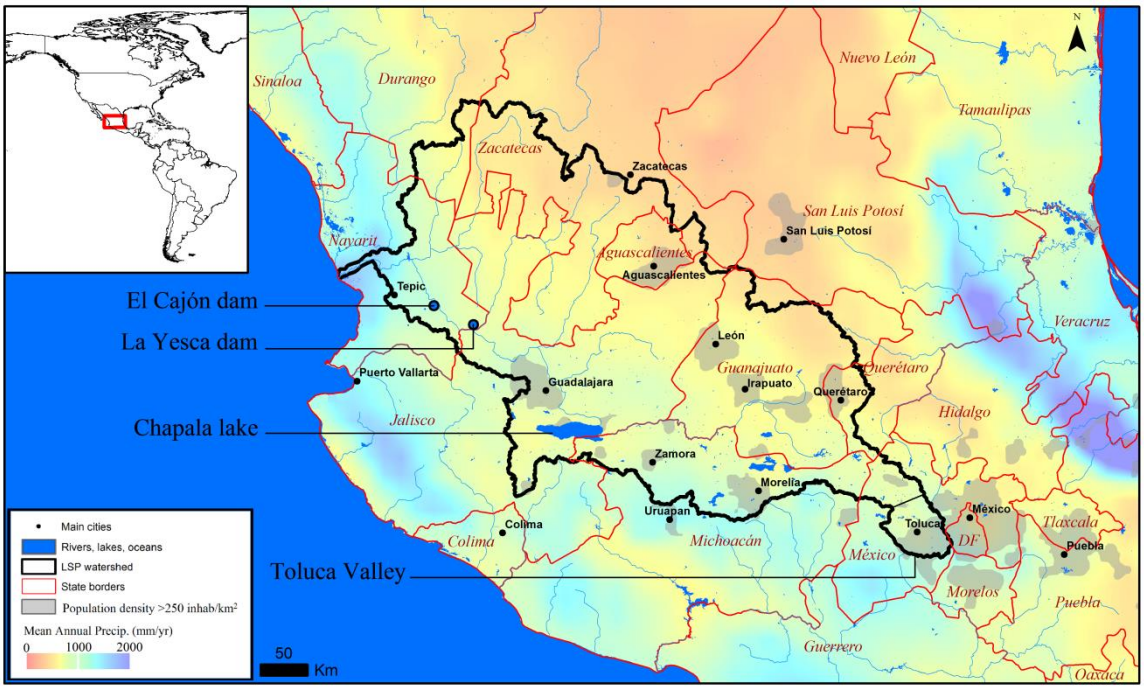

Figure 1: Annual precipitation rates (WorldClim – Hijmans et al. 2005), highly populated areas (CIESIN/CIAT, 2005), and main cities of Central Mexico. The location of the LSP basin, Mexico's largest lake (Chapala lake), and two recent hydroelectric dams are also presented.

This chapter is published as: Castellazzi et al. (2016), Groundwater depletion in Central Mexico: Use of GRACE and InSAR to support water resources management, Water Resour. Res. 52, 5985–6003, http://dx.doi.org/10.1002/2015WR018211

Several regional studies were conducted in several parts of the basin: in the Toluca Valley (Esteller et al, 2002; Rudolph et al. 2006; Calderhead et al. 2011, 2012a, 2012b; Davila-Hernandez et al. 2014; Del Campo et al. 2014, Castellazzi et al. 2016a), in Morelia (Avila-Olivera et al. 2010; Cabral-Cano et al. 2010; Cigna et al. 2012; Castellazzi et al. 2016a), in the Queretaro region (Gutiérrez-Carrillo et al. 2002; Castellazzi et al. 2016a; Huizar-Alvarez et al. 2011), and in Aguascalientes Valley (Castellazzi et al. 2016a; Pacheco-Martínez et al. 2013). While literature reports high rates of groundwater drawdowns and land subsidence in several municipalities or region, no study has been done in an integrated manner at the watershed scale.

To manage groundwater resources, *Comisión Nacional del Agua (*CONAGUA) calculates the mean annual availability of groundwater for each of the 653 administrative aquifers of Mexico. It represents the volume of groundwater that can be withdrawn while preserving the balance of ecosystems relying on groundwater (springs, baseflow). According to Mexican water regulations, no further groundwater extraction allowance can be emitted in depleting aquifers. However, current allowances can be exchanged, hence the unofficial water market between users.

The aquifer budget approach used by CONAGUA relies either on (1) a groundwater-budget approach, if sufficient data are available, or (2) a water-budget approach. The groundwater budget method is based on groundwater flow. Although it is linked to surface flow such as precipitation, evapotranspiration and runoff, such parameters do not appear directly. The budget is calculated as a balance between groundwater inflows from recharge area and outflows to discharge areas or pumping centers. The volume of groundwater inflowing from recharge area and outflowing to discharge areas is evaluated following the Darcy's low. The main advantage of such method is that evapotranspiration estimates is not necessary, and its related error not reported in the groundwater availability estimation. The groundwater storage change is measured by observing water table fluctuations (Scanlon et al. 2002). If no sufficient hydrogeological data are available, a simple water-budget method is used. In this approach, all the variables, i.e. precipitation, evapotranspiration, surface runoff, and change in soil water are estimated. The recharge is set equal to the residual. The evapotranspiration, the key parameter in such estimation, is calculated following the method described by Turc

This chapter is published as: Castellazzi et al. (2016), Groundwater depletion in Central Mexico: Use of GRACE and InSAR to support water resources management, Water Resour. Res. 52, 5985–6003, http://dx.doi.org/10.1002/2015WR018211

(1962). For long-term averaged steady-state conditions, the variation of soil water content is assumed to be negligible (Scanlon et al. 2002).

4.3. DATA

4.3.1. GRACE

The TWS monthly grids are based on the RL05 monthly GRACE models derived by the Center for Space Research, University of Texas, USA, for the period April 2002 to April 2014. The details of the RL05 processing can be found in Bettadpur (2012). The GRACE models do not include the spherical degree-one terms, and Swenson et al.'s predictions (2008a) are added to each monthly GRACE model. As the monthly degree-two term time-series is better determined by the satellite laser ranging (Cheng et al. 2013), it was used to replace the corresponding term of each GRACE model. The surface water storage (SWS) data were gathered from two main surface water management agencies of Mexico: *Comisión Nacional del Agua* (CONAGUA) and *Comisión Federal de Electricidad* (CFE). The SMS estimates were taken from five LSM: VIC10, CLM10, MOSAIC10 (MOS10), NOAH10, and NOAH025), all included within The Global Land Data Assimilation System (GLDAS-1 - Rodell et al. 2004). To select the best SMS estimates among the available LSM, a comparison with *in situ* data was performed. To convert point-based soil moisture probe measurements into 1D soil water retention curves time-series, samples and data were obtained: the grain size from sediment samples at the three drilling sites, daily precipitation from rain gauges, runoff rates from a previous study (Calderhead et al. 2012b), NDVI from LandSAT time-series, and daily temperatures from a local weather station.

4.3.2. INSAR

The SAR images used for SBAS-InSAR processing were taken with the Phased Array type L-band Synthetic Aperture Radar (PALSAR) sensor aboard ALOS-1 satellite. They can be downloaded free of charge and directly in Single Look Complex format (SLC - Level 1.1) from the Alsakan Satellite Facility (ASF) web portal (https://www.asf.alaska.edu/). While their resolution is approximately 10m in Azimuth, it varies in range depending on the acquisition Line Of Sight (LOS) angle.

4.3.3. WATER MANAGEMENT DATA AND OTHERS

The Mexican water regulation agency, Comisión Nacional del Agua (CONAGUA) is responsible for publishing the results of water budget estimates of the 653 aquifers of Mexico according to the NOM-011-CONAGUA-2000 norm. Among these administrative aquifers, 96 are present within the LSP basin. Data used for this study were taken from CONAGUA (2009a, 2013a). The land use map was adapted from INEGI (2005).

4.4. METHODS

4.4.1. GRACE

To infer the GWS storage component from GRACE, several contributions need to be removed from the TWS measured by GRACE (Eq. 2):

$$\Delta GWS = \Delta TWS - (\Delta SWS + \Delta SMS + \Delta SPS) \quad (2)$$

Where *ΔGWS* is the groundwater storage variation, *ΔTWS* is the total water storage variation measured by GRACE satellites, *ΔSWS* is the surface water storage variation, *ΔSMS* is the water storage variation within the unsaturated zone, and *ΔSIS* is the snow and ice water storage variation. All variables are in WTE (Water Thickness Equivalent) per year [LT^{-1}], or if integrated over an area, in volume/time [L^3T^{-1}].

a) Total Water Storage change (ΔTWS)

A two-step method was used to extract the gravity change signal from the GRACE models (Huang et al. 2012). First, a de-striping step as described by Swenson and Wahr (2006) was used to correct the GRACE model coefficients. An additional de-striping criterion wad applied on the RMS ratio between the original and de-striped coefficients to minimize signal loss. Second, a statistical test step similar to Davis et al.'s (2008) was used to identify signal-dominant coefficients that do not require filtering, and to apply non-isotropic Gaussian filtering (Han et al. 2005) solely to the remaining coefficients. This two-step method minimizes the resulting signal loss from the three methods while retaining their efficiency and effectiveness in extracting the signal.

b) Subtracting Soil Moisture Storage (ΔSMS) influence

Variations in the water content within the vadose zone (or unsaturated zone) (ΔSMS) were extracted from LSM. These large scale models combine *in situ* and space-based

observations to estimate land surface state and parameters of the water cycle such as evapotranspiration, run off and recharge (Georgakakos and Baumer, 1996; Moran et al. 2004). The removal of ΔSMS from GRACE data has been widely performed in previous studies (Chen et al. 2009; Tiwari et al. 2009; Rodell et al. 2007; Scanlon et al. 2012; Huang et al. 2012). While these studies often only rely on large scale LSM-derived estimates, we suggest that comparing them with available *in situ* data prevents possible unrealistic ΔSMS estimates to be integrated within the final GRACE signal decomposition. From August 2010 to August 2011, Soil Moisture Probes (SMP) monitored soil water content at three locations and at three depths (5, 10 and 15m) within the Toluca Valley (Salas-Garcia, 2012): the Nevado de Toluca site, the Taborda site, and the Zolocatepec site. Hereafter, they will be called SMP 1, 2 and 3, respectively.

The HYDRUS-1D package (Simunek et al. 2005) is a physically based model that can fully represents the physical processes involved when water migrates within the vadose zone. This model was used to solve Richards 'equation, which describes the movement of water in unsaturated soils over a 1D soil column. Such calculation was performed on daily data spanning from august 2010 to august 2011 and at three locations within the Toluca Valley (Southern part of the watershed, see Figure 1). In this perspective, boundary conditions were implemented: atmospheric conditions at the surface of the column, and a free drainage condition at its base. The soil hydraulic functions were assessed by analysing the soil samples gathered during drilling operations and calculated using the ROSETTA software (Schaap et al. 2001). The recharge inflow was calculated using a simple water-budget method (Eq. 3), where the fluid flux across the soil surface boundary $q(t)$ [LT^{-1}] is related to precipitation P [LT^{-1}], to actual evapotranspiration ETR [LT^{-1}], and to surface runoff R_n [LT^{-1}]:

$$q(t) = P - ETR - R_n \quad (3)$$

The methodology used to assess actual evapotranspiration is based on the approach developed by Wang et al. (2007), who developed a simple regression equation relying on the net radiation R_{net}, the Normalized Difference Vegetation Index $NDVI$, the daytime averaged day temperature T, and three correlation coefficients c_0, c_1, and c_2 (Eq. 4) :

$$ETR = R_{net}(c_0 + c_1 NDVI + c_2 T) \quad (4)$$

By combining Equation 3 and 4, we obtain Equation 5:

$$q(t) = P - R_n(c_0 + c_1 NDVI + c_2 T) - R_n \quad (5)$$

To estimate the water content at the three sites with HYDRUS 1D model, initial soil hydraulic parameters and the surface boundary condition (*q(t)*) were calibrated with respect to the soil water content measured at three depths in each well. This calibration process aims to minimize the differences between measured water content and numerically predicted values from HYDRUS 1D. Thus, hydraulic parameters of the unsaturated zone and the surface boundary condition (*q(t)*) were estimated by using an iterative procedure, in which the transient water contents were fitted to three *in situ* measures. As a result, optimized water content time series were obtained. Integration along the soil column and monthly averaging allowed direct comparison with values from the LSM grids. The comparison was performed on the pixel over which the field probes are, rather than with the basin-average. After selecting the best LSM to estimate ΔSMS storage, they were filtered to make them compatible with GRACE data. The LSM-derived SMS estimates were converted to the GRACE-like spherical harmonic models, truncated to spherical harmonics of degree and order 60, and filtered using the two step filtering applied over the GRACE models (see Huang et al. 2012). They are simply called the filtered SMS estimates hereafter.

c) Subtracting Surface Water Storage (ΔSWS) influence

Within LSP basin, most of the 1254 surface water bodies are managed for irrigation, recreational, and hydroelectricity production purposes. In order to analyse their trends, they were divided into two groups: (1) the water bodies with less than 40 MCM of storage, mainly used for irrigation during the dry season, and (2) the 12 larger water bodies, with storage capacity ranging from 40 to 6600 MCM. A trend analysis was performed over the storage time-series of the 12 larger surface water bodies. Among them, three show significant trends during 2002-2014. The level of Chapala Lake, the most extensive lake in Mexico, is controlled through water management schemes encouraging its recovery to past storage level. La Yesca and El Cajon dams showed significant storage increases, as they were still in their initial filling stages in 2014. The storage time-series of these three water bodies were converted into a Water Thickness

This chapter is published as: Castellazzi et al. (2016), Groundwater depletion in Central Mexico: Use of GRACE and InSAR to support water resources management, Water Resour. Res. 52, 5985–6003, http://dx.doi.org/10.1002/2015WR018211

Equivalent (WTE) grid, and was filtered similarly to the GRACE model and the SMS estimates.

The analysis accounted for 72% of the total surface water storage capacity (in each dam, it is referred to as *Nivel de Aguas Máximas Ordinarias* or NAMO, see e.g. CONAGUA, 2013b) within the watershed. The remaining 28% of the capacity is stored by smaller dams, which are mainly used for irrigation purposes in farming communities. Their level typically reaches its maximum during rainy season, when water overflows through the structure. Consequently, they are not likely to bias the ΔSWS trend estimates.

d) Forward Modelling the InSAR map for GWS trend error estimation

By taking the LSM-derived SMS trend map as a good estimation of the GRACE TWS trend spatial pattern, it can be truncated and filtrated similarly to the GRACE solution (forward modelling) to estimate the error induced by GRACE's low resolution over the basin-average TWS trend estimates (e.g. Huang et al. 2012). However, the spatial patterns of the LSM-derived SMS trend might not be related to the spatial patterns of the GWS trend. Given that InSAR detects land subsidence, a phenomenon directly linked to groundwater depletion, we suggest that it is a better approximation of the GWS trend spatial patterns, and that it can be used to simulate the influence of resolution over GWS trend estimates. In this perspective, the InSAR land subsidence map was integrated into a GRACE-like pixel grid, truncated and filtrated similarly to the GRACE solution, and averaged over the basin. The resulting basin-average was compared to the basin-average computed with the original InSAR data. Their ratio was taken as an error estimate of the GRACE-derived GWS trend, and helped in interpreting GRACE-derived GWS trend estimates at the scale of LSP basin.

4.4.2. INSAR

a) Processing

Vertical velocity measurements were taken from Chaussard et al. (2014b), who relied on over 600 SAR images from 15 ascending tracks acquired by the ALOS satellite between 2007 and 2011. Three thousand interferograms with small spatial (<1.5 km) and temporal (<1 yr) baselines were produced following the D-InSAR technique, relying on the ROI_PAC processing software (Rosen et al. 2004). These interferograms

were integrated in an interconnected network and inverted for the phase change through time relative to the first SAR acquisition according to the SBAS technique (Berardino et al. 2002). A temporal coherence mask preserving the displacement values corresponding to coherence of 0.7 to 1 was applied over each time-series. Vertical velocity maps were produced by assuming the displacement entirely vertical. By considering the subsidence rates generally constant in time (as observed in: Chaussard et al. 2014b; Castellazzi et al. 2016a), the maps were stacked into one annually averaged vertical velocity map, regardless of each initial InSAR measurements time span within 2007-2011. To ease data processing and handling, the final large scale InSAR map was down-sampled to a resolution of 60 m by 60 m using a Nearest Neighbour algorithm. In order to fulfill the gaps created in low coherence areas by the coherence mask, and restore the continuity of the land subsidence map in vegetated areas, a bilinear interpolation algorithm was applied. Values below a detection threshold of 1 cm/yr of subsidence were set to 0. Although the final InSAR-derived land subsidence map only covers 64% of the basin area, it covers 94% of the total population within the basin.

b) Interpretation

Groundwater withdrawal is the only known cause of land subsidence in the study area. Thus, InSAR-derived vertical ground displacement measurements are considered to be entirely related to aquifer compaction. As defined by the poro-elastic model (Terzaghi, 1925; Biot, 1941), and assuming the geostatic load and the total stress σ_T constant, the variation of effective stress $\Delta\sigma_e$ [$ML^{-1}T^{-2}$], and the interstitial fluid pressure Δp [$ML^{-1}T^{-2}$] are related to the changes in hydraulic head Δh [L], such that (Eq. 6):

$$\Delta\sigma_e = -\Delta p = -\rho\, g\, \Delta h \qquad (6)$$

where ρ is the water density [ML^{-3}] and g is the gravitational constant [LT^{-2}]. When such pressure change applies over a compressible aquifer matrix, change in the grain to grain spacing occurs. According to the Terzhagi one-dimensional compaction model, the related deformation at the surface Δu [L] can be expressed as a function of the pore pressure change Δp [$ML^{-1}T^{-2}$] affecting an aquifer characterized by its compressibility α [$M^{-1}L\ T^2$] and thickness b [L], such that (Eq. 7):

$$\Delta u = \Delta p\ \alpha\ b = \rho\ g\ \alpha\ b\ \Delta h = Ssk\ b\ \Delta h = Sk\ \Delta h \qquad (7)$$

Where S_k and S_{sk} are respectively the skeletal storage, and the specific skeletal storage coefficients. Most of the exploited aquifers within the basin are unconfined (Castellazzi et al. 2016a). They are assumed to be directly in contact with the bedrock, i.e. the geostatic stress decrease related to water extraction does not induce expansion of the underlying lithological layers. For unconfined conditions, the hydraulic head change (*Δh)* can be related to the ΔGWS in WTE as measured by either GRACE or groundwater budgets, and the aquifer Specific yield (S_y), such that (Eq. 8):

$$\Delta h = \Delta GWS / S_y \quad (8)$$

Given the relative unavailability of lithological data throughout the basin, the conversion of land subsidence measurements into volume of groundwater depletion cannot be performed with sufficient precision. Specific yield (S_y), compressibility (α), and aquifer thickness (b) are highly variable spatially, and large scale estimates would be labor-intensive and costly to obtain. Consequently, we suggest a sensitivity analysis over the poro-elastic model (Eq. 7) for two of the three governing parameters (α and b) in order to relate InSAR observations to both GRACE and groundwater budget *ΔGWS* estimates. The third parameter (S_y – Eq. 8) is set at a constant value of 0.2, typical for the aquifers occurring in the study area. For such analysis, both *ΔGWS* and *Δu* can either be expressed in WTE and cm\yr of subsidence, or in total water and void volumes per year integrated over the study area.

c) Groundwater uses and mass losses

The presence of water mass change greatly depends on uses and fate of the extracted groundwater, which is related to land use in the pumping areas. In order to approximate the proportions of the different groundwater uses and the related returns to aquifers, a land use map (adapted from INEGI, 2005) was co-registered over the InSAR-derived land subsidence map. The land use map was modified by grouping classes into urban area, farmland, irrigated farmland and others. A 3-km buffer area around cities (called here peri-urban area) was used to account for mixed water usage in city surroundings and for the horizontal effects of aquifer compaction. An analysis of the cumulative histograms describing the occurrence of land subsidence in each land use class was performed. The annual subsidence volume (in MCM/yr), corresponding to the loss in aquifer matrix porosity related to compaction, was computed for each land use class by

multiplying every pixel of the subsidence grid by its ground area and summing the resulting values for each class. The approach assumes the reaction drawdown/compaction as spatially homogeneous, and that the buffer area around cities entirely accounts for both mixed urban and agricultural water uses and the horizontal component of land subsidence.

4.5. RESULTS AND DISCUSSION

4.5.1. GRACE-DERIVED GWS TREND

Soil Moisture Storage (SMS) *in situ* measurements are point-based and only cover a limited area of the LSP basin: they are all within the 2,000 km^2 of the Toluca Valley. They are compared with the corresponding pixel within each LSM grid (Figure 2c), rather than with the basin-average taken for GRACE signal decomposition (Figure 2a and 2b). They are also limited in time: they span over one year, which limits their ability to reveal SMS trends. However, they are the only direct and reliable SMS measurements to support SMS signal removal from GRACE TWS data. We suggest that a comparison with available field data increases confidence in the LSM-derived SMS estimates, and is more reliable that the common approach relying solely on LSM (e.g. Rodell et al. 2009; Famiglietti et al. 2011; Huang et al. 2012).

Comparison between the three Soil Moisture Probes (SMP) and LSM (Figure 2) confirms that LSM-derived SMS estimates are realistic. It confirms the absence of significant SMS trend and the low impact of SMS over the GRACE TWS trend. It also suggests that CLM10 is the most suitable to represent ΔSMS over SMP 2 and 3, and that VIC10 is most suitable for SMP 1 (Figure 2, Table 1). Toluca Valley is a typical setting in LSP watershed: recharge areas are located in highlands (Calderhead et al. 2012a, 2012b), and groundwater flows toward the lower part where fine grained sediment layers are more abundant. SMP 1 is located in a recharge zone and its phreatic level is deeper (70 m) than SMP 2 and 3 (20 to 30m). It has higher infiltration rates and annual amplitude of vadose zone water storage. While VIC10 shows good accuracy over the SMP 1 groundwater recharge area, CLM10 shows accuracy in the lowlands area where recharge rates are typically low. Because the two models represent well the ΔSMS in two settings with typical low and high extremes rates of recharge, they are taken as the best available estimate of the spatial variability of ΔSMS change over the

This chapter is published as: Castellazzi et al. (2016), Groundwater depletion in Central Mexico: Use of GRACE and InSAR to support water resources management, Water Resour. Res. 52, 5985–6003, http://dx.doi.org/10.1002/2015WR018211

watershed. Over the basin and at GRACE's resolution, CLM10 and VIC10 show slightly positive trends of +91 and +39 MCM/yr (Figure 2; Table 1).

Table 1: Comparison between ΔSMS estimates from 5 LSM and 3 in-situ measurement location in Toluca Valley from 08-2011 to 08-2012, LSM SMS signal amplitude loss related to GRACE resolution (variance ratio original vs filtered) and trends of the ΔSMS estimates at GRACE's resolution.

	Deviation of LSM ΔSMS estimates for each Soil Moisture Probe (%)				SMS trend at GRACE's resolution
	SMP1	SMP2	SMP3	Mean	
CLM10	213	-52	-12	49	+91
MOS10	-53	-88	-77	-73	-14
NOAH10	-159	-106	-133	-133	+248
NOAH025	-40	-96	-104	-80	+254
VIC10	-7.4	-82	-68	-52	+39
Average	-9.6	-85	-79	-58	+124
Std. Dev.	122	18	40	60	+122
Average VIC10/CLM10	103	-67	-40	-4.6	+65

This chapter is published as: Castellazzi et al. (2016), Groundwater depletion in Central Mexico: Use of GRACE and InSAR to support water resources management, Water Resour. Res. 52, 5985–6003, http://dx.doi.org/10.1002/2015WR018211

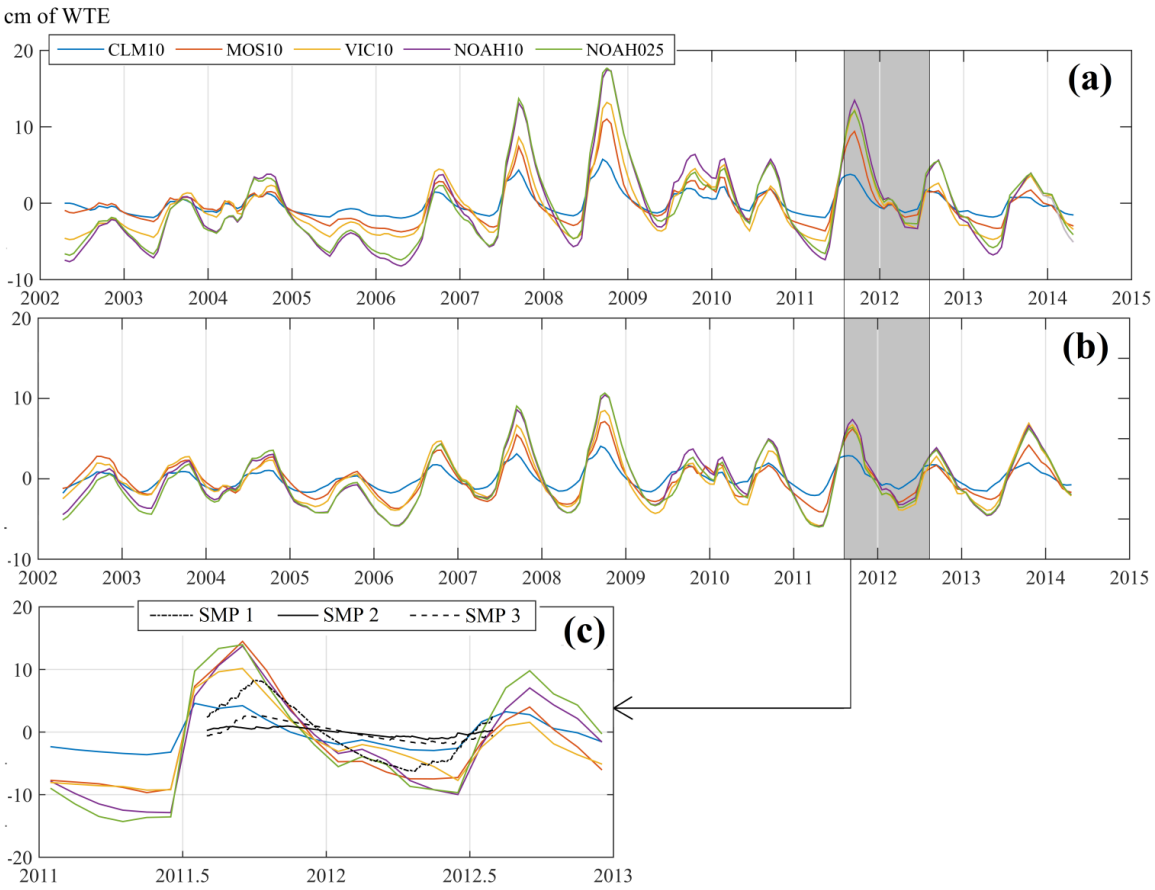

Figure 2: ΔSMS estimates from 5 LSM over LSP basin (a), ΔSMS estimates from 5 LSM over LSP basin at GRACE's resolution (b), and comparison between ΔSMS estimates from 5 LSM over Toluca Valley and in situ data taken in 3 locations of Toluca Valley (c).

It is observed that neither SMS, TWS, nor SWS are showing significant trends (Figure 2 and 3). TWS is decreasing by 112 MCM/yr over the basin and for the period 04-2002 to 04-2014 (Figure 3c). SWS change estimates shows a slightly positive trend of 39 MCM/yr (Figure 3a), due to: (1) the effect of volume restoration policies of Chapala Lake, the main natural lake of the watershed; and (2) the construction of two new dams, El Cajón in 2007 and La Yesca in 2012. Once fully operational, they will store respectively 5000 and 2500 MCM. However, forward modeling the impact of SWS on GRACE TWS data shows that SWS has a very limited impact on the signal at GRACE resolution (+7 MCM/yr - Figure 3b). It is partly due to the location of the surface water bodies, near the watershed boundary, implying an important outward signal loss during

filtering. After signal decomposition (Eq. 2), GRACE-derived GWS trend is estimated at -158 MCM/yr using VIC10 and at -211 MCM/yr using CLM10 (Figure 4). Error in the estimation arises mainly from GRACE limited resolution.

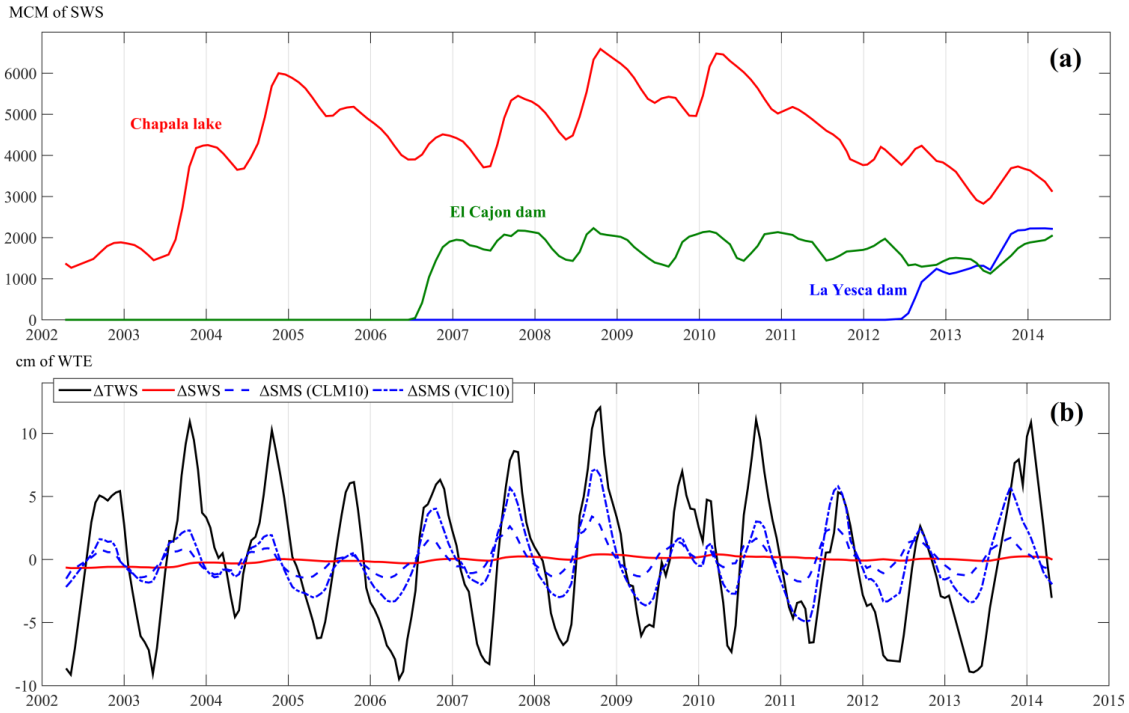

Figure 3: SWS increased due to volume restoration policies of Chapala Lake and the construction of two new dams (a). GRACE TWS, filtered SMS from VIC and CLM, and filtered SWS time-series are used to infer the GWS trend (b). While SWS increased (a), its effect on GRACE signal is relatively small (b, red line).

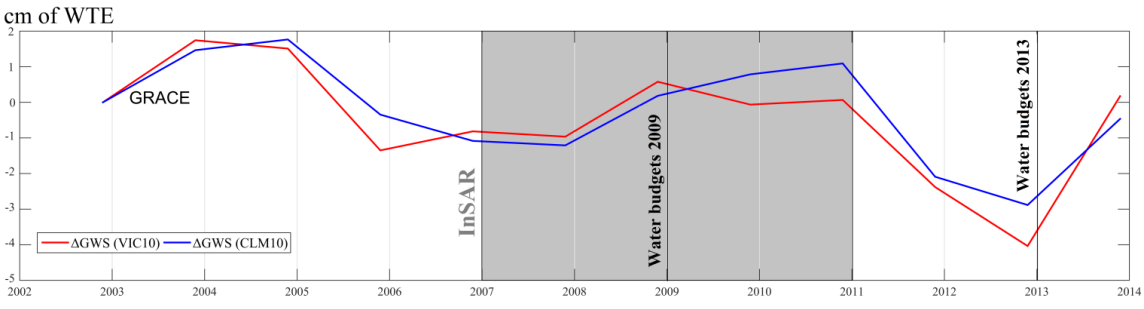

Figure 4: Annually averaged ΔGWS change from GRACE over LSP watershed from 2002 to 2014. Filtered CLM10 and VIC10 are used to subtract SMS influence from TWS. While a slightly negative trend is visible, it is significantly lower to what is expected given the important groundwater drawdowns reported in the literature, in the

This chapter is published as: Castellazzi et al. (2016), Groundwater depletion in Central Mexico: Use of GRACE and InSAR to support water resources management, Water Resour. Res. 52, 5985–6003, http://dx.doi.org/10.1002/2015WR018211

official water budgets, and suggested by InSAR observations. The time overlap with other types of data used in this study is also presented: InSAR-derived land subsidence maps from 2007 to 2011 and official aquifer budgets published by CONAGUA in 2009 and 2013.

Due to the low resolution of the GRACE system, GWS trend estimates can be influenced by leakages inward and outward of the study area. Leakages effects are estimated through forward modelling of the InSAR map. The comparison between the original and the modelled map shows a decrease in the basin-average by a ratio of 2.7 (Figure 5). As the InSAR map is mainly centered over the basin area (see extent on Figure 5a), and as its surroundings are not fully covered, the simulation might underestimate leakages inward. Given that the basin area has a higher population density than its surroundings (with the exception of Mexico City, see Figure 1), groundwater depletion is more likely occurring inside the basin than outside the basin. If the InSAR map comprises all the groundwater deficit areas within and beyond the watershed boundary, GRACE would only detect 37% of the groundwater deficit (Figure 5). If land subsidence observations are missing within the InSAR map outside of the watershed because of its limited extent, GRACE would detect more than 37% of the groundwater deficit. The value of 37% (1/2.7) is taken as a conservative GWS trend error estimate. The final GRACE-derived GWS trend estimation ranges from the lowest value, using VIC10, to the highest, using CLM10 multiplied by 2.7. Indeed, it ranges from -158 to -569 MCM/yr.

This chapter is published as: Castellazzi et al. (2016), Groundwater depletion in Central Mexico: Use of GRACE and InSAR to support water resources management, Water Resour. Res. 52, 5985–6003, http://dx.doi.org/10.1002/2015WR018211

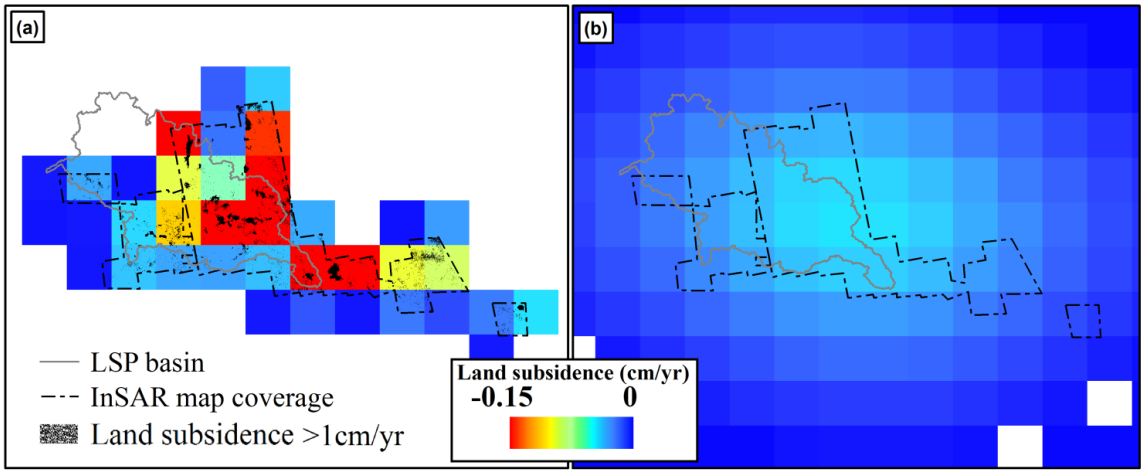

Figure 5: Integration of InSAR-derived land subsidence measurement on a GRACE-like 1-by-1 degree grid where the detected subsidence values are spread over the pixel area (a), truncation and filtering according to the GRACE model (b). Basin averaging shows a decrease of the land subsidence values by a factor 2.7, which is taken as a conservative GWS trend error estimate.

4.5.2. COMPARING GEODETIC OBSERVATIONS WITH GROUNDWATER MANAGEMENT

While GRACE GWS trend estimates shows a groundwater mass loss of the order of 158 to 569 MCM/yr (Figure 6b), the accumulation of the official aquifer water budgets within the same area suggested a total groundwater deficit of 1998 MCM/yr in 2009 (Figure 6c) and 2095 MCM/yr in 2013 (Figure 6d). At least 72% of the deficit estimated by the official water budgets is not detected by GRACE.

Important regional groundwater deficits are occurring in several regions of the watershed. These are observed in both land subsidence (Figure 6e) and water budget maps (Figure 6c and 6d), which generally show good agreement. Comparison between Figures 6c, 6d and 6e shows that the aquifers with the highest rates of deficit (larger than 50 MCM/yr) are generally well detected by InSAR-derived land subsidence mapping. Spatial patterns of land subsidence (Figure 6e) are notably restricted to valleys and basins filled by alluvial and lacustrine quaternary sediments. These sediments constitute extensively used aquifers where severe groundwater withdrawal has taken place and is the leading cause of land subsidence. Few areas showing high deficit rates

This chapter is published as: Castellazzi et al. (2016), Groundwater depletion in Central Mexico: Use of GRACE and InSAR to support water resources management, Water Resour. Res. 52, 5985–6003, http://dx.doi.org/10.1002/2015WR018211

do not show land subsidence, probably due to the absence of compressible lithological layers.

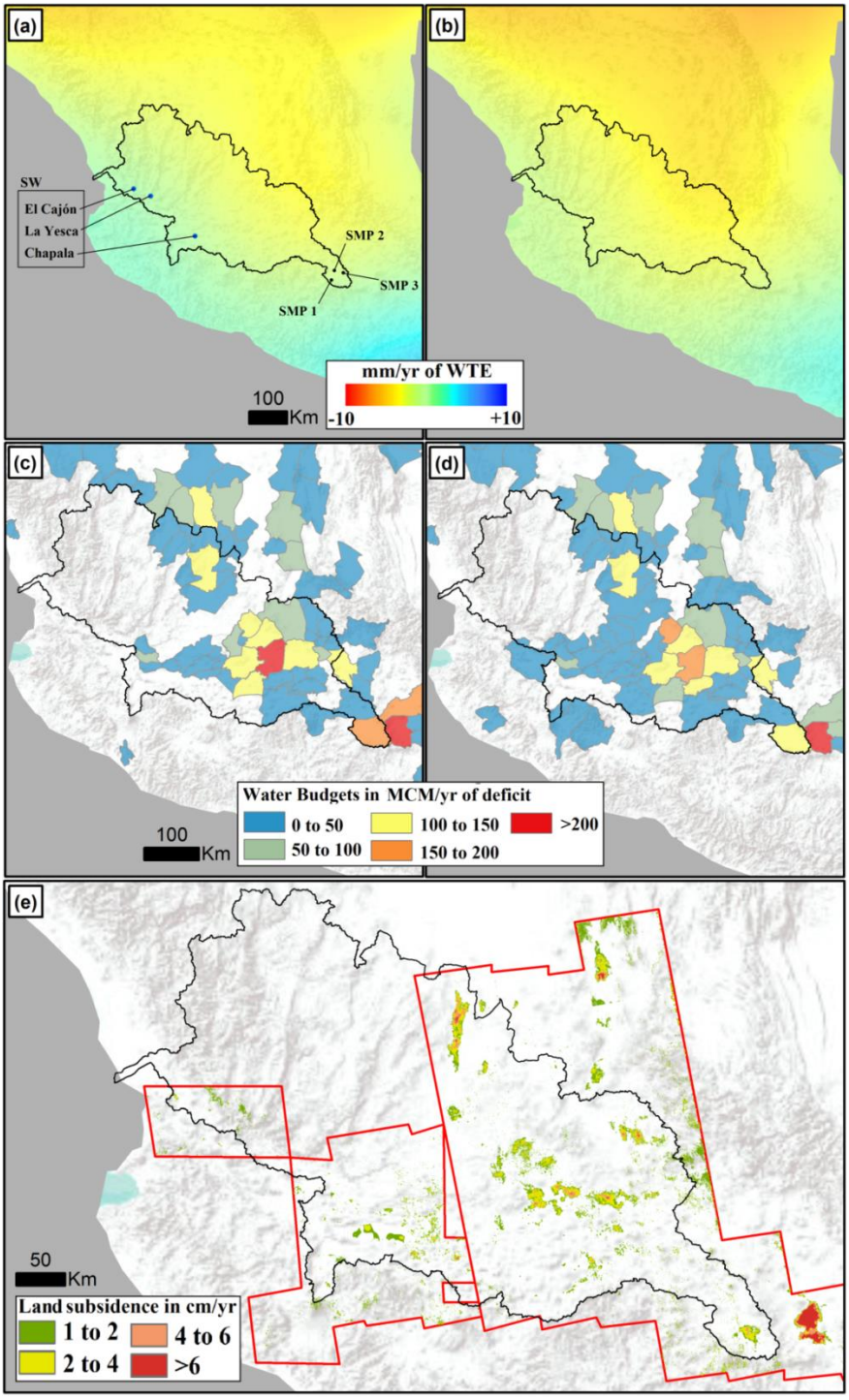

Figure 6: TWS storage trend over 2002-2014 from GRACE satellites, location of the major surface water bodies and location of the Soil Moisture Probes (a); GWS storage trend over 2002-2014 computed by removing the filtered ΔSWS and ΔSMS estimates from ΔTWS (average VIC/CLM was used for SMS - b); Water balance in aquifers

measured with the official method in 2009 (c) and in 2013 (d); Extent of the InSAR survey and InSAR-derived annual vertical ground displacement averaged over 2007-2011 (e).

Most of the exploited aquifers within the basin are unconfined, with the exception of the semi-confined aquifer of Toluca Valley (Calderhead et al. 2010, 2011, 2012a, 2012b, Davila-Hernandez et al. 2014). Their thickness typically ranges from 60 to 200 m (see an overview of the different aquifers in Castellazzi et al. 2016a). According to the InSAR results, 4.1% of the basin area subsides at rates over 1 cm/yr and the total annual volume of subsidence, i.e. the total loss of void volume in aquifer matrices, is 101 MCM/yr. By assuming a Specific yield (S_y) of 0.2, a typical value for an unconfined aquifer, it is possible to observe how the other parameters of the poro-elastic model (Eq. 6 and 7) vary to match the compaction rates in respect with groundwater depletion estimates from both GRACE and water budgets. To explain a total porosity loss of 101 MCM/yr and groundwater depletion according to GRACE estimates (from 158 to 569 MCM/yr), the average aquifer compressibility should be approximately $10^{-7.5}$ Pa^{-1} (Figure 7). Hence, we consider that such compressibility, corresponding to compressible clays, is not a realistic estimate when considering a whole aquifer or water basin. Conversely, the value of $10^{-8.5}$ Pa^{-1}, resulting from the interpretation of the GWS estimates from water budgets with the poro-elastic model, is more realistic. We conclude that InSAR observations agree more with the official water budgets than with GRACE ΔGWS trend estimates. However, we note that the heterogeneity in aquifer thickness and compressibility throughout the watershed, along with the lack of field data, limits the inversion of the InSAR measurements into volume of depleted groundwater.

This chapter is published as: Castellazzi et al. (2016), Groundwater depletion in Central Mexico: Use of GRACE and InSAR to support water resources management, Water Resour. Res. 52, 5985–6003, http://dx.doi.org/10.1002/2015WR018211

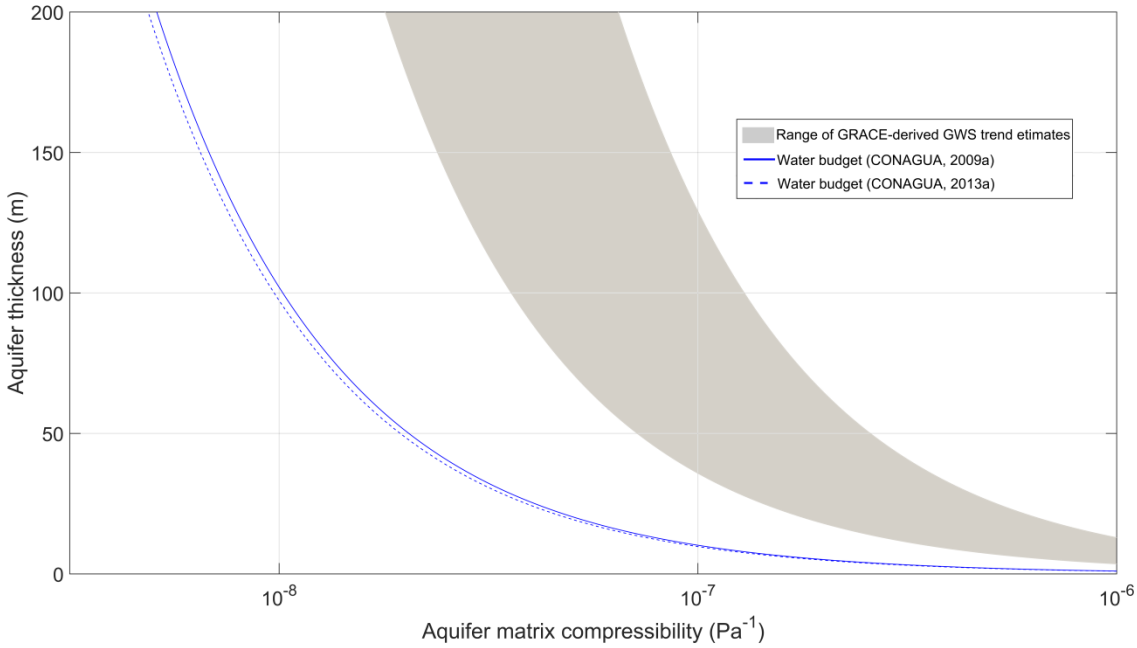

Figure 7: Possible combinations of aquifer compressibility (α) and thickness (b) values, which would explain the total aquifer void volume loss as measured by InSAR. Given the current hydrogeological knowledge of the area, the parameters values suggested by the official water budgets (CONAGUA, 2009a, 2013a) are more realistic than the range suggested by the GRACE-derived GWS trend estimates.

4.5.3. FROM GROUNDWATER EXTRACTION TO MASS LOSSES

In the basin, groundwater deficits occur mainly in urban and irrigated farmland areas (Figure 8). In Aguascalientes (Figure 8a) and in Celaya-Irapuato-Salamanca agricultural corridor (Figure 8e), land subsidence limits match well irrigated land limits, reinforcing the idea that irrigation is an important cause of deficit and land subsidence. The Guadalajara area (Figure 8b) is not facing important land subsidence despite its population density (Figure 1), because of incompressible substrate (Chaussard et al. 2014b) and water supplies relying mainly on the surrounding dams. The Toluca Valley (Figure 8c) faces important land subsidence. In this region, groundwater extraction provides water to the city of Toluca, to irrigation, and also to Mexico City through the 396 wells of the *Lerma System*. Some areas, such as Zamora and Tepic (Figure 8b and 8d) are subject to land subsidence, but are not officially declared as groundwater depletion areas by water managers (Figure 8b).

This chapter is published as: Castellazzi et al. (2016), Groundwater depletion in Central Mexico: Use of GRACE and InSAR to support water resources management, Water Resour. Res. 52, 5985–6003, http://dx.doi.org/10.1002/2015WR018211

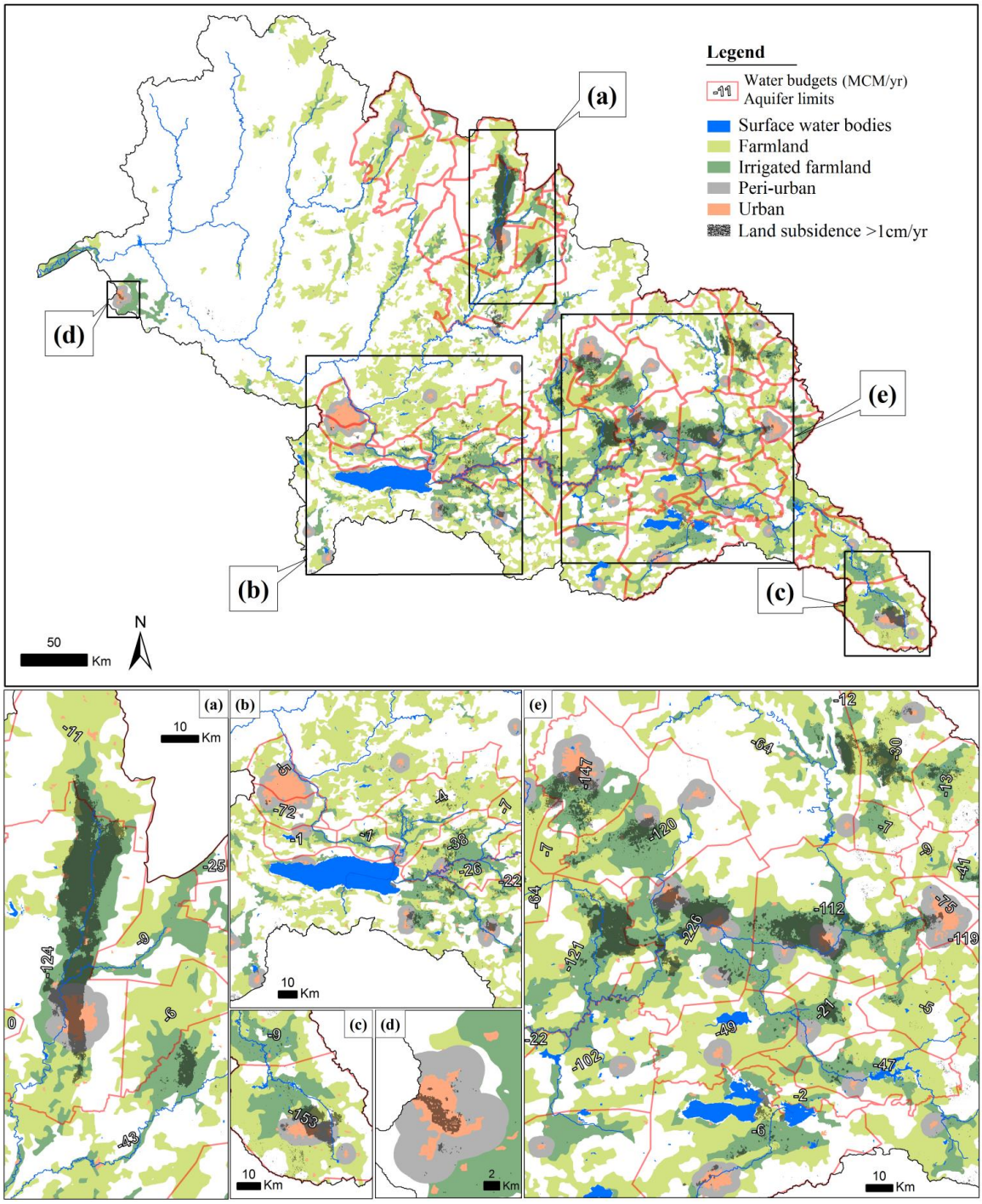

Figure 8: Land uses, land subsidence and deficit in administrative aquifers (CONAGUA, 2009a) with detailed views over Aguascalientes Valley (a), Guadalajara, Chapala Lake and Zamora area (b), Toluca (c), Tepic (d), and the Celaya-Irapuato-Salamanca Valley (e - including Morelia area in the South). Only aquifers with negative water budget balances are delimited.

This chapter is published as: Castellazzi et al. (2016), Groundwater depletion in Central Mexico: Use of GRACE and InSAR to support water resources management, Water Resour. Res. 52, 5985–6003, http://dx.doi.org/10.1002/2015WR018211

The occurrence of groundwater mass losses detectable by GRACE depends on water uses. When wastewater is discharged into natural systems, the increased hydraulic head on permeable soils and riverbeds can induce local groundwater recharge (Bouwer, 1991; Foster et al. 2004), which is not accounted in aquifer water budgets estimates. In the field, it is commonly observed that municipal and industrial wastewaters are discharged into surface water canals and streams. Infiltration events are largely observed throughout the watershed (Figure 9). Furthermore, land subsidence in highly heterogeneous lithological settings (Chaussard et al. 2014b; Castellazzi et al. 2016a) is likely enhancing infiltration through fracturing and recurring drainage failures. Surface water infiltrations due to subsidence faults have been largely observed in the region, either continuously (Rodriguez et al. 2005) or unexpectedly (e.g. fractures in Laguna Almoloya in 2008, Figure 9c, see CONAGUA, 2009b). Conversely, during irrigation, ET rates are generally high and more than 70% of the extracted water is expected to produce mass losses. Indeed, the typical annual water balance in watersheds located in semi-arid zones is approximately, in % of the total annual precipitation: ET = 70% or higher, Runoff = 20 to 25%, and Recharge = 10%.

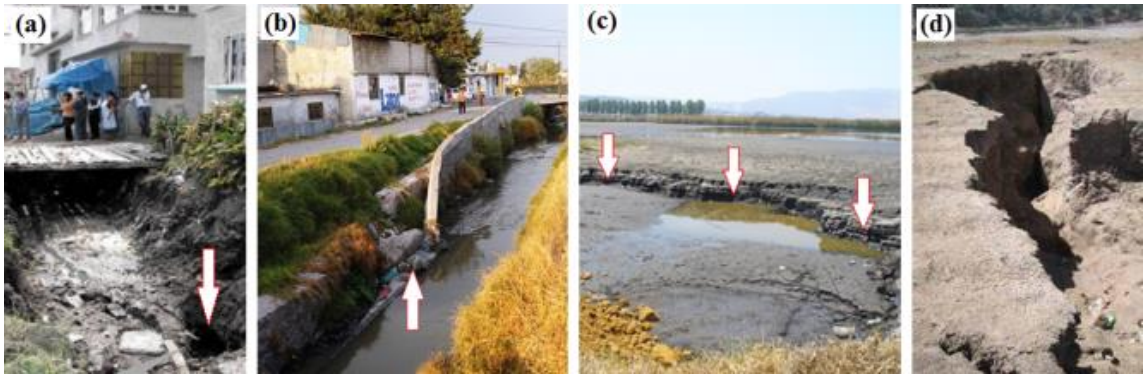

Figure 9: Examples of wastewater infiltrations in groundwater systems: wastewater canal broken by faults in San Pedro Totoltepec (Toluca Valley) in 2013 (a) and 2014 (b); sudden draining of Laguna Almoloya in San Nicolas Coatepec due to fracturing in march 2008 (c) and in a location nearby in June 2006 (d). Arrows show the fractures causing wastewater infiltrations.

While these field observations suggest higher groundwater return rates in settings where groundwater is pumped for municipal or industrial uses (namely: Urban Area,

Farmland, and Others) than for irrigation, the exact rate of water returns to the aquifers remains unknown. In such areas, the most probable fate of the extracted groundwater are: (1) recharge by infiltration in the wastewater discharge areas, (2) contribution to surface water flow, (3) direct evaporation from retention wastewater lagoons, and (4) recharge through leaks in the water distribution systems. Further studies are needed to better understand the fate of wastewater and its contribution to groundwater flow systems.

The approach suggested in section 4.3 is used to infer the importance of different water uses and their relative contribution to the observed groundwater mass loss at the watershed scale. The approach estimates the proportions of land subsidence related to the different land (and water) uses. From 29% to 44% (with and without accounting for the buffer area - Figure 10a and 10b) of the volume of compaction is potentially linked to pumping in settings where important groundwater returns occur. The analysis of GRACE-derived GWS change and related error concluded that at least 72% of the deficit estimated by the official water budgets was not detected by GRACE. These results suggest that groundwater returns, along with the error within GRACE-derived GWS trend estimates, are not fully explaining the gap between the GWS change estimates from GRACE and the official water budgets.

This chapter is published as: Castellazzi et al. (2016), Groundwater depletion in Central Mexico: Use of GRACE and InSAR to support water resources management, Water Resour. Res. 52, 5985–6003, http://dx.doi.org/10.1002/2015WR018211

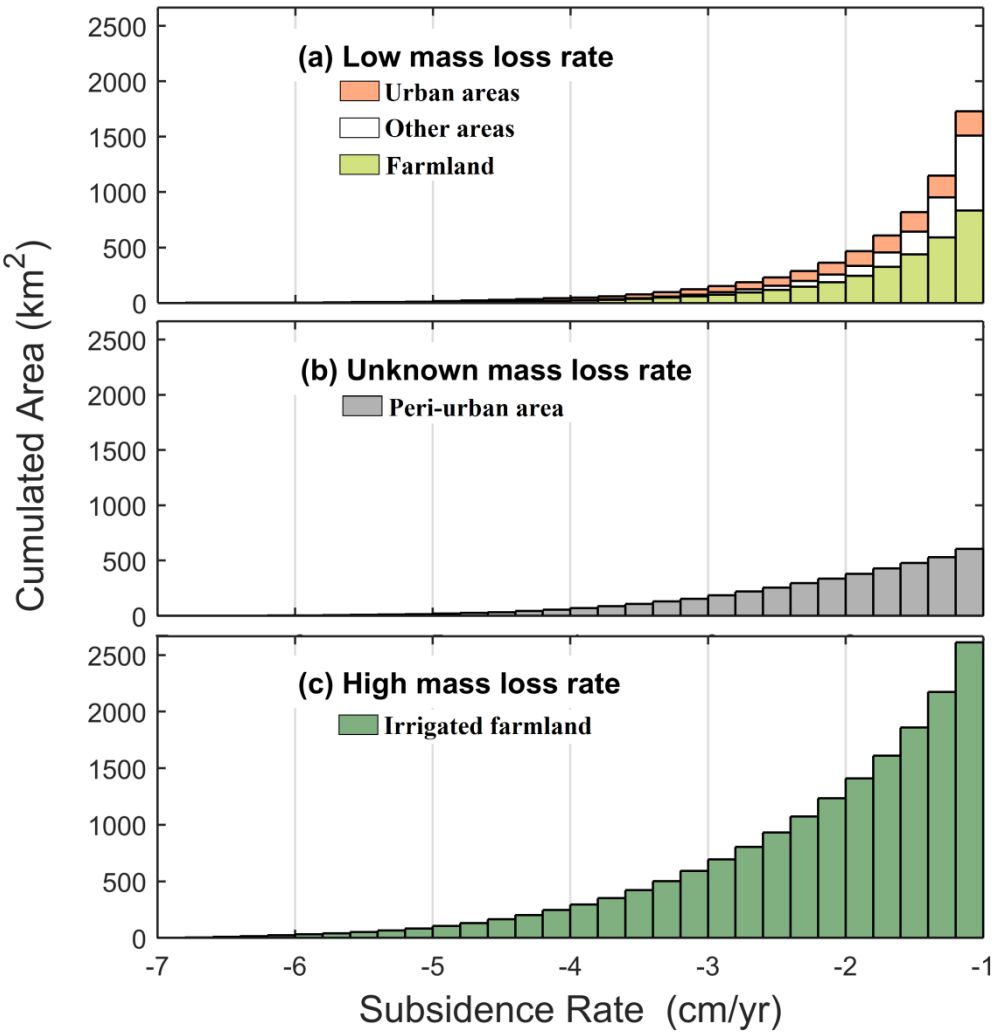

Figure 10: Cumulative histogram of the subsiding area occurring in different land use classes within LSP basin. Subsidence rates are presented according to the related groundwater mass losses occurring while fulfilling the different water needs supposed for every land use classes: low (a), unknown (b), and high (c). A direct comparison of the relative importance of groundwater uses and related mass losses can be observed by comparing the volumes of the three graphs.

We suggest that the water budget method applied for water governance in Central Mexico (CONAGUA, 2009a, 2013a) underestimates recharge due to leaks in water distribution systems and wastewater canals (see for e.g. Foster et al. 2004). Other inputs are not precisely estimated, e.g. rainfall is considered as a constant value determined for each administrative aquifer. As output, the cumulative volumes of groundwater

extraction permits are considered. Since wells are typically not equipped with flow meters, the exact amount of water extracted per well is not exactly known, hence the validity of aquifer outflow estimates is questionable. Furthermore, illegal wells are frequently reported throughout the watershed.

4.5.4. COMPARING INSAR, GRACE, AND WATER BUDGETS

Table 2 presents an overview of the ability of GRACE, InSAR and aquifer water budgets to account for the main possible returns into aquifer systems. InSAR and GRACE provide a complete 'all-integrated' perspective on deficits through compaction (InSAR) and mass loss (GRACE), but they do not account similarly for recharge occurring after large scale surficial flow. The scale at which water can flow on the surface through streams before infiltrating can vary significantly and remains unknown. While InSAR is commonly used at local or regional scales, GRACE is typically used at watershed scale, resulting in possible differences in encompassing such returns of water into the groundwater systems. Theoretically, increased recharge out of the pumping area could be detected by InSAR, but would probably not induce ground level change beyond the L-band detection threshold (around 1cm/yr). Short wavelength SAR sensor (X or C), higher revisit cycle frequency, and the PSI algorithm could be used to retrieve such small movements (Rucci et al. 2012).

This chapter is published as: Castellazzi et al. (2016), Groundwater depletion in Central Mexico: Use of GRACE and InSAR to support water resources management, Water Resour. Res. 52, 5985–6003, http://dx.doi.org/10.1002/2015WR018211

Table 2: Ability of each technique to account for groundwater returns into aquifers. Water managers use either a groundwater budget or a water budget approach to monitor the availability of groundwater in each administrative aquifer unit (detailed explanation in 2. Study area).

Returns to GW systems	InSAR	GRACE	Official groundwater governance tools	
			Flow-based groundwater budgets	Water budgets
Leaks in water distribution systems	Integrated	Integrated	Approximated	Not included
Local scale recharge by wastewater disposal	Integrated	Integrated	Not included	Not included
Large scale recharge by wastewater disposal and flow	Not included	Integrated	Not included	Not included
Recharge by irrigation	Integrated	Integrated	Approximated	Not included

4.6. CONCLUSIONS AND PERSPECTIVES

We address the possibility of assessing groundwater sustainability through the use of GRACE, InSAR, and groundwater budgets. The groundwater management agency estimated the groundwater volume loss of the administrative aquifers within LSP basin at 1998 MCM/yr in 2009 and 2095 MCM/yr in 2013. Contrastingly, GRACE only detects 158 to 210 MCM/yr of deficit. GRACE ΔGWS estimates are subject to large errors when integrated at the 100,000 -150,000 km^2 scale. Forward modeling using InSAR data is used to assess leakages effects, which only explains up to a total of 569 MCM/yr of deficit within the LSP basin.

In order to investigate these discordant observations, and by assuming a relation between land and groundwater uses, we analysed the subsidence for each land use classes and suggested mass loss rates for every class. The analysis assesses the relative importance of groundwater mass losses within the total extraction independently from GRACE data. The results suggest that approximately one third of the groundwater depletion is allocated to municipal and industrial settings, where, as observed in the field, wastewater is discharged into canals and streams. We suggest that a large part of this wastewater comes back into aquifer systems and that these returns are likely enhanced by surficial faulting related to aquifer compaction processes. The return of

This chapter is published as: Castellazzi et al. (2016), Groundwater depletion in Central Mexico: Use of GRACE and InSAR to support water resources management, Water Resour. Res. 52, 5985–6003, http://dx.doi.org/10.1002/2015WR018211

extracted groundwater to the aquifer systems limits the watershed scale groundwater depletion and suggests upcoming groundwater quality issues. Leaks in water distribution networks and uncertainties within the official water budgets are among the other possible explanations for the observed low groundwater mass loss.

While several recent studies pointed out the potential of using GRACE to globally assess groundwater sustainability and stress (Famiglietti, 2014; Richey et al. 2015), we show that the absence of groundwater mass losses on a large scale is not necessarily a proof of aquifer sustainability. Studying the fate of the extracted groundwater is essential when interpreting GRACE data. Getting the most out of different independent observation tools (including geodetic observations, *in situ* data, and local expertise), and keeping in mind their respective limitations, allows to better understand groundwater storage changes and its dynamics at different scales. Such a comprehensive understanding is a necessary step while GRACE and InSAR observations are aimed to understanding groundwater storage evolution and improve related management policies.

The combination of GRACE and InSAR observations holds promise for high resolution volumetric mapping of groundwater depletion. GRACE has a low resolution and is quantitative; InSAR has a high resolution and is not directly quantitative. The increasing coverage and availability of SAR data (e.g. Sentinel 1A/1B IW or ALOS-2 ScanSAR data) will enhance land subsidence mapping at GRACE's scale of application. Combined applications where InSAR is taken as the spatial *a priori* for mass concentrations (e.g. Farinotti et al. 2015) to refine GRACE GWS trend maps will arise. Understanding discordances between geodetic observations such as presented in this article is necessary in the perspective of such novel applications.

4.7. ACKNOWLEDGEMENTS

The authors would like to thank the Ministère des Relations internationales Francophonie et Commerce extérieur du Québec (MRIFCE - Quebec) and the Consejo Nacional de Ciencia y Tecnología (CONACyT - Mexico) for their financial support. The technical support of CONAGUA was essential for the success of the study; the authors particularly acknowledge the help of Sergio Murillo, Martin Velasco, and Oswaldo Valdez. The authors also thank Laurent Longuevergne (CNRS - Rennes,

France), Shimon Wdowinski (RSMAS - Univ. of Miami), Devin L. Galloway (USGS), and Michel Parent (Geological Survey of Canada) for their advice.

GRACE data were processed by Sean Swenson, supported by the NASA MEaSUREs Program, and are available at http://grace.jpl.nasa.gov. The GLDAS-1 data were acquired as part of the mission of NASA's Earth Science Division and archived and distributed by the Goddard Earth Sciences (GES) Data and Information Services Center (DISC).

5. ASSESSING GROUNDWATER DEPLETION AND DYNAMICS USING GRACE AND INSAR: POTENTIAL AND LIMITATIONS

Pascal Castellazzi

Institut national de la recherche scientifique, Centre Eau, Terre et Environnement, Université du Québec, 490 rue de la Couronne, Québec, QC, Canada, G1K 9A9, Phone: 418-570-3630, Fax: 418-654-2600. Email: pascal.castellazzi@ete.inrs.ca

Richard Martel

Institut national de la recherche scientifique, Centre Eau, Terre et Environnement, Université du Québec, 490 rue de la Couronne, Québec, QC, Canada, G1K 9A9, Phone: 418-654-2683, Fax: 418-654-2600. Email: richard.martel@ete.inrs.ca

Devin L. Galloway

United States Geological Survey, Water Science Field Team – West, 5957 Lakeside Boulevard, Indianapolis, IN 46278-0000, Phone: 916-801-2040. Email: dlgallow@usgs.gov

Laurent Longuevergne

Géosciences Rennes, UMR CNRS 6118. Université Rennes 1. Campus Beaulieu. 35042 Rennes Cedex, France. Phone: +33 223-236-546. Email : laurent.longuevergne@univ-rennes1.fr

Alfonso Rivera

Geological Survey of Canada, Natural Resources Canada, 490, rue de la Couronne, Quebec (Quebec) G1K 9A9, Canada. Phone 418-654-2688, Fax: 418-654-2615. Email: alfonso.rivera@canada.ca

This chapter is published as: Castellazzi et al. (2016), Assessing Groundwater Depletion and Dynamics Using GRACE and InSAR: Potential and Limitations, Groundwater 54, 768–780. https://doi.org/10.1111/gwat.12453

Keywords

Remote sensing, groundwater depletion, subsidence, gravity, InSAR, GRACE.

Abstract

In the last decade, remote sensing of the temporal variation of ground level and gravity has improved our understanding of groundwater dynamics and storage. Mass changes are measured by GRACE satellites whereas ground deformation is measured by processing SAR satellites data using the InSAR techniques. Both methods are complementary and offer different sensitivities to aquifer system processes. GRACE is sensitive to mass changes over large spatial scales (over 100,000 km^2). As such, it fails in providing groundwater storage change estimates at local or regional scales relevant to most aquifer systems, and at which most groundwater management schemes are applied. On the other hand, InSAR measures ground displacement due to aquifer response to fluid-pressure changes. InSAR applications to groundwater depletion assessments are limited to aquifer-systems susceptible to measureable deformation. Furthermore, the inversion of InSAR-derived displacement maps into volume of depleted groundwater storage (both reversible and largely irreversible) is confounded by vertical and horizontal variability of sediment compressibility. During the last decade, both techniques have shown increasing interest in the scientific community to complement available *in situ* observations where they are insufficient. In this review, we present the theoretical and conceptual bases of each method, and present idealized scenarios to highlight the potential benefits and challenges of combining these techniques to remotely assess groundwater storage changes and other aspects of the dynamics of aquifer systems.

5.1. INTRODUCTION

Groundwater systems play a central role in sustaining ecosystems and providing humanity with high quality freshwater (Taylor et al. 2013). The reliance on groundwater will probably intensify under climate change, as it affects precipitation patterns, and as adaptation strategies generally rely on groundwater resources (Kundzewicz 2007, Green et al. 2011), pointing out the necessity of adequate observation tools for management.

This chapter is published as: Castellazzi et al. (2016), Assessing Groundwater Depletion and Dynamics Using GRACE and InSAR: Potential and Limitations, Groundwater 54, 768–780. https://doi.org/10.1111/gwat.12453

As a diffusive media storing water, groundwater systems respond to natural and human-induced changes in external and internal boundary fluxes (recharge and discharge) by changes in storage and fluid pressure (head), which in turn affect flow. Groundwater depletion is one of the many objective and subjective factors used to determine the sustainability of groundwater resources. Overexploited aquifer systems typically exhibit groundwater depletion, i.e. a long-term decrease in the volume of stored groundwater (Konikow 2015). Groundwater extraction modifies the groundwater flows to satisfy pumping rates. Groundwater storage decreases as water is released from storage; the groundwater system converges towards a new equilibrium constrained by the capture of available water sources; where capture refers to both potential increased recharge and decreased discharge. For a detailed discussion of capture and groundwater depletion, see Konikow and Leake (2014). Depending upon what is deemed as acceptable consequences (environmental, economic and social) of the groundwater depletion and the effects of any induced recharge or reduced discharge such as decreased springflow or streamflow or drying lakes and wetlands, the development and use of groundwater may or may not be considered sustainable (Alley et al. 1999, Armandine et al. 2014).

Large-scale monitoring of head and storage changes generally relies on temporal responses to natural and/or anthropogenic stresses, measured as water-level changes in wells. The distribution of monitoring wells is often sparse at the scale of the groundwater system and individual wells tend to represent local conditions of the penetrated hydrogeologic units within the system. Two processes offer “distant” actions and allow observations of groundwater behavior and its spatial variability from the surface or from space. The first one is gravity: water storage changes directly participates to the changes in the mass balance and induce temporal variations of the gravity field (Pool, 2008). The second one is poro-elastic deformation; head changes induce media deformation that can be measured at the surface (e.g. Chaussard et al. 2014a, Schuite et al. 2015). These two distant actions might be measured remotely: InSAR (Interferometry of Synthetic Aperture Radar) measures Earth’s surface deformation and GRACE (Gravity Recovery and Climate Experiment) mission (Tapley et al. 2004, Schmidt et al. 2008) is sensitive to water mass changes. Both observation systems offer a new vision on groundwater response to anthropic and climatic pressures and the impact of heterogeneity on flow patterns. This paper addresses the potential and synergy of the two remote sensing tools to monitor the sustainable use of groundwater

This chapter is published as: Castellazzi et al. (2016), Assessing Groundwater Depletion and Dynamics Using GRACE and InSAR: Potential and Limitations, Groundwater 54, 768–780. https://doi.org/10.1111/gwat.12453

resources. The methods and prospective approaches presented in the following sections focus on enhancing estimates of groundwater depletion at aquifer scale that can be used by water resource managers and stakeholders to formulate criteria for the sustainable use of groundwater systems.

5.1.1. GROUNDWATER DEPLETION

Groundwater storage change (ΔGWS) can be computed using a water-budget (mass balance) approach for a specified non-equilibrium accounting period (usually annual or multi-annual) where ΔGWS is the residual of aquifer-system inflows and outflows (Eq. 1):

Equation 1: $\Delta GWS = R - (D + P)$

where R is the rate of groundwater recharge, D is the groundwater discharge rate, and P is the net rate of extraction from pumping. Another common approach uses changes in water levels to compute ΔGWS (Eq. 2):

Equation 2: $\Delta GWS = \Delta h\ A\ S$

where Δh is the change in water level (expressed as hydraulic head) for some specified time, A is the area of the aquifer representative of the head change, and S is the aquifer storage coefficient or storativity. This approach is used in numerical groundwater flow models on a per model-cell basis to compute cell-by-cell and integrated ΔGWS for the model domain. Both approaches generally rely on typically inaccurate and sparsely available field data to constrain the ΔGWS estimates, which is exacerbated by high heterogeneity of the geological media (Marsily et al. 2005), and difficulties in estimating recharge (Eq. 1) and storativity (Eq. 2).

5.1.2. AQUIFER RESPONSE: CONFINED VS UNCONFINED

To understand physical changes within depleting aquifers, it is important to examine aquifer storativity (S), i.e. the ratio between the volume of water taken into or released from storage per unit area of aquifer, per unit of hydraulic head change, which can expressed by rearranging Equation 2 as (Eq. 3):

Equation 3: $S = \Delta GWS/(\Delta h\ A)$.

This chapter is published as: Castellazzi et al. (2016), Assessing Groundwater Depletion and Dynamics Using GRACE and InSAR: Potential and Limitations, Groundwater 54, 768–780. https://doi.org/10.1111/gwat.12453

S can be calculated for unconfined (Eq. 4) and confined aquifers (Eq. 5):

Equation 4: $S = Sy + b\ Ss \sim Sy$

Equation 5: $S = b\ Ss = b\ (Ss_k + Ss_w,) = b\ (\rho\ g\ (\alpha + n\ \beta_w))$

where *Sy* is the drainage porosity, also called unconfined storativity or Specific yield, *b* is the aquifer thickness, *Ss* is the specific storage coefficient (*Ss=S/b*), Ss_k is the skeletal specific storage, related to aquifer matrix compressibility (α), Ss_w is the water specific storage, related to water compressibility (β_w), ρ is fluid density, g is the gravitational acceleration and *n* is aquifer porosity. Note that because the development of the classical groundwater storage coefficient (*S*) assumes one-dimensional vertical stress and strain, the vertical ground displacement *Δu* resulting from a change in vertical stress expressed in terms of *Δh* can be defined as (Eq. 6), where *Δu/b* is the vertical strain:

Equation 6: $\Delta u = b\ Ss\ \Delta h$

Typical values of storativity range from 5.10^{-5} to 5.10^{-3} (Todd 1980) in confined aquifers and 1.10^{-1} to 3.10^{-1} in unconfined aquifers (Lohman 1972); i.e. unconfined storativity (Sy) is about two to four orders of magnitude larger than confined storage. The ideal aquifer response (drawdown, or *Δh*) to pumping at a specified rate in both types of aquifers of infinite extent (assuming similar hydraulic conductivity and other aquifer properties) results in a larger extension/volume of the cone of depression for confined aquifers. Put another way, the change in storage (ΔGWS) needed to supply the pumping volume is derived from a larger volume of the aquifer material for confined versus unconfined conditions. This analysis applies to porous media only.

5.1.3. HYDRAULIC HEAD RESPONSE

The Cooper-Jacob solution is an approximation of the Theis non-equilibrium method (Theis 1935) for the calculation of the radius of influence of a steadily pumping well as a function of storativity and time in an ideal confined aquifer (Cooper and Jacob 1946; Dragoni 1998). It relies on the assumptions of horizontal isotropic, homogeneous aquifers of infinite extent, and fully penetrating wells. It can be used for unconfined aquifers with proper correction. Figure 1 shows the radius of influence (Figure 1a) and the drawdown (h_0-h; where h_0 is the initial head prior to the imposed pumping stress) as a function of aquifer storativity (*S*) using the Theis (Fig 1b) and the Cooper-Jacob (Fig

This chapter is published as: Castellazzi et al. (2016), Assessing Groundwater Depletion and Dynamics Using GRACE and InSAR: Potential and Limitations, Groundwater 54, 768–780. https://doi.org/10.1111/gwat.12453

1b) solutions. Note that: (1) the Cooper-Jacob solution should not be used for unconfined conditions without Jacob's correction for partial dewatering of water-table aquifers (e.g. transmissivity changes, see Halford et al. 2006); and (2) the Theis solution can be used for unconfined conditions only when the late-time segment of the Theis well function is considered (Theis 1935; Van der Kamp 1985; Kruseman and De Ridder 1991), i.e.when the delayed water-table response can be overlooked.

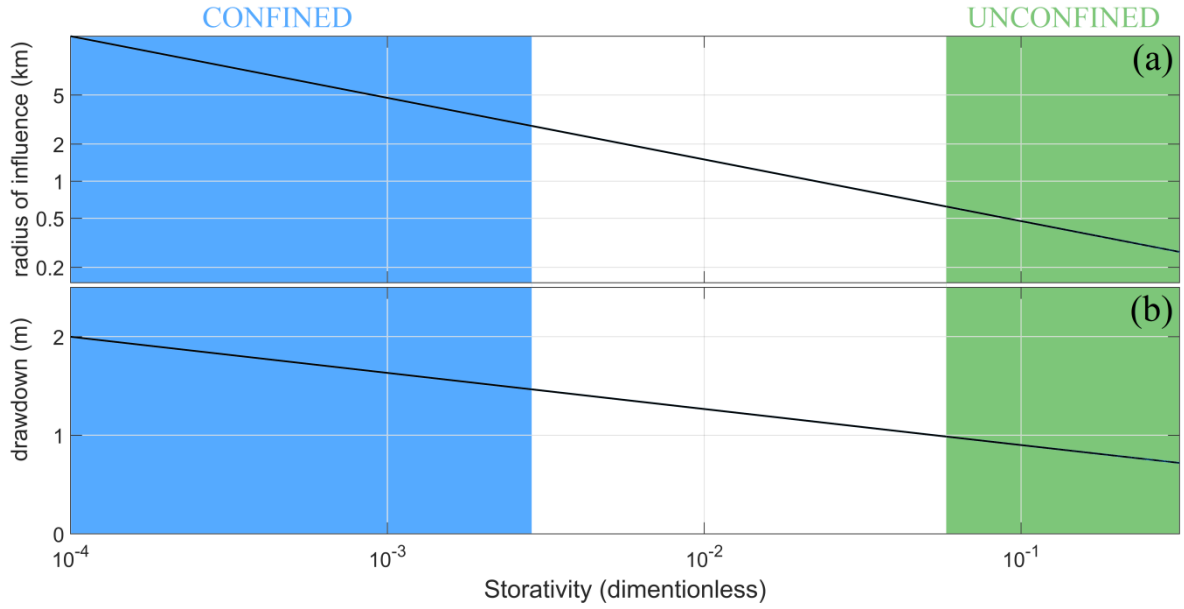

Figure 1: a) Storativity vs radius of influence according to the Cooper-Jacob approximation; b) storativity vs drawdown in an observation well located 50 m distant from a pumping well according to the Theis non-equilibrium equation. Typical values of storativity are highlighted in blue for confined conditions, and in green for unconfined conditions. Transmissivity is 100 m2/day, 100 days of pumping at a constant rate of 200 m3/day.

The radius of influence, i.e. the horizontal effect of head loss, increases strongly when storativity decreases (Figure 1a). The cone of depression is deeper near the pumping well and spreads more widely for confined versus unconfined conditions. While the total mass change is equivalent for both cones of depression, the mass changes nearby the pumping center are larger for the unconfined aquifer compared to the confined aquifer. This partially explains good correlations between water levels and local microgravity measurements in areas near hydraulic stresses and in unconfined aquifers (Pool and Eychaner 1995, Pool 2008). For confined aquifer conditions, the correlation is

This chapter is published as: Castellazzi et al. (2016), Assessing Groundwater Depletion and Dynamics Using GRACE and InSAR: Potential and Limitations, Groundwater 54, 768–780. https://doi.org/10.1111/gwat.12453

poorer (e.g. Pool 2008), because mass changes are less concentrated in the near-field region around the pumping well.

5.1.4. AQUIFER SYSTEM COMPACTION

Groundwater depletion can lead to ground subsidence. Analysis and simulation of aquifer-system compaction have been addressed primarily using two approaches: one based on the conventional groundwater flow theory (Jacob 1940) and one based on the linear poro-elasticity theory (Biot 1941). The former approach is a special case of the latter, and both approaches are based on the principle of effective stress (Terzaghi, 1925). For the discussions here we follow the approach of Hoffmann et al. (2003b) based on conventional groundwater flow theory. Assuming incompressible solid grains, and only vertical effective stresses and vertical strains, the effective stress principle can be expressed (Eq. 7):

Equation 7: $\sigma_t = \sigma_e + p$

where p is the interstitial fluid pressure, σt is the total vertical stress, and σ_e is the vertical effective stress. For the case of constant total stress (where $\Delta\sigma_t = 0$), Equation 6 can be simplified and expressed in terms of changes (Δ) in stress (Eq. 8):

Equation 8: $\Delta\sigma_e = -\Delta p = -\rho\, g\, \Delta h$

where ρ is the water density and g is the gravitational constant.

The response of saturated geological media to increase in effective stress is governed by the matrix and fluid compressibilities embodied in the skeletal and water specific storage terms constituting the aquifer storativity of the material (Eq. 5). The most compressible and porous materials are clay and silt, and the least compressible have a compressibility of the same order of magnitude as water (Domenico and Mifflin 1965; Freeze and Cherry 1979). In these compressible materials, the effective stress increases the compression of the aquifer skeleton, decreasing porosity, and to a certain extent decreasing *Ss* and hydraulic conductivity (*K*). Additionally, compressible, typically low-permeability fine-grained units in layered heterogeneous aquifer systems play a major role in impeding vertical groundwater flow between more permeable, typically coarser-

This chapter is published as: Castellazzi et al. (2016), Assessing Groundwater Depletion and Dynamics Using GRACE and InSAR: Potential and Limitations, Groundwater 54, 768–780. https://doi.org/10.1111/gwat.12453

grained hydrogeologic units. Depending on the continuity of the fine grained units and their position within the aquifer system, they usually form either confining units between aquifer systems, or discontinuous interbeds within the aquifers. In overexploited unconfined aquifers, decrease in the effective stress occurs in underlying confined aquifers according to the decreased in geostatic stress. This phenomenon should be taken into account when interpreting or predicting ground displacements Δu related to depleting unconfined aquifers (see e.g. Leake and Galloway, 2007). For a more complete description and review of land subsidence caused by aquifer-system compaction see Galloway and Burbey (2011).

5.2. DETECTION OF GROUNDWATER DEPLETION

5.2.1. INSAR

Several techniques are available to measure ground displacements, including primarily borehole extensometers, GPS, conventional surveying, LiDAR, and InSAR. It is possible to monitor both trends and seasonal variations of the ground level with proper use of any of these techniques. InSAR is increasingly used in hydrogeology (Galloway and Hoffmann 2007; Galloway 2014) due to its precision reaching a few mm/yr, its spatial coverage typically between 100 to 5,000 km^2, and its cost-efficiency.

a) Principle and application

InSAR consists in interpreting phase shift between several Synthetic Aperture Radar (SAR) acquisitions taken from the same orbital track. Parameters influencing the phase shift, such as the perspective change due to difference in satellite position in space between acquisitions (spatial baseline) and the atmospheric effects can be estimated and removed from the measured phase shift. The remaining phase shift component is the temporal change of the satellite Line Of Sight (LOS) distance.

There are currently three main InSAR processing workflows used in hydrogeological applications: Differential (D), Small Baseline Subset (SBAS), and Persistent Scatterers Interferometry (PSI). With the D-InSAR technique, two SAR images acquired at different times are used to create a phase shift map, called interferogram (Rocca et al. 1997; Massonnet and Feigl 1998). The phase difference map is wrapped over phase cycles ($-\pi$ to $+\pi$), and can be converted to real displacement values using a spatial phase

This chapter is published as: Castellazzi et al. (2016), Assessing Groundwater Depletion and Dynamics Using GRACE and InSAR: Potential and Limitations, Groundwater 54, 768–780. https://doi.org/10.1111/gwat.12453

unwrapping algorithm. The SBAS technique uses numerous (usually tens to hundreds) interferograms selected within all possible combination offered by several SAR acquisitions. The interferograms are produced and corrected following the D-InSAR approach and the SBAS algorithm (Berardino et al. 2002; Lanari et al. 2004) is used to retrieve surface displacement through time along the SAR images time-series. PSI is also a time-series technique but only the phase history of highly coherent and stable scattering targets is used (Ferretti et al. 2000a, 2001). The spatial phase unwrapping used in SBAS or D-InSAR is replaced by a temporal phase unwrapping calculated for each target using the temporal history of the phase individually for each target. Consequently, PSI provides a greater accuracy over persistent and coherent targets than SBAS (Pasquali et al. 2011) but is limited to areas with a high density of stable targets (e.g. buildings or bedrock outcrops), making it less appropriate for non-urban settings (e.g. agricultural areas relying on groundwater-supplied irrigation).

Galloway and Hoffmann (2007) enumerate the main uses of InSAR in hydrogeology: (1) Identify litho-stratigraphic and structural boundaries in groundwater-flow systems; (2) identify aquifer-system heterogeneity; (3) estimate aquifer-system hydro-mechanical properties; and (4) constrain numerical models of groundwater flow, aquifer-system compaction and land subsidence. The most comprehensive use of InSAR in hydrogeology is its integration in flow model calibration (e.g. Hoffmann et al. 2003a, Yan and Burbey 2008, Siade et al. 2014). More recently, InSAR-derived ground displacement mapping has been used to: (1) estimate storage change within a well-known lithological context (e.g. Chaussard et al. 2014b); (2) improve lithological knowledge and define specific geological structures such as fractures (e.g. Hernandez-Marin and Burbey 2009, Xu et al. 2012; Zhang et al. 2014; Castellazzi et al. 2016a); (3) predict future land subsidence rates (e.g. Calderhead et al. 2011); and (4) infer changes in hydraulic head after a calibration period relating ground and groundwater levels (Reeves et al. 2011; Chaussard et al. 2014a).

b) Resolution, accuracy and challenges

The large variety of SAR sensors available and the diversity of acquisition options in LOS angle, resolution, and coverage, make the technique adaptable to detect displacement in almost any settings. SAR acquisitions have spatial resolution ranging

from 1 m to 50 m and extend over 10 to 200 km in both length and width (more strictly, range and azimuth).

In the case of D and SBAS-InSAR, the resolution should be decreased by a factor of 2 to 5 to improve the signal/noise ratio and allow a consistent spatial phase unwrapping. The development of InSAR processing algorithms combined with the rising availability of large SAR images stacks allow to routinely monitor ground displacements with an accuracy of 1 to 4 mm/yr (e.g. Samsonov et al. 2010, 2014).

The main challenges of InSAR application to water science is linked to the loss of coherence in natural system (vegetated, agricultural areas). The loss of interferometric coherence is usually proportional to the vegetation height and inversely proportional to the SAR wavelength. While patches of trees in urban settings are usually smoothened by down-sampling or compensated by interpolating the final results, the lack of coherence is a problem where high vegetation is dominant throughout the land cover (e.g. crops, forest). For example, short wavelength SAR (e.g. 3.1 cm wavelength of TerraSAR-X) would not allow ground displacement detection in farmland and scrublands, and coherence would only be sufficient in urban settings. To overcome the problem, longer SAR wavelengths (e.g. 23 cm wavelength of ALOS-1/2) can be used at the cost of larger displacement detection threshold (around 1 cm/yr) and a lower vertical precision. Atmospheric effects also affect InSAR results at the scale of up to few mm/yr, but they can be almost completely taken into account while using recent sensors and methodological improvements (Ferretti et al. 2007, Rucci et al. 2012). In hydrogeology, the displacement detected by InSAR is often assumed to be entirely linked to aquifer compaction. At the cm/yr scale, the spatial patterns of aquifer compaction are usually well distinguishable from sediment erosion, sediment deposition, landslides, volcanism, or tectonic fault movements. While the potential application arising by retrieving ground displacements at the mm/yr scale are important (Schuite et al. 2015), their interpretation remains a challenge when several displacement causes may coexist.

The SAR phase should be comparable between successive acquisitions. If the differential movement between two acquisitions of a SAR time-series is higher than the length of a SAR wave phase, and if this movement is not spatially progressive, phase ‘jumps’ occur and the inversion of the phase into displacement is compromised. For this

This chapter is published as: Castellazzi et al. (2016), Assessing Groundwater Depletion and Dynamics Using GRACE and InSAR: Potential and Limitations, Groundwater 54, 768–780. https://doi.org/10.1111/gwat.12453

reason, the temporal density of an InSAR images stack, i.e. the time interval between images, should adequately match the expected displacement rates, which can often be roughly anticipated (+/-50%) considering either the hydrogeological knowledge of the area, previous InSAR studies, other available ground displacement measurements, or comparable cases. Ideally, to retrieve a constant subsidence rate of 5 cm/yr with the original PSI technique (i.e. PSInSAR^{TM}, see Ferretti et al. 2001), the SAR time-series should be constructed of at least seven images per year in X-Band, four images per year in C-band, and one image per year in L-band (wavelength of 3.1, 5.6, and 23 cm, respectively). If the subsidence is spatially progressive, stronger subsidence rates can be retrieved through the spatial phase unwrapping typically used in D and SBAS, and implemented in some PSI algorithms (see Crosetto et al. 2016). Other parameters should be taken into account e.g. the noise level of the SAR data, the phase unwrapping technique, and the temporal variability of the ground displacements. Consequently, a comfortable margin in the temporal density of the time-series is always preferred. Users should be aware that the temporal density of the acquisition forming a SAR time-series is limited by the orbital cycles of the spacecraft, usually from 10 to 46 days. The recent Sentinel-1A and 1B system provides comparable images every 6 days.

c) Data availability, current developments, and future missions

Several space-borne SAR launch mission are currently operating: Radarsat-2 (C-Band, Canadian Space Agency), Sentinel-1A and 1B (C-Band, European Space Agency), TerraSAR-X (X-Band, German Aerospace Center), COSMO-SkyMed (X-Band, Italian Space Agency) and ALOS-2 (L-Band, Japan Aerospace eXploration Agency). Archived SAR time-series from past or current missions are increasingly available at no cost. Data from ERS-1, ERS-2, and ENVISAT are available upon application (https://earth.esa.int). They are covering the periods 1991-2000, 1995-2011, and 2002-2011, respectively. ALOS-1 data covers 2006-2011 and are available upon registration (https://www.asf.alaska.edu). From 2014, Sentinel-1 mission provides free and high quality data to InSAR specialists (https://sentinel.esa.int or https://peps.cnes.fr).

Recent advancement in space-borne SAR sensor, as seen in the recent Sentinel mission, provides: 1) an ever improving signal/noise ratio, allowing to produce and unwrap interefrograms at full resolution and to retrieve fine spatial details of ground deformation; 2) a higher repeat path frequency, allowing e.g. to infer seasonal ground

This chapter is published as: Castellazzi et al. (2016), Assessing Groundwater Depletion and Dynamics Using GRACE and InSAR: Potential and Limitations, Groundwater 54, 768–780. https://doi.org/10.1111/gwat.12453

level variations with high temporal details, and relate them to seasonal recharge and discharge patterns; and 3) an increased spatial coverage, allowing e.g. its use at GRACE scale and related applications as described in this article.

At least two new SAR mission are planned for launch in the next years: Radarsat Constellation (C-Band, Canadian Space Agency) and NiSAR (L and S-Band, US National Aeronautics and Space Administration and The Indian Space Research Organisation). Some of the recent (e.g. Sentinel) and upcoming missions consist in positioning two to three SAR satellites on different orbital configurations, allowing to: (1) cover the entire earth surface more frequently; (2) generate Digital Elevation Model (DEM) with large-baseline interferometry of two synchronous SAR acquisitions taken from different spacecraft; and (3) simulate an higher repeat path frequency to improve earth deformation monitoring with time-series InSAR.

5.2.2. GRACE

The GRACE satellite mission (Tapley et al. 2004) has provided new insights into mass redistribution within the Earth's system and offers new perspectives in hydrology.

a) Principle and application

As the first two satellites of their generation, GRACE is monitoring spatio-temporal changes in the Earth's gravity field with an unprecedented resolution, allowing interpretation of mass changes within hydrosystems (see e.g. Cazenave and Chen, 2010). The system comprises two satellites on a ~450 km altitude orbit track and about 200 km apart. Distance between the satellites is measured at the micrometer level allowing detection of a one centimeter Water Thickness Equivalent (WTE) distributed over an area at the scale of the system's altitude, i.e. with a diameter of a few hundred kilometers. Gravity has two fundamental advantages. First, the link between gravity and mass storage is direct, independent of lithology and requiring no calibration. Second, the distant effect allows to penetrate Earth's at depth and record mass storage in groundwater systems. GRACE integrates vertically all water storage components. The groundwater contribution can be inferred by removing all other components from the Total Water Storage change (ΔTWS) measured by GRACE (Eq. 9):

Equation 9: $\Delta GWS = \Delta TWS - (\Delta SWS + \Delta SMS + \Delta SIS)$

This chapter is published as: Castellazzi et al. (2016), Assessing Groundwater Depletion and Dynamics Using GRACE and InSAR: Potential and Limitations, Groundwater 54, 768–780. https://doi.org/10.1111/gwat.12453

where ΔSWS is the surface water storage variations; ΔSMS is the water storage variations in the soil unsaturated zone; and ΔSIS is the snow and ice water storage variations. In quantitative hydrogeology, the main difficulty of using GRACE is gathering enough field data and/or model output to account for surface-water, soil-moisture and snow/ice storage. Typically, ΔSIS and ΔSWS can be estimated using in situ or satellite altimetry data, and ΔSMS can be estimated using large scale models (Land Surface Models - LSM). ΔSWS, ΔSMS, and ΔSIS contribute to uncertainties in GWS estimation.

Since 2002, GRACE has provided unique and decisive data to understand, monitor, and model continental water cycle and exchanges between storage compartments (continents, atmosphere, and oceans). GRACE allowed monitoring of groundwater storage changes in natural or engineered systems (e.g. Rodell et al. 2009; Famiglietti et al. 2011; Huang et al. 2012, Richey et al. 2015). The approach was validated by comparison with well data in various climatic contexts (Scanlon et al. 2012, Shamsudduha et al. 2012, Feng et al. 2013, Forootan et al. 2014). Integration of GRACE data in groundwater studies includes the assimilation into models (as validation or calibration) to improve their predictive ability (Guntner et al. 2007, Zaitchik et al. 2008, Sun et al. 2012, Xie et al. 2012, Döll et al. 2012, Eicker et al. 2014, Hu and Jiao, 2015).

b) Resolution, accuracy and challenges

GRACE is sensitive to large scale storage changes. Several authors have suggested that GRACE data could be safely interpreted for basins of at least 200,000 km², and with a sensitivity of ~10 mm (i.e. ~ 2 km^3). Yet, GRACE is not a regular remote sensing tool, and offers a gravitational resolution, i.e. sensitive to mass. Several papers have shown that the same mass concentrated over small area are recoverable (Longuevergne et al. 2013, Tourian et al. 2015). Therefore, there are potential to monitor high storage variability, such as the recharge zone of an aquifer system (Huang et al. 2015).

GRACE range rate data (distances between the two satellites - Level 1B data) should be processed and converted into mass changes and water storage changes in WTE (Level-3 data) to be used for hydrological applications. The most common processing strategies rely on converting the signal into Spherical Harmonics coefficients (Stockes

This chapter is published as: Castellazzi et al. (2016), Assessing Groundwater Depletion and Dynamics Using GRACE and InSAR: Potential and Limitations, Groundwater 54, 768–780. https://doi.org/10.1111/gwat.12453

coefficients, Level 2). Then, the coefficients are combined to spatial domain over a grid and filtered. Because of its sensitivity to larger scales, computed mass changes are generally affected by amplitude loss and require rescaling to produce Level-3 data. Landerer and Swenson (2012) and Long et al. (2015) proposed the use of scaling factors based on a-priori mass variations from LSM. In the recent years, with increasing experience of GRACE data, several novel processing strategies have arisen to improve the spatial resolution (e.g. Bruinsma et al. 2010; Ramillien et al. 2011; Save et al. 2012). Among them, mass concentration solutions, or 'mascons', are particularly suited for hydrological applications (e.g. Watkins et al. 2015, Sakumura et al. 2016). Inter-comparison of different products has been recently carried out by Farinotti et al. (2015) and shows the large potential of these new datasets to work at scales closer to the groundwater management scale (scales ~ 100,000 km²). For details on GRACE TWS processing to extract GWS contribution, associated uncertainties linked to GRACE large-scale sensitivity (truncation, filtering, leakage), and estimation of storage compartments (Equation 9), the interested reader can refer to Longuevergne et al. (2010), Scanlon et al. (2012), and Long et al. (2016).

c) Data availability, current developments, and future missions

Several versions of GRACE data are available online and free of charge. Official solutions from The Center for Space Research (CSR – USA), The Jet propulsion Laboratory (JPL – USA) and The GFZ German Research Centre for Geosciences (GFZ – Germany) are popular (see http://gracetellus.jpl.nasa.gov/). Other solutions are available online at The Institute of Theoretical Geodesy and Satellite Geodesy (Graz University of Technology - Austria) and The Research Group for Space Geodesy (GRGS - French National Space Center) websites. The University of Colorado and GRGS created interactive portals to compute GRACE time-series over a region, a country, or a watershed (http://geoid.colorado.edu/grace and http://thegraceplotter.com/).

The use of GRACE in hydrogeology is still limited to the largest systems, for which it can be considered as one of the observation system in the hydrogeologist's toolbox (Alley and Konikov, 2015). For further application and resolution of scientific challenges, the main limitation of GRACE is the limited spatial resolutions as well as the limited length of the available observations (see e.g. Scanlon et al. 2015). A recent

This chapter is published as: Castellazzi et al. (2016), Assessing Groundwater Depletion and Dynamics Using GRACE and InSAR: Potential and Limitations, Groundwater 54, 768–780. https://doi.org/10.1111/gwat.12453

consensus on the science and user needs for future satellite gravity observing systems has been synthetized in Pail et al. (2015). Waiting for the next generation of satellite gravity missions, the GRACE follow-on mission is planned for 2017.

5.3. THEORETICAL SCENARIOS

Identical groundwater withdrawal and use in each situation results in identical storage change volumes when integrated across the system area, while the spatial distributions of storage changes and compaction can be different for each case (Figure 2). In this section, the differences are discussed for three typical and theoretical types of hydrogeological settings, where water is extracted from an unconfined aquifer (A), from the confined part of a regional aquifer (B), and from a confined (C_1) or semi-confined aquifer (C_2).

In an unconfined aquifer (Figure 2A), groundwater is extracted from the unconfined storage or drainage porosity (Sy), the radius of influence due to pumping is focused on the pumping center and is smaller compared to a confined aquifer setting (see the effect of confinement on the radius of influence on Figure 1), i.e. mass losses would be detectable by microgravity measurements located near the pumping center. InSAR and GRACE could both detect groundwater depletion if water is pumped beyond the sustainable rate and for InSAR only if the aquifer contains compressible sediments. Often, the return flows of the non-consumptive-use fraction of the extracted groundwater are difficult to assess and may not be properly accounted in groundwater budgets (see e.g. Foster et al. 2004). These components of the water budget typically are approximated, and may be based on available observed responses of the aquifer system, such as water levels, compaction or mass loss.

Regional aquifer system with focused recharge (Figure 2B) typically occur in sedimentary basins, where fine grained sediments with low permeability occur in lowlands and highly coarse and permeable sediments occurs in the higher elevation and slopes (e.g. Calderhead et al. 2012b). Often, urban developments and groundwater extraction take place in the lowest altitude of the valley. In these settings, mass losses attributed to groundwater storage changes over the area of head loss would be diffusely spread throughout the confined aquifer (larger radius of influence). In this section of the aquifer, and if it is susceptible to compaction, the detectable gravity change could be

This chapter is published as: Castellazzi et al. (2016), Assessing Groundwater Depletion and Dynamics Using GRACE and InSAR: Potential and Limitations, Groundwater 54, 768–780. https://doi.org/10.1111/gwat.12453

attributable in part to aquifer compaction. In fact, there are two mechanisms of gravity change in compacting aquifers, elevation change and mass change. Elevation change is linked to the storage derived from compaction, while gravity change is a measure of total storage change if corrected for elevation change. The area of hydraulic head changes (see Figure 1b) may spread to the recharge area, which lead to head decline in the unconfined section of the aquifer, and where head changes correlates well with mass losses. Additionally, head losses in the pumping area can be partially compensated by regional flows. However, given that the typical groundwater transport times over large areas covered by GRACE are of long duration, this regional-scale adjustment to the pumping area does not likely affect the reliability of ΔGWS assessment from GRACE. In such settings, the water budget should integrate a wider area, encompassing recharge and discharge areas, and integrating spatially variable inflows and outflows. Compaction of susceptible aquifer systems typically occurs nearby pumping areas, where detection through local microgravity measurements corresponds to the change in groundwater storage derived principally from skeletal storage (Ss_k) and the change in land-surface altitude (Pool, 2008). Both InSAR and microgravity measurements will be sensitive to spatial variability in the response of the aquifer system, while GRACE would integrate the whole affected area.

In a closed, non-leaky, confined and fossil aquifer (Figure $2C_1$), extracted groundwater is derived from the confined storage, i.e. the matrix and fluid compressibilities embodied in S_{sk} and S_{sw}, respectively. Mass losses spread horizontally due to low storativity (large radius of influence, see Figure 1), any compaction and resulting land subsidence is similarly distributed. The water balance (Eq. 1) is inexorably negative. Because the groundwater resource in this aquifer is finite, consumptive uses of the groundwater constitute groundwater mining, though some return flow of non-consumptively used groundwater extracted from the aquifer could replenish a shallow, hydraulically isolated overlying unconfined aquifer. The negative balance for the confined aquifer could theoretically be detectable by GRACE, but this measurement can possibly be confounded by infiltration of any return flow (recharge) to soil-moisture storage and/or an overlying unconfined aquifer. InSAR alone cannot be used to determine the state of the water balance for that system, but can provide evidence of groundwater depletion in the confined aquifer (inelastic compaction and largely irreversible land subsidence) in affected areas within the system. The volume of land

This chapter is published as: Castellazzi et al. (2016), Assessing Groundwater Depletion and Dynamics Using GRACE and InSAR: Potential and Limitations, Groundwater 54, 768–780. https://doi.org/10.1111/gwat.12453

subsidence mapped using InSAR could be used as an estimate of the volume of largely irreversible storage depletion owing to the inelastic compressibility of the aquifer skeleton.

When the same type of aquifer receives water derived from leakage of an overlying unconfined aquifer (Figure 2C$_2$), the horizontal spread of drawdowns, mass losses and compaction are limited proportionally to the leakage.

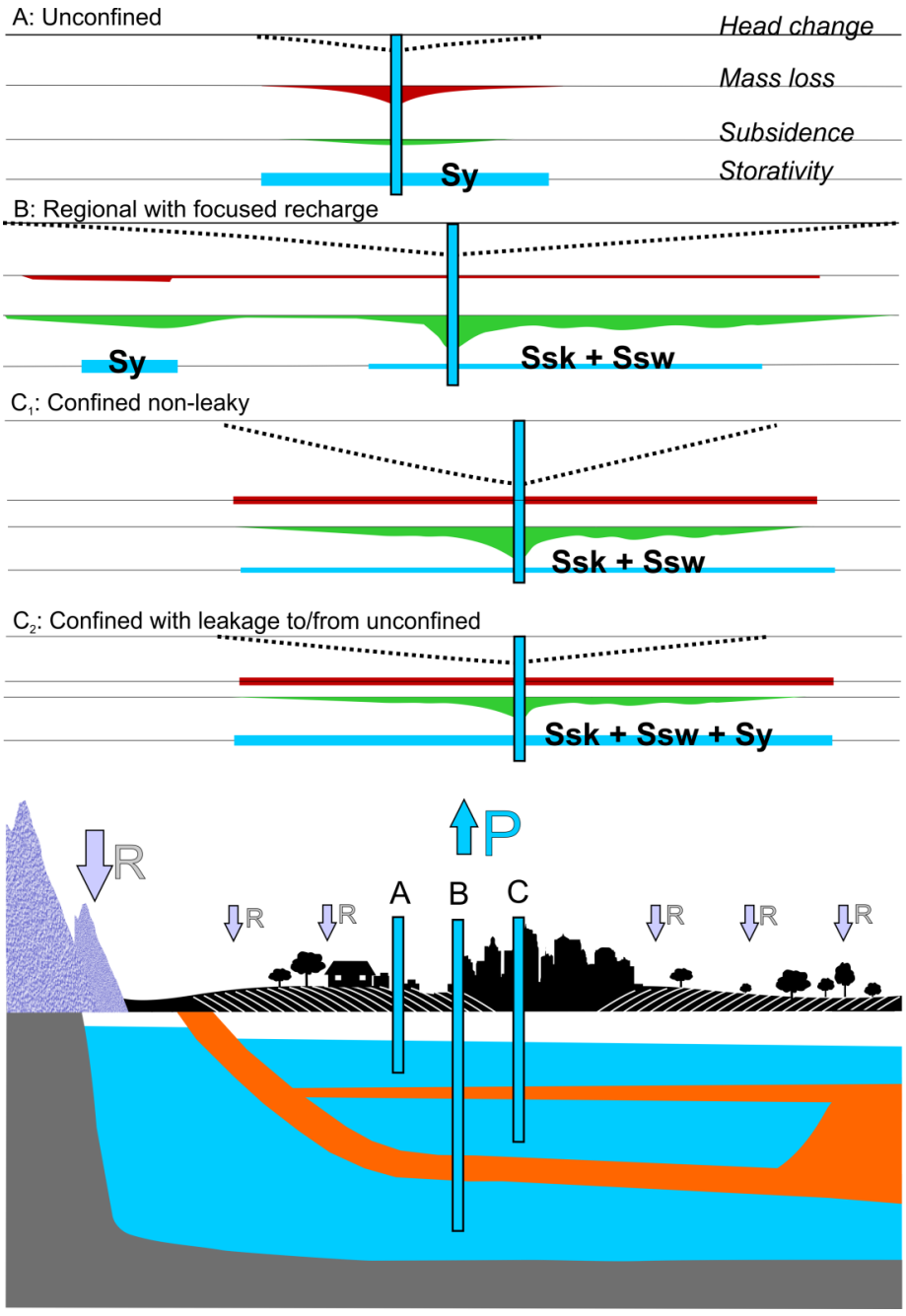

Figure 2: Conceptual models of land subsidence and mass losses occurrence in different idealized depleting aquifers (P: Pumping; R: Recharge).

This chapter is published as: Castellazzi et al. (2016), Assessing Groundwater Depletion and Dynamics Using GRACE and InSAR: Potential and Limitations, Groundwater 54, 768–780. https://doi.org/10.1111/gwat.12453

5.4. POTENTIAL BENEFITS OF COMBINING GRACE AND INSAR

In the perspective of enhancing the capabilities of both techniques, we discuss four different potential approaches based on their combination.

5.4.1. TOWARD HIGH RESOLUTION AND VOLUMETRIC GROUNDWATER DEPLETION MAPPING

The global volumetric and high spatial resolution mapping of groundwater storage changes is needed to fully support groundwater governance and assure sustainability of groundwater resources. Toward this objective, and where aquifer-system compaction is systematically linked to groundwater storage loss, InSAR can be used to partially overcome GRACE resolution limitations.

InSAR-derived groundwater depletion mapping can be used as a quantitative or non-quantitative synthetic data as input into GRACE GWS change estimates. Indeed, while scaling factors derived from soil moisture models fails in downscaling GRACE-derived GWS trend maps, InSAR provides the proper downscaling data. The injection of InSAR measurement into GRACE data assumes that the reaction hydraulic head/compaction is stable throughout a large study area. Additionally, InSAR can also be inserted into the GRACE estimates as a groundwater depletion detection tool in a non-quantitative manner, providing only a spatial *a priori* of mass loss concentrations for GRACE GWS trend maps. Such approach was tested with success for glacier mass losses detection using GRACE (Farinotti et al. 2015). In all cases, compressible hydrogeologic units need to be present throughout the study area and drawdown should be large enough to induce compaction and subsidence within the detectability range of InSAR. Another limitation of such approach resides in the confusion between climatic and anthropogenic GWS change in GRACE data.

5.4.2. REMOTE ASSESSMENT OF AQUIFER REACTION TO PUMPING

Both short-term fluctuations (daily-to-seasonal) and long-term trends of groundwater levels can cause temporal variations in aquifer-system deformation and accompanying land-surface movements. Early applications of InSAR to detect aquifer-system compaction and land subsidence focused on demonstrating the utility of the InSAR technique (e.g. Galloway et al. 1998, Amelung et al. 1999; Galloway et al. 2000,

This chapter is published as: Castellazzi et al. (2016), Assessing Groundwater Depletion and Dynamics Using GRACE and InSAR: Potential and Limitations, Groundwater 54, 768–780. https://doi.org/10.1111/gwat.12453

Hoffmann et al. 2001, 2003a, Lu and Danskin 2001, Heywood et al. 2002, Schmidt and Bürgmann 2003) to evaluate seasonal and inter-annual trends in compaction and the governing parameters controlling the hydromechanical response, principally to groundwater extractions, but also to natural recharge (Lu and Danskin 2001). The development of robust time-series InSAR methods greatly enhanced the potential for the monitoring of elastic and seasonal land-surface movements (e.g. with the SBAS-InSAR method: Reeves et al. 2011, 2014; Chaussard et al. 2014b). After a calibrating period of a few years using paired observations of water level variations and ground displacements, it is possible to infer seasonal water table level changes by monitoring ground displacements, provided that the water table moves according to the previously calibrated range of seasonal variations, and that the effective stress does exceed the pre-consolidation stress. By replacing *in situ* measurements by GRACE-derived GWS variations, it would be possible to relate ground deformation with larger scale groundwater-storage changes with limited field data available. The approach shows potential for: (1) estimating water level changes within the elastic range of deformation in areas devoid of monitoring wells; and (2) detecting transgression from an elastic deformation accompanying seasonal head variations above critical pre-consolidation heads. Three main challenges remain, however: (1) InSAR should be applied over large areas to reach GRACE scale (e.g. Chaussard et al. 2014b); (2) GRACE and InSAR should measure variations of the same water stocks; and (3) the spatial heterogeneity of storativity and compressibility can be accounted for.

5.4.3. ANTHROPOGENIC/CLIMATIC STORAGE CHANGES

While InSAR and GRACE used to map groundwater storage changes at different scales, the increasing availability of SAR data now allow the production of ground motion maps at GRACE scale (e.g. Chaussard et al. 2014b). Furthermore, the increased sensitivity brought by recent InSAR developments (Rucci et al. 2012) shows great potential for ground motion detection induced by non-anthropogenic water storage change, likely slower than for groundwater depletion nearby pumping centers. As InSAR is not directly quantitative, there is a limited interest of using it alone. However, InSAR would be able to provide an angle of view over the relative importance of the anthropogenic and non-anthropogenic components of a given water storage change integrated by GRACE over a larger area. For such application: (1) the anthropogenic

groundwater depletion areas have to be limited and well-defined throughout a typical GRACE footprint; (2) compressible hydrogeologic units should be sufficiently present throughout the study area. The non-anthropogenic storage change and induced ground motion are expected to be close or smaller than the typical InSAR detection threshold of few 3-5 mm/yr (PSI method and C-Band radar data). As a results, the most important parameter for such application is the precision of InSAR measurement in natural settings. Atmospheric patterns influence radar waves. As this influence can be accounted for, this is still the major sources of error within InSAR measurements. Rucci (2012) explains how a sub-milliter precision could be obtained in the near future, in settings with large density of coherent ground targets and using the most recent SAR systems. Density of such targets is typically low in natural settings: motion detection with high precision in natural settings is still a major challenge for InSAR specialists.

5.4.4. TOWARD THE REMOTE ASSESSMENT OF AQUIFER CONFINEMENT AND DYNAMICS

As shown on Figure 2, the spatial extent of mass loss and land subsidence depend on aquifer confinement. Given the current development of higher resolution gravimetric sensors (Thales Alenia Space 2010; Famiglietti et al. 2013; Watkins et al. 2013), there is great hope for mass losses recovery at local to regional scale. Thus, through comparison between theoretical concepts (see Figure 2) and case studies, hydrogeologists could potentially infer aquifer configuration and flow dynamics through spatial analysis of subsidence and mass losses occurrence.

5.5. SUMMARY

In this review, we presented the general principles of two methods to remotely assess groundwater storage changes though gravity changes and aquifer-system compaction. While compaction measurements (e.g. InSAR) rely principally on the presence of fine-grained (clays and silts) compressible hydrogeologic units to reveal storage change, gravimetric methods (depending on their resolution) can be sensitive to aquifer confinement. Compaction occurs as a consequence of hydraulic pressure drop and the matrix compressibility of aquifer-system material, while gravity variations occur as a consequence of fluid mass changes, and to a certain extent, changes in the position of land surface owing to compaction and accompanying land subsidence.

This chapter is published as: Castellazzi et al. (2016), Assessing Groundwater Depletion and Dynamics Using GRACE and InSAR: Potential and Limitations, Groundwater 54, 768–780. https://doi.org/10.1111/gwat.12453

Land subsidence detection takes advantage of a variety of resolutions, image footprint and precision options from several SAR imaging spacecraft currently operating. Imaging options range from semi-continental scales (e.g. ScanSAR or TOPSAR modes in ALOS-2 or Sentinel-1 satellites) to city scales (e.g. Radarsat-2 Ultrafine mode). Vertical precision usually ranges from millimeters when using short waves (e.g. X-Band used by TerraSAR-X, 3.1cm wavelength) to centimeters when using longer waves (L-Band used by ALOS PALSAR, 23 cm wavelength). Shorter waves allow better vertical precision while longer waves allow better detection in less coherent areas (e.g. farmland).

Although no studies exist on the remote detection of aquifer-system confinement through the analysis of land subsidence spatial patterns, we argue that this is theoretically possible with minimal lithological data. Indeed, due to the important difference in storativity, confined aquifers show ampler radius of influence and head drop than unconfined aquifers, which could reflect on amplitude and extent of land subsidence. Case studies in well-known hydrogeological settings, where *in situ* data are available, would allow to better understand the remaining challenges of such applications.

Microgravity surveys are costly, labor intensive and spatially limited. GRACE data are freely available and of increasing ease of use, but because of the minimum critical area of usability it is unsuitable at most typical aquifer scales. While microgravity measurements can provide information on local aquifer flow dynamics and confinement, GRACE does not. As none of these methods' resolution matches adequately the typical water management scales, there is a methodological gap left to be fulfilled.

The possibility of combining gravity and subsidence measurements to better assess aquifer dynamics shows potential but is currently limited by methodological issues. Nevertheless, there is both hope and expectations for a valid option in the future regarding the remote assessment of aquifer confinement and groundwater flow dynamics.

This chapter is published as: Castellazzi et al. (2016), Assessing Groundwater Depletion and Dynamics Using GRACE and InSAR: Potential and Limitations, Groundwater 54, 768–780. https://doi.org/10.1111/gwat.12453

5.6. ACKNOWLEDGEMENTS

The authors would like to thank the *Ministère des Relations Internationales Francophonie et Commerce Extérieur du Québec* (MRIFCE - Québec) and the *Consejo Nacional de Ciencia y Tecnología* (CONACyT - Mexico) for their financial support. Additionally, the authors would like to thank Luc Aquilina, René Lefebvre, and Jasmin Raymond, who initiated the collaboration between *Institut National de la Recherche Scientifique* in Québec and *University of Rennes 1* in France. Through the creation of a *Laboratoire International Associé* (LIA) France-Québec, they made this research possible.

This chapter is published as: Castellazzi et al. (2016), Assessing Groundwater Depletion and Dynamics Using GRACE and InSAR: Potential and Limitations, Groundwater 54, 768–780. https://doi.org/10.1111/gwat.12453

7. COMBINING GRACE AND INSAR FOR QUANTITATIVE MAPPING OF GROUNDWATER DEPLETION AT THE WATER MANAGEMENT SCALE

Pascal Castellazzi

Institut national de la recherche scientifique, Centre Eau, Terre et Environnement, Université du Québec, 490 rue de la Couronne, Québec, QC, Canada, G1K 9A9, Phone: 418-570-3630, Fax: 418-654-2600. Email: pascal.castellazzi@ete.inrs.ca

Laurent Longuevergne

Géosciences Rennes, UMR CNRS 6118. Université Rennes 1. Campus Beaulieu. 35042 Rennes Cedex, France. Phone: +33 223-236-546. Email : laurent.longuevergne@univ-rennes1.fr

Richard Martel

Institut national de la recherche scientifique, Centre Eau, Terre et Environnement, Université du Québec, 490 rue de la Couronne, Québec, QC, Canada, G1K 9A9, Phone: 418-654-2683, Fax: 418-654-2600. Email: richard.martel@ete.inrs.ca

Alfonso Rivera

Geological Survey of Canada, Natural Resources Canada, 490, rue de la Couronne, Quebec (Quebec) G1K 9A9, Canada. Phone 418-654-2688, Fax: 418-654-2615. Email: alfonso.rivera@canada.ca

Charles Brouard

Institut national de la recherche scientifique, Centre Eau, Terre et Environnement, Université du Québec, 490 rue de la Couronne, Québec, QC, Canada, G1K 9A9. Phone: 418-654-2524 ext.4443. Email: charles.brouard@ete.inrs.ca

Estelle Chaussard

State University of New York at Buffalo. 417 Hochstetter Hall, Buffalo, NY 14260-1350, USA. Phone: 716 645 4291. E-mail: estellec@buffalo.edu

This chapter is published as: Castellazzi et al. (2017), Combining GRACE and InSAR for quantitative mapping of groundwater depletion at the water management scale. Submitted to Remote Sensing of Environment on March 23rd 2017. Under Review.

Highlights

- InSAR determines where groundwater-related mass changes occur
- GRACE-derived groundwater mass changes data are focused to the water management scale
- Discrepancies between GRACE solutions limits further use of GRACE for water management

Keywords

Geodesy, Groundwater depletion, GRACE, InSAR, groundwater management.

Abbreviations

CFE: Comisión Federal de Electricidad
CONAGUA / CNA: Comisión Nacional del Agua
DKK: Deccorelation filter for GRACE data created by J. Kusche (GFZ, Posdam, Germany).
GLDAS: Global Land Data Assimilation System (LSM output dataset)
GRACE: Gravity Recovery and Climate Experiment
GWS: Groundwater Storage
InSAR: Interferometric Synthetic Aperture Radar
LOS: (Satellite) Line Of Sight
LSM: Land Surface Model
RMS: Root Mean Square
SAR: Synthetic Aperture Radar
SBAS-InSAR: Small Baseline Subset Interferometry
SH: Spherical Harmonics
SMS: Soil Moisture Storage
SWS: Surface Water Storage
TWS: Total Water Storage
WTE: Water Thickness Equivalents (unit)

Abstract

GRACE gravity variation recovery and InSAR-derived ground displacement data show promise in supporting and assessing groundwater management policies. However, GRACE system's resolution is too low, and the inversion of InSAR data into volume of groundwater storage loss requires extensive and often unavailable lithological data. Here we present how InSAR can be used to constrain and spatially focus GRACE-derived groundwater mass loss to depletion areas, reducing the gap between the GRACE scale and the typical water management scales. While we highlight the tremendous potential of a fully geodetic, quantitative, and high resolution mapping of groundwater storage loss, we also point out the crucial need for producing guidelines on the proper GRACE solution to use for any study area and/or application.

In order to illustrate the GRACE/InSAR combination procedure, we present a case study in Central Mexico, where groundwater depletion of ~4000 MCM/yr is reported by the water governance agencies and is well documented in the scientific literature. However, in this region, not all GRACE solutions provide reasonable groundwater depletion estimates. Using two of them, an inversion is performed to focus the groundwater-related GRACE signal over different mass distribution maps. Several mass distributions are tested, including two from InSAR-derived aquifer compaction mapping. The results show that the regions of Mexico City and Bajio, an agricultural and industrial corridor 250km North of Mexico City, are the main contributors to the regional groundwater depletion. The mass distribution map produced directly from InSAR lead to results closer to official groundwater budgets than the others tested.

This chapter is published as: Castellazzi et al. (2017), Combining GRACE and InSAR for quantitative mapping of groundwater depletion at the water management scale. Submitted to Remote Sensing of Environment on March 23rd 2017. Under Review.

7.1. INTRODUCTION

Intensive groundwater withdrawal exceeding natural replenishment occurs in numerous arid and semi-arid areas of the World (FAO, 2011). Humanity reliance on non-renewable or overexploited groundwater resources presents a growing risk to water and food production. The implementation of efficient groundwater management practices is essential to solve existing water supply issues while complying with the growing water needs. Nowadays, groundwater monitoring schemes usually rely on water budgets, where storage change is considered as the residual of the incoming and exiting flows equilibrium. Major concerns arise while using such estimates. First, it overlooks aquifer dynamics and changes within the local water cycle occurring as groundwater storage changes (Bredehoeft, 2002). Second, the lack of methodological consensus and the complexity of estimating incoming and exiting fluxes prevent such estimates to be comparable between different managing agencies and make them highly sensitive to political influences. The need for efficient and independent groundwater management tools arises along with the ever-growing pressure on groundwater resources.

Geodesy provides interesting perspectives toward the development of global and independent groundwater monitoring techniques. Geodetic methods have the advantage of being independent from politics, of global extent, and often widely available. Several of these methods can be used to study groundwater, in order of historical appearance: Multispectral imaging, Synthetic Aperture Radar (SAR) imaging, and time-variable gravity monitoring (GRACE satellites). Multispectral images were the first available and are used in numerous water-related applications: generate Digital Elevation Model (DEM), identify geomorphologic patterns, map and monitor the evolution of land and water use, delimit water features, detect groundwater outflows (springs), and enables better understanding of key water balance parameters such as evaporation and recharge (Meijerink, 2007). Applications of SAR data in groundwater science started in the late 1990's. Their main contribution into groundwater science came with the development of ground displacement data derived from Interferometric SAR processing (InSAR, Massonet and Feigl, 1998). Ground displacement data allowed to detect groundwater depletion areas, map lithological boundaries, infer confined aquifer storage properties, and calibrate groundwater models (Galloway and Hoffmann, 2007). The development of interferometry time-series algorithms in the early 2000's (Ferretti et al. 2001;

This chapter is published as: Castellazzi et al. (2017), Combining GRACE and InSAR for quantitative mapping of groundwater depletion at the water management scale. Submitted to Remote Sensing of Environment on March 23rd 2017. Under Review.

Berardino et al. 2002) enhanced its integration into groundwater science, as it allowed reducing atmospheric artefacts and monitor finer displacements, such as the aquifer reaction to pumping and recharge over time (Chaussard et al. 2014a). Since then, processing algorithms kept improving along with the increasing imaging capability and data availability (including open access options) from the most recent orbital SAR systems (Crosetto et al. 2016).

Finally, gravity field variation time-series from the Gravity Recovery And Climate Experiment (GRACE – Tapley et al. 2004) provides a very novel insight into groundwater systems (Alley and Konikow, 2015). Being sensitive to mass variations, GRACE provides a direct and quantitative insight into groundwater storage changes. The system orbits the Earth since 2002, but the assimilation of these novel data by groundwater scientists really only started in the 2010's, after reaching a maturity upon processing strategies and time-variable gravity data interpretation.

Among the geodetic methods available, only GRACE and InSAR provide a direct insight on groundwater storage variations. However, as groundwater management tools, they both have limits. First, the aquifer volume responds to pressure changes according to its compressibility, which is highly variable in space. Indeed, even if pressure change seems to physically affect the structure of the least compressible aquifer (Schuite et al. 2015), not all depleting aquifers are subject to ground deformation beyond the typical InSAR detection threshold of 3 to 10 mm/yr for typical data and processing strategies. Consequently, the use of InSAR is limited to the most compressible aquifer systems. In most regions, the inversion of InSAR into volume of storage change is limited by the lack of compressibility data. The scale of InSAR applications varies from the city scale (Castellazzi et al. 2016b) up to the state/country scale (e.g. Chaussard et al. 2013; Chaussard et al. 2014b). The increasing availability of large scale SAR imaging modes such as ScanSAR and TOPSAR helps in providing ground deformation maps at the scale of states or water basins (Figure 1). On the other hand, GRACE data provide a direct insight into groundwater storage change (Scanlon et al., 2012; Feng et al., 2013), assuming that other mass changes can be accounted and subtracted accurately. However, GRACE has a maximum mass field resolution estimated between 450 to 750 km (Longuevergne et al. 2010, 2013), which is insufficient to be used to support groundwater governance at the aquifer scale (Figure 1).

In this study, we investigate how InSAR can help interpreting GRACE data at a higher resolution, closer to the groundwater management scale. InSAR detects groundwater depletion areas that compact, for which the groundwater mass losses are integrated within GRACE data at its own resolution. Thus, InSAR can be used as *a spatial* a priori to focus GRACE signal and improve its resolution, as suggested in Castellazzi et al., (2016a). To test the proposed procedure, we propose a case study in Central Mexico.

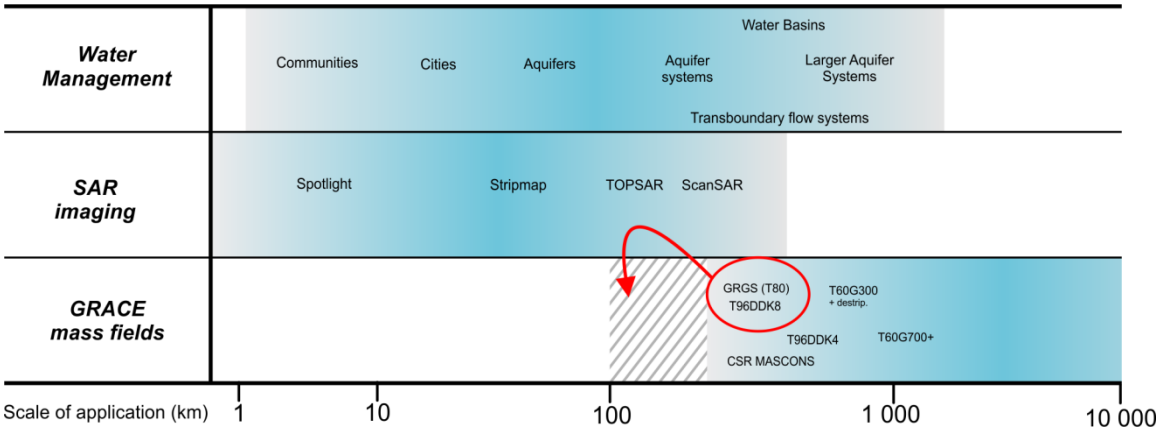

Figure 1: Scales of application of InSAR, GRACE, and the water management practices. This study aims to take advantages of the information from InSAR to reduce the gap between aquifer-scale water management and GRACE groundwater storage trend estimates of the highest resolution available (red arrow). Typical SAR imaging products and GRACE processing strategies are presented (T60/80/96: Degrees of spherical harmonic truncation; G/DDK: Type of filtering (Gaussian or DDK filters); Destrip: Destripping method presented by Swenson and Wahr, 2006).

7.2. STUDY AREA

7.2.1. BACKGROUND

Central Mexico faces important groundwater depletion which threatens the sustainability of several economic activities in the agricultural and industrial sectors. It also has important consequences for assuring the basic access to clean water. Several land subsidence areas related to groundwater over extraction are reported (Chaussard et al. 2014b, Castellazzi et al. 2016a, 2016b) and are generally occurring where high

population density occurs in low precipitation areas (Figure 2). Land subsidence also takes place in some irrigated farmland areas (Castellazzi et al. 2016b), mainly between Queretaro and San Luis Potosi, and around the Aguascalientes Valley. Recently, Castellazzi et al. (2016b) compared an unconstrained GRACE solution (from Huang et al. 2012) with InSAR measurements and the official groundwater budget data (CONAGUA, 2009a, 2013a) and noticed important discordances. They suggested that the surprising low depletion rates of mass loss as observed by this GRACE solution are partly related to wastewater infiltrations at different scales and basin closure processes (Molle et al. 2010).

7.2.2. GROUNDWATER GOVERNANCE

Mexico's groundwater management scheme relies on groundwater budgets calculated by CONAGUA for each of the 653 administrative aquifer units of Mexico (Figure 2). The Mexican water regulation does not allow the creation of new groundwater extraction allowance in aquifer having negative groundwater balance, i.e. depleting aquifers. Depending on data availability for each aquifer, such calculation is based either on a flow-based groundwater budget approach comparing inputs to outputs, or on a water-budget approach, where recharge is calculated as a residual of a typical water budget equation. More details are provided in Castellazzi et al. (2016b).

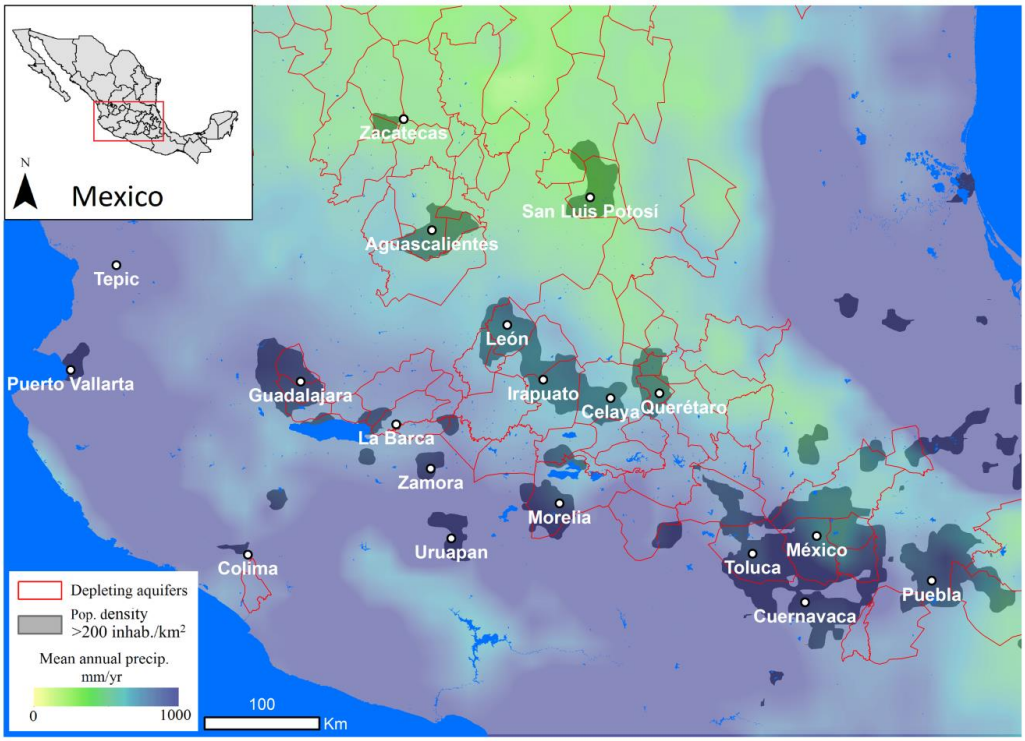

Figure 2: Map of the study area. Groundwater depletion often occurs in highly populated areas and where precipitation rates are below 1000 mm/yr. Several other depletion areas are located in less populated regions where groundwater is pumped for agricultural purposes (Castellazzi et al. 2016b). Precipitation data are from Hijmans et al. (2005), population density data are from CIESIN/CIAT (2005), and the administrative aquifer depletion map is from CONAGUA (2009a).

7.3. Data and Methods

7.3.1. SAR data and InSAR processing

All SAR data used in this study are from ALOS-1 satellite and are available from the Alaskan Satellite Facility web portal (ASF - http://www.asf.alaska.edu). Ground deformation data are based on two InSAR processing batch. First, the main part of the coverage was taken from Chaussard et al. (2014b), who relied on more than 600 ALOS-1 images. Second, 104 additional ALOS-1 images from 6 time-series were added for this study to increase the total spatial coverage to 179 870 km^2. Both processing are based on the SBAS-InSAR algorithm (Berardino et al. 2002) and interpolated in low coherence areas similarly to Castellazzi et al. (2016b) in order to restore data continuity.

Only vertical displacements beyond a nominal detection threshold of 1 cm/yr of subsidence are considered. For the inversion, the resulting vertical ground displacement map at 60m resolution was down-sampled to a 0.25 degree grid in which pixel values represent the mean subsidence within each 0.25 by 0.25 degree cell footprint.

7.3.2. GRACE DATA AND SIGNAL DECOMPOSITION

Four versions of GRACE data are considered: a typical unconstrained solution from the Center for Space Research (CSR RL05 - http://www.csr.utexas.edu/grace) complete up to Spherical Harmonics (SH) degree and order 60, destripped according to Swenson and Wahr (2006), and filtered by a 200km radius Gaussian smoother; the CSR regularized MASCONS solution from Save et al. (2016); an unconstrained solution using CSR RL05 complete up to SH degree and order 96 and destripped/smoothened in a single step by applying the DDK8 filter (Kusche, 2007, 2009); the stabilized solution complete up to SH degree and order 80 from the Space Geodesy Research Group (GRGS - http://grgs.obs-mip.fr/grace). Throughout the article, these solutions are referred to as T60G200, CSR MASCON, T96DDK8, and GRGS, respectively.

The Soil Moisture Storage (SMS) trend was estimated using four Land Surface Models (LSM) included in GLDAS v2.0 (Rodell et al. 2004). Even though Castellazzi et al. (2016b) observed that SWS trend is negligible in the study area, SWS trend from 11 lakes and dams were taken into account. To make them compatible in terms of spatial resolution, LSM-derived SMS estimates and SWS data were filtered similarly to the GRACE TWS data. The SMS and SWS trend maps at GRACE resolution were subtracted to the GRACE TWS trend map to produce the GRACE-derived GWS trend map used for the inversion.

7.3.3. MASCONS DELINEATION AND INVERSION

Five large regions, or ‘MASCONs’ (see e.g. Farrinoti et al. 2015), were delimited according to water usage (Castellazzi et al. 2016b), climatic conditions (Figure 1), and aquifer types (Castellazzi et al. 2016a). The inversion process consists in attributing a GWS change value to each of the five MASCONs and modeling the WTE change as

perceived by GRACE. The set of the five GWS change values is optimized in order to minimize the pixel-to-pixel RMS of the residual between the simulated map and the GRACE-derived GWS map. Three mass concentration strategies are tested: one without any spatial *a priori* of mass distribution, considering masses as uniform within each MASCON, referred to as 'uniform'; one consisting of distributing masses equally over subsiding pixels above an arbitrary threshold of 1MCM/yr of subsidence volume per 0.25 degree pixel, referred to as 'uniform InSAR'; and one consisting of distributing masses on all subsiding pixels proportionally to their subsidence rates, referred to as 'weighted InSAR'. The inversion procedure is performed identically for the three mass distributions and the two solutions. Two solvers are used to find the set of values minimizing the RMS with the original GRACE-derived GWS trend map: a Genetic algorithm-based solver and a Pattern Search solver.

Genetic algorithms (GAs) are stochastic evolutionary algorithms (Goldberg, 1989; Holland, 1992) inspired by natural selection and involving genetic operators such as mutation, crossover, and selection. The first generation is created by selecting a random and uniformly distributed set of 200 individuals with parameter values taken from a realistic range. The subsequent generations are formed by 5% of the most efficient individuals from the previous generation (usually referred to as elite population) and 50% of crossovers. These crossovers are created by randomly mixing parameter values from two solutions of the previous generation. The 45% remaining individuals, referred to as 'mutants', are created by randomly adding a value from a Gaussian distribution to each parameter of a solution taken from the previous generation. The Gaussian distribution is center on 0 and has a variable standard deviation decreasing at each generation. The selection process used to produce the crossovers and mutants are based on a random process with selection probability being a linear function of the relative fitness of the solution. All individuals of the new generation created are then evaluated by the fitness function. This iterative process is repeated until convergence is achieved, usually around 100 to 200 generations.

In order to assure the robustness of the results, a Pattern Search (Hooke and Jeeves, 1961; Kolda et al. 2003) solver is also implemented. Pattern search is a non-gradient based algorithm, making adjustment to each parameter value independently in order to iteratively converge toward a stable solution. Results are considered as reliable when

both Pattern Search and Genetic solvers lead to results within 3%. The residual maps are used to assess the validity of the inversion procedure and are produced by subtracting the result of the inversion at GRACE resolution to the GRACE GWS trend map.

7.4. Results and Discussion

7.4.1. InSAR data and MASCONs delineation

The combination of the InSAR-derived vertical displacement map from Chaussard et al. (2014b – Figure 3a) and the newly processed area (Figure 3b) allows a total coverage of 179 870 km^2. Five new subsidence patches are revealed, with vertical subsidence rates up to 20 cm/yr in the Chaparrosa area (Figure 3b). These valleys are facing important subsidence rates probably due to the groundwater extraction needed to sustain intensive agricultural activities in a low precipitation area (around 450 mm/yr – Hijmans et al. 2005).

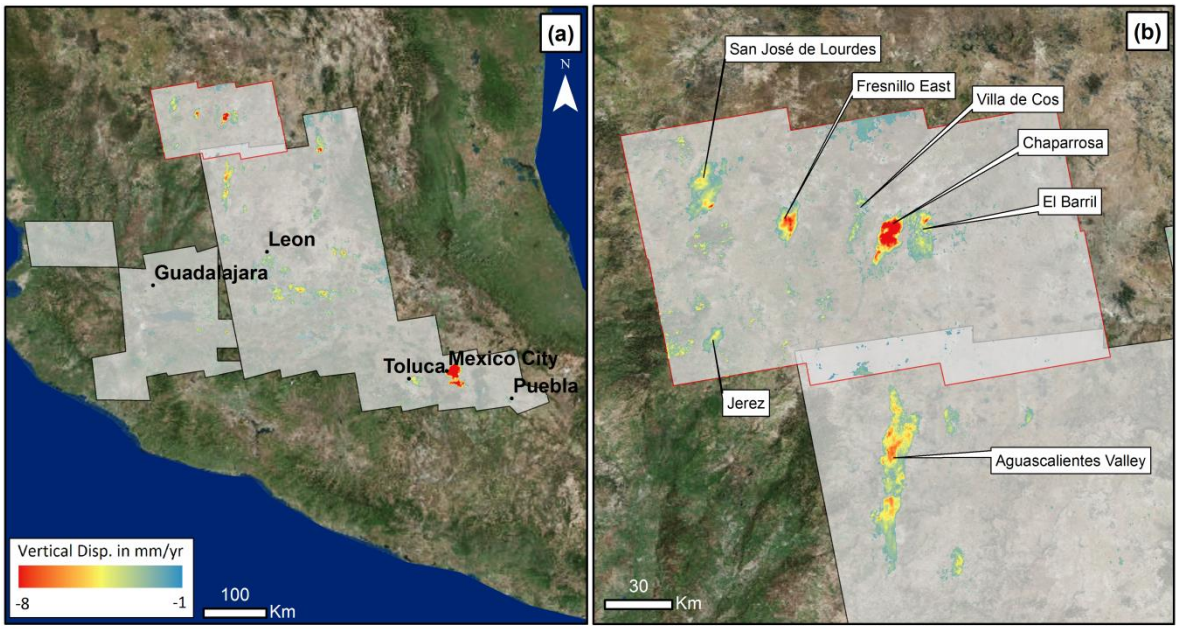

Figure 3: Global InSAR-derived ground displacement map (a). Main cities over 100 000 inhabitants are shown for spatial reference. The black contour represents the coverage from Chaussard et al. (2014b), whereas the red contour delimits the coverage of the new SBAS-InSAR processing performed for this study. Newly discovered subsidence patches are shown in (b).

This chapter is published as: Castellazzi et al. (2017), Combining GRACE and InSAR for quantitative mapping of groundwater depletion at the water management scale. Submitted to Remote Sensing of Environment on March 23rd 2017. Under Review.

Using the map shown on Figure 3b, a 0.25 by 0.25 degree vertical subsidence pixel grid was created (Fig 4). Two versions were used as spatial *a priori* of mass concentration to constraint the inversion: one respecting the mean subsidence with each pixel footprint (Figure 4a), and one uniform mass distribution only including pixels subsiding above an arbitrary value of 1 MCM/yr of volume of vertical subsidence (Figure 4b).

Using the InSAR 0.25 degree map and the hydrogeological knowledge of the study area (Castellazzi et al. 2016b), five MASCONs are delineated (Fig 4a). 'Mexico' delimits the region of Mexico City and other surrounding cities such as Toluca and Puebla. It is constituted of multilayered complex aquifers of volcanogenic and lacustrine origins, often described as semi-confined. 'Bajio' includes the intensively exploited unconfined aquifers located in the Queretaro-Celaya-Salamanca-Irapuato industrial and agricultural corridor (Wester et al. 2011). 'High Plateau' includes the agricultural valleys of Laguna Seca and Jaral de Berrios regions (see e.g. Fig.1 in Wester et al. 2011) up to San Luis Potosi. 'Aguascalientes' delimits the unconfined aquifer of the Aguascalientes Valley and other agricultural Valley in the state of Zacatecas, all affected by important subsidence up to 10cm/yr related to municipal and agricultural groundwater extraction. Finally, the 'Lower LS' region delimits the downstream portion of the Lerma-Santiago basin (the upstream part of the larger Lerma-Siantiago-Pacifico basin), where both groundwater extraction and land subsidence are less important due to the abundance of natural SW bodies and dams supporting in parts the water needs of the region. MASCONs cover a total area of 253 565 km^2 (Table 1). While the total MASCON area is covered at 74% by the InSAR survey, it includes all densely populated and irrigated farmland areas where groundwater depletion may occur. The subsiding area of Tepic (Figure 4a) was not taken into account for the study. The area is isolated from the rest of Central Mexico, it receives higher precipitations rates due to the proximity to the Pacific Ocean, and groundwater depletion might not be a major contributor of the GRACE TWS trends.

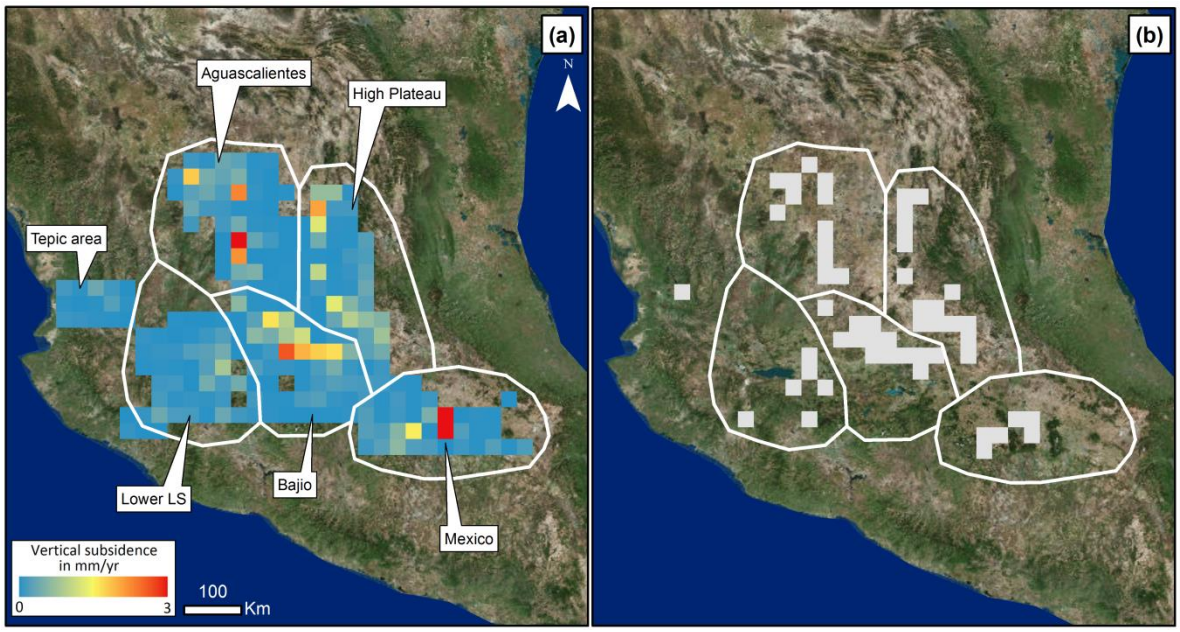

Figure 4: The InSAR map is integrated into a 0.25 degree pixel grid and then used to focus the GRACE-derived groundwater mass loss signal. (a) and (b) show two of the mass distribution strategies tested: mass distribution proportional to the total subsidence within each pixels (a – referred to as 'Weighted InSAR'), and uniform mass change for each subsiding areas (b – referred to as 'Uniform InSAR'). A third mass distribution is tested, consisting in considering the each MASCON as having an uniform mass distribution, referred to as 'Uniform'.

Table 1: Size, main cities, population, and precipitation rates within the five MASCONs. Precipitation data are from Hijmans et al. (2005) and population data are from CIESIN/CIAT (2005).

MASCON name	Size (km^2)	Main cities	Mean Precipitation (mm/yr)	Total Population (10^6 inhab.)
Mexico	51230	Puebla Mexico Toluca	855	25,2
Bajio	39616	Querétaro Celaya Irapuato Salamanca León Morelia	842	6,3
Lower LS	56049	Guadalajara Ciudad Guzman	892	8,0
Aguascalientes	50358	Aguascalientes Zacatecas	468	2,0
H.P.	56310	San Luis Potosi	533	3,1

7.4.2. GRACE DATA AND SIGNAL DECOMPOSITION

It is important to note that the MASCONs delineated for this study area delineated around a region known to undergo severe groundwater depletion and several subsidence areas (Castellazzi et al. 2016a, 2016b; Chaussard et al. 2014b). Among the four GRACE solutions (Figure 5), only two show groundwater depletion in the study area (Figure 5c and 5d). While the groundwater governance data show a total depletion rate of 3710 MCM/yr, the total mass anomaly over and around the study area corresponds to a total of approximately 1900 and 2700 MCM/yr of TWS depletion and 2720 and 3620 MCM/yr of groundwater depletion, for the GRGS RL03 and T96DDK8 solutions, respectively. As observed in Castellazzi et al. (2016b), typical unconstrained solutions such as T60G200 estimate the GWS trend as almost stable (Fig.5a).

Major discordances between an unconstrained GRACE solution from Huang et al. (2012), InSAR observations, and the official governance data (CONAGUA, 2009a, 2013a) were studied in Castellazzi et al. (2016b), who interpreted it to result from hydrodynamics processes related to basin closure (Molle et al. 2010) unaccounted in official governance data. While the GRACE solutions GRGS RL03 and T96DDK8

(Figure 5c and 5d) will be used for the inversions performed in this study, the question of determining the most appropriate GRACE solution to use for the study area remains unsolved. In areas of stronger trend signals (e.g. Farinotti et al. 2015), the relative agreement between solutions allows to assume the ensemble mean of different solution as the best GRACE TWS estimates available. In the case of Central Mexico, major discordances exist between solutions resulting from different processing strategies (Figure 5). The GRACE solutions considered for the inversion are decomposed using the data shown in Figure 6, and the resulting trends are considered being entirely related to GWS change.

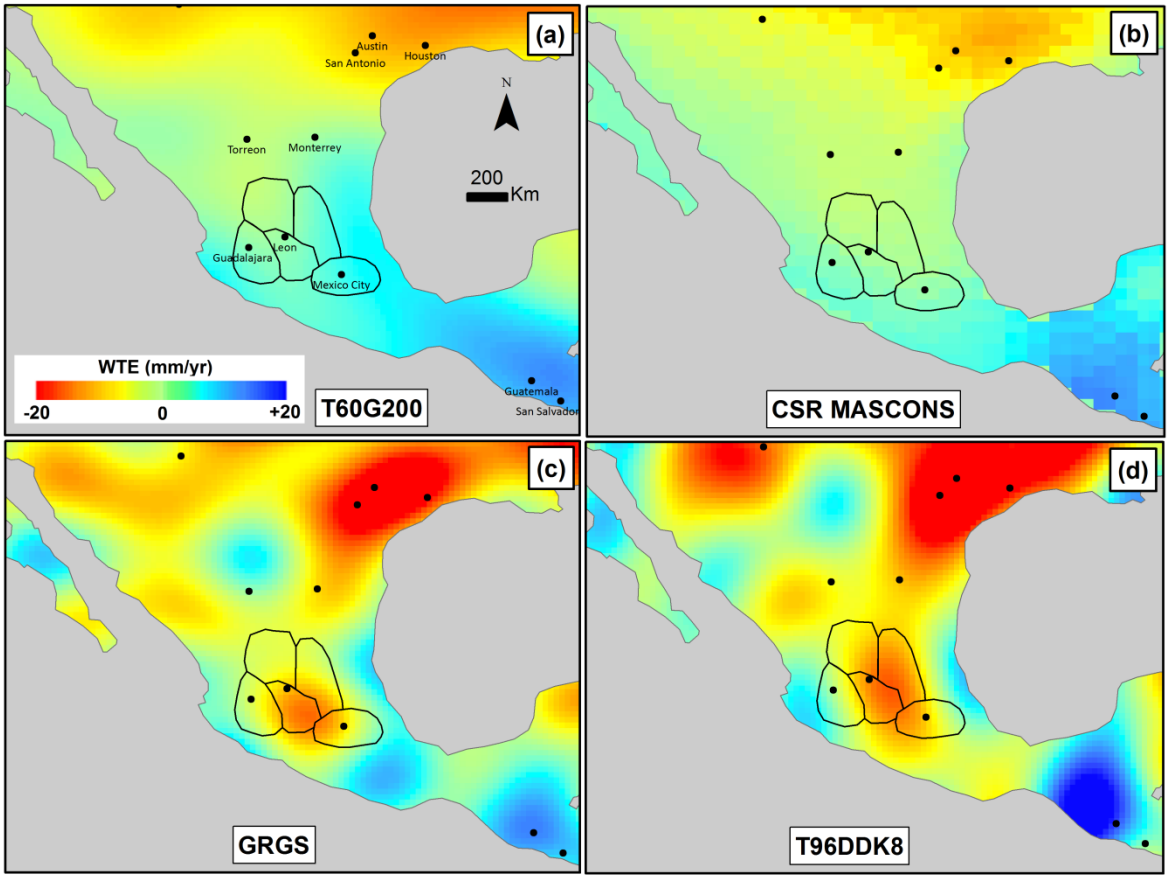

Figure 5: GRACE TWS trend for the period 08-2002 to 08-2014 using the CSR RL05 unconstrained solutions complete up to degree and order 60 of SH Stokes coefficients, destripped (Swenson and Wahr, 2006) and filtered using a 200km radius Gaussian smoother (a), a regularized MASCON solution (Save et al. (2016) - b), a stabilized solution complete up to degree and order 80 of SH Stokes coefficients (c), and an unconstrained solution complete up to degree and order 96 of SH Stokes coefficients, destripped/smoothened in a single step using the DDK8 filter (Kusche et al. 2009).

Conversely to solutions (a) and (b), (c) and (d) show a significant TWS trend over the study area, coinciding with the official groundwater management data (CONAGUA, 2009a, 2013a).

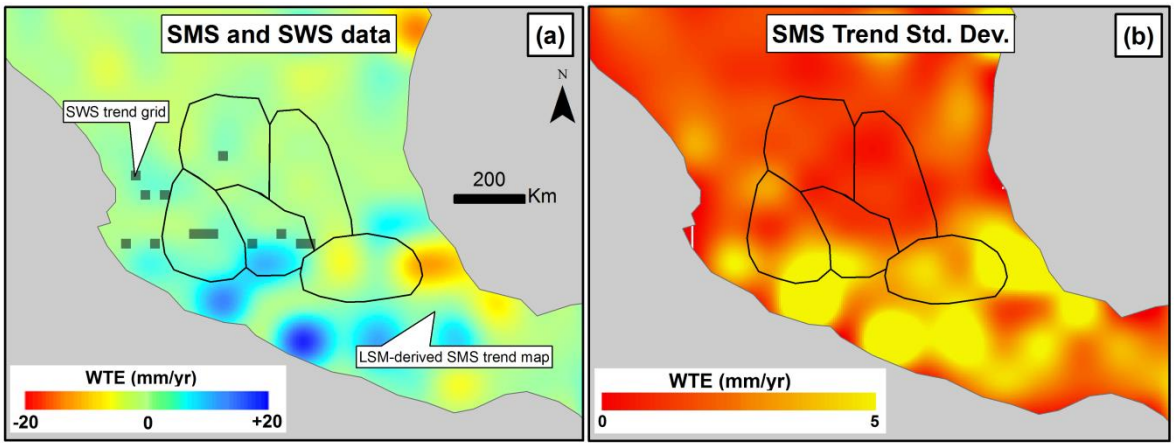

Figure 6: Soil Moisture storage Trend for the study period using the mean of the four LSM within GLDAS v2.0 (a). Their standard deviation is shown in (b). Lake storage trend data are assembled over a 0.25 degree grid (a). For use with GRACE data, SWS and SMS (a) grids are always truncated and filtered similarly to the GRACE solution they are combined with.

7.4.3. DOWNSCALING GRACE SIGNAL TO THE GROUNDWATER MANAGEMENT SCALE

GRGS and CSR T96DKK8 solutions agree that Mexico and Bajio regions are important contributors to the regional groundwater depletion (Table 2). Both solutions also agree reasonably well for the Aguascalientes MASCON. The main difference between GRGS and CSR T96DDK8 are in the groundwater mass loss distribution for the Lower LS and H.P. MASCONs, where GRGS provides higher values in Lower LS, and CSR T96DDK8 provides higher values in H.P. The Lower LS and the H.P. MASCONs are oriented on both east and west ends of the study area. Thus, they may be influenced differently by stripping residues, as different destripping strategies are used by the two solutions.

Table 2: Results of GRACE ΔGWS estimations using the different spatial a priori of mass distributions (see section 6.2). 'None' refers to a simple spatial averaging; 'Uniform' refers to a complete and homogenous mass distribution within MASCONs; 'Uniform InSAR map' refers to a uniform mass repartition within pixels from the simplified InSAR map (Figure 4b); 'Weighted InSAR map' refers to a mass distribution respecting values from the original 0.25 degree InSAR map (Figure 4a). All inversions (all GRACE GWS estimations but the simple spatial averaging 'None') are constrained to a maximum of 0. Groundwater management data from CONAGUA (2009) are shown for comparison. All data are in MCM/yr.

GRACE solution	Spatial *a priori* of Mass distribution	Mexico	Bajio	Aguasc.	Lower LS	H.P.	Total	Figure
T60G200	None	183	-71	-107	-90	-9	-95	-
	Uniform	0	0	-275	-326	0	-607	-
CSR MASCON	None	122	81	-33	155	13	338	-
GRGS RL03 T80	Uniform	-461	-1216	-225	-527	0	> -2429	-
	Uniform InSAR	-685	-633	-299	-872	0	> -2493	8d, 9b, 10d
	Weighted InSAR	-574	-835	-227	-751	0	> -2387	8f, 9d, 10f
CSR RL05 T96DDK8	Uniform	-350	-1651	-572	0	-809	> -3382	-
	Uniform InSAR	-644	-1505	-487	0	-598	> -3234	8c, 9a, 10c
	Weighted InSAR	-515	-1621	-458	0	-598	> -3192	8e, 9c, 10e
Official Management scheme (CONAGUA, 2009a)		-1228	-1144	-157	-684	-497	-3710	7a, 7b

The GRACE/InSAR inversion using GRGS and CSR T96DDK8 generally provides comparable results to the groundwater governance data for 4 of the 5 MASCONs (Figure 7 and 8). Discrepancies between the final geodetic groundwater depletion map and official governance data can be observed in Figure 9. Different factors can explain them. First, the original GRACE-derived ΔGWS estimates never entirely reflect the regional groundwater depletion regardless of the GRACE solution considered (Table 2). These differences can be partly explained by the influences of unaccounted leakages, stripping residues, or GWS signal removal by the destripping and filtering applied to the T96DDK8 solution. Second, 15% of the pixels of the groundwater management map at a 0.25 degree resolution (Figure 7b) are unaccounted in the InSAR map at the same resolution used as mass distribution *a priori* (Figure 4a). It suggests that some depleting aquifers do not show subsidence, or undergo compaction at rates below the InSAR detection threshold. It is also important to notice that almost all pixels with groundwater depletion rates beyond approximately 65 MCM/yr are detected by InSAR, and are consequently present into the inversion mass distribution map (Figure 9). Third, GRACE and official groundwater budgets do not exactly measure groundwater depletion similarly. GRACE provides a view on the groundwater-related mass loss, including all dynamic effects within aquifers, but is contaminated by spatial leakages inherent to its mass field resolution. On the other hands, official groundwater budgets overlook the dynamic effects of aquifers depletion (changes in recharge or discharge; Bredehoeft, 2002), wastewater recharge, or infiltration from water distribution systems. The latter is known to be enhanced by aquifer compaction and associated ground fracturing (Castellazzi et al. 2016b).

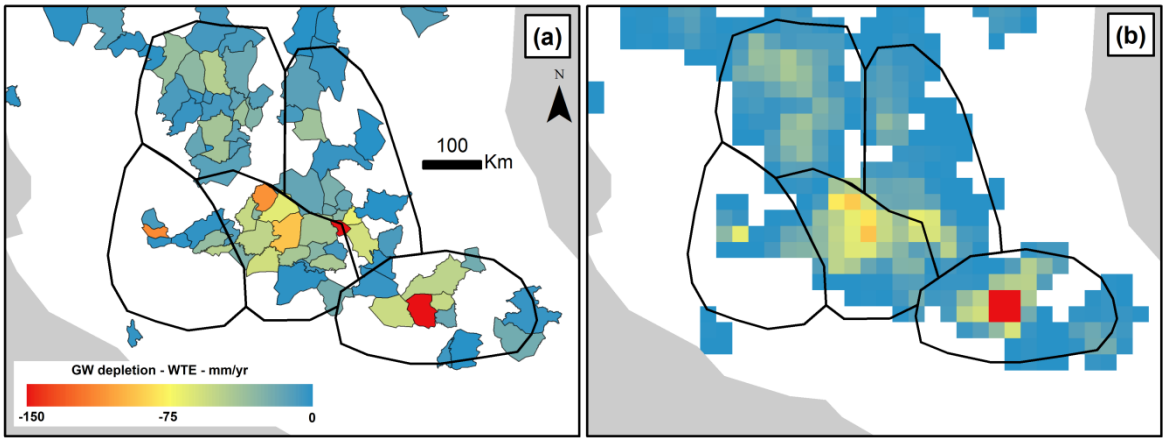

Figure 7 (previous page): Official groundwater budgets used for groundwater governance at the administrative aquifer resolution (a) and resampled on a 0.25 degree GRACE-like pixel grid (b) for comparison with the fully geodetic InSAR/GRACE groundwater depletion map.

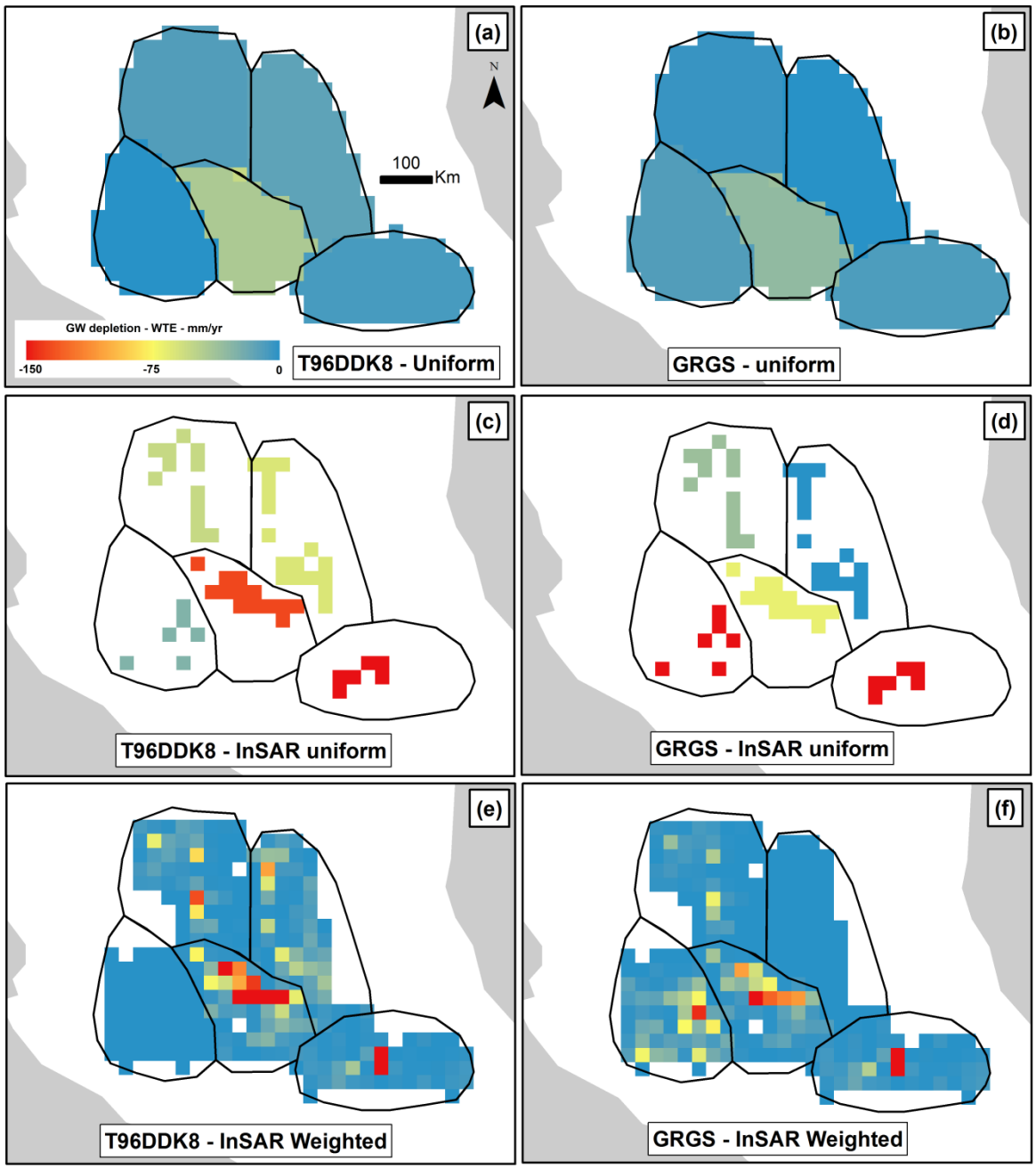

Figure 8: GRACE/InSAR-derived groundwater mass loss using the two solutions and the three types of mass distribution maps previously described (Table 2).

InSAR-weighted mass distribution provides a notably better groundwater depletion map (Figure 8), suggesting that InSAR measurements provide not only a spatial *a priori* of groundwater mass loss occurrence, but also significant quantitative information. Furthermore, it also suggests that an important correlation exists between the groundwater depletion rates and the subsidence rates, even though lithology (aquifer confinement, thickness, and compressibility) varies within the study area. The two solutions used present notably different influences from the two coasts, in a direction parallel to the stripes related to GRACE orbits. The influencing signal patterns are notable on the inversion residual map (Figure 10), where the most important residuals are located on the east and west sides for the T96DDK8 solution. These signals patterns could not be explained through the InSAR-derived mass distribution map, which suggests that the side signals may not be entirely imputable to groundwater storage change. This might explain the variable inversion results for the Lower LS and H.P. MASCONs.

The residual patterns of the GRACE-derived GWS maps after inversion show a low degree of sensitivity to the different mass distribution tested for the T96DDK8 solution (Fig.10 a/c/e). Conversely, notable differences are observed in the inversion results (Table 2) and the residual maps (Figure 10 b/d/f) for the GRGS solution. This points out that the GRGS solution, which is not filtered, provides better resolution allowing to discriminate mass patterns from the different distribution tested. On the other hand, the T96DKK8, even though being among the most resolution-preserving filter, decreases significantly the resolution and smooths the mass distribution. Thus, very similar inversion results are obtained for the different mass distributions tested with the T96DDK8 solution. Such observation proves the potential of the combined GRACE/InSAR inversion procedure as proposed in this article for application over non-filtered solutions from the the generations of GRACE missions to come, which are expected to have an improved spatial resolution.

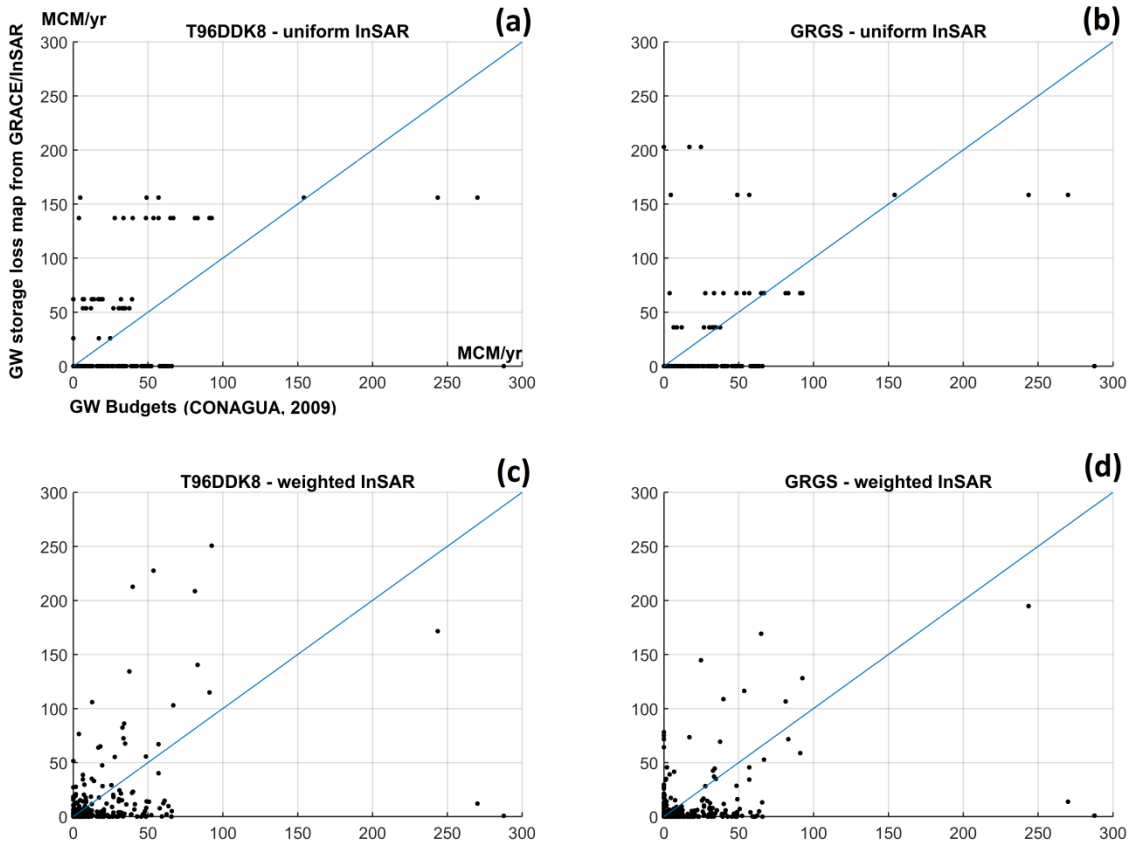

Figure 9: Scatter plots of the pixel per comparison between 0.25 degree pixel grid of the four groundwater depletion maps derived from geodesy vs the groundwater budgets from CONAGUA (2009a).

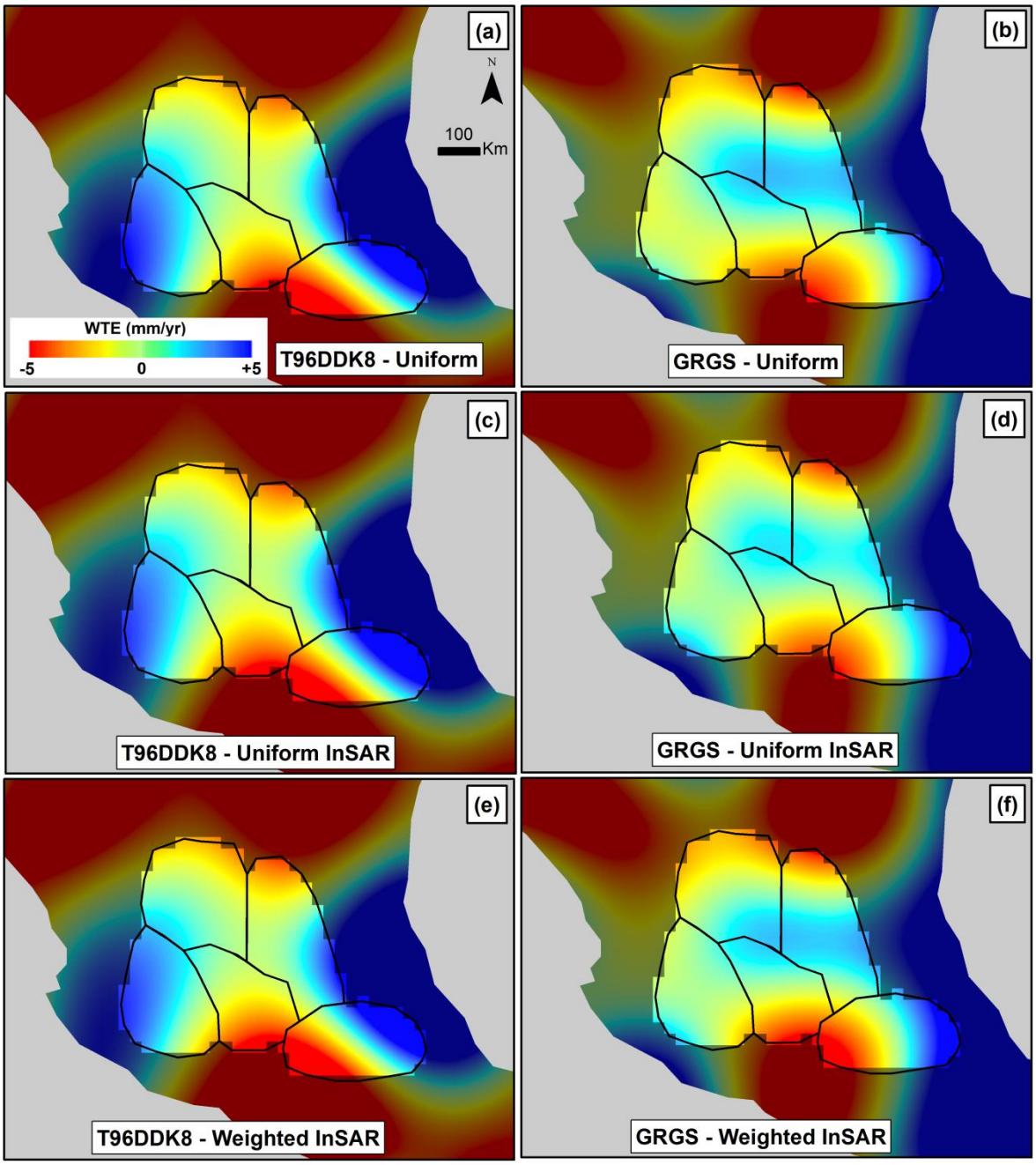

Figure 10: Residuals after inversion of GRACE-derived GWS trend data using the two solutions tested and the three different a priori of groundwater mass loss distribution. Note that a 1/4 exaggeration factor applies to the color scale for comparison with Figure 5. The zone outside the comparison area for lowering and optimizing the RMS with the GRACE-derived GWS signal is darkened.

7.5. CONCLUSION

This study shows that InSAR can be used to focus GRACE-derived GWS trend maps up to a resolution close to the groundwater management scale. The methodology is used to produce GWS change maps usable for comparison with the current groundwater governance scheme. We show that focusing GRACE GWS signal using InSAR data as a spatial *a priori* map of groundwater mass loss distribution is able to provide quantitative and high resolution information about the occurrence of groundwater depletion.

The validity of the procedure is limited by three main factors. First, selecting from the multitude of GRACE solutions available for any given study area, which often remains at the discretion of the user even though important discrepancies may occur between results of different processing strategies. Second, the ability of the GRACE decomposition procedure to account for all groundwater-related mass changes within the TWS change and to produce a map respecting the spatial patterns of the real GWS change. Third, the inversion results depend on the ability to reliably detect groundwater depletion areas using InSAR, which suggests that all depleting aquifers are subsiding beyond the InSAR detection threshold (approximately 1 cm/yr for the L-band data presented in this study).

In the study area, the most significant uncertainty lies predominantly in the choice of GRACE data processing strategy, as different GRACE solutions show very different TWS trends in both their regional-averaged values and their spatial patterns. However, InSAR is efficient in mapping the groundwater-related mass loss patterns and providing a groundwater mass loss distribution map.

Focusing GRACE data through an inversion procedure constraint by InSAR data is a promising first step towards creating a fully-geodetic groundwater depletion map at the groundwater governance resolution (100km scale). When using the GRGS and T96DDK8 GRACE solutions, the results show a reasonable correlation with the groundwater budget map used for groundwater governance in Mexico. However, given the lack of guidelines regarding the appropriate GRACE solution to use according to the study settings, the method proposed in this study cannot be implemented directly as a groundwater management tool. A consensus is therefore needed regarding which

solution to use for any given application and study area. Such processing guidelines are necessary to make the method proposed in this study applicable globally.

An important axis of research lies within the observation of discrepancies between mass-balance measurements and other typical quantitative methods. While the official groundwater depletion map allows a unique comparison with the inversed GRACE result, it differs by essence from mass field measurements like GRACE (Castellazzi et al. 2016c). It is therefore difficult to compare and fully validate such maps. Interpolated microgravity data at the pixel-scale (approx. 25 km) might provide a better point of comparison, but are still labor-intensive to produce at such scales.

7.6. ACKNOWLEDGMENTS

The authors would like to thank The Ministère of International Relations and La Francophonie (MRIF - Quebec) and the Consejo Nacional de Ciencia y Tecnología (CONACyT - Mexico) for their financial support. The technical support of CONAGUA was essential for the success of the study; the authors particularly acknowledge the help of Sergio Murillo, Martin Velasco, and Oswaldo Valdez. The authors also thank Shimon Wdowinski (RSMAS - Univ. of Miami) for his advice and Dr. Wei Feng for the publication of The GRACE Toolbox, a MATLAB-based GRACE data processing platform. GRACE data were accessed via the Center for Space Research (CSR - http://www.csr.utexas.edu/grace) and the Space Geodesy Research Group (GRGS - http://grgs.obs-mip.fr/grace) web portals. The GLDAS-2 data were acquired as part of the mission of NASA's Earth Science Division and archived and distributed by the Goddard Earth Sciences (GES) Data and Information Services Center (DISC). ALOS data are provided by the Japan Aerospace Exploration Agency (JAXA) and are accessible in SLC format directly via the Alaskan Satellite Facility (ASF) web portal upon registration. Additionally, the authors would like to thank Luc Aquilina, René Lefebvre, and Jasmin Raymond, who initiated the collaboration between Institut National de la Recherche Scientifique in Québec and University of Rennes 1 in France. Through the creation of a Laboratoire International Associé (LIA) France-Québec, they made this research possible.

8. AUTRES CONTRIBUTIONS

Cette section de la thèse décrit les autres contributions scientifiques lors de mes études doctorales. J'ai contribué à la rédaction de quatre autres articles scientifiques, 12 conférences internationales et quatre rappports de recherche.

8.1. AUTRES ARTICLES SCIENTIFIQUES

Martel R., **Castellazzi P.**, Gloagen E. A multidisciplinary approach for karst mapping under urban areas: the case of Quebec City, Canada. Soumission au journal *Geomorphology* en Septembre 2017

Jaramillo F, Brown I., **Castellazzi P.**, Espinosa L., Guittard A., Hong S.H., Rivera-Monroy V., Wdowinski S. Assessment of hydrologic connectivity and restoration in ungauged wetlands with Interferometric SAR observations. *Environmental Earth Sciences.* Soumission au journal *Environmental Research Letters* le 4 Juillet 2017.

Castellazzi, P., R. Martel, J. Garfias, A. I. Calderhead, J. Salas-García, J. Huang, and A. Rivera (2014), Groundwater deficit and land subsidence in central Mexico monitored by GRACE and RADARSAT-2, article de conférence présenté au *2014 IEEE Geoscience and Remote Sensing Symposium*, 13-18 July 2014, Quebec City, Canada.

Martel, R., **Castellazzi P.**, L. Trépanier, M. Laporte-Saumure, and S. Brochu (2014), Accuracy of Lysimeters for Dissolved Copper, Antimony, Lead, and Zinc Sampling under Small Arms Backstop, *Vadose Zone Journal*, 13(8).

8.2. COMMUNICATIONS LORS DE CONFÉRENCES INTERNATIONALES

Castellazzi P., Martel R, Calderhead A.I. (2016). InSAR to understand groundwater flow systems and support groundwater management. 43th International Association of Hydrogeologist Congress. Montpellier, France. September 30th.

Castellazzi P., Martel R., Rivera A., Calderhead A.I., Garfias J., Chaussard E. (2016). Groundwater depletion in Central Mexico: the use of InSAR and GRACE to support groundwater management. *69th National Conference of the Canadian Water Resources Association*, Montreal, QC, Canada. May.

Castellazzi P., Martel R., Rivera A., Calderhead A.I, Garfias J. (2015). Évaluer la durabilité des ressources en souterraine par télédétection…l'eau souterraine vue de

l'espace. Congrès Étudiant INRS-ETE, Passé, Présent et Futur 3 perspectives de l'environnement, Québec, 6 novembre.

Martel R, Gabriel U., Trépanier L., Tranquille Temgoua A.G., **Castellazzi P.,** Bordeleau G., Parent M. (2015) Groundwater Characterisation of military range training areas, Presented at Department of Physical & Applied Geology, Eötvös Loránd University, Budapest, Hungary Oct 15th.

Martel, R, U. Gabriel, L. Trépanier, A.-G. Tranquille Temgoua, **P. Castellazzi**, G. Bordeleau and M. Parent (2015) Characterisation of groundwater of military range training areas, In proceedings of STO-MP-AVT-244 Munitions-Related Contamination, Applied Vehicle Technology Panel (AVT) Specialists' *NATO-AVT-244* Meeting 12-14 October, Prague, Czech Republic.

Castellazzi P., Martel R., Rivera A., Huang J., Calderhead A.I, Chaussard E., Garfias J. (2015). Remote sensing and hydrogeology: GRACE and InSAR to assess groundwater sustainability in Central Mexico. *NGWA Groundwater Summit*. San Antonio, TX, USA. March.

Calderhead A.I., Hinton M., Logan C., Sharpe D., Russell H., Oldenborger G., **Castellazzi P.**, Pugin A., Martel R., Rivera A.(2014). Remote sensing techniques for understanding the groundwater flow dynamics of a buried valley aquifer. *IGARSS. IEEE*. Quebec, QC, Canada. July.

Castellazzi P., Martel R., Garfias-Soliz J., Calderhead A.I, Salas-Garcia J., Huang J.,Rivera A. (2014). Groundwater deficit and land subsidence in Central Mexico monitored by GRACE and RADARSAT-2. *IGARSS. IEEE*. Quebec, QC, Canada. July.

Castellazzi P., Martel R., Garfias-Soliz J., Calderhead A.I, Salas-Garcia J., Huang J.,Rivera A. (2014). Groundwater deficit and land subsidence in the Lerma-Santiago-Pacifico Watershed, Mexico. *NGWA Groundwater Summit*. Denver, CO, USA. May.

Calderhead, A I, Hinton, M., Logan, C., Sharpe, D., Russell, H A J., Oldenborger, G., Pugin, Rivera, A., Castellazzi, P., and R. Martel (2013). A Groundwater flow dynamic simulations of a buried valley aquifer calibrated with field and remotely sensed data presented at *American Geophysical Union*, Fall Meeting 2013, San Francisco, CA, United States, Dec. 2013

Castellazzi P., Martel R., Calderhead I.A. Garfias, J.,Rivera A. (2012). Sobrexplotación y subsidencia en el acuífero del valle de Toluca y en la cuenca Lerma-Santiago, México. *Convención Nacional Geológica*. Mexico city, Mexico. November.

Castellazzi P., Martel R., Calderhead A.I., Garfias J, Rivera A. (2012). Estudio de la sobreexplotación y la subsidencia en el acuífero del valle de Toluca y en la cuenca Lerma-Santiago, México. *Congreso Internacional de Hidrogeología y Recursos Hídricos*. Sucre, Bolvia. October.

8.3. RAPPORTS DE RECHERCHE

Martel, R., Trépanier, L., Gloaguen, E., Lavoie, D., Varfalvy, V., Laflèche, M., **Castellazzi, P.**, Perret D., Calderhead A., Parent M., Gabriel U., Boutin M., Bernier, M., Gauthier, Y., Deschênes-Rancourt, C., Levesque R., Millet, E., Jouveau, M.J., Normand, J. (2014). Étude des grottes de Courville à partir de méthodes quantitatives en sciences de la terre – 4.7 Interférométrie par images satellitaires. INRS-ETE, Research report R-1494.

Martel R., Gabriel U., Varfalvy V., Deschênes-Rancourt, C., Jouveau M.J, **Castellazzi P**. (2014) Drilling and groundwater sampling at the CFAD Dundurn destruction area and at 17 wing Winnipeg DET Dundurn. INRS-ETE, Research report R-1485.

Martel, R., Trépanier, L., **Castellazzi, P.**, Deschênes-Rancourt, C. et Gosselin, J.-S. (2013). Suivi des lysimètres installés dans le champ de tir de petit calibre 30 lignes BFC Farnham. INRS-ETE, Research report R-1400.

Martel R., Trepanier L., Deschênes-Rancourt C., **Castellazzi P.**, Lafond S., Jaotombo N. (2012). Sondage CPT, analyse de l'eau et des sols au champ de tir B à la garnison Farhnam et suivi des lysimètres aux champs de tir Nicosie et Famagusta et à la butte expérimentale de Valcartier. INRS-ETE, Research report R-1341.

Bibliographie

Aguirre-Díaz, G. J., J. Nieto-Obregón, and F. R. Zúñiga (2005), Seismogenic basin and range and intra-arc normal faulting in the central Mexican Volcanic Belt, Querétaro, México, *Geological Journal*, *40*(2), 215-243.

Alley, W. M., and L. F. Konikow (2015), Bringing GRACE Down to Earth, *Groundwater*, *53*(6), 826-829.

Alley, W. M., T. E. Reilly, and O. L. Franke (1999), *Sustainability of ground-water resources*, US Department of the Interior, US Geological Survey.

Amelung, F., D. L. Galloway, J. W. Bell, H. A. Zebker, and R. J. Laczniak (1999), Sensing the ups and downs of Las Vegas: InSAR reveals structural control of land subsidence and aquifer-system deformation, *Geology*, *27*(6), 483-486.

Aranda-Gomez, J. J., et al. (2013), Active sinking at the bottom of the Rincon de Parangueo Maar (Guanajuato, Mexico) and its probable relation with subsidence faults at Salamanca and Celaya, *Boletin De La Sociedad Geologica Mexicana*, *65*(1), 169-188.

Armandine Les Landes, A., L. Aquilina, J. De Ridder, L. Longuevergne, C. Pagé, and P. Goderniaux (2014), Investigating the respective impacts of groundwater exploitation and climate change on wetland extension over 150 years, *Journal of Hydrology*, *509*, 367-378.

Armienta, M. A., and N. Segovia (2008), Arsenic and fluoride in the groundwater of Mexico, *Environmental Geochemistry and Health*, *30*(4), 345-353.

ASTER, G. (2009), Validation Team: ASTER Global DEM Validation–Summary Report, *METI & NASA*, *28*.

Avila-Olivera, J. A., and V. H. Garduno-Monroy (2008), A GPR study of subsidence-creep-fault processes in Morelia, Michoacan, Mexico, *Engineering Geology*, *100*(1-2), 69-81.

Avila-Olivera, J. A., P. Farina, and V. H. Garduno-Monroy (2008), Unmasking sinkings zones caused by Subsidence-Creep-Fault Processes in Morelia, Michoacan, using Insar and GIS, in *GIS in Geology and Earth Sciences*, edited by K. Oleschko, S. Cherkasov,

J. L. PalacioPrieto, V. TorresArguelles, C. I. GaonaSalado, A. G. CastanedaMiranda and S. A. ZamoraCastro, pp. 273-273.

Avila-Olivera, J. A., P. Farina, and V. H. Garduno-Monroy (2008), Integration of InSAR and GIS in the study of surface faults caused by subsidence-creep-fault processes in Celaya, Guanajuato, Mexico, in *GIS in Geology and Earth Sciences*, edited by K. Oleschko, S. Cherkasov, J. L. PalacioPrieto, V. TorresArguelles, C. I. GaonaSalado, A. G. CastanedaMiranda and S. A. ZamoraCastro, pp. 200-211.

Avila-Olivera, J. A., P. Farina, and V. H. Garduno-Monroy (2010), Land subsidence monitored by satellite interferometry in Mexican cities, in *Land Subsidence, Associated Hazards and the Role of Natural Resources Development*, edited by D. CarreonFreyre, M. Cerca, D. L. Galloway and J. J. SilvaCorona, pp. 316-318.

Avila-Olivera, J. A., V. H. Garduno-Monroy, and P. Farina (2010), Integrated study of land subsidence in Morelia, Michoacan, Mexico, in *Land Subsidence, Associated Hazards and the Role of Natural Resources Development*, edited by D. CarreonFreyre, M. Cerca, D. L. Galloway and J. J. SilvaCorona, pp. 185-190.

Bai, L., L. Jiang, H. Wang, and Q. Sun (2016), Spatiotemporal characterization of land subsidence and uplift (2009-2010) over Wuhan in Central China revealed by TerraSAR-X InSAR analysis, *Remote Sensing*, *8*(4).

Bamler, R., and P. Hartl (1998), Synthetic aperture radar interferometry, *Inverse Problems*, *14*(4), R1-R54.

Bell, J. W., F. Amelung, A. Ferretti, M. Bianchi, and F. Novali (2008), Permanent scatterer InSAR reveals seasonal and long-term aquifer-system response to groundwater pumping and artificial recharge, *Water Resources Research*, *44*(2).

Berardino, P., G. Fornaro, R. Lanari, and E. Sansosti (2002), A new algorithm for surface deformation monitoring based on small baseline differential SAR interferograms, *IEEE Transactions on Geoscience and Remote Sensing*, *40*(11), 2375-2383.

Bettadpur, S. (2012), UTCSR Level-2 Processing Standards Document for Level-2 Product Release 0005, GRACE 327-742, CSR Publ, *GR-12-xx, Rev*, *4*.

Billah, M. M., J. L. Goodall, U. Narayan, J. T. Reager, V. Lakshmi, and J. S. Famiglietti (2015), A methodology for evaluating evapotranspiration estimates at the watershed-scale using GRACE, *Journal of Hydrology*, *523*, 574-586.

Biot, M. (1941), General theory of three-dimensional consolidation. *Journal of Applied Physics* 12(2):155 – 164

Biot, M. A. (1941), General theory of three-dimensional consolidation, *Journal of applied physics*, *12*(2), 155-164.

Bouwer, H. (1991), Ground-water recharge with sewage effluent, *Water Science and Technology*, *23*(10-12), 2099-2108.

Bozzano, F., I. Cipriani, P. Mazzanti, and A. Prestininzi (2011), Displacement patterns of a landslide affected by human activities: insights from ground-based InSAR monitoring, *Natural hazards*, *59*(3), 1377-1396.

Bredehoeft, J. D. (2002), The water budget myth revisited: Why hydrogeologists model, *Ground Water*, *40*(4), 340-345.

Broussolle, J., V. Kyovtorov, M. Basso, G. Ferraro Di Silvi E Castiglione, J. Figueiredo Morgado, R. Giuliani, F. Oliveri, P. F. Sammartino, and D. Tarchi (2014), MELISSA, a new class of ground based InSAR system. An example of application in support to the Costa Concordia emergency, *ISPRS Journal of Photogrammetry and Remote Sensing*, *91*, 50-58.

Bru, G., G. Herrera, R. Tomas, J. Duro, R. De la Vega, and J. Mulas (2013), Control of deformation of buildings affected by subsidence using persistent scatterer interferometry, *Struct. Infrastruct. Eng.*, *9*(2), 188-200.

Bruinsma, S., J.-M. Lemoine, R. Biancale, and N. Valès (2010), CNES/GRGS 10-day gravity field models (release 2) and their evaluation, *Advances in Space Research*, *45*(4), 587-601.

Brunori, C., C. Bignami, M. Albano, F. Zucca, S. Samsonov, G. Groppelli, G. Norini, M. Saroli, and S. Stramondo (2015), Land subsidence, Ground Fissures and Buried Faults: InSAR Monitoring of Ciudad Guzmán (Jalisco, Mexico), *Remote Sensing*, *7*(7), 8610.

Burbey, T. J. (2002), The influence of faults in basin-fill deposits on land subsidence, Las Vegas Valley, Nevada, USA, *Hydrogeology Journal*, *10*(5), 525-538.

Burgess, D., and M. J. Sharp (2008), Recent changes in thickness of the Devon Island ice cap, Canada, *Journal of Geophysical Research-Solid Earth*, *113*(B7).

Burgmann, R., P. A. Rosen, and E. J. Fielding (2000), Synthetic aperture radar interferometry to measure Earth's surface topography and its deformation, *Annual Review of Earth and Planetary Sciences*, *28*, 169-209.

Cabral-Cano, E., D. Solano-Rojas, T. Oliver-Cabrera, S. Wdowinski, E. Chaussard, L. Salazar-Tlaczani, F. Cigna, C. DeMets, and J. Pacheco-Martínez (2015), Satellite geodesy tools for ground subsidence and associated shallow faulting hazard assessment in central Mexico, *Proceedings of the International Association of Hydrological Sciences*, *372*, 255.

Cabral-Cano, E., et al. (2010), Is there a tectonic component to the subsidence process in Morelia, Mexico?, in *Land Subsidence, Associated Hazards and the Role of Natural Resources Development*, edited by D. CarreonFreyre, M. Cerca, D. L. Galloway and J. J. SilvaCorona, pp. 164-169.

Calderhead, A. I., R. Martel, J. Garfias, A. Rivera, and R. Therrien (2010), Pumping effects on land subsidence in the Toluca Valley, Mexico, in *Land Subsidence, Associated Hazards and the Role of Natural Resources Development*, edited by D. CarreonFreyre, M. Cerca, D. L. Galloway and J. J. SilvaCorona, pp. 461-466.

Calderhead, A. I., R. Martel, J. Garfias, A. Rivera, and R. Therrien (2012a), Sustainable Management for Minimizing Land Subsidence of an Over-Pumped Volcanic Aquifer System: Tools for Policy Design, *Water Resources Management*, *26*(7), 1847-1864.

Calderhead, A. I., R. Martel, J. Garfias, A. Rivera, and R. Therrien (2012b), Pumping dry: an increasing groundwater budget deficit induced by urbanization, industrialization, and climate change in an over-exploited volcanic aquifer, *Environmental Earth Sciences*, *66*(7), 1753-1767.

Calderhead, A. I., R. Martel, P. J. Alasset, A. Rivera, and J. Garfias (2010), Land subsidence induced by groundwater pumping, monitored by D-InSAR and field data in the Toluca Valley, Mexico, *Canadian Journal of Remote Sensing*, *36*(1), 9-23.

Calderhead, A. I., R. Therrien, A. Rivera, R. Martel, and J. Garfias (2011), Simulating pumping-induced regional land subsidence with the use of InSAR and field data in the Toluca Valley, Mexico, *Adv. Water Resour.*, *34*(1), 83-97.

Carreon-Freyre, D., M. Cerca, and M. Hernandez-Marin (2003), Correlation of near-surface stratigraphy and physical properties of clayey sediments from Chalco Basin, Mexico, using Ground Penetrating Radar, *Journal of Applied Geophysics*, *53*(2-3), 121-136.

Castellazzi, P., N. Arroyo-Domínguez, R. Martel, A. I. Calderhead, J. C. L. Normand, J. Gárfias, and A. Rivera (2016a), Land subsidence in major cities of Central Mexico: Interpreting InSAR-derived land subsidence mapping with hydrogeological data, *International Journal of Applied Earth Observation and Geoinformation*, *47*, 102-111.

Castellazzi, P., R. Martel, A. Rivera, J. Huang, G. Pavlic, A. I. Calderhead, E. Chaussard, J. Garfias, and J. Salas (2016b), Groundwater depletion in Central Mexico: Use of GRACE and InSAR to support water resources management, *Water Resources Research*, *52*(8), 5985-6003.

Castellazzi, P., R. Martel, D. L. Galloway, L. Longuevergne, and A. Rivera (2016c), Assessing Groundwater Depletion and Dynamics Using GRACE and InSAR: Potential and Limitations, *Groundwater*.

Castellazzi, P., R. Martel, J. Garfias, A. I. Calderhead, J. Salas-García, J. Huang, and A. Rivera (2014), Groundwater deficit and land subsidence in central mexico monitored by grace and RADARSAT-2, paper presented at 2014 *IEEE Geoscience and Remote Sensing Symposium*, 13-18 July 2014.

Castellazzi P., Martel R., Garfias J., Rivera A. (2017a), InSAR to support sustainable urbanization over compacting aquifers: the case of Toluca Valley, Mexico. *International Journal of Applied Earth Observation and Geoinformation*, *63*, 33-34.

Castellazzi P., Longuevergne L., Martel R., Rivera A., Brouard C., Chaussard E. (2017b – en revision), Combining GRACE and InSAR for quantitative mapping of groundwater depletion at the water management scale. (Soumis à la revue *Remote Sensing of Environment* le 23 mars 2017). En révision.

Cazenave, A., and J. Chen (2010), Time-variable gravity from space and present-day mass redistribution in theEarth system, *Earth and Planetary Science Letters*, *298*(3), 263-274.

Center for International Earth Science Information Network - CIESIN - Columbia University, and Centro Internacional de Agricultura Tropical - CIAT. (2005), Gridded Population of the World, Version 3 (GPWv3): Population Density Grid. Palisades, NY: NASA Socioeconomic Data and Applications Center (SEDAC). http://dx.doi.org/10.7927/H4XK8CG2.

Chaussard, E., F. Amelung, H. Abidin, and S. H. Hong (2013), Sinking cities in Indonesia: ALOS PALSAR detects rapid subsidence due to groundwater and gas extraction, *Remote Sensing of Environment*, *128*, 150-161.

Chaussard, E., R. Bürgmann, H. Fattahi, R. M. Nadeau, T. Taira, C. W. Johnson, and I. Johanson (2015), Potential for larger earthquakes in the East San Francisco Bay Area due to the direct connection between the Hayward and Calaveras Faults, *Geophysical Research Letters*, *42*(8), 2734-2741.

Chaussard, E., R. Bürgmann, M. Shirzaei, E. J. Fielding, and B. Baker (2014a), Predictability of hydraulic head changes and characterization of aquifer-system and fault properties from InSAR-derived ground deformation, *Journal of Geophysical Research: Solid Earth*, *119*(8), 6572-6590.

Chaussard, E., S. Wdowinski, E. Cabral-Cano, and F. Amelung (2014b), Land subsidence in central Mexico detected by ALOS InSAR time-series, *Remote Sensing of Environment*, *140*, 94-106.

Chen, J. L., C. R. Wilson, B. D. Tapley, Z. L. Yang, and G. Y. Niu (2009), 2005 drought event in the Amazon River basin as measured by GRACE and estimated by climate models, *Journal of Geophysical Research-Solid Earth*, *114*.

Cheng, M., B. D. Tapley, and J. C. Ries (2013), Deceleration in the Earth's oblateness, *Journal of Geophysical Research: Solid Earth*, *118*(2), 740-747.

Chinnasamy, P., and G. Agoramoorthy (2015), Groundwater Storage and Depletion Trends in Tamil Nadu State, India, *Water Resources Management*, *29*(7), 2139-2152.

Cigna, F., B. Osmanoglu, E. Cabral-Cano, T. H. Dixon, J. A. Avila-Olivera, V. H. Garduno-Monroy, C. DeMets, and S. Wdowinski (2012), Monitoring land subsidence and its induced geological hazard with Synthetic Aperture Radar Interferometry: A case study in Morelia, Mexico, *Remote Sensing of Environment*, *117*, 146-161.

Cigna, F., E. Cabral-Cano, B. Osmanoglu, T. H. Dixon, S. Wdowinski, and Ieee (2011), Detecting subsidence-induced faulting in Mexican urban areas by means of persistent scatterer interferometry and subsidence horizontal gradient mapping, *2011 Ieee International Geoscience and Remote Sensing Symposium (Igarss)*, 2125-2128.

CONAGUA (2009a), Acuerdo por el que se da a conocer la ubicación geográfica de 371 acuíferos del territorio nacional, se actualiza la disponibilidad media anual de agua subterránea de 282 acuíferos, y se modifica, para su mejor precisión. México, Comisión Nacional del Agua. http://www.conagua.gob.mx/CONAGUA07/Noticias/DOF-28-08-2009.pdf

CONAGUA (2009b), Actualización de la disponibilidad media anual de agua subterránea acuífero (1501) Valle de Toluca. Estado de México. Diario oficial de la Federación, Mexico. http://www.conagua.gob.mx/Conagua07/Aguasubterranea/pdf/DR_1501.pdf

CONAGUA (2013a), Acuerdo por el que se actualiza la disponibilidad media anual de agua subterránea de los 653 acuíferos de los Estados Unidos Mexicanos, mismos que forman parte de las regiones hidrológico-administrativas que se indican. México, Comisión Nacional del Agua, Mexico.

CONAGUA (2013b), Estadísticas del Agua en México, Edición 2013. http://www.conagua.gob.mx/CONAGUA07/Noticias/SGP-2-14Web.pdf

Cooper, A. H., and R. Calow (1998), Avoiding gypsum geohazards: guidance for planning and construction.

Cooper, H. H., and C. E. Jacob (1946), A generalized graphical method for evaluating formation constants and summarizing well-field history, *Eos, Transactions American Geophysical Union*, *27*(4), 526-534.

Couture, R., and S. Riopel (2008), Landslide hazards mapping and permafrost slope InSAR monitoring, Mackenzie Valley, Northwest Territories, Canada, 1151-1155 pp.

Crosetto, M., O. Monserrat, M. Cuevas-González, N. Devanthéry, and B. Crippa (2016), Persistent Scatterer Interferometry: A review, *ISPRS Journal of Photogrammetry and Remote Sensing*, *115*, 78-89.

Davila-Hernandez, N., D. Madrigal, J. L. Exposito, and X. Antonio (2014), Multi-temporal analysis of land subsidence in Toluca Valley (Mexico) through a combination of Persistent Scatterer Interferometry (PSI) and historical piezometric data, *Advances in Remote Sensing, 2014*.

Davis, J. L., M. E. Tamisiea, P. Elósegui, J. X. Mitrovica, and E. M. Hill (2008), A statistical filtering approach for Gravity Recovery and Climate Experiment (GRACE) gravity data, *Journal of Geophysical Research: Solid Earth*, 113, B04410, doi:10.1029/2007JB005043.

de Marsily, G., F. Delay, J. Gonçalvès, P. Renard, V. Teles, and S. Violette (2005), Dealing with spatial heterogeneity, *Hydrogeology Journal*, *13*(1), 161-183.

del Campo, M. A. M., M. V. Esteller, J. L. Exposito, and R. Hirata (2014), Impacts of urbanization on groundwater hydrodynamics and hydrochemistry of the Toluca Valley aquifer (Mexico), *Environmental Monitoring and Assessment*, *186*(5), 2979-2999.

Densmore, J., K. Ellett, J. Howle, M. Carpenter, and M. Sneed (2010), Monitoring land-surface deformation on Bicycle Lake playa, Fort Irwin, California, USA, in *Land Subsidence, Associated Hazards and the Role of Natural Resources Development*, edited by D. CarreonFreyre, M. Cerca, D. L. Galloway and J. J. SilvaCorona, pp. 39-43.

Dixon, T. H., F. Amelung, A. Ferretti, F. Novali, F. Rocca, R. Dokka, G. Sella, S.-W. Kim, S. Wdowinski, and D. Whitman (2006), Space geodesy: Subsidence and flooding in New Orleans, *Nature*, *441*(7093), 587-588.

Döll, P., H. Hoffmann-Dobrev, F. T. Portmann, S. Siebert, A. Eicker, M. Rodell, G. Strassberg, and B. Scanlon (2012), Impact of water withdrawals from groundwater and surface water on continental water storage variations, *Journal of Geodynamics*, *59*, 143-156.

Domenico, P. A., and M. D. Mifflin (1965), Water from low-permeability sediments and land subsidence, *Water Resources Research*, *1*(4), 563-576.

Dong, S., S. Samsonov, H. Yin, S. Ye, and Y. Cao (2014), Time-series analysis of subsidence associated with rapid urbanization in Shanghai, China measured with SBAS InSAR method, *Environmental earth sciences*, *72*(3), 677-691.

dos Reis Júnior, J. A., D. L. de Castro, A. Casas, M. Himi, and F. P. Lima-Filho (2015), ERT and GPR survey of collapsed paleocave systems at the western border of the Potiguar Basin in northeast Brazil, *Near Surface Geophysics*, *13*(4), 369-381.

Dragoni, W. (1998), Some considerations regarding the radius of influence of a pumping well, *Hydrogeologie*(3), 21-26.

Eicker, A., M. Schumacher, J. Kusche, P. Döll, and H. M. Schmied (2014), Calibration/Data Assimilation Approach for Integrating GRACE Data into the WaterGAP Global Hydrology Model (WGHM) Using an Ensemble Kalman Filter: First Results, *Surv Geophys*, *35*(6), 1285-1309.

Esteller, M. V., and C. Diaz-Delgado (2002), Environmental effects of aquifer overexploitation: A case study in the highlands of Mexico, *Environmental Management*, *29*(2), 266-278.

Esteller, M. V., and J. M. Andreu (2005), Anthropic effects on hydrochemical characteristics of the Valle de Toluca aquifer (central Mexico), *Hydrogeology Journal*, *13*(2), 378-390.

Esteller, M. V., R. Rodriguez, A. Cardona, and L. Padilla-Sanchez (2012), Evaluation of hydrochemical changes due to intensive aquifer exploitation: case studies from Mexico, *Environmental Monitoring and Assessment*, *184*(9), 5725-5741.

Famiglietti, J. S. (2014), The global groundwater crisis, *Nature Climate Change*, *4*(11), 945-948.

Famiglietti, J. S., and M. Rodell (2013), Water in the Balance, *Science*, *340*(6138), 1300-1301.

Famiglietti, J. S., M. Lo, S. L. Ho, J. Bethune, K. J. Anderson, T. H. Syed, S. C. Swenson, C. R. de Linage, and M. Rodell (2011), Satellites measure recent rates of groundwater depletion in California's Central Valley, *Geophysical Research Letters*, *38*.

Farina, P., J. Alejandro Avila-Olivera, V. Hugo Garduno-Monroy, and F. Catani (2008), DInSAR analysis of differential ground subsidence affecting urban areas along the Mexican Volcanic Belt (MVB), *Rivista Italiana Di Telerilevamento*, *40*(2), 103-113.

Farinotti, D., L. Longuevergne, G. Moholdt, D. Duethmann, T. Mölg, T. Bolch, S. Vorogushyn, and A. Güntner (2015), Substantial glacier mass loss in the Tien Shan over the past 50 years, *Nature Geoscience*, *8*(9), 716-722.

Farr, T. G., et al. (2007), The shuttle radar topography mission, *Reviews of Geophysics*, *45*(2).

Feng, W., M. Zhong, J.-M. Lemoine, R. Biancale, H.-T. Hsu, and J. Xia (2013), Evaluation of groundwater depletion in North China using the Gravity Recovery and Climate Experiment (GRACE) data and ground-based measurements, *Water Resources Research*, *49*(4), 2110-2118.

Fernando, L. G., and O. F. Gerardo (1999), Feasibility study for the attenuation of groundwater exploitation impacts in the urban area of Aguascalientes, Mexico, 181-187 pp.

Ferrari, L., T. Orozco-Esquivel, V. Manea, and M. Manea (2012), The dynamic history of the Trans-Mexican Volcanic Belt and the Mexico subduction zone, *Tectonophysics*, *522*, 122-149.

Ferretti, A., A. Fumagalli, F. Novali, C. Prati, F. Rocca, and A. Rucci (2011), A new algorithm for processing interferometric data-stacks: SqueeSAR, *IEEE Transactions on Geoscience and Remote Sensing*, *49*(9), 3460-3470.

Ferretti, A., C. Prati, and F. Rocca (2000a), Analysis of permanent scatterers in SAR interferometry, paper presented at Geoscience and Remote Sensing Symposium, 2000. Proceedings. IGARSS 2000. IEEE 2000 International, IEEE.

Ferretti, A., C. Prati, and F. Rocca (2000b), Non-linear subsidence rate estimation using permanent scatterers in differential SAR interferometry, *IEEE Transactions on Geoscience and Remote Sensing*, *38*(5), 2202-2212.

Ferretti, A., C. Prati, and F. Rocca (2001), Permanent scatterers in SAR interferometry, *IEEE Transactions on Geoscience and Remote Sensing*, *39*(1), 8-20.

Ferretti, A., G. Savio, R. Barzaghi, A. Borghi, S. Musazzi, F. Novali, C. Prati, and F. Rocca (2007), Submillimeter accuracy of InSAR time series: Experimental validation, *IEEE Transactions on Geoscience and Remote Sensing*, *45*(5), 1142-1153.

Figueroa Vega, G.E. (2004), El agrietamiento de la ciudad de Toluca. Informe preparado a solicitud del Gobierno del estado de México, 27 p.

Forootan, E., R. Rietbroek, J. Kusche, M. A. Sharifi, J. L. Awange, M. Schmidt, P. Omondi, and J. Famiglietti (2014), Separation of large scale water storage patterns over Iran using GRACE, altimetry and hydrological data, *Remote Sensing of Environment*, *140*, 580-595.

Foster, S. S., H. Garduño, A. Tuinhof, K. Kemper, and M. Nanni (2003), Urban wastewater as groundwater recharge: Evaluating and managing the risks and benefits, in *GW-MATE Briefing Note Series*, edited, Banco Mundial.

Freeze, R. A., and J. A. Cherry (1979), Groundwater, *Groundwater*.

Freyre, D. C. (2010), Land subsidence processes and associated ground fracturing in central Mexico, in *Land Subsidence, Associated Hazards and the Role of Natural Resources Development*, edited by D. CarreonFreyre, M. Cerca, D. L. Galloway and J. J. SilvaCorona, pp. 149-157.

Galloway, D. L. (2014), Retrospective of InSAR/DInSAR contributions to hydrogeology by way of bibliographic search, paper presented at Geoscience and Remote Sensing Symposium (IGARSS), 2014 IEEE International, 13-18 July 2014.

Galloway, D. L., and T. J. Burbey (2011), Review: Regional land subsidence accompanying groundwater extraction, *Hydrogeology Journal*, *19*(8), 1459-1486.

Galloway, D. L., and J. Hoffmann (2007), The application of satellite differential SAR interferometry-derived ground displacements in hydrogeology, *Hydrogeology Journal*, *15*(1), 133-154.

Galloway, D., R. Bürgmann, E. Fielding, F. Amelung, and R. Laczniak (2000), Mapping recoverable aquifer-system deformation and land subsidence in Santa Clara Valley, California, USA, using space-borne synthetic aperture radar, paper presented at Proceedings of the 6th International Symposium on Land Subsidence.

Galloway, D. L., K. W. Hudnut, S. E. Ingebritsen, S. P. Phillips, G. Peltzer, F. Rogez, and P. A. Rosen (1998), Detection of aquifer system compaction and land subsidence using interferometric synthetic aperture radar, Antelope Valley, Mojave Desert, California, *Water Resources Research*, *34*(10), 2573-2585.

Georgakakos, K., and O. W. Baumer (1996), Measurement and utilization of on-site soil moisture data, *Journal of Hydrology*, *184*(1-2), 131-152.

Gleeson, T., Y. Wada, M. F. P. Bierkens, and L. P. H. van Beek (2012), Water balance of global aquifers revealed by groundwater footprint, *Nature*, *488*(7410), 197-200.

Goldberg, D. E. (1989), Genetic Algorithms in Search, Optimization and Machine Learning, 372 pp., Addison-Wesley Longman Publishing Co., Inc.

Gonzalez-Sosa, E., N. R. Ramos-Salinas, and C. A. Mastachi-Loza (2010), Climate change impact and anthropogenic effects in land subsidence of Queretaro valley, Mexico, in *Land Subsidence, Associated Hazards and the Role of Natural Resources Development*, edited by D. CarreonFreyre, M. Cerca, D. L. Galloway and J. J. SilvaCorona, pp. 514-518.

Gray, L. (2011), Using multiple RADARSAT InSAR pairs to estimate a full three-dimensional solution for glacial ice movement, *Geophysical Research Letters*, *38*.

Green, T. R., M. Taniguchi, H. Kooi, J. J. Gurdak, D. M. Allen, K. M. Hiscock, H. Treidel, and A. Aureli (2011), Beneath the surface of global change: Impacts of climate change on groundwater, *Journal of Hydrology*, *405*(3-4), 532-560.

Güntner, A., R. Schmidt, and P. Döll (2007), Supporting large-scale hydrogeological monitoring and modelling by time-variable gravity data, *Hydrogeology Journal*, *15*(1), 167-170.

Halford, K. J., W. D. Weight, and R. P. Schreiber (2006), Interpretation of transmissivity estimates from single-well pumping aquifer tests, *Ground Water*, *44*(3), 467-471.

Hernandez-Marin, M., and T. J. Burbey (2009), The role of faulting on surface deformation patterns from pumping-induced groundwater flow (Las Vegas Valley, USA), *Hydrogeology Journal*, *17*(8), 1859-1875.

Hernandez-Marin, M., J. Pacheco-Martinez, A. Ramirez-Cortes, T. J. Burbey, J. A. Ortiz-Lozano, M. E. Zermeno-de-Leon, J. Guinzberg-Velmont, and G. Pinto-Aceves (2014), Evaluation and analysis of surface deformation in west Chapala basin, central Mexico, *Environmental Earth Sciences*, *72*(5), 1491-1501.

Heywood, C. E., D. L. Galloway, and S. V. Stork (2002), Ground displacements caused by aquifer-system water-level variations observed using interferometric synthetic aperture radar near Albuquerque, New Mexico.

Hijmans, R. J., S. E. Cameron, J. L. Parra, P. G. Jones, and A. Jarvis (2005), Very high resolution interpolated climate surfaces for global land areas, *International Journal of Climatology*, *25*(15), 1965-1978.

Hilley, G. E., R. Burgmann, A. Ferretti, F. Novali, and F. Rocca (2004), Dynamics of slow-moving landslides from permanent scatterer analysis, *Science*, *304*(5679), 1952-1955.

Hoffmann, J., D. L. Galloway, and H. A. Zebker (2003), Inverse modeling of interbed storage parameters using land subsidence observations, Antelope Valley, California, *Water Resources Research*, *39*(2).

Hoffmann, J., H. A. Zebker, D. L. Galloway, and F. Amelung (2001), Seasonal subsidence and rebound in Las Vegas Valley, Nevada, observed by synthetic aperture radar interferometry, *Water Resources Research*, *37*(6), 1551-1566.

Hoffmann, J., S. Leake, D. Galloway, and A. M. Wilson (2003), MODFLOW-2000 ground-water model--User guide to the subsidence and aquifer-system compaction (SUB) package, DTIC Document.

Holland, J. H. (1992), Genetic algorithms, *Scientific american*, *267*(1), 66-72.

Hooke, R., and T. A. Jeeves (1961), `` Direct Search" Solution of Numerical and Statistical Problems, *J. ACM*, *8*(2), 212-229.

Hooper, A., H. Zebker, P. Segall, and B. Kampes (2004), A new method for measuring deformation on volcanoes and other natural terrains using InSAR persistent scatterers, *Geophysical Research Letters*, *31*(23).

Hu, L., and J. J. Jiao (2015), Calibration of a large-scale groundwater flow model using GRACE data: a case study in the Qaidam Basin, China, *Hydrogeology Journal*, *23*(7), 1305-1317.

Huang, J., J. Halpenny, W. van der Wal, C. Klatt, T. S. James, and A. Rivera (2012), Detectability of groundwater storage change within the Great Lakes Water Basin using GRACE, *Journal of Geophysical Research-Solid Earth*, *117*.

Huang, Z., Y. Pan, H. Gong, P. J. F. Yeh, X. Li, D. Zhou, and W. Zhao (2015), Subregional-scale groundwater depletion detected by GRACE for both shallow and deep aquifers in North China Plain, *Geophysical Research Letters*, *42*(6), 1791-1799.

Huizar-Alvarez, R., L. M. Mitre-Salazar, S. Marin-Cordova, J. Trujillo-Candelaria, and J. Martinez-Reyes (2011), Subsidence in Celaya, Guanajuato, Central Mexico: implications for groundwater extraction and the neotectonic regime, *Geofisica Internacional*, *50*(3), 255-270.

INEGI - Instituto Nacional de Estadística y Geografía (2015), Encuesta Intercensal 2015.

Instituto Nacional de Estadística y Geografía – INEGI (2005), Conjunto de Datos Vectoriales de la Carta de Uso del Suelo y Vegetación, Escala 1:1'000,000 Serie II (Continuo Nacional), INEGI, Mexico.

Jacob, C. E. (1940), On the flow of water in an elastic artesian aquifer, *Eos, Transactions American Geophysical Union*, *21*(2), 574-586.

Jiang, Y., M. Liao, Z. Zhou, X. Shi, L. Zhang, and T. Balz (2016), Landslide deformation analysis by coupling deformation time series from SAR data with hydrological factors through data assimilation, *Remote Sensing*, *8*(3).

Junez-Ferreira, H. E., and G. S. Herrera (2013), A geostatistical methodology for the optimal design of space-time hydraulic head monitoring networks and its application to the Valle de Quer,taro aquifer, *Environmental Monitoring and Assessment*, *185*(4), 3527-3549.

Khakim, M. Y. N., T. Tsuji, and T. Matsuoka (2013), Detection of Localized Surface Uplift by Differential SAR Interferometry at the Hangingstone Oil Sand Field, Alberta,

Canada, *Ieee Journal of Selected Topics in Applied Earth Observations and Remote Sensing*, *6*(6), 2344-2354.

Khan, S. D., Z. Huang, and A. Karacay (2014), Study of ground subsidence in northwest Harris county using GPS, LiDAR, and InSAR techniques, *Natural Hazards*, *73*(3), 1143-1173.

Kolda, T. G., R. M. Lewis, and V. Torczon (2003), Optimization by Direct Search: New Perspectives on Some Classical and Modern Methods, *SIAM Review*, *45*(3), 385-482.

Konikow, L. F. (2015), Long-Term Groundwater Depletion in the United States, *Groundwater*, *53*(1), 2-9.

Konikow, L. F., and S. A. Leake (2014), Depletion and Capture: Revisiting "The Source of Water Derived from Wells", *Groundwater*, *52*, 100-111.

Kruseman, G. P., and N. A. Ridder (1990), Analysis and evaluation of pumping test data, *Analysis and evaluation of pumping test data.*(47).

Kundzewicz, Z. W., L. J. Mata, N. W. Arnell, P. Döll, P. Kabat, B. Jiménez, K. A. Miller, T. Oki, Z. Sen, and I. A. Shiklomanov (2007), Freshwater resources and their management, *Climate Change 2007: Impacts, Adaptation and Vulnerability. Contribution of Working Group II to the Fourth Assessment Report of the Intergovernmental Panel on Climate Change*, 173-210.

Kusche, J. (2007), Approximate decorrelation and non-isotropic smoothing of time-variable GRACE-type gravity field models, *Journal of Geodesy*, *81*(11), 733-749.

Kusche, J., R. Schmidt, S. Petrovic, and R. Rietbroek (2009), Decorrelated GRACE time-variable gravity solutions by GFZ, and their validation using a hydrological model, *Journal of Geodesy*, *83*(10), 903-913.

Lan, H. X., L. P. Li, H. J. Liu, and Z. H. Yang (2012), Complex Urban Infrastructure Deformation Monitoring Using High Resolution PSI, *Ieee Journal of Selected Topics in Applied Earth Observations and Remote Sensing*, *5*(2), 643-651.

Lanari, R., F. Casu, M. Manzo, G. Zeni, P. Berardino, M. Manunta, and A. Pepe (2007), An overview of the small BAseline subset algorithm: A DInSAR technique for surface deformation analysis, *Pure and Applied Geophysics*, *164*(4), 637-661.

Lanari, R., P. Lundgren, M. Manzo, and F. Casu (2004), Satellite radar interferometry time series analysis of surface deformation for Los Angeles, California, *Geophysical Research Letters*, *31*(23).

Landerer, F. W., and S. C. Swenson (2012), Accuracy of scaled GRACE terrestrial water storage estimates, *Water Resources Research*, *48*.

Leake, S., and D. L. Galloway (2007), MODFLOW Ground-Water Model-User Guide to the Subsidence and Aquifer-System Compaction Package (SUB-WT) for Water-Table Aquifers*Rep. 2328-7055*, Geological Survey (US).

Li, B., M. Rodell, B. F. Zaitchik, R. H. Reichle, R. D. Koster, and T. M. van Dam (2012), Assimilation of GRACE terrestrial water storage into a land surface model: Evaluation and potential value for drought monitoring in western and central Europe, *Journal of Hydrology*, *446–447*, 103-115.

Li, X. P., L. Wang, D. L. Chen, K. Yang, and A. H. Wang (2014), Seasonal evapotranspiration changes (1983-2006) of four large basins on the Tibetan Plateau, *Journal of Geophysical Research-Atmospheres*, *119*(23), 13079-13095.

Liu, G. X., H. G. Jia, R. Zhang, H. X. Zhang, H. L. Jia, B. Yu, and M. Z. Sang (2011), Exploration of Subsidence Estimation by Persistent Scatterer InSAR on Time Series of High Resolution TerraSAR-X Images, *Ieee Journal of Selected Topics in Applied Earth Observations and Remote Sensing*, *4*(1), 159-170.

Lohman, S. W. (1972), *Ground-water hydraulics*, US Government Printing Office.

Lollino, G., D. Giordan, G. B. Crosta, J. Corominas, R. Azzam, J. Wasowski, and N. Sciarra (2015), *Engineering Geology for Society and Territory–Volume 2*, Springer.

Long, D., L. Longuevergne, and B. R. Scanlon (2015), Global analysis of approaches for deriving total water storage changes from GRACE satellites, *Water Resources Research*, *51*(4), 2574-2594.

Long, D., X. Chen, B. R. Scanlon, Y. Wada, Y. Hong, V. P. Singh, Y. Chen, C. Wang, Z. Han, and W. Yang (2016), Have GRACE satellites overestimated groundwater depletion in the Northwest India Aquifer?, *Scientific Reports*, *6*.

Longuevergne, L., B. R. Scanlon, and C. R. Wilson (2010), GRACE Hydrological estimates for small basins: Evaluating processing approaches on the High Plains Aquifer, USA, *Water Resources Research*, *46*.

Longuevergne, L., C. R. Wilson, B. R. Scanlon, and J. F. Crétaux (2013), GRACE water storage estimates for the Middle East and other regions with significant reservoir and lake storage, *Hydrol. Earth Syst. Sci.*, *17*(12), 4817-4830.

Lu, Z., and W. R. Danskin (2001), InSAR analysis of natural recharge to define structure of a ground-water basin, San Bernardino, California, *Geophysical Research Letters*, *28*(13), 2661-2664.

Macciotta, R., M. Hendry, and C. D. Martin (2016), Developing an early warning system for a very slow landslide based on displacement monitoring, *Natural Hazards*, *81*(2), 887-907.

Martinez-Reyes, J., and L. M. Mitre-Salazar (2010), Geological setting of active faulting associated with land subsidence at the Aguascalientes and Queretaro valleys, Mexico, in *Land Subsidence, Associated Hazards and the Role of Natural Resources Development*, edited by D. CarreonFreyre, M. Cerca, D. L. Galloway and J. J. SilvaCorona, pp. 191-194.

Massonnet, D., and K. L. Feigl (1998), Radar interferometry and its application to changes in the Earth's surface, *Reviews of geophysics*, *36*(4), 441-500.

Mattar, K. E., P. W. Vachon, D. Geudtner, A. L. Gray, I. G. Cumming, and M. Brugman (1998), Validation of Alpine glacier velocity measurements using ERS tandem-mission SAR data, *Ieee Transactions on Geoscience and Remote Sensing*, *36*(3), 974-984.

Mazzotti, S., A. Lambert, M. Van der Kooij, and A. Mainville (2009), Impact of anthropogenic subsidence on relative sea-level rise in the Fraser River delta, *Geology*, *37*(9), 771-774.

Mei, S., V. Poncos, and C. Froese (2008), Mapping millimetre-scale ground deformation over the underground coal mines in the Frank Slide area, Alberta, Canada, using spaceborne InSAR technology, *Canadian Journal of Remote Sensing*, *34*(2), 113-134.

Mexico News Daily (2015), The train that budget cuts have not stopped. Mexico News Daily, Saturday, March 21, 2015. http://mexiconewsdaily.com/news/train-budget-cuts-not-stopped/

Mitchell, M. (1995), Genetic algorithms: An overview, *Complexity*, *1*(1), 31-39.

Moran, M. S., C. D. Peters-Lidard, J. M. Watts, and S. McElroy (2004), Estimating soil moisture at the watershed scale with satellite-based radar and land surface models, *Canadian Journal of Remote Sensing*, *30*(5), 805-826.

Ng, A. H.-M., L. Ge, X. Li, H. Z. Abidin, H. Andreas, and K. Zhang (2012), Mapping land subsidence in Jakarta, Indonesia using persistent scatterer interferometry (PSI) technique with ALOS PALSAR, *International Journal of Applied Earth Observation and Geoinformation*, *18*, 232-242.

Normand, J. C. L., and E. Heggy (2015), InSAR Assessment of Surface Deformations in Urban Coastal Terrains Associated With Groundwater Dynamics, *Ieee Transactions on Geoscience and Remote Sensing*, *53*(12), 6356-6371.

Osmanoglu, B., T. H. Dixon, S. Wdowinski, E. Cabral-Cano, and Y. Jiang (2011), Mexico City subsidence observed with persistent scatterer InSAR, *International Journal of Applied Earth Observation and Geoinformation*, *13*(1), 1-12.

Pacheco, J., J. Arzate, E. Rojas, M. Arroyo, V. Yutsis, and G. Ochoa (2006), Delimitation of ground failure zones due to land subsidence using gravity data and finite element modeling in the Queretaro valley, Mexico, *Engineering Geology*, *84*(3-4), 143-160.

Pacheco-Martinez, J., and J. Arzate-Flores (2007), Multilayered analysis of subsidence in the valley of Queretaro, Mexico, *Revista Mexicana De Ciencias Geologicas*, *24*(3), 389-402.

Pacheco-Martinez, J., J. Arzate-Flores, R. Lopez-Doncel, R. Barboza-Gudino, J. L. Mata-Segura, A. Del-Rosal-Pardo, and J. Aranda-Gomez (2010), Zoning map of ground failure risk due to land subsidence of San Luis Potosi, Mexico, in *Land Subsidence, Associated Hazards and the Role of Natural Resources Development*, edited by D. CarreonFreyre, M. Cerca, D. L. Galloway and J. J. SilvaCorona, pp. 179-184.

Pacheco-Martinez, J., M. Hernandez-Marin, T. J. Burbey, N. Gonzalez-Cervantes, J. A. Ortiz-Lozano, M. E. Zermeno-De-Leon, and A. Solis-Pinto (2013), Land subsidence and ground failure associated to groundwater exploitation in the Aguascalientes Valley, Mexico, *Engineering Geology*, *164*, 172-186.

Padilla-Gil, L. L., J. A. Avila-Olivera, G. A. Huape-Padilla, and M. E. Granados-Garcia (2010), Need to integrate land subsidence into the legal instruments of Mexico: Morelia, Michoacan case study, in *Land Subsidence, Associated Hazards and the Role of Natural Resources Development*, edited by D. CarreonFreyre, M. Cerca, D. L. Galloway and J. J. SilvaCorona, pp. 432-434.

Pail, R., et al. (2015), Science and User Needs for Observing Global Mass Transport to Understand Global Change and to Benefit Society, *Surv Geophys*, *36*(6), 743-772.

Pasquali, P., A. Cantone, P. Riccardi, M. Defilippi, F. Ogushi, S. Gagliano, and M. Tamura (2014), Mapping of ground deformations with interferometric stacking tecniques. Land applications of RADAR remote sensing, edited, InTech.

Pearse, J., V. Singhroy, S. Samsonov, and J. H. Li (2014), Anomalous surface heave induced by enhanced oil recovery in northern Alberta: InSAR observations and numerical modeling, *Journal of Geophysical Research-Solid Earth*, *119*(8), 6630-6649.

Poncos, V., D. Teleaga, M. A. Boukhemacha, S. A. Toma, F. Serban, and Ieee (2014), Study of urban instability phenomena in Bucharest City based on PS-InSAR, in *2014 Ieee International Geoscience and Remote Sensing Symposium*, edited, Ieee, New York.

Pool, D. R. (2008), The utility of gravity and water-level monitoring at alluvial aquifer wells in southern Arizona, *GEOPHYSICS*, *73*(6), WA49-WA59.

Pool, D. R., and J. H. Eychaner (1995), Measurements of Aquifer-Storage Change and Specific Yield Using Gravity Surveys, *Groundwater*, *33*(3), 425-432.

Pratesi, F., D. Tapete, G. Terenzi, C. Del Ventisette, and S. Moretti (2015), Rating health and stability of engineering structures via classification indexes of InSAR Persistent Scatterers, *International Journal of Applied Earth Observation and Geoinformation*, *40*, 81-90.

Qin, Y., and D. Perissin (2015), Monitoring Ground Subsidence in Hong Kong via Spaceborne Radar: Experiments and Validation, *Remote Sensing*, *7*(8), 10715.

Ramillien, G., R. Biancale, S. Gratton, X. Vasseur, and S. Bourgogne (2011), GRACE-derived surface water mass anomalies by energy integral approach: Application to continental hydrology, *Journal of Geodesy*, *85*(6), 313-328.

Reeves, J. A., R. Knight, H. A. Zebker, P. K. Kitanidis, and W. A. Schreüder (2014), Estimating temporal changes in hydraulic head using InSAR data in the San Luis Valley, Colorado, *Water Resources Research*, *50*(5), 4459-4473.

Reeves, J. A., R. Knight, H. A. Zebker, W. A. Schreüder, P. S. Agram, and T. R. Lauknes (2011), High quality InSAR data linked to seasonal change in hydraulic head for an agricultural area in the San Luis Valley, Colorado, *Water Resources Research*, *47*(12).

Richey, A. S., B. F. Thomas, M. H. Lo, J. T. Reager, J. S. Famiglietti, K. Voss, S. Swenson, and M. Rodell (2015), Quantifying renewable groundwater stress with GRACE, *Water Resources Research*, *51*(7), 5217-5237.

Rocca, F., C. Prati, A. Ferretti, and Esa (1997), An overview of ERS-SAR interferometry, in *Third Ers Symposium on Space at the Service of Our Environment, Vol 1*, edited, pp. XXVII-XXXVI.

Rodell, M., I. Velicogna, and J. S. Famiglietti (2009), Satellite-based estimates of groundwater depletion in India, *Nature*, *460*(7258), 999-U980.

Rodell, M., J. L. Chen, H. Kato, J. S. Famiglietti, J. Nigro, and C. R. Wilson (2007), Estimating groundwater storage changes in the Mississippi River basin (USA) using GRACE, *Hydrogeology Journal*, *15*(1), 159-166.

Rodell, M., et al. (2004), The global land data assimilation system, *Bulletin of the American Meteorological Society*, *85*(3), 381-+.

Rodell, M., and J. S. Famiglietti (1999), Detectability of variations in continental water storage from satellite observations of the time dependent gravity field, *Water Resources Research*, *35*(9), 2705-2723.

Rodriguez, R., A. Ramos, J. A. Mejia, and J. Berlin (2000), *Subsidence and aquifer vulnerability: The Salamanca case*, 95-99 pp.

Rodriguez, R., J. Lira, and I. Rodriguez (2012), Subsidence risk due to groundwater extraction in urban areas using fractal analysis of satellite images, *Geofisica Internacional*, *51*(2), 157-167.

Rodriguez, R., M. A. Armienta, and J. A. M. Gomez (2005), Arsenic contamination of the Salamanca aquifer system in Mexico: a risk analysis, 77-83 pp.

Rosen, P. A., S. Hensley, G. Peltzer, and M. Simons (2004), Updated repeat orbit interferometry package released, *Eos, Transactions American Geophysical Union*, *85*(5), 47-47.

Rucci, A., A. Ferretti, A. Monti Guarnieri, and F. Rocca (2012), Sentinel 1 SAR interferometry applications: The outlook for sub millimeter measurements, *Remote Sensing of Environment*, *120*, 156-163.

Rudolph, D. L., R. Sultan, J. Garfias, and R. G. McLaren (2006), Significance of enhanced infiltration due to groundwater extraction on the disappearance of a headwater lagoon system: Toluca Basin, Mexico, *Hydrogeology Journal*, *14*(1-2), 115-130.

Rudolph, D., R. Sultan, J. Garfias, and R. McLaren (2007), Analysis of interactions of surface water and groundwater: influences an wetland disappearance, *Ingenieria Hidraulica En Mexico*, *22*(1), 15-30.

Sakumura, C., S. Bettadpur, H. Save, and C. McCullough (2016), High-frequency terrestrial water storage signal capture via a regularized sliding window mascon product from GRACE, *Journal of Geophysical Research: Solid Earth*, *121*(5), 4014-4030.

Samsonov, S. V., N. d'Oreye, P. J. Gonzalez, K. F. Tiampo, L. Ertolahti, and J. J. Clague (2014), Rapidly accelerating subsidence in the Greater Vancouver region from two decades of ERS-ENVISAT-RADARSAT-2 DInSAR measurements, *Remote Sensing of Environment*, *143*, 180-191.

Samsonov, S., K. Tiampo, P. J. Gonzalez, V. Manville, and G. Jolly (2010), Ground deformation occurring in the city of Auckland, New Zealand, and observed by Envisat

interferometric synthetic aperture radar during 2003-2007, *Journal of Geophysical Research-Solid Earth*, *115*, 12.

Save, H., S. Bettadpur, and B. D. Tapley (2012), Reducing errors in the GRACE gravity solutions using regularization, *Journal of Geodesy*, *86*(9), 695-711.

Save, H., S. Bettadpur, and B. D. Tapley (2016), High-resolution CSR GRACE RL05 mascons, *Journal of Geophysical Research: Solid Earth*.

Scanlon, B. R., L. Longuevergne, and D. Long (2012), Ground referencing GRACE satellite estimates of groundwater storage changes in the California Central Valley, USA, *Water Resources Research*, *48*, 9.

Scanlon, B. R., Z. Zhang, R. C. Reedy, D. R. Pool, H. Save, D. Long, J. Chen, D. M. Wolock, B. D. Conway, and D. Winester (2015), Hydrologic implications of GRACE satellite data in the Colorado River Basin, *Water Resources Research*, *51*(12), 9891-9903.

Schaap, M. G., F. J. Leij, and M. T. van Genuchten (2001), ROSETTA: a computer program for estimating soil hydraulic parameters with hierarchical pedotransfer functions, *Journal of Hydrology*, *251*(3-4), 163-176.

Schmidt, D. A., and R. Bürgmann (2003), Time-dependent land uplift and subsidence in the Santa Clara valley, California, from a large interferometric synthetic aperture radar data set, *J. Geophys. Res.*, *108*(B9).

Schmidt, R., F. Flechtner, U. Meyer, K. H. Neumayer, C. Dahle, R. König, and J. Kusche (2008), Hydrological Signals Observed by the GRACE Satellites, *Surv Geophys*, *29*(4-5), 319-334.

Schroeder, A., and R. Rodriguez (2010), Subsidence faulting and aquifer vulnerability - their relation in Irapuato, Mexico, in *Land Subsidence, Associated Hazards and the Role of Natural Resources Development*, edited by D. CarreonFreyre, M. Cerca, D. L. Galloway and J. J. SilvaCorona, pp. 502-504.

Schuite, J., L. Longuevergne, O. Bour, F. Boudin, S. Durand, and N. Lavenant (2015), Inferring field-scale properties of a fractured aquifer from ground surface deformation during a well test, *Geophysical Research Letters*, *42*(24), 10696-10703.

Short, N., A. M. LeBlanc, W. Sladen, G. Oldenborger, V. Mathon-Dufour, and B. Brisco (2014), RADARSAT-2 D-InSAR for ground displacement in permafrost terrain, validation from Iqaluit Airport, Baffin Island, Canada, *Remote Sensing of Environment*, *141*, 40-51.

Simunek, J., M. T. van Genuchten, and M. Sejna (2008), Development and applications of the HYDRUS and STANMOD software packages and related codes, *Vadose Zone Journal*, *7*(2), 587-600.

Singhroy, V., J. Li, S. Samsonov, L. Shen, J. Pearse, and Ieee (2014), InSAR monitoring of surface deformation induced by steam injection in the Athabasca oil sands, Canada, in *2014 Ieee International Geoscience and Remote Sensing Symposium*, edited.

Singhroy, V., R. Couture, P.-J. Alasset, V. Poncos, and Ieee (2007), InSAR monitoring of landslides on permafrost terrain in Canada, in *Igarss: 2007 Ieee International Geoscience and Remote Sensing Symposium, Vols 1-12: Sensing and Understanding Our Planet*, edited, pp. 2451-2454.

Singhroy, V., K. Murnaghan, J. Zhang, and Ieee (2009), InSAR monitoring of landslides using RADARSAT, in *2009 Ieee International Geoscience and Remote Sensing Symposium, Vols 1-5*, edited, pp. 21-24.

Stancliffe, R. P. W., and M. W. A. van der Kooij (2001), The use of satellite-based radar interferometry to monitor production activity at the Cold Lake heavy oil field, Alberta, Canada, *Aapg Bulletin*, *85*(5), 781-793.

Strassberg, G., B. R. Scanlon, and D. Chambers (2009), Evaluation of groundwater storage monitoring with the GRACE satellite: Case study of the High Plains aquifer, central United States, *Water Resources Research*, *45*.

Swenson, S., and J. Wahr (2006), Post-processing removal of correlated errors in GRACE data, *Geophysical Research Letters*, *33*(8).

Swenson, S., D. Chambers, and J. Wahr (2008a), Estimating geocenter variations from a combination of GRACE and ocean model output, *Journal of Geophysical Research: Solid Earth*, 113, B08410, doi:10.1029/2007JB005338.

Swenson, S., J. Famiglietti, J. Basara, and J. Wahr (2008b), Estimating profile soil moisture and groundwater variations using GRACE and Oklahoma Mesonet soil moisture data, *Water Resources Research*, 44, W01413, doi:10.1029/2007WR006057.

Tapete, D., R. Fanti, R. Cecchi, P. Petrangeli, and N. Casagli (2012), Satellite radar interferometry for monitoring and early-stage warning of structural instability in archaeological sites, *Journal of Geophysics and Engineering*, *9*(4).

Tapley, B. D., S. Bettadpur, J. C. Ries, P. F. Thompson, and M. M. Watkins (2004a), GRACE measurements of mass variability in the Earth system, *Science*, *305*(5683), 503-505.

Tapley, B. D., S. Bettadpur, M. Watkins, and C. Reigber (2004b), The gravity recovery and climate experiment: Mission overview and early results, *Geophysical Research Letters*, *31*(9), L09607, doi:10.1029/2004GL019920.

Tarantola, A. (2004), *Inverse Problem Theory and Methods for Model Parameter Estimation*, Society for Industrial and Applied Mathematics.

Taylor, R. G., et al. (2013), Ground water and climate change, *Nature Climate Change*, *3*(4), 322-329.

Teatini, P., L. Tosi, T. Strozzi, L. Carbognin, U. Wegmuller, and F. Rizzetto (2005), Mapping regional land displacements in the Venice coastland by an integrated monitoring system, *Remote Sensing of Environment*, *98*(4), 403-413.

Terzaghi, K. (1925), Principles of soil mechanics, IV—Settlement and consolidation of clay, *Engineering News-Record*, *95*(3), 874-878.

Tiwari, V. M., J. Wahr, and S. Swenson (2009), Dwindling groundwater resources in northern India, from satellite gravity observations, *Geophysical Research Letters*, *36*.

Turc, L. (1961), Estimation of irrigation water requirements, potential evapotranspiration: a simple climatic formula evolved up to date, *Ann Agron*, *12*(1), 13-49.

Vangenuchten, M. T. (1980), A closed-form equation for predicting the hydraulic conductivity of unsaturated soils, *Soil Science Society of America Journal*, *44*(5), 892-898.

Wada, Y., L. P. H. van Beek, C. M. van Kempen, J. W. T. M. Reckman, S. Vasak, and M. F. P. Bierkens (2010), Global depletion of groundwater resources, *Geophysical Research Letters*, 37, L20402, doi:10.1029/2010GL044571.

Wahr, J., M. Molenaar, and F. Bryan (1998), Time variability of the Earth's gravity field: Hydrological and oceanic effects and their possible detection using GRACE, *Journal of Geophysical Research: Solid Earth*, *103*(B12), 30205-30229.

Wang, K. C., P. Wang, Z. Q. Li, M. Cribb, and M. Sparrow (2007), A simple method to estimate actual evapotranspiration from a combination of net radiation, vegetation index, and temperature, *Journal of Geophysical Research-Atmospheres*, *112*(D15).

Westen, C. J. V. (2004), Geo-Information tools for landslide risk assessment: an overview of recent developments, in *Landslides: Evaluation and Stabilization/Glissement de Terrain: Evaluation et Stabilisation, Set of 2 Volumes*, edited, pp. 39-56, CRC Press.

Wilson, S. S., N. C. Crawford, L. A. Croft, M. Howard, S. Miller, and T. Rippy (2006), Autonomous robot for detecting subsurface voids and tunnels using microgravity, paper presented at Proceedings of SPIE - The International Society for Optical Engineering.

Xu, W. B., Z. W. Li, X. L. Ding, C. C. Wang, and G. C. Feng (2012), Application of small baseline subsets D-InSAR technology to estimate the time series land deformation and aquifer storage coefficients of Los Angeles area, *Chinese Journal of Geophysics-Chinese Edition*, *55*(2), 452-461.

Yan, T. T., and T. J. Burbey (2008), The value of subsidence data in ground water model calibration, *Ground Water*, *46*(4), 538-550.

Yan, Y. J., M. P. Doin, P. Lopez-Quiroz, F. Tupin, B. Fruneau, V. Pinel, and E. Trouve (2012), Mexico City Subsidence Measured by InSAR Time Series: Joint Analysis Using PS and SBAS Approaches, *Ieee Journal of Selected Topics in Applied Earth Observations and Remote Sensing*, *5*(4), 1312-1326.

Yeh, P. J. F., S. C. Swenson, J. S. Famiglietti, and M. Rodell (2006), Remote sensing of groundwater storage changes in Illinois using the Gravity Recovery and Climate Experiment (GRACE), *Water Resources Research*, 42, W12203, doi:10.1029/2006WR005374.

Yerro, A., J. Corominas, D. Monells, and J. J. Mallorquí (2014), Analysis of the evolution of ground movements in a low densely urban area by means of DInSAR technique, *Engineering Geology*, *170*, 52-65.

Yuill, B., D. Lavoie, and D. J. Reed (2009), Understanding subsidence processes in coastal Louisiana, *Journal of Coastal Research*, 23-36.

Zhang, M., and T. J. Burbey (2016), Inverse modelling using PS-InSAR data for improved land subsidence simulation in Las Vegas Valley, Nevada, *Hydrological Processes*, *30*(24), 4494-4516.